

New ethylene oxide-based catanionic mixtures – investigations towards potential applications



Dissertation

zur Erlangung des Doktorgrades der Naturwissenschaften (Dr. rer. nat.)
der Fakultät Chemie und Pharmazie
der Universität Regensburg

vorgelegt von

Lydia Zahnweh

aus Wartenberg
2019

Promotionsausschuss

1. Gutachter	Prof. Dr. Werner Kunz, Institut für Physikalische und Theoretische Chemie, Universität Regensburg (Deutschland)
2. Gutachter	Prof. Dr. Jean-Marie Aubry, UCCS, Université des Sciences et Technologies de Lille (France)
3. Prüfer	Prof. Dr. Hubert Motschmann, Institut für Physikalische und Theoretische Chemie, Universität Regensburg (Deutschland)
Vorsitzender	Prof. Dr. Henri Brunner

Promotionsgesuch eingereicht am: 7. Februar 2019

Datum der mündlichen Prüfung: 26. März 2019

Diese Doktorarbeit entstand in der Zeit von November 2014 bis Dezember 2018 am Institut für Physikalische und Theoretische Chemie der Universität Regensburg unter der Betreuung von Prof. Dr. Werner Kunz in Kooperation mit der Firma BASF, Ludwigshafen.

ACKNOWLEDGEMENT

Die Anfertigung dieser Arbeit wäre ohne eine Großzahl an Menschen nicht möglich gewesen, bei welchen ich mich im Folgenden bedanken möchte.

An erster Stelle möchte ich mich bei Herrn Prof. Dr. Werner Kunz bedanken. Vielen Dank für die Bereitstellung des Themas, die Möglichkeit, dieses an Ihrem Lehrstuhl bearbeiten zu dürfen und die vielen hilfreichen Diskussionen. Nur mit Ihrer Hilfe war es möglich, solch eine gute Kooperation mit der BASF durchzuführen.

Ein großes Dankeschön geht an viele Personen in der BASF in Ludwigshafen. Zuallererst möchte ich mich bei Dr. Matthias Kellermeier für seine Unterstützung durch zahlreiche Ideen in den letzten Jahren und die Möglichkeit, viele Messungen in seinen Laboren durchführen zu dürfen, bedanken. Ebenfalls ein großer Dank geht an: Dr. Nadine Engelhardt und Dr. Susanne Engert für die Synthese der in dieser Arbeit untersuchten Moleküle und für die gute Zusammenarbeit während des Projekts; Dr. Günther Oetter für seine konstruktiven Beiträge und die vielen durchgeführten Messungen in seinem Labor; Dr. David Ley für die Durchführung mehrere High-Throughput Screenings; Dr. Andreas Ott für seine Mühe, oft schwierige Proben zu TEM Bildern zu verwandeln; Nicole Lichterfeld-Weber und Marco Czink für viele Messunterstützungen; Van-Tay Nguyen für die Hilfe bei QCM Problemen; und zu guter Letzt möchte ich mich bei Werner Wacker, Peter Stangl, Elisabeth Wagner und Bernd Kümmerling für ihre Hilfe und besonders für ihr freundliche Art bedanken. Ich hatte viel Spaß mit euch.

Außerdem möchte ich mich bei allen Kollegen und besonders Bürokollegen am Lehrstuhl für die schöne Zeit und ihre Unterstützung bedanken, im Besonderen bei Tessa für die vielen amüsanten Mittagspausen und Bürogespräche, sowie bei der Physik-Kaffee-Crew für Erholungen am Nachmittag. Des Weiteren möchte ich mich bei Barbara für die Durchführung der Cytotox-Tests bedanken.

Der größte Dank gehört meinen Eltern, die mich mein ganzes Leben und auch im Laufe der letzten Jahre in jeder erdenklichen Weise unterstützt haben. „Was macht die Forschung?“ „Die Forschung ist fertig, Mama!“ ;)

Und das Beste zum Schluss: Danke Peter für Alles!

Lydia Zahnweh

ABSTRACT

The topic of this work was the investigation of new catanionic mixtures with the focus on potential application in foaming, spreading, washing and emulsions. To this purpose, a new group of catanionic mixtures consisting of newly synthesized anionic and cationic surfactants by BASF was introduced. These substances have a linear molecular structure with an alkyl chain of different lengths and number of ethylene oxide (EO) group(s) combined with an ionic headgroup, a sulfate group for the anionic species and a choline group for the cationic species. The intention of inserting EO groups in the catanionic surfactant structure was to increase the scope of potential applications by improving their solubility, which is known to be low, especially around equimolar ratio. For understanding the influences of different structural aspects on properties and performances, the experimental data were correlated to molecular properties to make predictions regarding their performance possible.

In the first part of the thesis, the catanionic mixtures were investigated at different anion-cation wt%-ratios from 9-1 to 1-9, regarding different physicochemical properties like solubility behavior, interfacial properties, adsorption behavior, and toxicity. An improved solubility, which could be led back to the present EO groups, could be confirmed. This precondition enabled the investigation of further properties. Synergistic effects were observed for the properties concerning the interfacial activity. For the cmc, as well as the surface tension reduction, small amounts of the oppositely charged surfactant were sufficient to reach the highest efficiency. High dynamics were found in combination with the anion SDS. For the adsorption on a hydrophobic and a hydrophilic surface, synergistic effects became obvious for the mixtures compared to the pure ionic surfactants. For the catanionic mixtures, a large variety of different aggregation structures was found with cryoTEM. A decrease in the toxicity of the cationic surfactant with the addition of an anionic surfactant was found. With the help of statistical analysis, several relations between the molecular and the observed physicochemical properties could be quantified. Especially for the solubility, the presence of EO groups is advantageous. The chain length influences the interfacial properties.

In the second part, a pre-screening over all catanionic mixtures regarding their foaming behavior was performed with a high-throughput robot. For a selection of catanionic mixtures, the foamability was investigated deeper considering the total foam height, the liquid volume of the foam and the average bubble size. The anion-cation ratio itself did not follow a clear trend. But for combinations having viscoelastic behavior, increasing foam stability was found. A lower solubility of the surfactant solution was

also favorable. A stabilization according to Pickering was suggested. Both methods, high-throughput robot and dynamic foam analyzer, showed the complexity of foams. By statistical analysis, a low surface tension of the surfactant solution could be correlated to higher foamability. The bubble size can be kept small, which correlates to high foam stability, by a small number of EO groups in the cationic surfactant, a small HLB value and a long average chain length of the surfactants.

In the third part, the fat removal behavior was investigated. In a first screening, the pure catanionic mixtures were tested with a quartz crystal microbalance (QCM). Four catanionic mixtures were further investigated in the in-house-built washing apparatus. The combination of SDS and C12EO1Ch gave the best results. The effect of a catanionic combination in a more complex washing system based on the three surfactants sodium dodecylbenzylsulfonate, Lutensol AO7, and Texapon N70 was examined in a next step. The addition of a cationic surfactant had positive effects, but only if EO groups were present in the cationic surfactant. A significant influence of the nonionic character in the washing solution was observed. But, the nonionic surfactant was not necessary for full extent if the cationic surfactant C12EO1Ch was added. It could compensate for the decrease of the nonionic surfactant. Further addition of an enzyme showed no positive effect, compared to approaches where only the cationic surfactant or only the enzyme was added to the washing solution. Both seemed to hinder each other. With the use of the cationic surfactant, the enzyme was not necessary. Consequently, the catanionic combination can be a substitute for the commonly used lipase.

In the fourth part, the spreading on a hydrophobic polyethylene surface was investigated. A synergistic effect of the mixtures was found. Around equimolar ratio, the contact angle was lowest for most mixtures. The combination of SDS and C12EO1Ch showed the behavior of a “super-spreader”. Three examples for a good, an intermediate and a bad wetting were examined via high-speed camera and compared to the wetting agent Plurafac LF300. The combination SDS-C12EO1Ch, mass ratio 5-5, gave the same good result as the wetting agent. A good spreading behavior was also confirmed on real plant leaves. Moreover, the three catanionic combinations were used to find a correlation to their physicochemical properties. The importance of the dynamics in the surfactant solutions and its surface activity became obvious. The same conclusion could be obtained by statistical analysis. For a good spreading behavior, EO groups were necessary to guarantee high solubility. A shorter chain length promoted spreading as well as high dynamics in the surfactant solution. With the investigated catanionic mixtures, the problem of precipitation, as it is often described in the literature, can be overcome by the insertion of EO groups. Thus, the maximal efficiency of them can be used, and super-spreaders can be tuned.

In the last part, the emulsification behavior was investigated via a screening of 10 different oils. Compared to the pure ionic surfactants, a lot of mixtures showed higher emulsion stability. But in general, the emulsification performance of the catanionic mixtures was lower than expected. Highest emulsion stability was obtained for the anion-cation mass ratio 5-5. Triolein was the oil which could be emulsified the best. A low interfacial tension was found to be a supporting factor for a stable emulsion. The combination of the anionic surfactant Texapon N70 and the cationic surfactant Dehyquart ACA, mass ratio 5-5, gave the best results on average. Thus, it was investigated further regarding the potential switchability of the catanionic emulsion system. The two parameters NaSCN content and temperature were found to influence the catanionic system. Their potential was investigated in an emulsion. An effect on the emulsion stability was found for the NaSCN content and the temperature, which could be used to destabilize the emulsion system. The principle concept could be confirmed, but further investigations are necessary to get a deeper insight into the influences and the emulsion capacity.

Within this work, the great potential of the catanionic mixtures for various applications could be shown. Catanionic mixtures have high potential especially due to their high efficiency at low concentrations. Their synergistic effect can enhance the performance. They can be tuned by changing different parameters like anion-cation ratio, number of EO groups or chain length. They can significantly improve surfactant properties and efficiency for several possible applications in industry as well as in household applications.

ZUSAMMENFASSUNG

Das Thema dieser Doktorarbeit war die Untersuchung neuer katanionischer Mischungen mit dem Fokus auf den potentiellen Anwendungsfeldern der Schäume, Benetzung von Oberflächen, Waschen und Emulsionen. Hierzu wurde eine Gruppe katanionischer Kombinationen aus neu synthetisierten anionischen und kationischen Tensiden der BASF vorgestellt. Die Grundstruktur der Tenside besteht aus einer linearen Molekülstruktur mit Ethylenoxid (EO)-Gruppe(n) zwischen einer Alkylkette mit unterschiedlicher Länge und einer ionischen Kopfgruppe, einer Sulfat-Gruppe für die Anionen und einer Cholin-Gruppe für die Kationen. Durch die EO-Gruppen in der Tensidstruktur soll das für diese Mischungen bekannte Ausfallen des Ionenpaares verhindert werden, um dadurch den Anwendungsbereich der Tenside zu vergrößern. Ein Verständnis der Struktureinflüsse auf Eigenschaften und Leistungen ist hierfür unabdingbar. Daher wurden die erhaltenen experimentellen Daten mit den molekularen Eigenschaften der katanionischen Kombinationen korreliert, um Vorhersagen über deren Auswirkung zu ermöglichen.

Im ersten Teil der Arbeit wurden die katanionischen Mischungen bei unterschiedlichen Anionen-Kation-Gewichtsverhältnissen von 9-1 bis 1-9 hinsichtlich verschiedener physikochemischer Eigenschaften wie Löslichkeitsverhalten, Grenzflächeneigenschaften, Adsorptionsverhalten und Toxizität untersucht. Eine verbesserte Löslichkeit, die auf die vorhandenen EO-Gruppen zurückgeführt werden kann, konnte festgestellt werden. Dies ermöglichte die Untersuchung weiterer Eigenschaften. So wurden synergistische Effekte für die Eigenschaften bezüglich der Grenzflächenaktivität beobachtet. Sowohl für die cmc als auch für die Verringerung der Oberflächenspannung reichten geringe Anteile des entgegengesetzt geladenen Tensids aus, um höchste Effizienz zu erreichen. In Kombination mit dem anionischen Tensid SDS wurde die höchste Dynamik gefunden. Für die Adsorption auf einer hydrophoben und einer hydrophilen Oberfläche wurden ebenfalls synergistische Effekte der Mischungen gegenüber den reinen ionischen Tensiden deutlich. Außerdem wurde eine Vielzahl unterschiedlicher Aggregationsstrukturen für die katanionischen Gemische mit Hilfe von cryoTEM-Aufnahmen gefunden. In Bezug auf die Zytotoxizität bei HaCaT-Zellen verringerte die Zugabe des anionischen zum kationischen Tensid die Toxizität verglichen mit dem reinen kationischen Tensid. Mit Hilfe einer statistischen Analyse konnten mehrere signifikante Beziehungen zwischen den molekularen und den beobachteten physikochemischen Eigenschaften gefunden werden: EO-Gruppen in der Molekülstruktur begünstigen die Löslichkeit. Die Alkylkettenlänge der Tenside beeinflusst die Grenzflächeneigenschaften.

Im zweiten Teil wurde zunächst mit einem High-Throughput Roboter ein Vorscreening aller katanionischen Gemische hinsichtlich ihres Schaumverhaltens durchgeführt. Für eine Auswahl an katanionischen Mischungen wurde das Schaumverhalten unter Berücksichtigung der gesamten Schaumhöhe, des Flüssigkeitsvolumens des Schaums und der durchschnittlichen Blasengröße untersucht. Das Anion-Kation-Verhältnis selbst zeigte keinen erkennbaren Einfluss auf das Schaumverhalten. Bei Kombinationen mit viskoelastischem Verhalten wurde eine erhöhte Schaumstabilität festgestellt. Eine niedrigere Löslichkeit der Tensidlösung war ebenfalls vorteilhaft. Eine Stabilisierung nach Pickering könnte der Grund hierfür sein. Beide Methoden, High-Throughput-Roboter und dynamic foam analyzer, zeigten die Komplexität von Schäumen. Durch statistische Analyse konnte eine Korrelation zwischen einer niedrigen Oberflächenspannung der Tensidlösung und einer höheren Schaumfähigkeit aufgezeigt werden. Die Blasengröße kann durch eine geringe Anzahl von EO-Gruppen im kationischen Tensid, einen geringen HLB-Wert und eine lange durchschnittliche Kettenlänge der Tenside klein gehalten werden, was eine hohe Schaumstabilität bewirkt.

Im dritten Teil der Arbeit wurde die Reinigungswirkung katanionischer Kombinationen anhand von Fettverschmutzungen untersucht. In einem ersten Screening wurden die reinen katanionischen Mischungen in einer Quarzkristall-Mikrowaage (QCM) getestet. In der hauseigenen Waschapparatur wurden vier katanionische Mischungen weiter untersucht. Die Kombination von SDS und C12EO1Ch zeigte die besten Reinigungsergebnisse. Die Auswirkung einer katanionischen Kombination in einem komplexeren Waschsysteem auf der Basis der drei Tenside Natriumdodecylbenzylsulfonat, Lutensol AO7 und Texapon N70 wurde daraufhin weiter untersucht. Die Zugabe eines kationischen Tensids hatte positive Wirkungen, jedoch nur, wenn EO-Gruppen im kationischen Tensid vorhanden waren. Es wurde ein signifikanter Einfluss des nichtionischen Charakters in der Waschlösung beobachtet. Wurde das kationische Tensid C12EO1Ch zugegeben, konnte die Konzentration des nichtionischen Tensids auf 1/3 verringert werden. Es konnte eine Erniedrigung der Konzentration des nicht-ionischen Tensids ausgleichen. Die Zugabe eines Enzyms zur Waschlösung zeigte keinen zusätzlichen positiven Effekt im Vergleich zu einer Waschlösung nur mit kationischem Tensid oder Enzym. Kationisches Tensid und Enzym schienen sich gegenseitig zu behindern. Bei Verwendung des kationischen Tensids war das Enzym nicht notwendig. Die katanionische Kombination kann als möglicher Ersatz der häufig verwendeten Lipase gesehen werden.

Im vierten Teil der Arbeit wurde das Spreitverhalten der katanionischen Mischungen auf einer hydrophoben Polyethylen-Oberfläche untersucht. Auch hier wurde ein synergistischer Effekt der Mischungen beobachtet. Bei äquimolarem Verhältnis war der Kontaktwinkel für die meisten Mischungen am geringsten. Die Kombination von SDS und C12EO1Ch zeigte sehr hohes Spreitverhalten und konnte als Superspreiter eingestuft werden. Drei Kombinationen wurden als Beispiele für einen guten, einen mittleren und einen schlechten Spreiter mit einer Hochgeschwindigkeitskamera untersucht und mit dem kommerziellen Benetzungsmittel Plurafac LF300 verglichen. Die Kombination SDS-C12EO1Ch, Verhältnis 5-5, ergab dasselbe gute Ergebnis wie bereits in vorherigen Tests beobachtet. Das gute Spreitverhalten wurde ebenfalls auf realen Pflanzenblättern bestätigt. Die physikochemischen Eigenschaften der drei katanionischen Kombinationen wurden mit ihrem Spreitverhalten korreliert. Die Bedeutung der Dynamik in den Tensidlösungen und deren Oberflächenaktivität wurde hierbei deutlich. Die gleiche Schlussfolgerung konnte durch statistische Analysen erzielt werden. Für ein gutes Spreitverhalten sind zum einen EO-Gruppen erforderlich, um eine hohe Löslichkeit zu gewährleisten. Zum anderen fördern eine kürzere Kettenlänge sowie eine hohe Dynamik in der Tensidlösung die Benetzung. Mit den untersuchten katanionischen Gemischen kann das in der Literatur oft beschriebene Ausfällungsproblem durch Einfügen der EO-Gruppen gelöst werden. Dadurch kann ihre hohe Effizienz genutzt und ihre Eignung für viele Anwendungen erleichtert werden.

Im letzten Teil der Arbeit wurde das Emulgierverhalten und die Stabilität der entstehenden Emulsion durch ein Screening mit zehn verschiedenen Ölen untersucht. Im Vergleich zu den reinen ionischen Tensiden zeigten viele Mischungen eine höhere Emulsionsstabilität. Im Allgemeinen war die Emulgieleistung der katanionischen Mischungen jedoch niedriger als erwartet. Die höchste Emulsionsstabilität wurde für das Anionen-Kation-Verhältnis 5-5 erhalten. Das Öl Triolein wurde am besten emulgiert. Eine niedrige Grenzflächenspannung erwies sich als unterstützender Faktor für eine stabile Emulsion. Die Kombination des anionischen Tensids Texapon N70 und kationischem Tensid Dehyquart ACA im Massenverhältnis 5-5 ergab im Durchschnitt die besten Ergebnisse. Daher wurde die potentielle Schaltbarkeit des katanionischen Emulsionssystems durch externe Parameter (pH, Temperatur, Salzzugabe, Alkoholzugabe) weiter untersucht. Für die beiden Parametern NaSCN-Konzentration und Temperatur konnte eine Veränderung des Systems festgestellt werden. Deshalb wurde der Effekt in konkreten Emulsionssystemen geprüft. Es wurde ein Einfluss der NaSCN-Konzentration und der Temperatur festgestellt, welcher zur Destabilisierung des Emulsionssystems verwendet werden könnte. Der Grundgedanke zur Schaltbarkeit

von Emulsionssystemen konnte bestätigt werden. Jedoch sind weitere Untersuchungen erforderlich, um einen tieferen Einblick in die Einflüsse und die Fähigkeit zur Emulsionsstabilisierung zu erhalten.

In dieser Arbeit konnte das Anwendungspotential der katanionischen Mischungen gezeigt werden. Insbesondere aufgrund ihrer hohen Wirksamkeit bei niedrigen Konzentrationen eignen sie sich als Alternative für kommerzielle Substanzen. Grund hierfür ist ein synergistischer Effekt zwischen den beiden ionischen Tensiden. Der große Vorteil der katanionischen Kombination ist die Möglichkeit, durch Anpassung verschiedener Parameter wie Anionen-Kation-Verhältnis, Anzahl der EO-Gruppen oder Kettenlänge ihre Eigenschaften speziell einzustellen.

TABLE OF CONTENTS

ACKNOWLEDGEMENT.....	V
ABSTRACT	VII
ZUSAMMENFASSUNG.....	XI
TABLE OF CONTENTS	XV
1 General introduction and motivation.....	1
2 Fundamental information about surfactants.....	5
2.1 General structure and classification.....	5
2.2 Self-assembly of surfactants in aqueous solutions	7
2.2.1 The packing parameter.....	7
2.2.2 Critical micelle concentration.....	8
2.3 Surfactant solubility and Krafft temperature	10
2.4 Adsorption of surfactants.....	11
2.4.1 Adsorption to a gas interface	11
2.4.2 Adsorption to solid surfaces.....	12
2.5 Toxicology and biodegradability.....	14
2.6 Ethylene oxide groups in the surfactant structure.....	16
3 Physicochemical characterization of new catanionic combinations.....	19
3.1 Introduction.....	19
3.2 Fundamental information on catanionics	21
3.2.1 Classification and properties	21
3.2.2 Aggregation behavior	23
3.2.3 Application.....	25
3.3 Results and discussion.....	27
3.3.1 Solubility in water	30
3.3.2 Critical micelle concentration.....	34
3.3.3 Interfacial tension.....	37
3.3.3.1 Surface tension against air	37
3.3.3.2 Interfacial tension against hexadecane.....	39
3.3.4 Adsorption behavior.....	43
3.3.5 Dynamic behavior.....	48

3.3.6	Aggregation behavior: DLS and cryoTEM	53
3.3.7	Cytotoxicity.....	58
3.3.8	Statistical analysis.....	61
3.4	Conclusion	66
3.5	Experimentals.....	69
3.5.1	Chemicals.....	69
3.5.2	Methods	69
3.5.2.1	Solubility Measurement	69
3.5.2.2	Interfacial tension measurements	70
3.5.2.3	Aggregation measurements	73
3.5.2.4	Adsorption measurement	73
3.5.2.5	Cytotoxicity.....	74
3.5.2.6	Statistical analysis.....	75
4	Towards application: catanionics as foaming agents	76
4.1	Introduction.....	76
4.2	Fundamental information	78
4.2.1	Definition, generation and differentiation	78
4.2.2	Stability of foams.....	78
4.3	Results and discussion.....	81
4.3.1	Pre-screening with the high-throughput robot.....	81
4.3.2	Deeper investigations on the foaming behavior of catanionic mixtures	86
4.3.2.1	Foam analysis	87
4.3.2.2	Statistical analysis.....	92
4.4	Conclusion	96
4.5	Experimentals.....	98
4.5.1	Chemicals.....	98
4.5.2	Methods	98
4.5.2.1	High-throughput robot	98
4.5.2.2	Dynamic foam analyzer	98
4.5.2.3	Statistical analysis.....	99
5	Towards application: catanionics as detergents for fat removal.....	100
5.1	Introduction.....	100

5.2	Fundamental information	102
5.2.1	The composition of the detergent formulations.....	102
5.2.1.1	Surfactants.....	102
5.2.1.2	Enzymes.....	103
5.2.1.3	Other ingredients	104
5.2.2	Influences on the washing process	104
5.2.3	Removal mechanisms.....	105
5.2.3.1	Liquid soil removal.....	106
5.2.3.2	Solid soil removal.....	108
5.3	Results and discussion.....	110
5.3.1	Pure cationic combinations	110
5.3.1.1	Pre-screening of the fat removal performance.....	110
5.3.1.2	Washing tests with the washing apparatus	118
5.3.2	Cationic combinations in complex washing systems	122
5.3.2.1	Reference systems and the influence of temperature.....	123
5.3.2.2	The influence of the soil on the washing result	126
5.3.2.3	Cationic surfactants as an additive to the standard mixture	130
5.3.2.4	Cationics as compensation for the decrease of AO7 concentration.....	136
5.3.2.5	Addition of enzyme	141
5.4	Conclusion	149
5.5	Experimentals.....	151
5.5.1	Chemicals.....	151
5.5.2	Methods	151
5.5.2.1	Preparation of the washing solution	151
5.5.2.2	Quartz microbalance	152
5.5.2.3	The in-house-built washing apparatus	154
5.5.2.4	Determination of the cmc	155
5.5.2.5	White light interferometry and scanning electron microscope	156
5.5.2.6	Enzyme stability tests	156
5.5.2.7	Contact angle measurements.....	156
5.5.2.8	Statistical analysis.....	157

6	Towards application: catanionics as spreading agents	158
6.1	Introduction.....	158
6.2	Fundamental information	160
6.2.1	Spreading and wetting	160
6.2.2	Surfactant-enhanced spreading	161
6.2.3	Spreading of catanionic combinations	163
6.3	Results and discussion.....	165
6.3.1	Contact angle on hydrophobic surfaces.....	165
6.3.1.1	Polyethylene.....	165
6.3.1.2	Plant leaves.....	174
6.3.2	Spreading behavior investigated with a high-speed camera	175
6.3.3	Correlation with other chemical properties.....	177
6.3.4	Statistical analysis.....	182
6.4	Conclusion	184
6.5	Experimentals.....	186
6.5.1	Chemicals.....	186
6.5.2	Methods	186
6.5.2.1	Contact angle measurement	186
6.5.2.2	High-speed camera recording	186
6.5.2.3	Interfacial tension measurement	187
6.5.2.4	Dynamic surface tension measurement.....	187
6.5.2.5	Cmc measurements.....	187
6.5.2.6	Adsorption behavior.....	187
6.5.2.7	Statistical analysis.....	188
7	Towards application: catanionics as an emulsifier	189
7.1	Introduction.....	189
7.2	Fundamental information	191
7.2.1	Definition and classification of an emulsion	191
7.2.1.1	Emulsion from the thermodynamical point of view	192
7.2.1.2	Interaction energy forces	193
7.2.1.3	Stability of emulsions	195
7.2.1.4	Catanionics systems in emulsions	198

7.2.2	Specific ion effects	199
7.3	Results and discussion	203
7.3.1	Emulsion screening.....	203
7.3.1.1	Correlations to the interfacial tension of the catanionic mixtures	210
7.3.1.2	Microscopic investigations with the CLSM.....	212
7.3.2	Deeper investigation of the system the system Tex-ACA, 5-5, 1 wt%	213
7.3.2.1	Basic characterization of the catanionic system	214
7.3.2.2	External influences on the Tex-ACA system	215
7.3.3	Tests on the switchability of emulsions	227
7.4	Conclusion	232
7.5	Experimentals	234
7.5.1	Chemicals.....	234
7.5.2	Methods	234
7.5.2.1	Emulsion stability	234
7.5.2.2	Spinning drop tensiometer.....	235
7.5.2.3	Turbidity measurement.....	236
7.5.2.4	Viscosity and density measurement.....	236
7.5.2.5	Confocal light scanning microscope	237
7.5.2.6	DLS measurement	237
7.5.2.7	SAXS measurement	237
8	General summary and outlook	239
9	Appendix	244
9.1	List of figures	244
9.2	Table of symbols.....	252
9.3	List of tables.....	254
9.4	List of equations	256
10	References.....	257
11	Eidesstattliche Erklärung	265

1 General introduction and motivation

Surfactants are omnipresent in our daily life and have developed in a way to fulfill the demands of consumers and industry. The economic aspect of surfactants is large. The turnover rates are several billion dollars only in the US. Due to their unique properties, their application ranges from personal care products to oilfield chemicals or food and packaging.^{1, 2}

Soaps are the oldest surfactants used by men already thousands of years ago. The alkaline reaction and the sensitivity towards water hardness of soaps are two main disadvantages, which result in the development and research of new surfactants. It was Fritz Günther of BASF Ludwigshafen who synthesized the first soap substitute, alkylated and sulfonated naphthalene, in 1917. Since then, different groups of synthetic surfactants made their way to several applications. E.g., alkyl sulfates can be found in many products and especially their ether derivatives are widely used due to their higher solubility.³

In the last years, the challenges for the surfactant industry have grown. Regulations regarding e.g. biocompatibility and energy saving are getting stricter. The awareness of consumers regarding the usage of products increases. The demand for “green” products is growing. Products which are milder for the consumer but also less damaging for the environment are desired. Moreover, the products should be cheap. They should work already at low temperature. So, energy for heating can be saved. Also, a minimum amount of used product is desired to protect resources. For this purpose, high-performing surfactants are needed, which work efficiently at low concentrations to decrease the amount of surfactant exposed to the environment and to save raw materials. A surfactant fulfilling all desired demands has not been developed yet. So, the adjustment of individual surfactants for special applications is necessary. To fulfill these requirements, the need for a deeper understanding of interactions and relationships between chemical structure and its physical and chemical influences is indispensable.¹

This is the basic idea of the present work. In this thesis, new anionic and cationic surfactants are introduced. They are combined as catanionic mixtures. The surfactant structure is based on the insertion of ethylene oxide groups in the linear structure of the anionic and cationic surfactant. Whereas it is already known for anions, like the commercial Texapon N70, this structural aspect has not been expanded to the cation side. For this purpose, one main aspect of this thesis is the creation

of a new group of cationic surfactants based on choline with ethylene oxide groups in the structure. Within this, two aspects are possible to be combined. Choline is a quaternary ammonium ion of biological origin with low toxicity and high biodegradability.⁴ Research has been done on choline as a counterion for long-chain anionic surfactants. A positive effect in reducing the Krafft point and thus an increase in the solubility could be found.^{5, 6} The positive effect of ethylene oxide groups within a molecule regarding the solubility is already known. The 2,5,8,11-tetraoxatridecan-13-olate (TOTO) anion is known to improve solubility due to the orientation of the ethylene oxide groups around a cation. The high flexibility in the molecular structure prevents precipitation.^{7, 8} The group of Akypo is a famous group of carboxylate anions produced by Kao Chemicals, which also benefits from the ethylene oxide-based structure.⁹

As already mentioned, this kind of positive structural effect has yet not been expanded to the group of cationic surfactants. The question arises if, with the combination of a cation and an anion, both including these structural aspects might have an even more positive effect than it can be observed for anionic surfactants alone. Especially, the problem of solubility when combining a cationic and an anionic surfactant, which normally leads to precipitation, might be lowered. In this way, two positive synergistic aspects can appear: the structural point of the ethylene oxide groups and the point of creating a catanionic combination where synergistic effects are already known.¹⁰ Unfortunately, their synthesis is complex. For this purpose, the expertise of an experienced company, BASF, could be used as a part of a cooperation for this field of research. With their expertise in the field of synthesis, they could provide a variety of the imagined compounds. The first idea was to combine these new cationic compounds with commercially available anions and with newly synthesized ones to characterize their physicochemical properties. Out of this, the aim was to apply these new combinations in several application fields like foaming, washing, spreading and emulsification.

The thesis is divided into five experimental chapters. In chapter 3, the newly synthesized catanionic combinations will be introduced. Several physicochemical properties will be investigated, and an overview of the characterization will be presented. Out of these results, chapter 4–7 will treat the four fields of potential application. Chapter 4 deals with foaming. Out of a screening, several catanionic combinations will be investigated deeper regarding their foaming behavior. The ability to spread will be investigated in chapter 5, where three examples of the catanionic mixtures were investigated to understand relations between spreading behavior and other physicochemical properties. In chapter 6, the application of catanionic combinations for fat removal is described. Tests

for a deeper understanding of the ability of different components to remove fat from a fiber were performed. Chapter 7 deals with the potential use of the catanionic combinations as emulsifiers and the possibility to change the stability of the emulsion with external parameters. The last chapter 8 will give a summary of the investigations and conclusions of this work.

2 Fundamental information about surfactants

2.1 General structure and classification

The term surfactant originates from “Surface Active Agents,” describing amphiphilic compounds.¹¹ They consist of a hydrophobic part (tail) and a hydrophilic part (headgroup) leading to the ability to adsorb at interfaces and thus change the interfacial properties of liquids. The hydrophobic part usually consists of a linear or branched alkyl chain of at least eight carbon atoms. These hydrocarbon-based surfactants are mainly obtained from petrochemicals, natural vegetable oil or natural animal fats. Since the purification and separation costs are high, most commercially used surfactants are mixtures without highest purity. They can differ in chain length or contain some impurities from synthesis, like alcohols.¹² The hydrophilic part can be of ionic or nonionic and water-soluble character. In the case of an ionic headgroup, a corresponding counterion is present. Generally, surfactants are subdivided due to their hydrophilic part into anionic, cationic, nonionic and zwitterionic surfactants. The groups can be further divided regarding the functional group.^{13, 14} Examples for the four classes of surfactants are shown in Figure 1. Depending on their headgroups, the surfactant classes show different behavior and are therefore used for different applications.^{15, 16}

Anionic and nonionic surfactants are the two groups of surfactants with the largest variety and the most used one with around 90 % of the overall surfactant production.¹⁷ Anionic surfactants can be found in cleaning products, emulsifiers, and foaming agents, but their applications can be limited by external conditions. Especially, carboxylates show a high sensitivity to hard water. That is why their application is limited. The presence of electrolytes can also affect anionic surfactants. Additionally, they are often not compatible with cationic surfactants since precipitation appears.¹⁵ Nonionic surfactants are compatible with all other surfactants and show no sensitivity against hard water. Additional electrolytes do not affect their performance. For this purpose, they are widely used. But, they show a temperature dependence in their physicochemical properties, e.g., their solubility decreases with increasing temperature. Cationic surfactants are the third largest group and consist mostly of surfactants with a nitrogen-based headgroup. Their synthesis is more expensive than other surfactant groups. Their field for the application concerns mainly the adsorption on surfaces, e.g. as anticorrosion agents on steel or as antistatic agents on plastic. Due to their high toxicity, they are often used as bactericides.¹⁸ They can also be affected by the presence of electrolytes and lower their performance in the presence of anionic surfactants. Zwitterionic surfactants are the smallest class of

surfactants.^{15, 18} They are compatible with all other surfactants and are not sensitive to water hardness.¹⁵ Their structure is defined by two distinct and opposite charges on the molecule at either adjacent or non-adjacent sites. Due to their structure, they show low toxicity for eye and skin contact. Thus, they are mostly used in personal care products.¹⁹


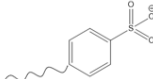


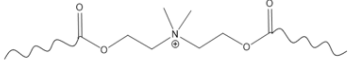
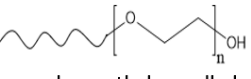
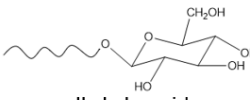
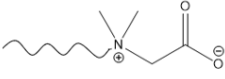
class	examples
anionic	 alkyl sulfate  alkyl benzenesulfonate  alkyl carboxylate
cationic	 quat. alkyl ammonium  alkyl ester quat
nonionic	 polyoxyethylene alcohol  alkyl glycoside
zwitterionic	 alkyl betaine

Figure 1. Classification of surfactants

The hydrophilic-lipophilic balance (HLB) value can be used as a characteristic of a nonionic surfactant. The HLB number developed by Griffin describes the relation of hydrophilic and lipophilic parts in the surfactant.²⁰ It is defined as the following:

$$\text{HLB} = 20 * \left(1 - \frac{M_l}{M}\right) \quad (\text{equation 1})$$

with the molar mass of the lipophilic part of the surfactant structure M_l and the total molecular mass M .

Surfactants with low HLB values from 0 to 10 are weakly hydrophilic and strongly lipophilic. For this purpose, they are oil soluble and suitable for W/O emulsions. Surfactants with high HLB values from 10 to 20 are weakly hydrophilic and strongly hydrophilic. Thus, they are soluble in water and used as emulsifiers in O/W emulsions.²¹

2.2 Self-assembly of surfactants in aqueous solutions

Surfactants are known for their aggregation forming a variety of different structures.²² Reason for this is their structure. Regarding their amphiphilic character in an aqueous solution, the hydration of the hydrophilic part will be energetically more favorable than the hydration of the hydrophobic part. For this purpose, the free energy of the hydrophobic part in the solution is higher than the hydrophilic part. The surfactants adsorb at interfaces to reduce the free energy. Their behavior reduces interfacial tension. Another possibility for free energy reduction is the formation of aggregates where the hydrophobic groups build an interior isolated from the outer medium and the hydrophilic parts directing to the surrounding aqueous medium. The formation of the aggregation is spontaneous. The molecules bind physically and not chemically together.¹¹

2.2.1 The packing parameter

The size and the shape of the aggregates can change with changing the parameters of the system like salt content or temperature.¹¹ Their shape can be predicted with the so-called “packing parameter” introduced by Israelachili *et al.* in 1976.²³ It is defined as the following:

$$p_p = \frac{V_t}{a l} \quad (\text{equation 2})$$

with the volume of the hydrophobic tail of the surfactant V_t , the area per molecule a and the length of the tail l .

Depending on the value of the packing parameter, the packing shape and thus the assembled structure can be predicted.²² An overview of the expected aggregate characteristics in relation to the surfactant packing parameter is shown in Figure 2. For common surfactants, the ratio of V/l is nearly constant. Consequently, the packing parameter is controlled by the value of a . The headgroup controls the aggregate structure: a decrease in the headgroup area brings p closer to a value of 1 resulting in bilayer structures; a large headgroup results in spherical micelles.










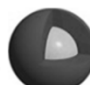
p_p	general surfactant type	expected aggregation structure		
< 0.33	single-chain surfactants with large headgroup	cone		spherical micelle 
$0.33 - 0.5$	single-chain surfactants with small headgroup	truncated cone		Cylindrical micelle 
$0.5 - 1$	double-chain surfactants with large headgroup and flexible chain	truncated cone		Vesicle, flexible bilayer 
1	double-chain surfactants with small headgroup or rigid chain	cylinder		Planar bilayer 
> 1	double-chain surfactants with small headgroup and large/bulky chain	wedge		Inverted structure 

Figure 2. Effect of the packing parameter on the packing shape and the assembled structure. The figure is based on reference ²⁴.

2.2.2 Critical micelle concentration

At very low concentrations, surfactant molecules appear as monomers in solution, which adsorb at present interfaces. The properties of an ionic surfactant are close to the ones of a strong electrolyte.¹³ At a specific concentration, the surfactant molecules start to form aggregates, mostly micelles. It is called the critical micelle concentration.²⁵

The formation of aggregates can be explained by the so-called “hydrophobic effect”.²⁶ It describes the phenomenon of aggregation by considering the interactions of the hydrophobic part of the surfactant molecule and the surrounding water. Water molecules are disturbed in their strong hydrogen bonding between each other by the addition of the surfactant. The entropy is lowered since the water molecules are hindered, and the enthalpy is increased since hydrogen bonds must be broken to get in contact with the surfactant. The formation of aggregates in the water phase with the hydrophobic parts isolated from the outer aqueous medium changes the energetic situation. The breakup of the hydrogen bonds results in a small positive enthalpy contribution. The entropy increases due to a smaller number of affected water molecules. Consequently, the free energy decreases and spontaneous formation of aggregates happens. The strength of the hydrophobic interactions responsible for aggregation is determined by several factors. It increases with decreasing temperature, increasing number of carbon atoms and increasing linearity of the tail.²⁷

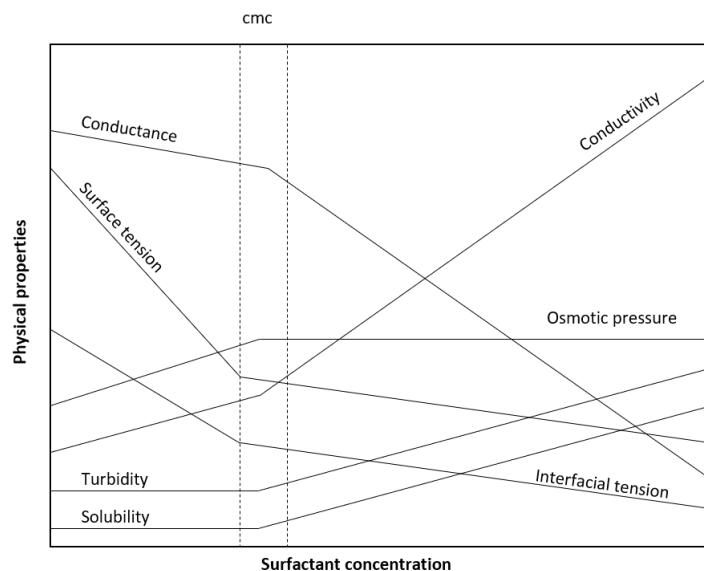


Figure 3: Schematic illustration of the dependence of different physicochemical properties of aqueous surfactant solutions on the surfactant concentration. The broken lines indicate the cmc range.

The formation of aggregates has several effects. By exceeding the critical micelle concentration (cmc), a sharp change in the physicochemical properties of the solution occurs. For this purpose, the determination of that concentration is possible with various methods. An overview of the change in physical properties as a function of the concentration of the surfactant is shown in Figure 3.

The cmc is an important characteristic for a surfactant, since most applications take advantage of micelles. For this purpose, it is useful to predict some influences on the cmc value. Some general trends can be stated:^{28, 29}

- Increasing hydrophobic chain length decreases the cmc due to the hydrophobic effect.
- Branching or double tailing increases the cmc compared to the same number of carbon atoms in a linear order.
- Ionic surfactants show higher cmc values compared to nonionic ones due to electrostatic repulsion.
- The cmc value depends on the present counterion. Stronger interactions between counterion and headgroup lower the cmc.
- Adding salt decreases the cmc values of ionic surfactants.

2.3 Surfactant solubility and Krafft temperature

The solubility of surfactants is the basic condition for any use of them. The temperature has a significant influence on the surfactant's solubility. At very low temperature, the solubility of a surfactant is very small. Figure 4 shows the solubility curve of a surfactant as a function of its concentration. The solubility increases sharply within a small area of temperature. It is called the 'Krafft phenomenon'. The 'Krafft temperature T_{Kr} ' is defined as the temperature where the solubility starts to increase. The reason is the formation of micelles indicated by the cmc line in Figure 4. Experimentally, T_{Kr} is often determined by heating up a 1 wt% surfactant solution and determine the temperature where a clear solution is observed.³⁰

The solubility of a surfactant is energetically in competition with the precipitation of the surfactant molecules. If the free energy of the crystalline state is lower, the surfactant molecules will not dissolve in solution. The free energy of the crystalline state depends on the packing effects and ionic interactions within the crystalline state. The more regular the packing in the crystalline state, the lower is its energy and thus the more favorable it is. A hindrance of this regular crystal packing of surfactants can increase the free energy and prevent early precipitation. Several different attempts are known:

- Changing the counterion: Increasing the steric of the counterion obstructs the regular packing of the crystal lattice. E.g., it has been shown by Klein et al. that the change of counterion from an alkali to a more steric choline ion increased the solubility of the surfactant significantly.^{5, 6}
- Changing the packing conditions by the introduction of branching or double bonds in the alkyl chain. The symmetry in the alkyl chain is disturbed which hinders a regular order of the chains in the solid state.
- Changing the packing conditions by the introduction of a hydrophilic group between the alkyl chain and the ionic group. Mostly ethylene oxide groups are used here. They show higher flexibility than the alkyl chains resulting in a higher entropy in the liquid phase and a hampered crystal packing in the solid phase. The effect is known for several types of surfactants like carboxylates and sulfates.^{9, 31}

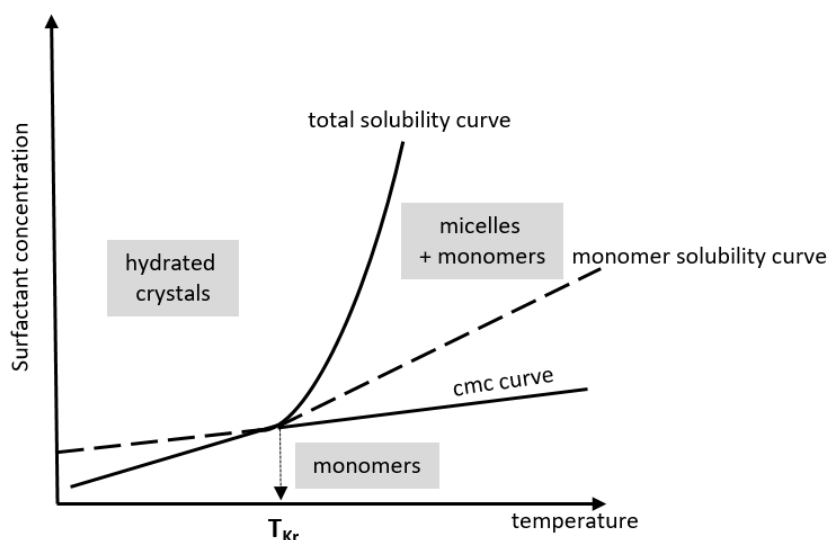


Figure 4: Temperature-dependence of the cmc, monomer solubility and total solubility of a surfactant. The intersection of the surfactant monomer solubility curve and the cmc curve defines the Krafft temperature (T_{Kr}). The figure is based on reference ³².

2.4 Adsorption of surfactants

2.4.1 Adsorption to a gas interface

Surfactants are known to adsorb on interfaces due to their amphiphilic character. The kinetics of that adsorption process is as interesting as the resulting surface tension reduction. This knowledge is of main interest in many applications such as foaming or emulsifying used in the industrial sectors of food, pharmaceuticals and oil recovery. Different influences change the ability of surfactants to move to an interface within a certain amount of time like temperature, concentration, and viscosity. But, the largest influence has the structure and the size of the molecule. They determine the ability to diffuse to and adsorb at the interface. The diffusion and the adsorption coefficient are parameters which describe these molecular properties.³³

The fact that there is a difference in the time needed for different surfactants to reach their final value of surface tension is known for a long time. It was Milner in 1907 who reported the diffusion of sodium oleate being responsible for the time dependence of its surface tension.³⁴ The work of Ward and

Tordai in 1946 set the basis of further discussions by inventing the quantitative diffusion model to describe the adsorption of surfactants at a liquid interface, as it is shown in equation 3.³⁵

$$\gamma_t = \gamma_{eq} - \frac{RT\Gamma^2}{2c} \left(\frac{D_L t_{surf}}{\pi} \right)^{0.5} \quad (\text{equation 3})$$

with the interfacial tension γ_t at surface age t_{surf} , the interfacial tension γ_{eq} of the solution in equilibrium, universal gas constant R , the temperature T , the equilibrium surface excess Γ , the concentration of the additive c and the diffusion constant D for long times/high concentrations.

The basic idea was that the transport of the surfactant to the interface is the main cause for the time dependence of the interfacial tension. The diffusion of the surfactant molecules from the bulk phase controls that transport, since the movement from the area right below the interface, the subsurface, to the interface is fast compared to the diffusion step. A constant surface area was assumed. This fact is not true for the formation of a bubble within the measurement with the maximum bubble pressure tensiometer. For this purpose, Joos and Rillaerts described the time dependence of the process of lowering the surface tension with a modified equation 4 with the assumption that the bubble remains spherical through the whole process.³⁶

$$\gamma_t = \gamma_0 - 2RTc \left(\frac{D_{eff} t_{surf}}{\pi} \right)^{0.5} \quad (\text{equation 4})$$

with the interfacial tension γ_t at surface age t_{surf} , the interfacial tension γ_0 of the pure solvent, the universal gas constant R , the temperature T , the concentration of the additive c and the effective diffusion constant D_{eff} for short times/small concentrations.

2.4.2 Adsorption to solid surfaces

The adsorption of surfactants on solid surfaces is of great interest in a lot of different fields like flotation, wetting, detergency or corrosion inhibition, since it modifies the character of the surface.³⁷ A lot of research on that topic has been done, and several mechanisms have been suggested. The origin of the adsorption of surfactants is the combination of several different forces between the adsorbed species and the solid surface. Depending on the character of the species, they can be covalent bonding, electrostatic attraction, hydrogen bonding or non-polar interactions. Additionally, lateral associative interactions, solvation, and desolvation are present.³⁸ From the energetical point

of view, a surfactant adsorbs on the solid surface, if the position at the interface is energetically favored compared to the bulk solution. It can be described with the standard free energy of adsorption ΔG^0_{ads} . It is defined as the sum of all driving forces:

$$\Delta G^0_{ads} = \Delta G^0_{elec} + \Delta G^0_{chem} + \Delta G^0_{c-c} + \Delta G^0_{c-s} + \Delta G^0_H + \Delta G^0_{H2O} + \dots \quad (\text{equation 5})$$

with the electrostatic interaction term ΔG^0_{elec} , the chemical term due to covalent bonding ΔG^0_{chem} , the free energy gained upon association of methyl groups in the hydrocarbon chain ΔG^0_{c-c} , the free energy due to interactions between the hydrocarbon chains and hydrophobic sites on the solid ΔG^0_{c-s} , the hydrogen bonding term ΔG^0_H and the term owing to dissolution or solvation of the adsorbate species or any species displaced from the interface due to adsorption ΔG^0_{H2O} .

Depending on the conditions of each surfactant-solid system, one or more of the forces mentioned earlier can be present and dominate the adsorption process. Electrostatic interactions ΔG^0_{elec} are only present in the case of ionic surfactants and a charged surface. If so, they play a crucial role in the adsorption process.³⁹ Chemical interactions ΔG^0_{chem} are present when covalent bonding is possible between the surfactant molecules and the solid and a chemisorption process can occur. It can happen in the case of precipitation of the surfactant due to the solubility limit. When surfactants adsorb on a substrate, they form two-dimensional aggregates at the interface. Here, the hydrophobic chains transfer from the aqueous medium to a hydrophobic interior of the aggregates. These aggregates are called hemi-micelles. The gain of free energy of this process is described as the driving force ΔG^0_{c-c} . The force depends on the number of $-CH_2$ groups in the surfactant structure. For adsorption on a hydrophobic surface, the hydrophobic interactions ΔG^0_{c-s} of the alkyl chain of the surfactant and the hydrophobic sites of the solid have an impact. For low concentrations, the surfactants attach to the hydrophobic surface parallel to the surface to have maximum contact. At higher concentrations, they attach vertically to the hydrophobic surface due to higher adsorption density. Hydrogen bonding ΔG^0_H can only happen if hydroxyl, phenolic, carboxylic or amine groups are present in the surfactant structure. A binding towards the solid surface is possible, if the interaction between the surfactant and the solid is stronger than the one with the surrounding water molecules. When a surfactant adsorbs, and parts of its hydration shell are removed, this is described by the desolvation energy ΔG^0_{H2O} . This is energetically unfavorable for the adsorption process.⁴⁰

An adsorption isotherm can describe the adsorption of a surfactant onto a surface. Depending on the type of surfactant, the adsorption isotherm differs and regions indicating different adsorption

processes can be seen. Depending on the shape, they are called L-type, S-type and L-S-type and are described by different models and equations. The most commonly known is the Langmuir isotherm for the L-type.⁴¹

A lot of research has been done on the topic of adsorption of surfactants. Since in commercial application generally a mixture of surfactants is used, the adsorption behavior of surfactant mixture has also been studied. Synergistic effects of mixing different types of surfactants could be observed. When regarding the mixture of anionic and cationic surfactants, the number of reported results is small because of the problematic precipitation.⁴⁰ Huang et al. studied the adsorption behavior of mixtures of anionic and cationic surfactants on silica.⁴² They found an enhanced adsorption behavior of the mixture. They assumed a formation of ion pairs as the excess adsorption of the mixture. Paria et al. investigated the adsorption of the mixture of sodium dodecylbenzenesulfonate and cetyltrimethylammonium bromide on a cellulosic surface.⁴³ They also found an increase of adsorption with the surfactant mixture and suggested the formation of ion pairs with less charge as a reason for their observation.

2.5 Toxicology and biodegradability

Surfactants are used in industrial processes as well as in the daily household. The usage in, e.g., detergents, cosmetics and in industrial processes leads to a release of the surfactants into the environment.⁴⁴ This can be harmful to organisms and whole ecosystems. The easiest way to prevent such problems is to use only non-toxic and biodegradable substances. The awareness of these problems has increased over the last decades, and the trend to replace traditional surfactants with new ones with lower toxic potential and based on natural raw materials is growing. The question of biodegradability, ecotoxicity, and cytotoxicity is highly important. There are two aspects regarding the usage of surfactant. The first is the potential danger of the components during application, e.g., the toxicity to the skin when applied in cosmetic products or the oral uptake. The second aspect is the potential danger of the components after application when they are released to the environment mostly with wastewater.

Toxicity

A lot of different tests are known to determine the toxicity of a substance. Normally, one test concentrates on one local aspect, e.g., skin irritation, or systematic effects, e.g., carcinogenicity. The toxicity of a surfactant is due to its interaction with biological structures like proteins or membranes.⁴⁵ Its intensity strongly depends on the molecular structure of the surfactant. Two aspects are important: the effect of the surfactant on the skin and the ability of the surfactant to penetrate through the skin membrane. The reason for the toxicity of surfactants on the skin is their ability to emulsify lipids which leads to a loss of moisture. The protection layer on the skin is disturbed, and chemical substances can penetrate easier through the skin. The penetration of ionic surfactants is relatively low, whereas nonionic surfactants tend to penetrate through the skin in greater numbers. But, the used amounts are in low ranges. So, they are regarded as not potentially hazardous. Regarding the molecular structure of surfactants, some general statements can be made:

- Cationic surfactants are more toxic than anionic surfactants, followed by nonionic surfactants.
- For an anionic surfactant, a saturated linear alkyl chain with a chain length of 10 to 12 carbon atoms has the highest potential of damage.⁴⁶
- Alkyl ether sulfates are less irritant than alkyl sulfates.⁴⁷

Ecotoxicity

Surfactants are released into the environment mainly through waste water. For this purpose, the toxicity of the surfactants against water organisms is of greatest interest. Many standardized tests are known to examine the aquatic toxicity of surfactants.⁴⁸ The LC/EC (median lethal or effect concentration) values are used to evaluate the results of acute toxicity tests. The tests are performed for 24, 48 or 96 h. The corresponding values are the LC/EC 0, 50 and 100 value. They describe the highest concentration for which no organism is dead/affected, the concentration which is expected to cause death/effects in 50 % of the organisms and the lowest concentration for which all organisms are dead/affected. Regarding the environmental aspect of cationic surfactants, their high tendency to adsorb on a variety of materials like natural sediments and soils is a problem.⁴⁹ The process is found to be mainly a process of ion exchange.⁵⁰ Adsorption on materials can prevent their biodegradation, and longer exposure to the environment is the consequence. Cationic surfactants are known to be toxic to aquatic organisms in the range of milligram per liter and for higher plants.

Biodegradability

When a surfactant is discharged into the environment, biodegradation is the only way to destruct the substance and remove it completely from the environment. It can be distinguished between primary and ultimate degradation. A degradation to a step where the surfactant has lost its surfactant properties is called primary degradation. It decreases undesired properties like foaming as well as the aqua toxicity. When the surfactant is converted to CO₂, H₂O, biomass and inorganic ions, the process is called ultimate degradation.⁵¹ Two structures, which appear in the environment due to their high usage, are the linear alkylbenzene sulfonates (LAS) and the alkyl phenol ethoxylates (APE). The commercially used anionic LAS is regarded as biodegradable under aerobic conditions. The degradation of the straight alkyl chain, the sulfonate group, and the benzene ring is necessary.⁵² APE is less biodegradable. Cationic surfactants are known to have a low biodegradability. Since they are known to stick closely to a variety of materials, fast biodegradation would be of high interest. Van Ginkel suggested an aerobic degradation for quaternary ammonium salts.⁵³ An anaerobic degradation is not known. Reason can be that appropriate metabolic pathways are not available and/or a possible toxic effect of the surfactant upon the relevant anaerobic microorganisms.⁵¹

2.6 Ethylene oxide groups in the surfactant structure

Ethylene oxide (further called EO) is a structural part which is present in different amounts in a lot of different molecules.⁵⁴ Its chemical structure is shown in Figure 5. Polyethylene oxide in its pure structure is known as a liquid for molecules with low molar mass and as solid for molecules with higher molar mass.⁵⁵ It is used in a variety of applications.⁵⁴ But, adducts based on ethylene oxide have gained nearly the same importance. EO as a structural element is, e.g., present in several surfactant structures. The most commonly known surfactant group are the nonionic surfactants where they are used as a hydrophilic headgroup in the surfactant structure.

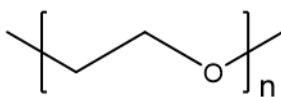


Figure 5: Chemical structure of an ethylene oxide (EO) group in a surfactant structure.

The insertion of an EO group has several consequences on the molecular properties. The EO units affect the area of the headgroup, and as a consequence, the packing parameter p .⁵⁶ EO moieties lead to lower charge intensity for the hydrophilic part of the surfactant. Both aspects can effectively decrease the electrostatic interactions between the surfactant molecules.⁵⁷ It was among others reported by Minero *et al.*. He stated that the EO moieties influence the dispersing of the charges in the headgroup. Consequently, the electrostatic repulsion is weakened.⁵⁸ With an increasing number of EO groups, the linear structure of the alkyl chain is less distinctive and stiff. The conformation of the molecule changes and larger steric hindrance is the result.⁵⁹ Comparing an alkyl carbon chain with an EO chain, the situation of hydration differs. The oxygen atom within the alkyl chain increases the polarity and can interact via hydrogen bonding with the surrounding water molecules. Stronger hydration for the EO chain is the consequence. Both, the higher steric hindrance and the higher hydration, influences the solubility and the interfacial activity.

Several studies were performed to investigate the influence of EO groups in surface-active substances. Hato *et al.* found that with an increasing number of EO groups, the surface activity was enhanced and the Krafft point was diminished.⁶⁰ Masuyama *et al.* examined a series of double-chain diols regarding the surface pressure-area isotherms. They found that the introduction of EO moieties made the hydrophobic chain of the surfactant more flexible, resulting in improved surface activity.⁶¹ It can also be named as the reason for the observation of Chen *et al.* who found that precipitation can be overcome by introducing EO moieties into the hydrophobic chain of some anionic or cationic surfactant molecules.⁶² Also, Cui *et al.* confirmed that the introduction of a poly(oxyethylene) separator between the hydrophobic part and the polar head of an anionic surfactant molecule could greatly improve the solubility of anionic/cationic complexes.⁶³ Li and Zhao argued in the same way when investigating 1:1 mixtures of anionic-cationic surfactant systems.⁶⁴

The effect of the presence of EO groups concerning the interfacial tension against hydrocarbons in the molecular structure of fatty acid methyl esters was investigated by Liu *et al.*⁶⁵ They confirmed an increasing solubility with an increasing number of EO groups. Moreover, they found a decrease in interfacial tension with an increasing number of EO groups and explained it with the enhancement of the interfacial hydrophobic interactions and the rearrangement of interfacial surfactant molecules. The influence of EO groups in polyelectrolyte–surfactant complexes was examined by Vleugels *et al.*⁶⁶ They varied the number of EO groups in the ionic surfactant sodium lauryl ether sulfate with two polycations and investigated the complexation behavior. They found influence on the stiffness of the

corresponding polycation. Zhan *et al.* reported on the influence of EO moieties on the microstructure of the mixture of cationic surfactant cetyltrimethyl ammonium bromide and anionic–nonionic carboxylate surfactants. An influence on the head-group areas and steric hindrance was found, which affect the arrangement of the surfactant molecules.⁶⁷

3 Physicochemical characterization of new catanionic combinations

3.1 Introduction

Surfactants are known and used in a broad variety of different applications for a long time. In general, they are classified according to their headgroup into anionic, cationic, nonionic and zwitterionic surfactants. They can either be used in pure form, meaning only one type of surfactant or as a mixture of different surfactants, also differing in their headgroup. When combined in a mixture of two or more different surfactants, they often show improved properties compared to the pure surfactants. This synergistic effect increases with the degree of charge difference between them. A problem is the very low solubility of the mixture.⁶⁸ Mixtures of different surfactants are often used in household and industrial application. The combination of anionic and nonionic surfactants is used the most. It can be found in a lot of formulations like detergents, personal care products or enhanced oil recovery.⁶⁹ Although the mixture of anion and cation should show the biggest synergistic effects, it is less commonly found in the industry, because of their low solubility around equimolar ratio. Application at higher concentrations is a problem. But, they are known to show extraordinary properties regarding several physical and chemical properties. For this purpose, research on the group of catanionic surfactants is growing over the last years.

In several investigations, different approaches for solving the problem of low solubility have been found. The concept of mixing a cationic and an anionic surfactant, resulting in a soluble so-called pseudo-nonionic surfactant ion pair was first introduced by Mehreteab *et al.*⁵⁷ They investigated the system of tetradecyltrimethylammonium bromide and an organic alkylpoly (oxyethylene) sulfate. They concluded that the insertion of additional water solubilizing groups within the surfactant structure could prevent precipitation. This hypothesis could be confirmed in several experiments. Anionic surfactants with additional water solubilizing groups are known and their higher solubility compared to the equivalent surfactant without water-soluble groups could be proven. Moreover, modifying the linear surfactant structure to a more branched hydrophobic structure showed the same effect.⁶⁸

Until now, the additional water solubilizing groups are only used in anionic surfactants. Alkyl ether sulfates and alkyl ether carboxylates are produced in large quantities by several companies like BASF

and Kao Chemicals. The question arises why this is only done on one-half of the available surfactants. The same would be possible on the cation side. Here, the modification in the structure is only based on the change in the structure by increasing the size of the headgroup or the hydrophobic part by branched chains. The insertion of a water solubilizing group like, e.g. an EO is not reported. Within this work, the focus will be on this topic. Within cooperation with BASF, new cationic surfactant structures based on an alkyl ether structure are synthesized. They are combined with anions which are partly on the market and partly also self-synthesized. They were investigated regarding their physicochemical properties and their potential for application. The focus is on the effect of the EO groups which are used as aid for higher solubility.

3.2 Fundamental information on catanionics

3.2.1 Classification and properties

The term 'catanionic' itself already describes the group of surfactants the best. Catanionic mixtures are defined as a mixture of a cationic and an anionic surfactant. The ratio between anion and cation can vary and has a great influence on the property of the mixture. A differentiation between 'true catanionic' and 'catanionic with excess salt' can be made. In true catanionic mixtures, the original counterions are not present. They are salt-free. They are removed after mixing the two surfactants, e.g. by dialysis.⁷⁰ Another possibility is the preparation of the catanionic mixture by neutralization. Here the counterions H^+ and OH^- react to the neutral molecule H_2O . If this is not the case and the corresponding counterions are still present in the catanionic mixture, it is described as a catanionic mixture with excess salt. Depending on the used raw materials, catanionic mixtures can be distinguished into three different cases:⁷¹

- a four-component-five species system where the two surfactants, the two counterions, and the solvent water is present
- a three-component system where the two surfactants and water are present. The two counterions H^+ and OH^- have reacted to water or have been removed.
- a catanionic system based on an alkyl amine oxide and a fatty acid. The proton from the organic base can transfer to the weak base oxide.

The preparation of catanionic mixtures is easy. The simple mixing of the two surfactant solutions is enough. When the two different charges are mixed, strong electrostatic attractions lead to a tight ion pair. Hydration water is removed from the interface at the mixed aggregate/solution interface. The resulting ion pair can be described as a pseudo-nonionic or a pseudo-double-tailed zwitterionic surfactant.⁷² Due to the two oppositely charged headgroups, they show several unique features. The most important aspects concerning catanionic mixtures are:

- Strong electrostatic attractions between the two headgroups leading to the formation of an ion pair
- Synergistic properties and solution behavior compared to the single surfactants
- Dependence of these properties on the molar ratio and the concentration
- Variety of different structures different in shape and size

- Spontaneous formation of vesicles
- Precipitation around equimolar ratio

The strongest synergistic effect of catanionic mixtures can be observed in high surface activity, enhanced adsorption, and low critical aggregation concentration. This has a great influence on the adsorption properties and the self-assembling.

A lot of different types of catanionic combinations have been investigated. The combination of two monomeric surfactants was the starting point and is still of great interest. The group of Thomas Zemb made deep investigations on the system of myristic acid and trimethyl alkyl ammonium and found a variety of different aggregations for this catanionic mixture.^{73, 74} The interest on catanionic combinations built of oligomeric surfactants increased in the last decades. They consist of two or more amphiphilic moieties which are linked at the headgroup with a spacer group. Reason for this is the fact that they show even more superior properties than the corresponding monomeric ones. The most investigated mixture is the one with bis-quaternary ammonium salts and the alkyl spacers in between.⁶⁸ This increases the solubility of the mixtures, and in the phase diagram, large areas of vesicle formation are observed due to their high asymmetry in the molecule structure. Another interesting mixture of catanionic is the mixture of surface-active ionic liquids. The combination of ionic liquid character and amphiphiles can be interesting. They show a high tendency to self-assemble and high surface activity. The mixture of imidazolium-based cations are the most investigated ones.⁷⁵

Forming catanionic mixtures with biologically active molecules and surfactants is another interesting field of research on catanionic mixtures. Either the anion or the cation can be a drug. For example, the catanionic combination with ibuprofen and 1-dodecyl-3-methylimidazolium chloride is studied by Sanan *et al.* Vesicle structures are formed which can have superior properties, e.g. regarding drug release in the body, compared to the pure drug. Another interesting group of catanionic mixtures is based on sugars. Menger *et al.* published the first example of a water-soluble catanionic surfactant based on a glycosidic amphiphile. The cation hexadecyltrimethylammonium ion was combined with glucuronate counterions. Also, Isabelle Rico-Lattes and her co-workers did a lot of research about sugar-based catanionic mixtures focusing mainly on the biocompatibility for pharmaceutical applications.^{76, 77}

3.2.2 Aggregation behavior

Catanionic mixtures show interesting phase behavior dominated by different interactions like electrostatic and hydrophobic interactions, steric effects and hydrogen bonding. The big advantage of catanionic mixtures is the possibility to control these interactions by changing the surfactant molecule and structure and thus changing the bulk properties.⁶⁸

When the two oppositely charged surfactants get in contact, they strongly interact by forming a tightly packed ion pair as it is schematically depicted in Figure 6. The ion pair can act as a pseudo-nonionic surfactant. The result of the formation of this tightly packed ion pair is a lower effective headgroup area compared to the value of each surfactant alone. Meanwhile, the volume of the hydrophobic part increases. Regarding the packing parameter p , the value comes closer to unity. For a packing parameter $p \approx 1$, structures of low curvature like vesicles and flexible bilayers are favorable.⁷⁸ For this purpose, spontaneous formation of vesicles in catanionic mixtures with long-term stability can occur in catanionic mixtures. This is of high interest since it can be used in several applications, e.g. in pharmaceutical formulations. They can be an alternative to phospholipid vesicles. It was Kaler *et al.* in 1989 who reported about the spontaneous formation of vesicles in aqueous mixtures of single tiled surfactants the first time.⁷⁹ They investigated aqueous mixtures of cetyl trimethylammonium tosylate and sodium dodecylbenzene sulfonate and observed vesicle formation. By varying the ratio of anionic to cationic surfactant, vesicle size, surface charge, and permeability could be changed.

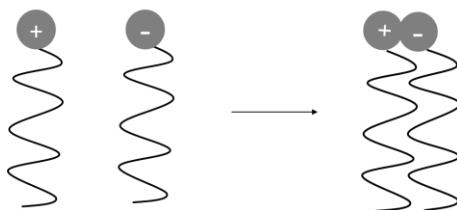


Figure 6: Formation of an ion pair of two oppositely charged ionic surfactants as it is the case for catanionic surfactants.

Regarding a typical phase diagram of a catanionic mixture, vesicles can be found in two lobes in the high diluted region, as it can be seen in Figure 7. As the position of the lobes indicates, vesicles are stabilized by the excess of one surfactant. By changing the molecular structure of the catanionic mixture, the region of vesicle formation can be modified. By changing external parameters like temperature or salt content, the size and shape of the aggregation structures can be varied. The

transition from one structure to another is of interest in several applications such as drug delivery. Research on different pathways in the phase diagram, especially regarding structural transitions, have been studied.

Around equimolarity of the two ions, a region of precipitation occurs. Reason for that is the strong electrostatic attraction of the oppositely charged surfactants. This is the main disadvantage of catanionic mixtures and the reason why they are only rarely used because it often leads to precipitation. By modifying the structure of the surfactants, the tendency to precipitate can be lowered. An increase in asymmetry of the hydrophobic part was reported by Jurasin *et al.* to be a possibility to prevent precipitation. By this, the hydrophobic attractions are weakened, and an efficient packing into a crystalline lattice is not possible.⁸⁰ Another approach is the use of additional water solubilizing groups within the molecule structure like EO groups.⁵⁷ Both approaches are possible and have proven to be a successful way to prevent precipitation. This is a precondition for any application.

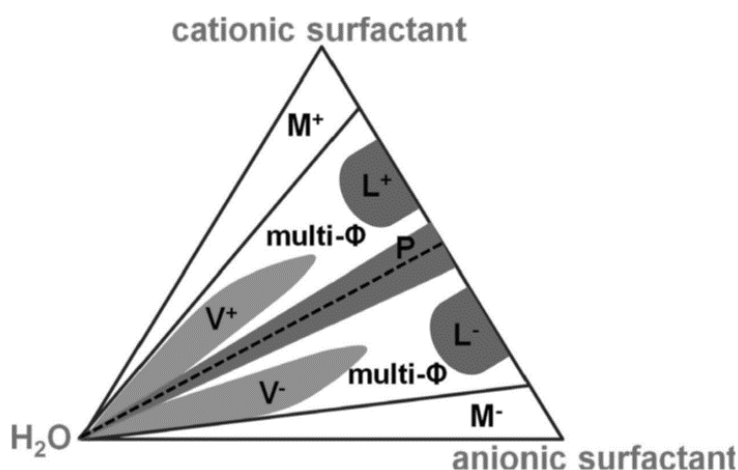


Figure 7: A schematic triangular phase diagram of the symmetric catanionic mixture at constant temperature and pressure. The dashed line denotes the equimolar line dividing the diagram into the cationic-rich and the anionic-rich region. Close to the charge neutrality line, a solid precipitate (*P*) is usually formed, but excess charge in the system usually leads to vesicle stabilization (denoted as *V*⁺ and *V*[−]). Mixed micelles (denoted as *M*⁺ and *M*[−]) are usually formed at the highest excess of the mixture components. Multiphase regions (*multi-Φ*) often involve a lamellar phase occurring at higher concentrations (denoted as *L*⁺ and *L*[−]). The figure is taken from reference ⁶⁸.

Besides vesicles, a variety of different aggregation forms are reported for catanionic mixtures in literature. Zemb *et al.* introduced self-assembled flat nanodiscs of the salt-free catanionic solutions of myristic acid and the hydroxide-exchanged form of cetyltrimethylammonium chloride.⁸¹ As

counterions, H^+ and OH^- were necessary as well as an excess of the cationic component. The diameter could be controlled to a constant size of 30 nm. In the same group, Dubois *et al.* found aggregates in salt-free catanionic solutions of the form of regular hollow icosahedra with the size of about one micrometer. The catanionic mixture was again cetyltrimethylammonium hydroxide and myristic acid. With the described method and the described conditions, icosahedra of the same size result.⁸²

3.2.3 Application

Unique properties and the control and change of them by changing the molecular structure are the main advantages of catanionic mixtures. Since it is possible to prevent strong precipitation by modifying the molecular structure, the field of application of catanionic mixtures has grown.

Especially in pharmaceuticals, their tendency to form vesicles is of interest since they mimic biological membranes. Moreover, they can be used as drug carriers and targeted drug delivery systems.⁸³ Vesicles can transport different species to cells. By tuning their physical state, the drug release can be controlled. Liposomes, natural polar lipids, are the most used substances for vesicle formations. But, their low stability against chemical degradation by hydrolysis and peroxidation is a problem. Here, catanionic vesicle can be a promising alternative. But until now, several problems like low encapsulation efficiency and permeability remain to be solved. One possibility would be the formation of vesicles where one ion is the amphiphilic drug.⁸⁴

Another field of application is the synthesis of advanced materials. Self-assembled aggregates are interesting in the preparation of new materials. Vesicles are often used as templates since their special structure allows reaction in four different environments within one solution: the bulk solution outside the vesicle, the inner part of the vesicle, the outside surface of the vesicle and the hydrophobic palisade layer of the vesicles.⁸⁵ Different inorganic materials have been synthesized with vesicle templates. Silica spheres were investigated by a lot of different groups. For example, Yuan *et al.* used long-chain imidazolium ionic liquid 1-dodecyl-3-methylimidazolium bromide and sodium dodecyl sulfate as a template for hollow silica spheres.⁸⁶

The application of catanionic mixtures for analytical methods is a rather young field of research but showed promising results. Again, the structuring of the catanionic mixtures is the crucial aspect. Selective capture and separation of oppositely charged solutes from a mixture of several solutes is

possible with charged vesicles. The charge can be controlled by the ratio of anionic and cationic surfactant.⁸⁷ Catanionic mixtures could also be successfully tested in a novel microextraction system by Kahe et al. A microextraction of various organic and inorganic compounds of real samples is described as a simple, safe, fast and low-cost technique.⁸⁸

Catanionic mixtures have also been investigated regarding their behavior of corrosion inhibition. Javadian et al. showed a positive effect of the catanionic mixture compared to the pure surfactant regarding the protective effects on a metal surface.⁸⁹ The strong adsorption on the metal surface enhances the formation of a protective surfactant film.⁶⁸

3.3 Results and discussion

The first point of interest was to gain a fundamental understanding of the influence of the insertion of one or more ethylene oxide (further called EO) groups into the anionic as well as into the cationic surfactant regarding several different physicochemical properties. The focus was on the positive effect of combining a cationic with an anionic surfactant on diverse properties. Kindly provided by BASF, several newly synthesized surfactants based on that idea were combined for that purpose. An overview of the compounds can be seen in Figure 10. The complete purification and desalination of the combinations would have been highly time-consuming or high quantity of the scantily present synthesized products would be required. Both was not possible and would not have been a realistic approach either, since applications with salt-free components are rare. For this purpose, the present counterions, sodium for the anionic surfactant and chloride for the cationic surfactant, were left in the investigated combinations. The nomenclature of the substances does not include the counterions, although they were always present. The compounds were named the same way. A schematic explanation is given in Figure 8.

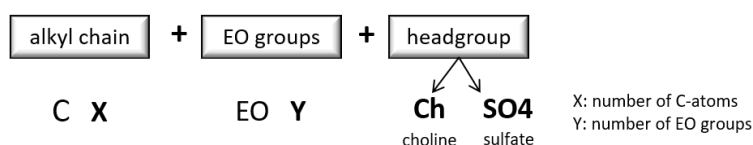


Figure 8: A schematic explanation for the nomenclature of the investigated compounds.

To have the possibility to compare the different substances with each other regarding only certain structural aspects, they were built up of the same basic molecule structure (see Figure 9). The cations contained a quarternium ammonium headgroup with three methyl groups. One long-chain alkyl tail of 12 carbon atoms was the hydrophobic part. The cations were all based on the structure of choline, which is known as a nutrient.⁴ Its structure is shown in Figure 9. It can be used to build biocompatible and highly water-soluble surfactant combinations.⁶ To the basic choline structure, a different number of EO groups and an alkyl chain were added. The idea was to combine the high solubility of choline, the positive effect of EO groups⁷ and the amphiphilic character due to a longer hydrophobic alkyl chain. The same chain of thought was applied to the anionic surfactant part. The basic anion structure consisted of a sulfate headgroup and one long-chain alkyl chain as hydrophobic part. Contrary to

cationic surfactants, for anionic surfactants, the basic structure with EO groups already exists. The commercially available Texapon N70® from BASF, which was one of the five anionic surfactants used in this study, was the inspiration for further derivatives.

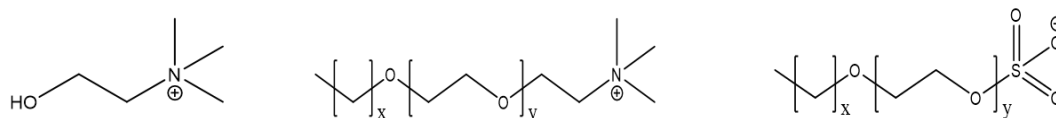


Figure 9: Chemical structure of choline (left), the basic structure of the choline derivatives (middle) and the SDS derivatives (right).

The selection of the surfactants was driven by several different aspects. First interest was the importance of the presence of EO groups. For this purpose, the commercial anion sodium dodecyl sulfate, further called SDS, and the commercial cation cetyl ammonium chloride, Dehyquart A-CA, further called ACA, were included as references into the surfactant scheme. The second interest was the effect of the number of EO groups within one ion side. For this purpose, at least two different amounts of EO groups were built into the basic anionic and cationic surfactant system. For the cationic surfactants, one and four EO groups were inserted. In the anionic counterpart, the commercially used Texapon N70, further called Tex, was used as an example for 2.5 EO groups and a C12 chain length. Anionic surfactants with four and six EO groups were synthesized. The third interest was the influence of the alkyl chain length. An anionic surfactant with an alkyl chain length of 18 was synthesized for comparison to the anionic surfactant with an alkyl chain length of 12. Different synthesis procedures were performed within the time of this thesis. The result was a slight difference in the structure of the cation. The cationic compound with one EO group was synthesized with an epoxide as starting material. Due to this, an additional hydroxy group was present in the molecule structure. It will be not considered in the following. This was not the case for the cationic surfactant with four EO groups. During the time of this thesis, the cationic surfactant C16EO1Ch was also synthesized. It was additionally investigated if the chain length on the cation side was an interesting factor.

In Figure 10, the scheme including the structure of the surfactants is depicted. It goes towards a higher amount of EO groups when going from the upper part to the lower part and when going from left to right. To see all different influences, especially the influence of the modification of the anionic

surfactant while keeping the cationic surfactant constant and vice versa, the combinations of all anions with all cations were investigated regarding the different properties. The commonly known combination of SDS and ACA at the top left could be regarded as the reference system. This combination has already been investigated in several studies⁹⁰⁻⁹² and symbolizes the “worst case”, meaning it contains no EO group. The potential flexibility due to this structural part within the molecule structure is at its minimum. Going from the upper left corner to the corner on the right bottom, the presence and the influence of the EO groups are more pronounced.

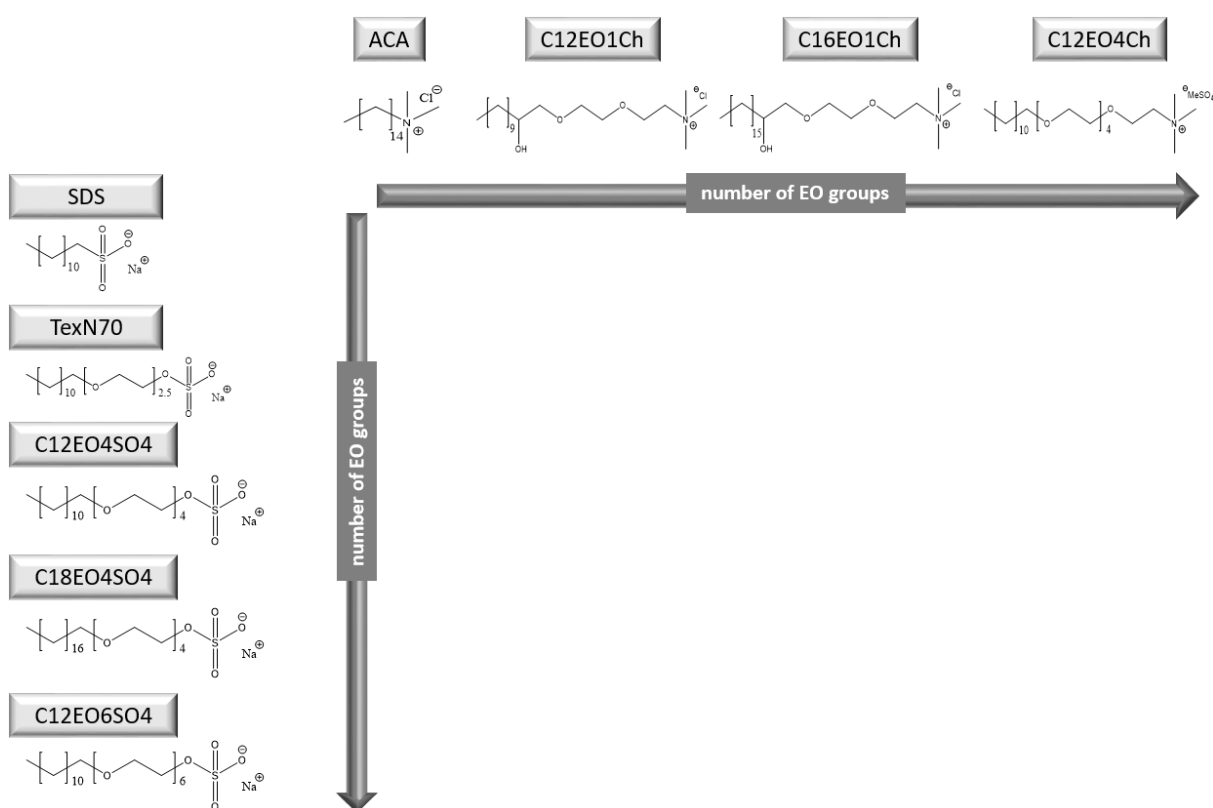


Figure 10: Overview of the investigated anionic surfactants and cationic surfactants. Cations are depicted on the horizontal line, and anions are shown on the vertical line.

Because several physical parameters could be varied during the measurement of the catanionic combinations, the following parameters were kept constant for the basic characterization:

- mass ratio anion-cation: for most investigations, under the condition that time needs were not outstandingly high, the ratios 0-10, 1-9, 2-8, 3-7, 4-6, 5-5, 6-4, 7-3, 8-2, 9-1 and 10-0 about mass percentage were investigated. The first number always related to the amount of anion, whereas the second number described the amount of cation.
- temperature: considering the general effort of lowering the energy requirement, chemical properties around room temperature were most interesting. For this purpose, for all experiments, if not mentioned otherwise, room temperature (25 °C) was set.
- pH value: the pH value was not adjusted for every single measurement, since the first tests did not show a significant dependence of the properties on the pH in case of the sulfate headgroup. The pH values ranged from around 5 to 7.
- concentration: if not written otherwise, the concentration was set to 0.1 wt% for all measurements. Using this value, it was ensured to be above the critical micellar concentration (see 3.3.2). In several investigations, when it came to concentration dependence, the value was varied, as it will be described in the corresponding section.
- water hardness: for standard characterization, the investigated compounds were solubilized in millipore water without any further additives, if not mentioned otherwise.

3.3.1 Solubility in water

One of the main intentions of changing the surfactant structure was the change in the interactions between the combined surfactant ions. An EO group within in the structure increases the flexibility of the alkyl chain.^{59, 61} If the alkyl chain is more flexible, they will not arrange completely linearly to each other. Consequently, the van der Waals interactions are lower between them compared to when they are packed closer together. Weaker interactions result in a lower tendency to precipitate. The solubility of the catanionic combinations increases.⁶³ Furthermore, the hydration situation changes with EO groups present. Hydration of an oxygen atom is significant compared to a carbon atom in an alkyl chain. More water molecules will orientate around the oxygen atom. It also leads to stronger isolation of the chain to other chains.

The first step for all catanionic combination was the investigation of their solubility at the concentration of 0.1 wt%. The two stock solutions of anionic and cationic surfactant were mixed in the appropriate ratio, and a simple optical evaluation was performed after a certain time. One week

was set as the time scale at which the determination of the samples was made. For all samples, photos were taken in front of a black background. So, turbidity could already be observed when only slightly present. An overview of the results is shown in Figure 11. The ratio of equimolarity calculated via their molar mass is indicated by a yellow stroke in the pictures.

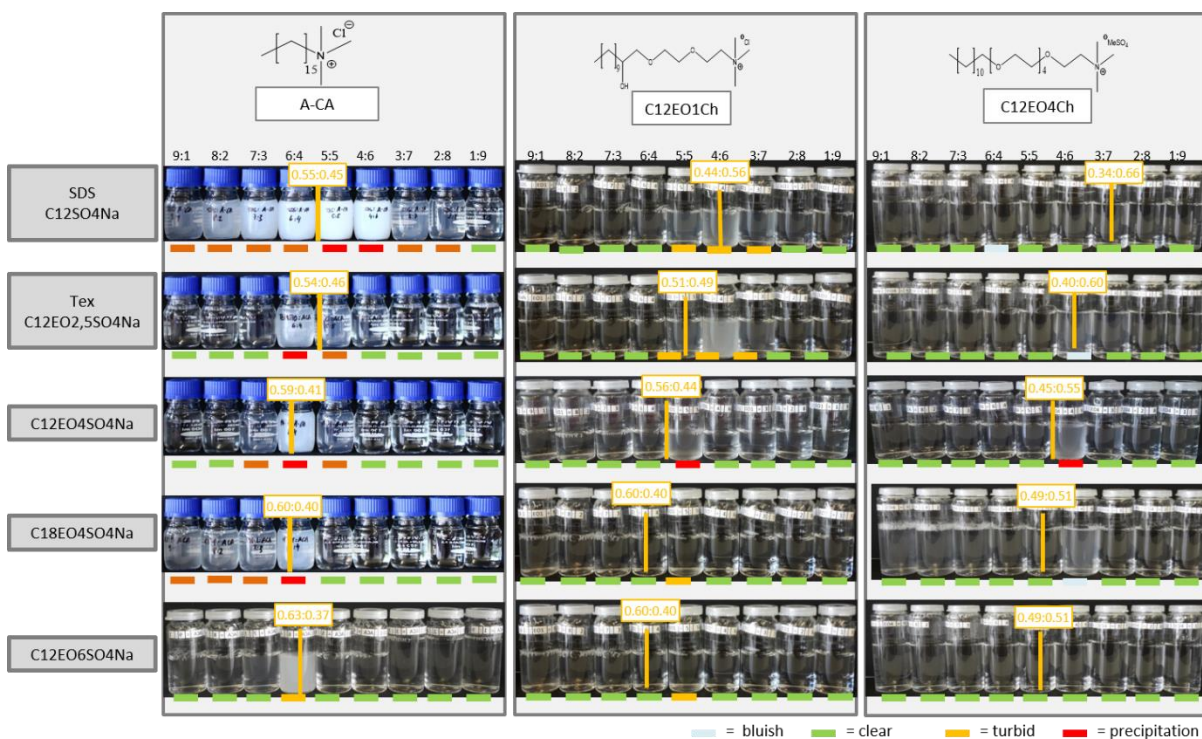


Figure 11: Optical evaluation of the solubility of the catanionic mixtures at a total surfactant concentration of 1 g/L in the anion-cation mass ratio 9-1 to 1-9 wt% after one week evaluated by eye; distinction was made into a clear solution with bluish glimmer (light blue), complete clear solution (green), turbid solution without precipitation (orange) and precipitation in the solution (red); the equimolar ratio is given in the yellow box respectively.

In Figure 11, several observations can be made. In general, the turbidity decreased from the pictures on the left to the right. The same trend was observed from the pictures above to pictures below. It confirmed the desired strategy towards a non-precipitation with the increase of EO groups within the molecule structure. The most critical range is the one near equimolar ratio. Here, the electrostatic interactions are the most dominant ones and together with the interactions between the alkyl chains, they can lead to precipitation. This phenomenon was less pronounced for combinations with a higher

amount of EO groups in the structure. The commonly known phenomenon of precipitation when combining a commercial anionic and cationic surfactant could be seen in the picture top left. Here, SDS and ACA were combined. Precipitation was observed for all samples, except for the ones with a maximal excess of ACA. Especially at ratios around equimolarity, precipitation occurred within seconds. The attraction forces between the molecules leading to precipitation were too strong to keep the mixture in solution. For all combinations with ACA, turbidity, mostly already precipitation, was observed after one week. So, the presence of EO groups only in the anionic surfactant seemed not to be enough to lead to a clear solution, which corresponds to complete solubility. On the lower right, completely clear solutions could be observed at all investigated ratios. The same was obtained for several combinations with C12EO1Ch. Comparing the two cationic surfactants containing EO groups, it could be assumed that the insertion of one EO group seemed to have already a significant impact on the solubility behavior. It appeared to be enough to increase the solubility enormously. Within the series of anionic surfactants, the changing structure seemed not to be a crucial factor. Already for the combinations with SDS, a significant increase in solubility was observed for both cationic surfactants. A decisive influence of the cation was also observed in combination with the anionic surfactant C18EO4SO4. Due to the longer alkyl chain, the solubility of the pure anionic surfactant was small at room temperature (see Figure 11). This is expected since a longer hydrophobic chain increases the Krafft temperature.^{47, 93} The combination with ACA showed no improvement. The ratios with an excess of anionic surfactant were turbid. At equimolar ratio, precipitation was observed. When combining the anionic with the new cationic surfactants, the situation changed. A significant increase of solubility was observable. The addition of the cationic surfactant brought the anionic surfactant into solution. Especially with C12EO4Ch, all samples were completely soluble. This confirmed the suggested hypothesis above. The EO groups within the cationic surfactant act as a solubilizer for the C18 alkyl chain in the anion. The effect of EO groups is also known from the TOTO anion. Long-chain quaternary ammonium cationic surfactants in combination with the TOTO anion form ion pairs with low melting points, due to the flexible character of the anion structure.⁹⁴

So far, only a qualitative impression was the criteria of evaluation. To confirm the observations quantitatively, the total carbon (TC) content in the solution of the samples was determined and correlated to the amount of carbon corresponding to 100 % dissolution as described in 3.5.2.1. The percentage of dissolved catanionic surfactants is shown in Figure 12. The TC measurements confirmed the observations from Figure 11. The same trends were observed. Nearly a complete dissolution of the catanionic compounds could be found for the cationic surfactant with the highest amount of EO

groups. TC confirmed the observation that the addition of this cationic surfactant helps to dissolve the non-soluble anionic surfactant C18EO4SO4. ACA showed precipitation at least at equimolar ratio for nearly all anions indicated by lower solubility values in Figure 12. For SDS together with ACA, the curve showed low solubility, as expected. The anionic surfactants with EO groups present but with an all in all shorter alkyl chain, Tex and C12EO4SO4, could form a catanionic combination that was more soluble compared to the one with the all in all longer alkyl chain, C18EO4SO4 and C12EO6SO4. Here, the effect of the overall chain length and the corresponding attraction forces seemed to dominate. In the case of C12EO6SO4, the effect of higher flexibility due to the EO groups could not compensate the attraction forces between the two molecules. In general, the solubility data showed that on the anionic surfactant side as well as on the cationic surfactant side, an EO group seemed to have a positive effect for solubilizing the catanionic compound at the investigated concentration of 0.1 wt%.

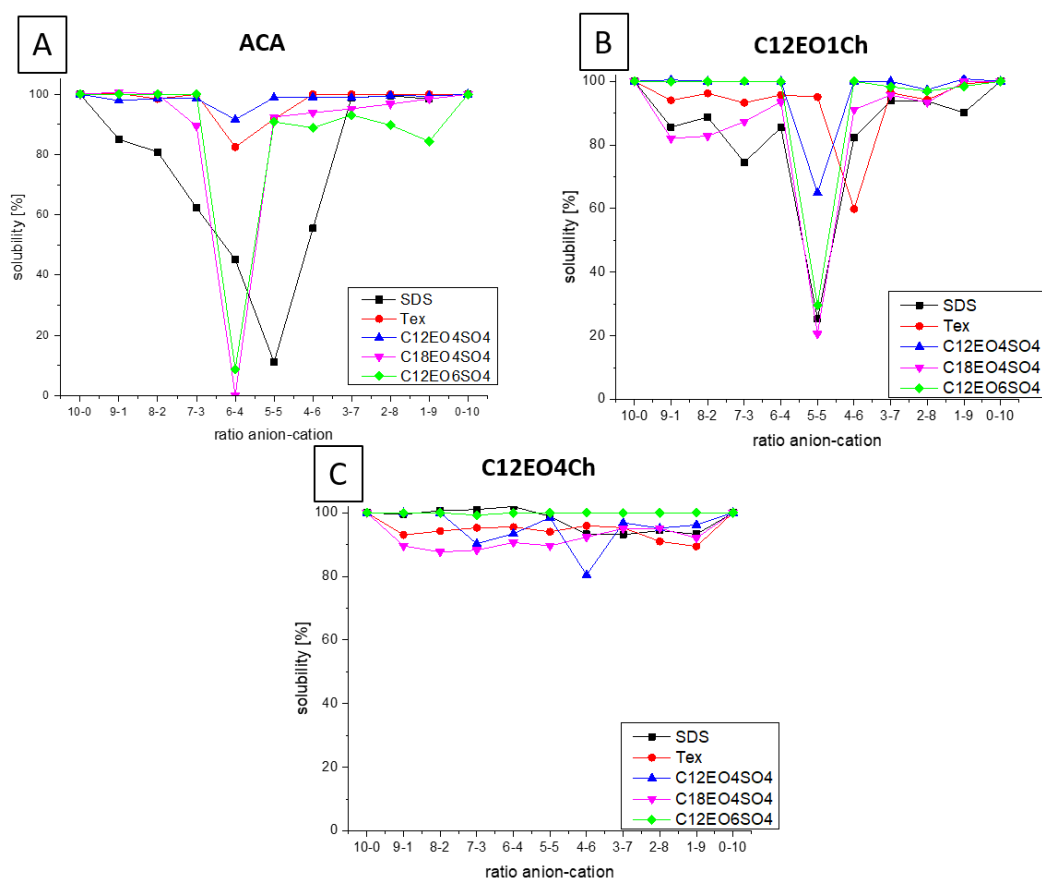


Figure 12: Results of the solubility measurements via Total Carbon determination as described in 3.5.2.1 in percentage of the catanionic combinations of the five anionic surfactants (SDS (black), Tex (red), C12EO4SO4 (blue), C18EO4SO4 (purple) and C12EO6SO4 (green)) and the cationic surfactants ACA (A), C12EO1Ch (B) and C12EO4Ch (C) at a total surfactant concentration of 1 g/L.

3.3.2 Critical micelle concentration

The critical micelle concentration (cmc) is an important property to describe the efficiency of a surfactant.⁹⁵ The property of forming micelles is essential for several applications like detergency⁹⁶ or emulsions.³ The lower the cmc value of a surfactant, the less amount is necessary. This is favorable regarding saving resources.¹ Thus, the determination of the critical micelle concentration was performed for the catanionic mixtures as described in 3.5.2.2. For the three ratios 8-2, 5-5 and 2-8 of anionic and cationic surfactant, the cmc values are exemplarily measured and compared to the pure surfactants. The results are depicted in Figure 13.

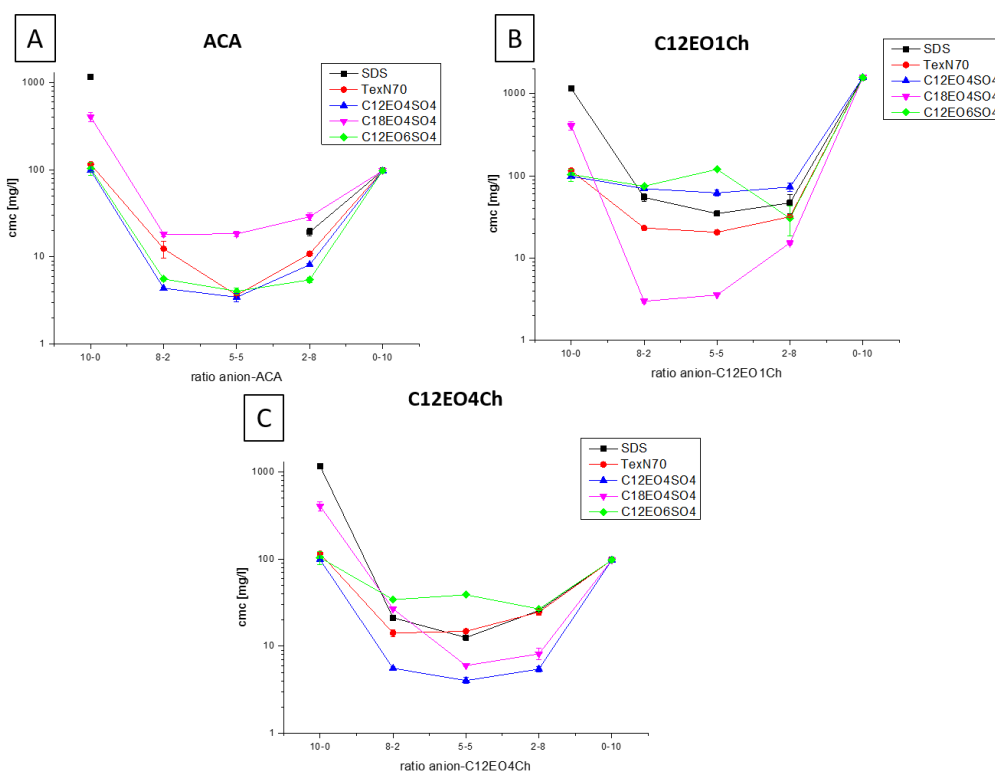


Figure 13: Results of the cmc determination as described in 3.5.2.2 in percentage of the catanionic combinations of the five anionic surfactants (SDS (black), Tex (red), C12EO4SO4 (blue), C18EO4SO4 (purple) and C12EO6SO4 (green)) and the cationic surfactants ACA (A), C12EO1Ch (B) and C12EO4Ch (C) at 25°.

For all investigated catanionic mixtures, a synergistic effect could be observed. The cmc values of the mixtures were significantly lower than the ones of the pure ionic surfactants. The cmc values for the

mixtures ranged from several mg/L to 20 mg/L, whereas the pure surfactants were around 100 mg/L or even higher. Depending on the cationic surfactant, the most efficient combination varied. The largest difference could be observed for the anionic surfactant C18EO4SO4. From the theoretical point, the surfactant with the longer alkyl chain should have a lower cmc value.^{1, 16, 97} But, a complete solubility of the substance is necessary for that. This was not completely given for the combination with ACA. If the molecules are not completely dissolved in the aqueous phase, they cannot act in a maximal extent. Combining the low soluble anionic surfactant C18EO4SO4 with the cationic surfactant C12EO1Ch changed the situation. Due to the interaction with the cation, the anion could be dissolved, indicated by a clear solution as it can be seen in 3.3.1. Subsequently, the effect of the longer alkyl chain could be observed in the cmc measurement. The cmc value decreased down to several mg/L. The combination of the two ions led to a more nonionic character. A nonionic character is also known to have lower cmc values.⁹⁸

For ACA, the combination with SDS showed only small solubility (see 3.3.1). So, a cmc value could not be determined for two combinations. When combining ACA with the three anionic surfactants with a C12 alkyl chain, the solubility increased. Low cmc values with a minimum value for the mass ratio 5-5 of 4-6 mg/L could be measured. For the two cationic surfactants with EO groups, C12EO1Ch and C12EO4Ch, the solubility was not a problem. Both cationic surfactants showed smaller cmc values in the catanionic mixtures than in pure form. Lowest values were obtained with the anionic surfactant C18EO4SO4 for C12EO1Ch and with C12EO4SO4 for C12EO4Ch. The combination with the anionic surfactant C12EO6SO4 did not give the best results. Both combinations have the maximum of EO groups in their series. In both cases, this was counterproductive. It seemed to be enough and even more effective if EO groups were present, either on the anionic side or the cationic side.

From the cmc measurement data, the surface excess concentration was determined. It is inversely proportional to the area per molecule at the surface A . The value of A was also calculated as described in 3.5.2.2 and is shown in Figure 14. It must be mentioned that the calculation assumes that the two surfactants are identical^{95, 99} and so, only the average value of A of anionic and cationic surfactant was calculated.

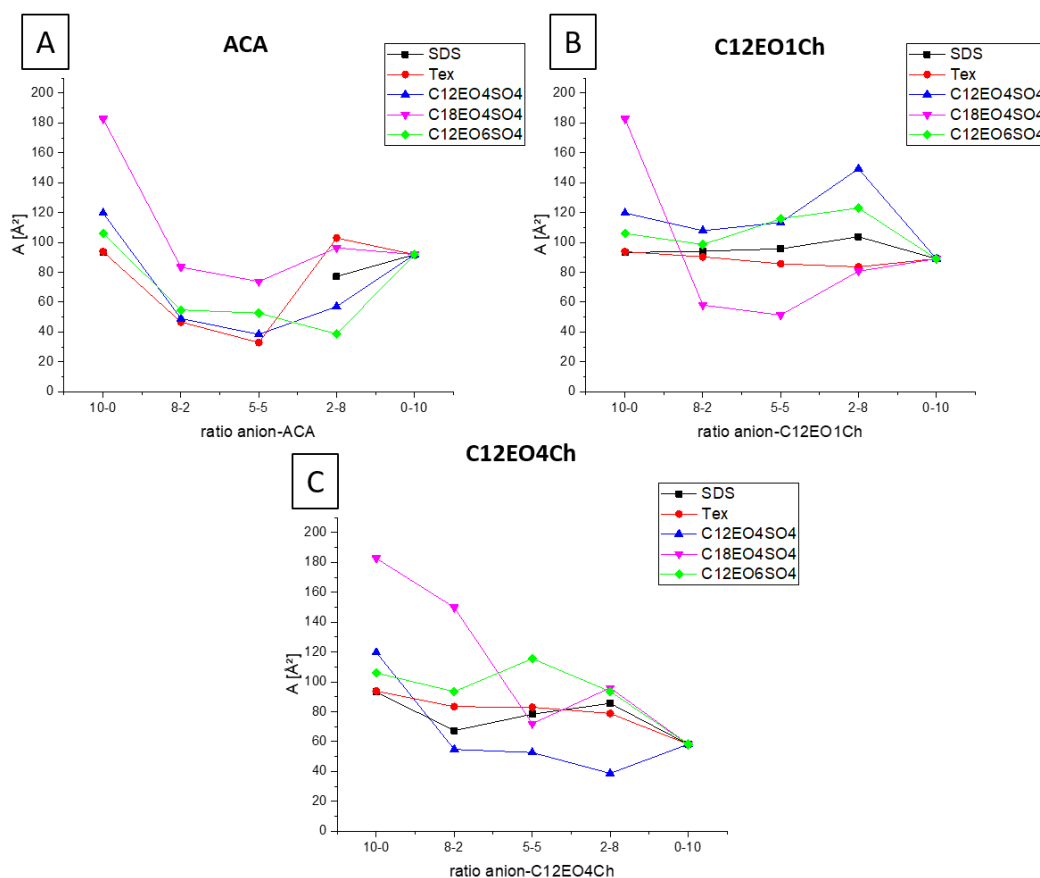


Figure 14: Area A per molecule at the surface A in \AA^2 calculated from the cmc data as described in 3.5.2.2 in percentage of the catanionic combinations of five anionic surfactants (SDS (black), Tex (red), C12EO4SO4 (blue), C18EO4SO4 (purple) and C12EO6SO4 (green)) and the cationic surfactants ACA (A), C12EO1Ch (B) and C12EO4Ch (C) at 25°C and a total surfactant concentration of 1 g/L.

In general, the area per molecule decreased when mixing the two surfactants. It was expected since the mixing led to an electrostatic attraction between the oppositely charged headgroups.⁷² For this purpose, a tighter packing was possible, resulting in a smaller area per molecule at the surface.²³ Some exceptions can be named. They all appeared at an excess of the cationic surfactant. Since the hydrophilic group did not only consist of the ionic headgroup but also of the hydrophilic EO groups, the ordering at the interface could be influenced by ordering of the EO groups. The reason could also be a practical one. Several combinations were difficult to measure since adsorption of the cationic surfactant at the plate occurred. This might adulterate the data and lead to slightly higher values. In average, C12EO1Ch gave the largest values for A . Here, except for C18EO4SO4, no decrease in A was observed. The values were in the same range as the pure surfactants. The surfactant molecules did

not seem to attract each other in a way that decreases the surface area. Either the new arrangement of the EO groups compensated it, or the one EO group was hindering a stronger attraction. For C12EO4Ch, the situation was similar. Except for C12EO4SO₄, no decrease in A was observed. Due to the flexibility of the EO groups and maybe also their hydration, the attraction seemed to be attenuated. A larger A value can be correlated to a less intense attraction between the two ionic surfactants. This agrees with the observed solubility in 3.3.1, since higher solubility corresponds to a less intense attraction between the two oppositely charged surfactants.

3.3.3 Interfacial tension

3.3.3.1 Surface tension against air

For all investigated catanionic combinations at the concentration of 0.1 wt%, the surface tension (ST) against air was measured as described in 3.5.2.2. The cmc measurements in 3.3.2 showed that 0.1 wt% was above the cmc for all catanionic combinations and the measured values corresponded to the values in application situations. The results of the ST measurements are shown in Figure 15. The observed trend was the same for all combinations. A synergistic effect of the mixing of the anionic and cationic surfactant could be seen. This is known from the literature.⁶³ Nonionic surfactants are known to have very low surface tension values.^{12, 100} A pseudo-nonionic character of the catanionic combinations could lead to a similar result. Compared to the pure surfactants, a significant decrease of at least ten mN/m in surface tension was observed at 0.1 wt%. The most pronounced difference was obtained for SDS, because the concentration of SDS was still below its cmc value (see 3.3.2). For the different anion-cation ratio, only small changes in surface tension were observed. The increase in nonionic character when going towards the equimolar ratio did not decrease the cmc value further. This means that a small amount of either anion or cation was enough to lower the surface tension of the mixture to a maximal extent.

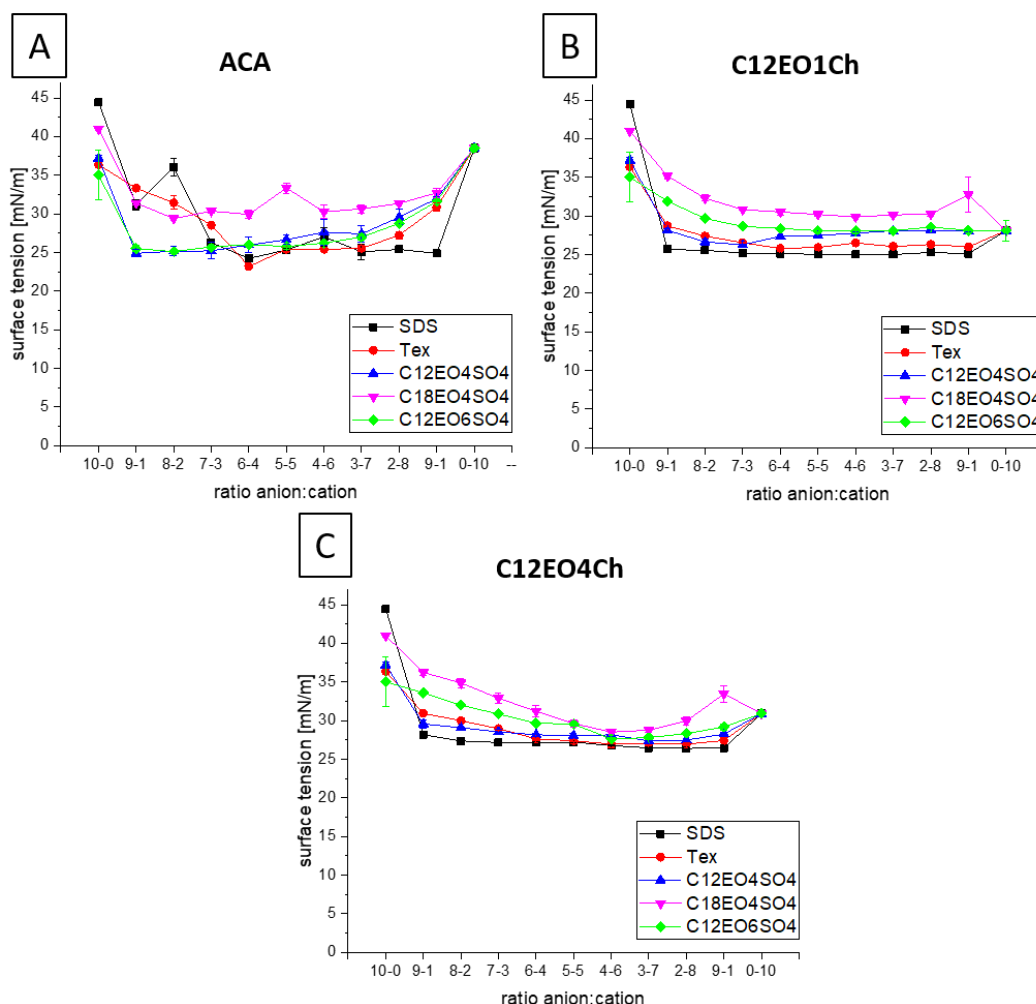


Figure 15: Results of surface tension via pendant drop measurements of the catanionic combinations of five anionic surfactants (SDS (black), Tex (red), C12EO4SO4 (blue), C18EO4SO4 (purple) and C12EO6SO4 (green)) and the cationic surfactants ACA (A), C12EO1Ch (B) and C12EO4Ch (C) at a total surfactant concentration of 1 g/L.

The two cationic surfactants with EO groups showed a lower surface tension value in their pure form at a concentration of 0.1 wt% than ACA. Their lower cmc value can be the reason for this. At the present concentration, ACA was not above the cmc concentration. For mixtures with ACA, the values seemed to follow no obvious trend. This might be due to the lower solubility of the catanionic mixture, which might disturb the pendant drop measurement. SDS gave the lowest surface tension values for all three cations with value down to 25 mN/m. This is a very small value. The value is even below the reported value for commercial obtainable nonionic surfactants based on alkyethoxyalcohols. E.g., Lutensol AO3 has a value of around 28 mN/m.¹⁰¹

The highest values were observed for the anionic surfactant C18EO4SO4 followed by C12EO6SO4. In both cases, the chain of the anionic surfactant was increased by a hydrophobic hydrocarbon chain for C18EO4SO4 and a hydrophilic EO chain for C12EO6SO4. Both two variants decreased the surface activity. Especially for C18EO4SO4, the higher surface tension values were not expected since hydrophobic parts in the chain normally lead to a decrease in surface tension.¹⁰² With the molecule having a larger hydrophobic area, the molecule will be pushed more easily towards the hydrophobic air interface. Tex and C12EO4SO4 showed only small differences. Compared to C18EO4SO4, the replacement of the hydrocarbon chain by EO groups had a positive effect on the surface efficiency. But, a too high number of EO groups seemed to be unfavorable as it could be seen with the comparison with C12EO6SO4. Regarding the three cations, C12EO4Ch gave slightly higher values than the other two cations, which were in the same range. EO groups in the cation structure seemed to have no positive effect. The surfactants were not more inclined to go to the interface. Hydration of the EO groups might be the reason for that.

In general, low surface tension values were obtained for the investigated catanionic mixtures. For the best catanionic combinations, the values were in the range of surface tension values known for nonionic surfactants. An increase in surface activity can be concluded compare to the pure ionic surfactants. This is an advantage: to reach low surface tension values, smaller amounts are necessary in the case of the catanionic mixtures.

3.3.3.2 Interfacial tension against hexadecane

The decrease of the surface tension against air is of main importance for several applications.^{2, 103} But, another interesting point regarding interfacial tension (IFT) is the reduction of interfacial tension against another liquid. This is especially important in the field of emulsions.⁹⁷ For this purpose, several catanionic combinations were investigated towards their interfacial behavior against hexadecane. Spinning drop measurements were performed over a time range of maximal 60 mins as described in 3.5.2.2. If the value was not at a constant level, the value after 60 mins was taken as the measured value. For each cationic surfactant, at least two combinations were investigated to make statements regarding structural influences possible.

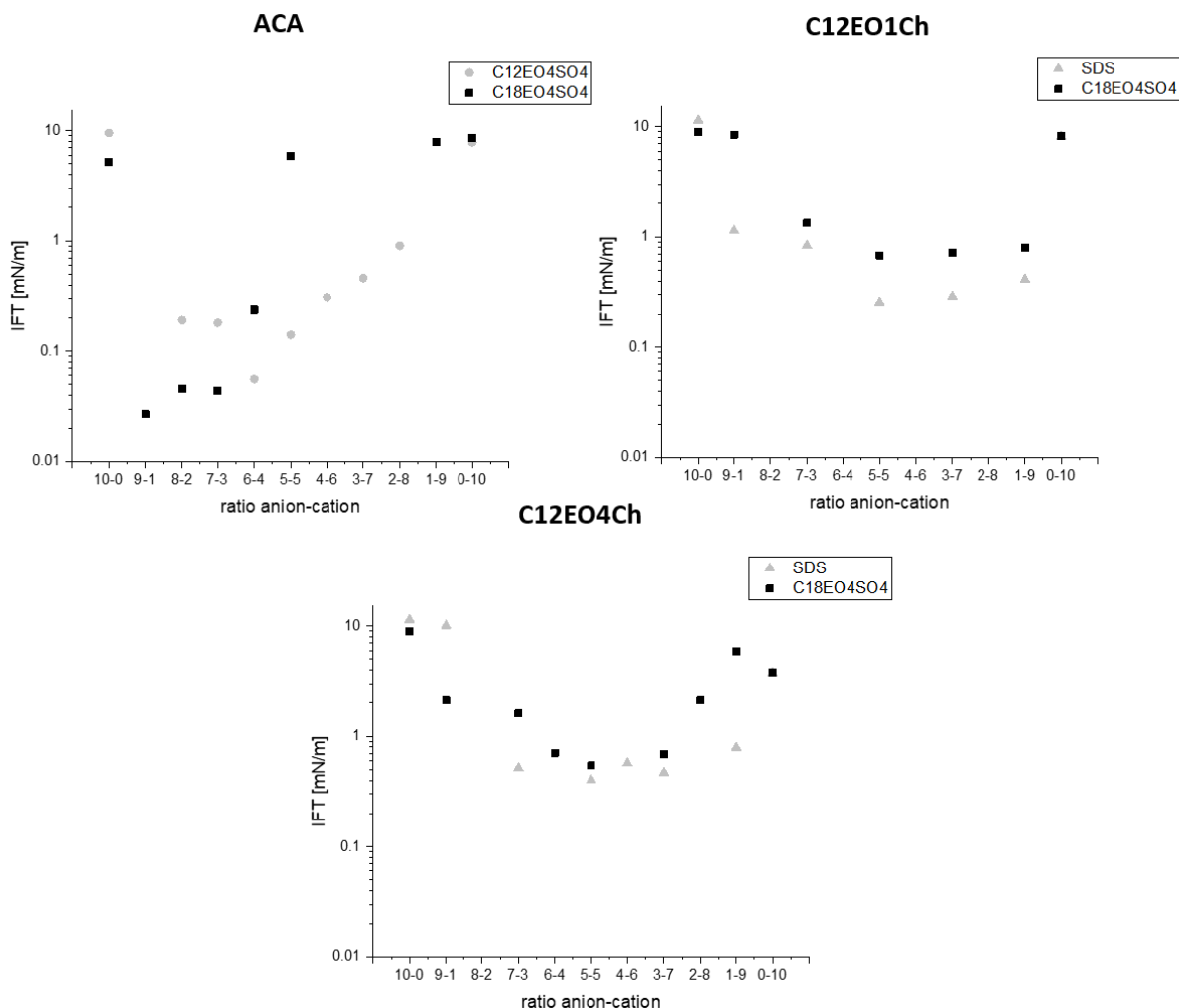


Figure 16: Interfacial tension results of six catanionic combinations of the three different cations (ACA (left), C12EO1Ch (middle) and C12EO4Ch (right)) at different mass ratios from 9-1 to 1-9 at 25 °C and a total surfactant concentration of 1 g/L measured as described in 3.5.2.2.

As shown in Figure 16, the determined interfacial tension values were extremely low for nearly all catanionic combinations compared to the pure surfactants. The measured values were below 1 mN/m. A nonionic surfactant is in the same range.¹⁰⁴ In the performed measurements, the synergistic effect of mixing an anionic and a cationic surfactant became again obvious. It could be seen that by mixing the two surfactants, a significant positive effect regarding their interfacial property can be achieved. The extent of the effect varied. For the two cationic surfactants with EO groups present in the structure, the effectiveness of the interfacial tension reduction was less intense than with the cation ACA. Both cationic surfactants showed similar values. They were combined with the same two

anionic surfactants, SDS and C18EO4SO4. In both cases, the combination with SDS gave lower values. The longer chain in combination with four EO groups did not show higher affinity to the interface. In combination with C12EO1Ch, the anionic surfactant SDS gave lower values than with C12EO4Ch. A higher number of EO groups within the cationic surfactant did not seem to promote the interfacial activity. A higher ethoxy number means higher hydrophilicity in the molecule. The EO groups are hydrated and the structural part is flexible. The interaction between the opposite charges is weakened.³¹ It might be weakened too much to gain a maximum of interfacial effectiveness. Moreover, SDS has a more hydrophobic character due to no EO groups in the structure. A more hydrophobic character can interact more intensively with the hydrophobic hexadecane. A lower interfacial tension value is the result.

For ACA, the combination with SDS was not reasonable, since the solubility limit was far below any concentration for a real application. For this purpose, only the two anionic surfactants C12EO4SO4 and C18EO4SO4 were mixed with ACA. They only differed in their carbon chain length. The trend within the ratio series was different. For ratios with an excess of anionic surfactant, the interfacial tension values were much lower than the ones discussed so far, whereas, with an excess of cationic surfactant, the values are higher. In these cases, the cationic surfactant was best used as an additive in small amounts. Within this range, the effectiveness was best. When the cationic surfactant is added, the anionic surfactant interacts with it, resulting in an ion pair with highly nonionic character. These ion pairs go more likely to the hydrophobic interface of hexadecane. With the ion pairs at the interface, part of the remaining anionic surfactant molecule also goes to the interface and assembles within the ion pairs. In small amounts, this seemed to be the most effective way to decrease the interfacial tension. With the increasing amount of anionic surfactant, the amount of ion pairs increased. But, ion pairs alone seemed not to be the most efficient in reducing the interfacial tension. The same could be seen for an excess of ACA.

In general, two observations should be pointed out. First, in the case of catanionic mixtures, lower concentrations are sufficient to result already in a high interfacial activity compared to the pure anionic surfactants. This is interesting for any application when considering the claim of sustainability and saving resources.¹ Second, the effectiveness of a catanionic surfactant mixture was in general significantly higher than the pure surfactants. This gives another advantage for several applications.

For applications, the usage of millipore water is not realistic. For this purpose, the influence of water hardness was tested on one catanionic combination. The anionic surfactant C12EO4SO4 was mixed with C16EO1Ch at 0 °dH and 5 °dH as the IFT is determined as described in 3.5.2.2. In Figure 17 – left, the results are shown. As it can be expected, the presence of additional ions does not change the situation to a great extent. The values for 5 °dH were slightly higher. From the point of the Hofmeister series, the added cations, Ca^{2+} and Mg^{2+} , will not interact strongly with the sulfate.¹⁰⁵ The added chloride ions were already present. Thus, the addition changed only the concentration of electrolytes in the solution. But in these concentrations, this did not affect the observed interfacial behavior.

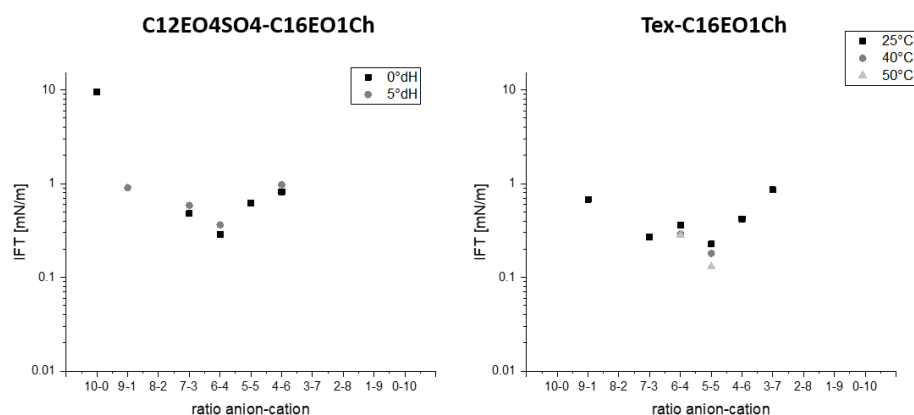


Figure 17: Comparison of the interfacial tension values for the influence of water hardness (0 °dH (black squares) and 5 °dH (grey circles)) for the catanionic combination of the anion C12EO4SO4 and the cation C16EO1Ch (left) and comparison of the influence of three different temperatures (25 °C (black squares), 40 °C (dark grey circles) and 50 °C (light grey triangles)) for the catanionic combination of the anion Tex and the cation C16EO1Ch (right). Experimental data is measured as described in 3.5.2.2 at a total surfactant concentration of 1 g/L.

The second tested influence was the temperature. The catanionic combination of Tex and C16EO1Ch was measured as described in 3.5.2.2 at three different temperatures, 25 °C, 40 °C and 50 °C for two different ratios. As it can be seen in Figure 17 (right), small differences could be observed. Around equimolar ratio, an increase in temperature results in a decreased in interfacial tension. Especially around equimolar ratio (mass ratio of 0.52:0.48 for C12EO4SO4 and 0.47:0.53 for Tex) around the mass ratio 5-5), the solubility was a problem. The higher temperature increased the solubility of the catanionic mixture. Since solubility limits the efficiency of the catanionic combination, higher temperatures increased the effectiveness of the combination. For the mass ratio 6-4, the solubility of

the catanionic mixture is higher. Thus, the observed differences are mainly due to temperature effect. The effect of increasing temperature was the same as for the mass ratio 5-5. This is known from the literature.¹⁰³ But the effect was not as decisive, because the influence of the solubility effect was reduced. Consequently, an increase in temperature for the catanionic mixtures influenced mostly the solubility character and had only small influences on the interfacial tension, when absolute solubility was already reached at lower temperatures.

3.3.4 Adsorption behavior

The adsorption of surfactants on the surface is interesting for several applications, e.g. in the field of coating surfaces.^{16, 106} An interesting aspect is the adsorption behavior of the combination of anionic and cationic surfactant in comparison to the pure surfactants. A surface can either be classified as hydrophobic or hydrophilic. The adsorption behavior of a substance strongly depends on the character of the surface. For this purpose, quartz crystal microbalance (QCM) measurements were performed on two different substrates exemplarily for some combinations. One substrate was a quartz crystal with a hydrophilic SiO₂ surface and the second one was a quartz crystal with a gold surface coated with a hydrophobic 1-octadecane thiol layer (SAM). The measurement procedure was the same for all measurements, as described in 3.5.2.4. The mass of adsorption after the surfactant step and the remaining mass on the quartz crystal after the last washing step were the two considered parameters. Depending on the application, both parameters are interesting: the ability to adsorb, but to be washed away again and the ability to adsorb and to stick to the surface, even if it gets in contact with water.

Four anionic surfactants were combined with the cation ACA and investigated regarding their adsorption behavior on the hydrophobic quartz crystal. For comparison, the cation C12EO4Ch was combined with SDS and C12EO6SO4. The results are shown in Figure 18. For all combinations, a large part of the adsorbed mass was washed away by the washing step. This was not surprising, since the molecules within the adsorbed layer were held together by intermolecular forces. The flow of the water acted as a constant force against it. So, the molecules were transported from the adsorption layer. The stronger the molecules stick to the surface and the stronger the forces, the larger will be the remaining part of the molecules.

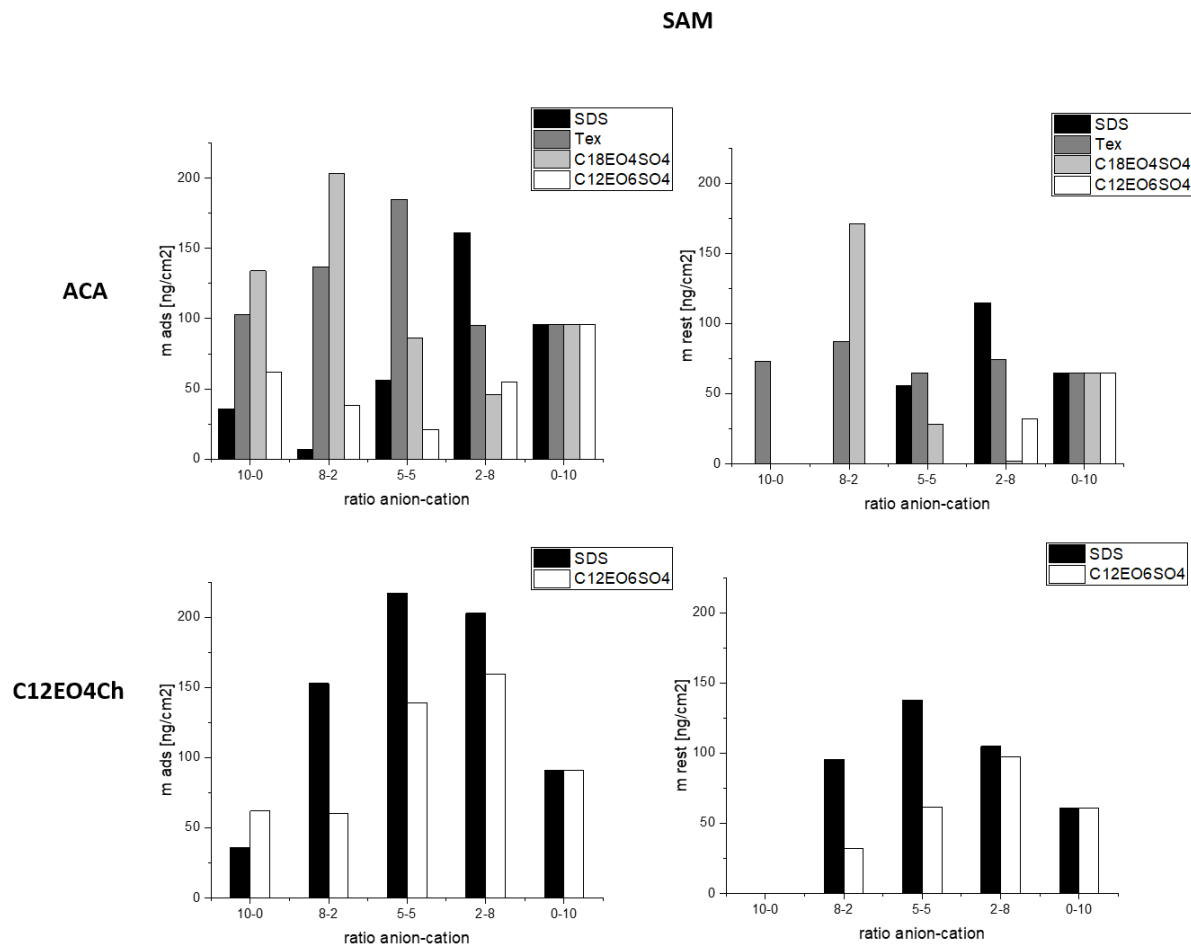


Figure 18: Results of the adsorbed mass after the surfactant step (left) and after the washing step (right) of the catanionic combinations with the cation ACA (above) and C12EO4Ch (below) at a total surfactant concentration of 1 g/L determined via QCM measurements on a SAM surface, as described in 3.5.2.4.

Comparing the different anionic surfactants for ACA on the hydrophobic surface, the situation differed. For Tex, all catanionic combinations showed higher adsorption than the pure surfactants. From the theoretical view, this was expected. By combining the two ionic surfactants, the overall character of the solutions gets more nonionic.²³ A nonionic character will interact better with a hydrophobic surface. Thus, the adsorbed mass should increase. For C18EO4SO4, the situation was similar. With SDS, only at a mass ratio of 2-8, adsorption could be observed. This might be because nearly all substance in the solution was precipitating and washed away by the solution. The surfactant molecules could not interact with the surface. For C12EO6SO4, the determined adsorption was extremely low compared to the pure surfactants. The molecules seemed not to interact with the

surface. They seemed to be disturbed by each other regarding their adsorption behavior. The interactions with the surface were too weak to stick to it. So, except for the two combinations of C18EO4SO4-ACA and SDS-ACA, all mixtures showed a weak adsorption behavior on the hydrophobic surface. The adsorption behavior of combinations with ACA differed from the one with C12EO4Ch. Here, all catanionic mixtures showed higher adsorption than the pure surfactants. The adsorbed mass after the first step was high compared to ACA, especially with SDS. Also, the amount of surfactant after the washing step was higher. For C12EO6SO4, an excess of cation was favorable. With SDS, 75 % of the original adsorbed mass stayed on the substrate for the mass ratio 5-5. The four EO groups within the cationic surfactant seemed to promote the adsorption on the hydrophobic surface. But, a maximal number of EO groups did not correspond to maximal adsorption. The additional six EO groups in the anionic surfactant did not improve but on the contrary weaken the adsorption.

The same catanionic combinations with the cation ACA were tested on a SiO₂ surface. The values were compared to two combinations with the cation C12EO1Ch. The results are depicted in Figure 19. To discuss the interaction on the SiO₂ surface, the information about the surface must be given. Silica has been intensively studied, since it is the major constituent of the earth's crust. From the chemical point of view, the surface of silica has a charged character defined by the relative concentrations of H⁺ and OH⁻. The isoelectric point for silica is at approximately pH 2.¹⁰⁷ The density of negative charges stays low until the solution pH reaches 6. Then a sharp increase is observed. Since the investigations were performed at pH 6, a less negatively charged, and more neutral surface could be assumed. The substrate had a hydrophilic character. So, for the adsorption on the substrate, hydrophilic parts of the surfactant structure were responsible.

In general, higher adsorption was observed for the SiO₂ substrate compared to the SAM substrate. The hydrophilic forces seemed to be more decisive. The pure surfactants were in the range of the maximal adsorption on the SAM substrate. Except for one combination, Tex-ACA, 5-5, the mixtures of ACA and the anions showed no higher adsorption than the pure ones. The reason for that is the argumentation above. The mixing of the two ions increased the nonionic, the more hydrophobic character. Thus, the hydrophilic part within the structure was weakened. The interaction with the hydrophilic substrate was less intense. The adsorption was reduced.

Regarding the mass remaining on the substrate after the washing step, some combinations were promising. Whereas the pure surfactants were washed away, the combinations stuck to the substrate.

Especially the two ratios 5-5 and 2-8 for the combination Tex-ACA gave high values for the remaining surfactant mass. So, compared to the pure surfactants, the mixtures adsorbed more difficultly on the substrate. But, when they adsorbed, they stuck to it and were more difficult to be removed. An interesting aspect was the adsorption behavior of the pure C12EO6SO₄. With a value of 360 ng/cm², it was the second highest value. Compared to the other anions, the interactions of C12EO6SO₄ with the hydrophilic substrate were stronger. Reason for this could be the larger hydrophilic part in the molecule consisting of six EO groups and one sulfate group. The EO groups seemed to be favorable for the adsorption on SiO₂. But, a higher number of them were necessary since the 2.5 EO groups in the Tex gave smaller values than the SDS.

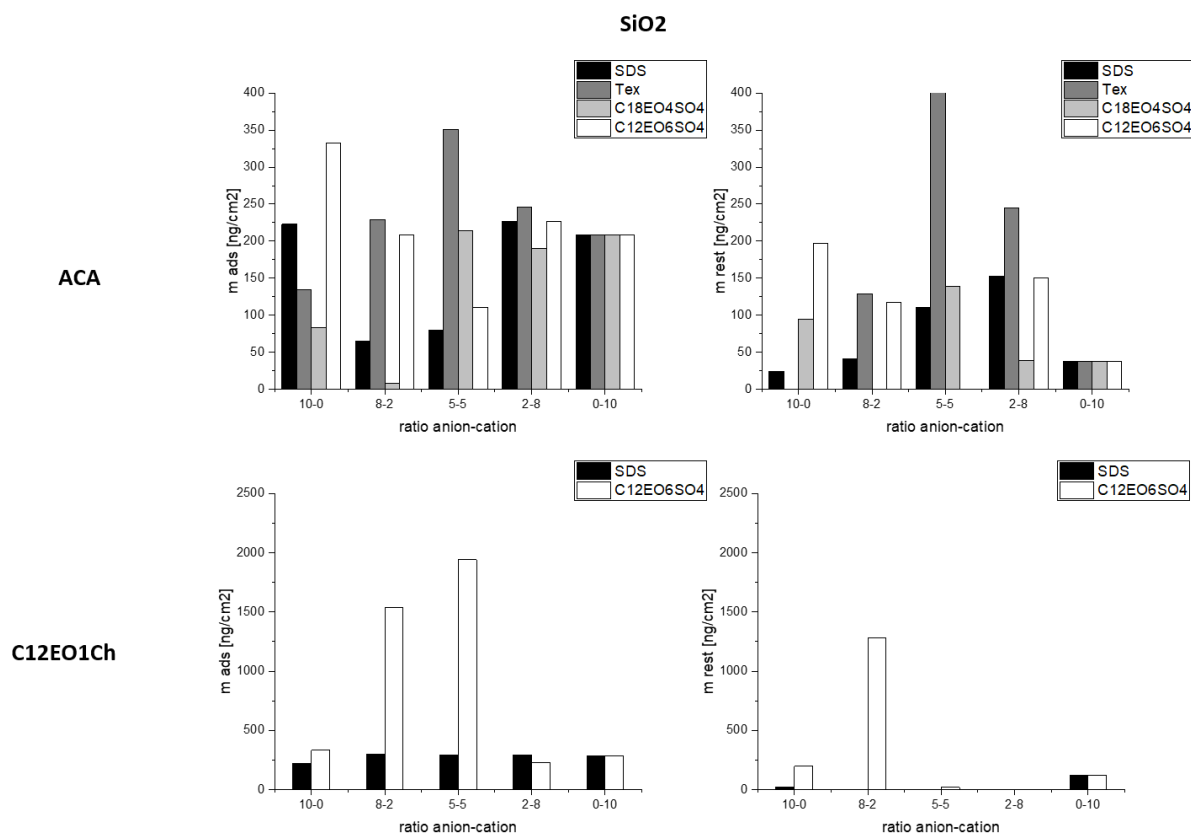


Figure 19: Results of the adsorbed mass after the surfactant step (left) and after the washing step (right) of catanionic combinations with the cationic surfactant ACA (above) and C12EO4Ch (below) at a total surfactant concentration of 1 g/L determined via QCM measurements on a SiO₂ surface, as described in 3.5.2.4.

C12EO1Ch in combination with SDS and C12EO6SO4 were measured for comparison. Compared to ACA, the cation had a larger hydrophilic part. Its effect can be seen when regarding the results. It must be paid attention to the larger scaling on the y-axis. All combinations with C12EO1Ch showed higher adsorption values after the first step. Especially the two values for the ratios 8-2 and 5-5 of the combination with C12EO6SO4 were extremely high. Combined with SDS, the values with changing the mass ratio were similar. No trend could be observed. The washing step removed most parts of the adsorbed surfactants in nearly all cases. C12EO6SO4-C12EO1Ch at the mass ratio 8-2 was the only combination where rest was left. When small forces like the water flow in the washing step were present, the adsorption forces were too weak for the surfactants to stay on the substrate.

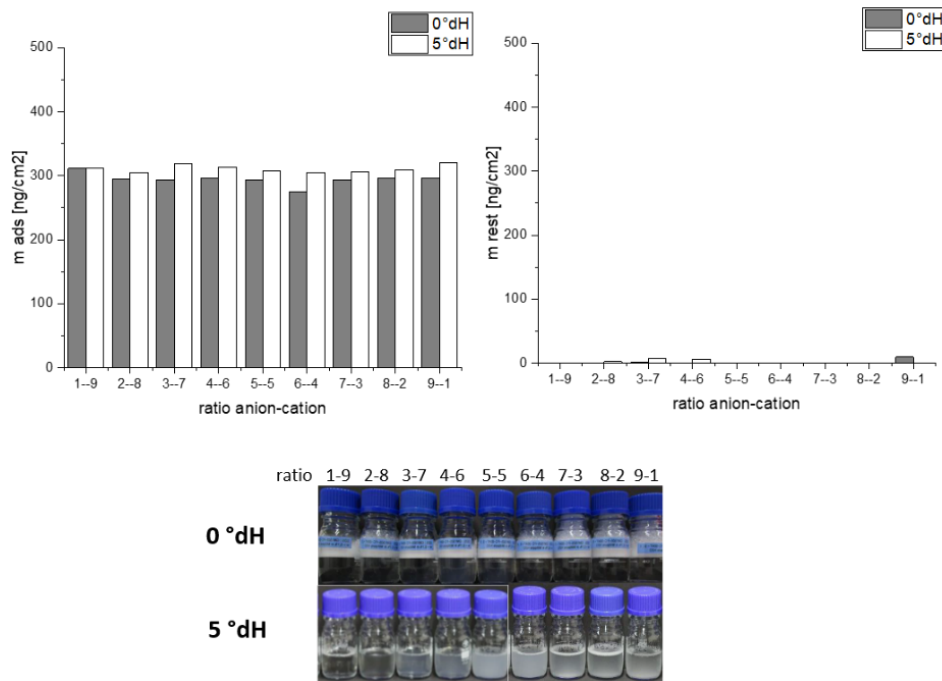


Figure 20: Investigation of the influence of water hardness on the adsorption behavior of the cationic combination SDS-C12EO1Ch at a total surfactant concentration of 1 g/L on a SiO₂ quartz crystal determined via QCM measurement, as described in 3.5.2.4. On the left: adsorbed mass after the first step of washing with the surfactant solution; on the right: adsorbed mass after the second step of washing with water; below: the optical appearance of the investigated samples.

Since in most applications, a water phase with dissolved ions is used, the influence of water hardness regarding the adsorption behavior of the cationic combinations was interesting. For this purpose,

the QCM measurements were performed for one catanionic combination, SDS-C12EO1Ch, at a water hardness of 5 °dH for all different ratios, including the one of equimolar ratio, to be compared to the tests with millipore water. The results are shown in Figure 20. No significant differences were observed with the presence of water hardness. Slightly higher values were measured for samples with 5 °dH. Water hardness indicates the presence of Ca^{2+} and Mg^{2+} . In pure form, SDS is sensitive towards such ions.¹⁰⁸ It builds strong ion pairs and precipitates. In combination with C12EO1Ch, this precipitation behavior was reduced. But, the turbidity of the samples on the anion-rich side could be seen. It must be mentioned that the pictures Figure 20 were taken after several days, whereas the measurement was performed after 24 h. So, the precipitation was not that intense. However, the higher tendency to precipitate could lead to higher values of adsorbed mass, since it could be deposited on the substrate. No adsorbed mass was left after the washing step. This confirmed the assumption, since precipitation could easily be washed away.

All in all, the performed QCM measurements showed a positive effect of the catanionic mixtures on the adsorption on the hydrophobic SAM surface. The increasing nonionic character around equimolar ratio led to maximal adsorption. The best adsorption result was obtained for the combination SDS-C12EO4Ch. The mixture of Tex-ACA, 8-2 remained on the SAM surface most effectively. On the hydrophilic SiO₂ surface, the adsorption was also positively influenced by the catanionic mixtures. But, the extent was not as decisive as on SAM, except for the mixture C12EO6SO₄-C12EO1Ch. Here, large adsorption, as well as a large remaining mass, could be detected. A dependence on the water hardness could not be detected. The use of catanionic mixtures showed the advantage of choosing the right combination and anion-cation ratio depending on the desired behavior.

3.3.5 Dynamic behavior

The dynamics of surfactants in the solution is of interest due to several aspects. High dynamics correspond to a fast movement of the surfactant molecules from the bulk phase to the water-air interface.¹⁰⁹ Especially when the application requires a fast process, high dynamics within the formulations are desired to achieve maximum efficiency. A high dynamic of the active substances in solution corresponds to higher efficiency in their function. This is necessary for example when the solution is sprayed onto a surface where it should work immediately after contact.

All catanionic combinations were investigated via a maximum bubble pressure tensiometer regarding their dynamic behavior as described in 3.5.2.2. The lifetime of the bubble was changed to higher values, and the corresponding surface tension is calculated via the detected bubble pressure as described in 3.5.2.2. For evaluation, the value of the decrease of the surface tension after 1 sec of bubble lifetime was taken for comparison. The results are shown in Figure 21.

Except for the combinations with ACA, all catanionic combinations showed a higher dynamic behavior than the pure anionic or cationic surfactant, which can be explained by the lower solubility of these mixtures. This could be seen especially for combinations of SDS and ACA with an excess of anionic surfactant. Already for the pure anionic surfactants, several aspects regarding the molecular structure could be observed. SDS showed only low dynamics. The molecules seemed to move slower through the bulk and adsorbed slower at the interface. In contrast to SDS, Tex gave high values. The insertion of 2.5 EO groups seemed to increase the dynamic behavior by a factor of three. Adding even more EO groups into the structure weakened the positive effect again. The behavior is less dynamic when going from Tex to C12EO4SO4 to C12EO6SO4. Another influencing aspect could also be the increased chain length, which could hinder diffusion and make the system less dynamic. This effect can be seen when comparing C12EO4SO4 and C18EO4SO4. The structure only differs in the length of the carbon chain. The received values for both anionic surfactants differed by a factor of three. For the longer alkyl chain, the values were in the range of SDS.

Consequently, for the pure anionic surfactant, the following structural influences could be concluded: the insertion of EO groups leads to a more dynamic surfactant. But, a longer chain gives a less dynamic system. This effect can be already seen when more EO groups are inserted and is even more pronounced when the hydrocarbon chain is lengthened. On the cationic surfactant side, the trends for the pure cations were different. ACA, the cation with the longest alkyl chain of 16 carbon atoms and no EO groups present, showed higher dynamic behavior than the cations with shorter chain length and EO groups. Also, a higher amount of EO groups seemed to be favorable in the pure cation solution.

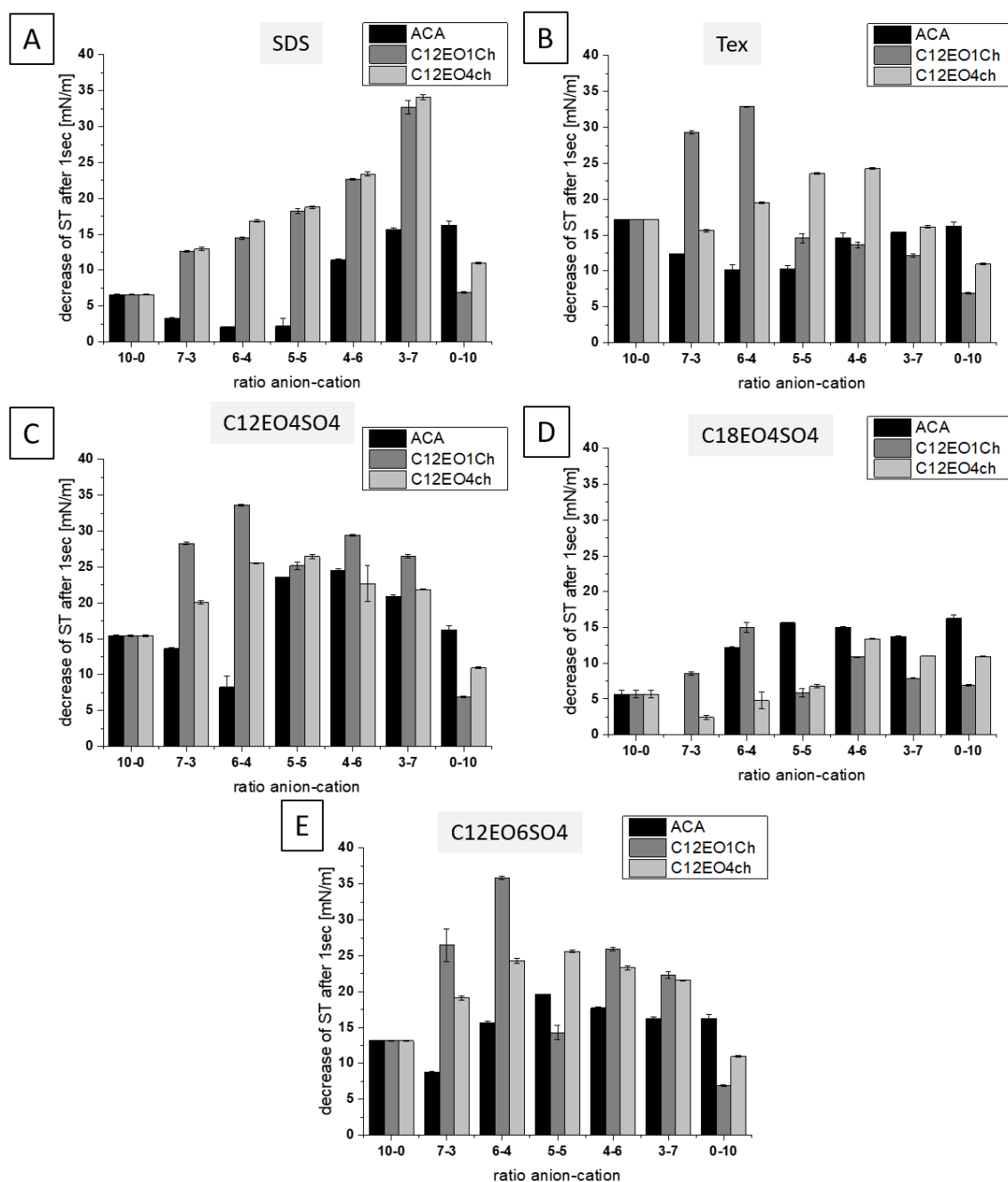


Figure 21: Dynamic surface tension measurements performed with a bubble tensiometer as described in 3.5.2.2 for the catanionic combinations consisting of the anionic surfactants SDS (A), Tex (B), C12EO4SO4 (C), C18EO4SO4 (D) and C12EO6SO4 (E) and the cationic surfactants ACA (black), C12EO1Ch (dark grey) and C12EO4ch (light grey); The evaluated value is the decrease in surface tension (ST) after a bubble lifetime of 1 sec.

When regarding the mixtures of the anionic and cationic surfactants described before, the situation depended strongly on the given case. In general, most combinations behaved more dynamic compared to the pure surfactants. This was especially the case for mixtures with C12EO1Ch and C12EO4Ch. Comparing the three different cationic surfactants in catanionic combinations, the same trend was observed for all combinations. In most cases, the cationic surfactant ACA gave the smallest values. The best results were obtained for C12O1Ch obtaining a decrease in surface tension of around 35 mN/m after 1 sec of bubble lifetime. Except for C18EO4SO₄, the combination of C12EO1Ch with each anion gave such high values. For SDS, both cationic surfactants with EO groups gave similar results. The trend within the different ratios was interesting for SDS. With the increasing amount of cationic surfactant, the measured values increased with its maximum at 3-7. Here, the synergistic effect was maximal. For the anionic surfactants Tex, C12EO4SO₄ and C12EO6SO₄, the trends were different. No linear increase was observed. The maximum was around the equimolar ratio in these cases. C18EO4SO₄ mixtures were less dynamic than mixtures with the other anionic surfactants. The values were highest mainly with ACA as cation but did not exceed the value of the pure cationic surfactant.

In summary, it is difficult to make a general statement about the trend influencing the dynamic behavior of the catanionic mixtures. But, some aspects can be concluded:

- A long alkyl chain, at least in the anionic surfactant, reduced the dynamics.
- In mixtures, the combination with a cationic surfactant with fewer EO groups gave best results in most combinations.
- In some cases, the presence of EO groups in the anionic surfactant could compensate the low dynamic of the ACA cationic surfactant.
- When an EO group was present in the cationic surfactant, an EO group was not necessary in the anionic one.

Two aspects influence the dynamic behavior as it was measured above.³³ One is the adsorption behavior of the surfactant molecule at the interface. The second part is the diffusion of the surfactant molecules in the bulk solution towards the interface. The diffusion coefficient describes the mobility of the molecules in the solution due to Brownian motion. If the diffusion coefficient is small, the molecules move slowly through the solution. Thus, the adsorption of the surfactant molecules at the interface is time-dependent on the rate of diffusion. The faster the molecules move through the

solution, the more dynamic is the system and less they dominate the time-dependent adsorption process at the interface. But regarding the impact of the diffusion for the dynamic surface tension, the diffusion in the bulk phase is not the appropriate factor. An adsorption barrier between the bulk phase and the interface has to be overcome.¹⁰⁹ This is considered in the effective diffusion coefficient from the bulk phase to the interface. It is calculated from the measurement data as described in 3.5.2.2 to give an idea of the diffusion part in these systems. The calculated values are depicted in Figure 22.

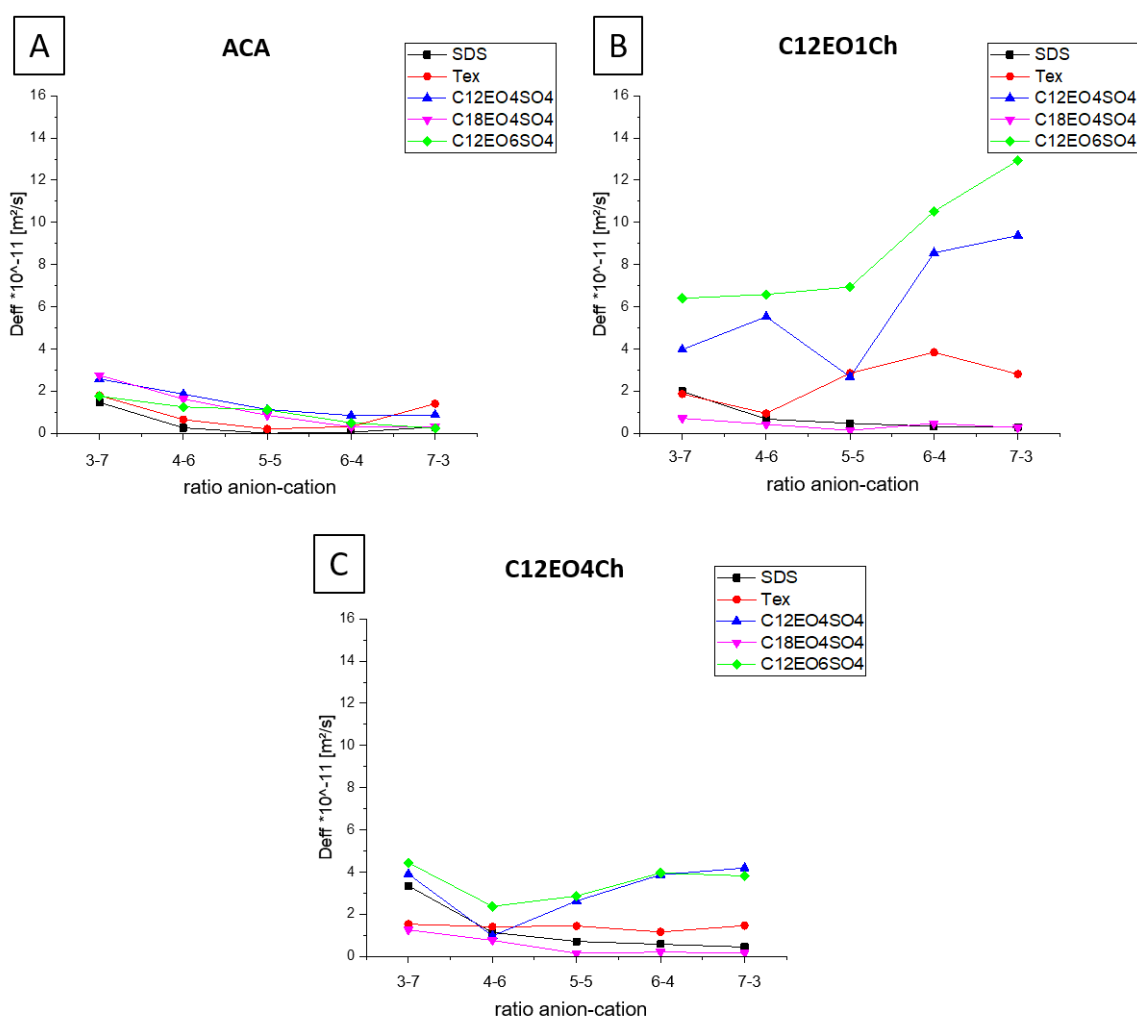


Figure 22: Calculated values for the effective diffusion coefficient from the dynamic surface tension measurement as described in 3.5.2.2 of the catanionic combinations of the five anionic surfactants (SDS (black), Tex (red), C12EO4SO4 (blue), C18EO4SO4 (purple) and C12EO6SO4 (green)) and the three cationic surfactants ACA (A), C12EO1Ch (B) and C12EO4Ch (C).

The calculated values for the effective diffusion coefficient from the bulk phase to the interface were relatively low when compared to values of diffusion coefficients within the liquid bulk phase. E.g., for pure SDS, a diffusion coefficient of one magnitude higher is given in literature.¹¹⁰ According to the mixed diffusion-kinetic controlled adsorption model, the reason for this can be the adsorption barrier.¹⁰⁹ Potential energy barrier, the correct orientation for adsorption and the presence of micelles can slow down the adsorption mechanism and thus decreases the corresponding diffusion coefficient. Moreover, the investigated substances were not of high purity. The salt of the counterions as well as potential byproducts of the synthesis were present in the solution. They could decrease the diffusion coefficient. C12EO1Ch gave much higher values by a factor of 4 to 6 for the diffusion coefficient for C12EO4SO4 and C12EO6SO4 compared to the other two cations. On the other hand, for ACA, the number of EO groups in the anionic surfactant did not play any role, for C12EO1Ch and C12EO4Ch an effect could be seen. C12EO6SO4 gave the highest values for both cationic surfactants. For nearly all combinations, no significant trend with one combination regarding the anion-cation ratio was observed. They were in the same range. For ACA, the diffusion coefficient decreased with higher amounts of the anionic surfactant.

For C12EO1Ch, the trend was the same for SDS and C18EO4SO4. For the other three anionic surfactants, the trend was the other way around. With a higher content of anionic surfactant, the diffusion coefficient increased. The catanionic mixture seemed to diffuse faster through the medium. For C12EO4Ch, the calculated values were nearly the same for each ratio. For the two anionic surfactants with a higher number of EO groups, a reduction could be seen at the mass ratio 4-6. This was around equimolar ratio. Maybe the strong interaction between the two ions hindered the movement within the solution. Since for most applications a high diffusion is desired, combinations of C12EO1Ch with anions with a higher number of EO groups are favorable regarding this property.

3.3.6 Aggregation behavior: DLS and cryoTEM

Catanionic combinations are known to aggregate into a variety of different structures.²² Size and structure of these aggregates, especially the formation of vesicles, is interesting for several applications, e.g. drug delivery.¹¹¹ In the given case of anion/cation mixtures, a variety of different structures with different size within the bulk solution could be expected. First, DLS measurements were performed as described in 3.5.2.3 with the catanionic solution used in other characterization

methods until now. A general impression of the average size of aggregates was of interest. For a more concrete insight of the aggregation in the catanionic mixtures solutions, cryoTEM measurements were performed.

For a general overview, all catanionic combinations were investigated via DLS. The solution of the samples was taken for measurement without any filtering. The average size of the aggregates was determined by a monomodal fit, and the resulted radii are summarized in Figure 23.

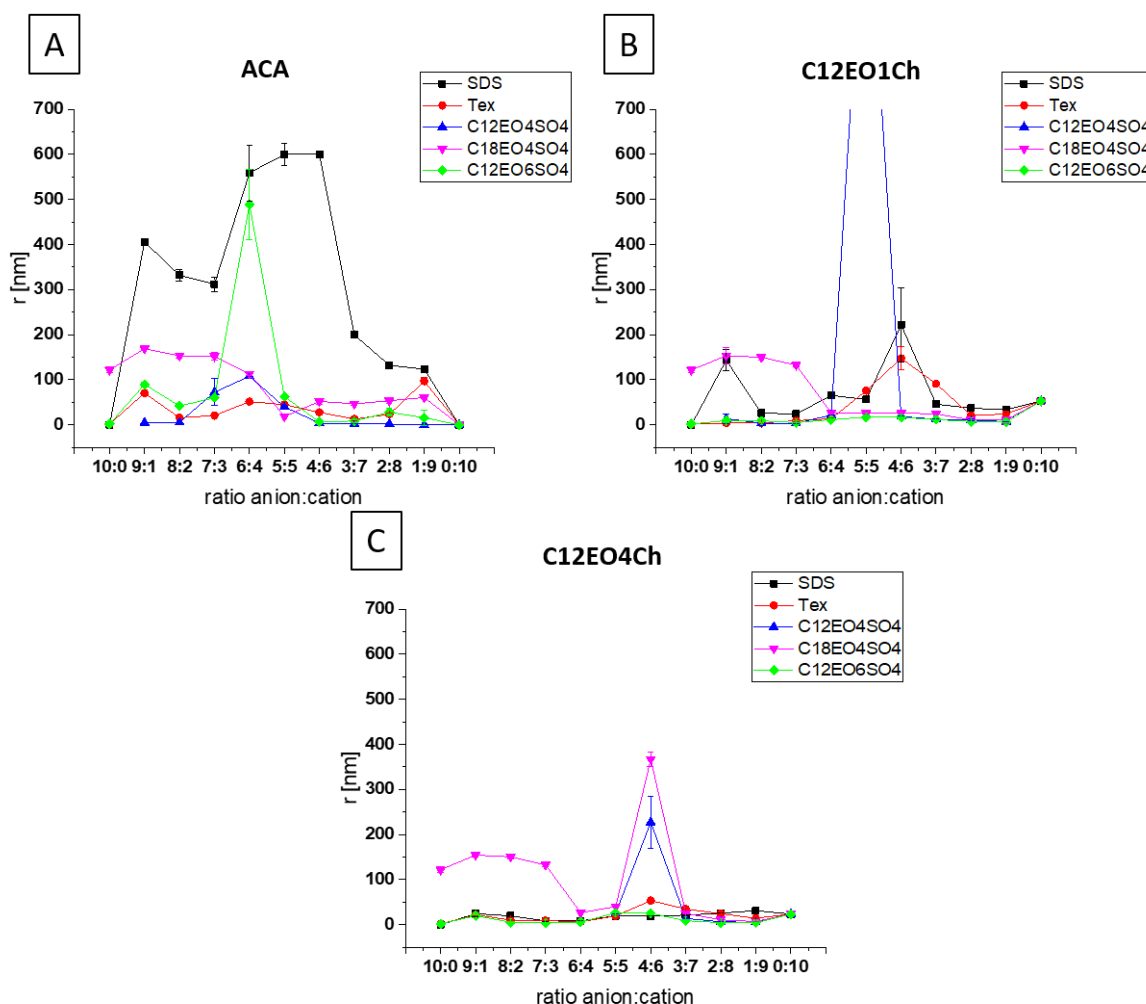


Figure 23: Radii, determined via monomodal fit of the corresponding DLS curves, as described in 3.5.2.3 of the catanionic combinations of five anionic surfactants (SDS (black), Tex (red), C12EO4SO4 (blue), C18EO4SO4 (purple) and C12EO6SO4 (green)) and the cationic surfactants ACA (A), C12EO1Ch (B) and C12EO4Ch (C) at 25°C and a total surfactant concentration of 1 g/L.

It must be mentioned that the stated radii are only a rough indication since the fitting relies on the assumption that a monodispersed system of spherical objects is present. This was not the case. Although a polydispersed system of different shapes of aggregation for catanionic mixtures could be assumed, the measured DLS curves looked monomodal and could be used for the determination of the average size of the particle in the solution. Hence, the DLS measurement could confirm the optical perception of the samples (see 3.3.1). For higher turbidity, a larger size of the aggregates should be measured. The determined radii confirmed that assumption. In samples with low solubility of the catanionic mixture, the radius was in the range of several hundred nm meaning the particle size was large enough so that the particle could be seen. The turbidity of the samples indicated this. Several mixtures could be assigned to that group of low solubility.

The combination of SDS and ACA showed high radii for ratios with higher anion content. Also, for the mixture of C12EO6SO₄ and ACA at the ratio around equimolar ratio, 6-4, and the mixture C12EO4SO₄ with C12EO1Ch, 5-5, the determined radii were very high. Both samples showed turbidity and even precipitation after a certain time. Also, for the combination of C12EO4Ch with the two anionic surfactants with four EO groups present, C12EO4SO₄ and C18EO4CO₄, the determined radii were several hundred nm. For the pure anionic surfactant C18EO4SO₄, the particle size was high, which was already indicated by the lower solubility at room temperature (see 3.3.1). Here, already the start of some precipitation was observed during the measurement. With higher amounts of cationic surfactant, the radius decreased. This indicated the better solubility of the mixture since smaller aggregates were present in the solution which did not tend to precipitate. In general, except for the named combinations, the determined radii were in the range of less than 50 nm for the two cations C12EO1Ch and C12EO4Ch. So, no larger particles could be assumed. The size is too large for normal micelle formation, which is normally in the range of only several nm as it could be seen for the pure surfactants. Here, the classical aggregation to spherical micelles is known (see 2.2.1). This indicated the presence of larger aggregates for the investigated catanionic mixtures. For the cationic surfactant ACA, the determined radii were slightly higher and were in the range up to 100 nm. Reason for this might be the tendency to lower solubility. Larger aggregates built, and result in particles which tend to precipitate with time. All in all, the DLS measurements suggest that by mixing the two oppositely charged surfactants, more than a mixed micelle formation happens. The determined average radii were too large to be due to spherical micelles. As known from the literature for catanionic mixtures, larger aggregates like wormlike micelles and larger vesicles can be expected.^{112, 113}

To get a deeper insight, cryoTEM measurements were exemplarily performed for six catanionic combinations as described in 3.5.2.3. The cryoTEM pictures were taken at 1 wt% to ensure a higher number of aggregates. The anion-cation mass ratio for each investigated combination was 5-5. The pictures give the possibility to show the real appearance of aggregates in the sample even if the probability of picturing a certain aggregate depended on the statistical presence in the solution. Especially under the consideration that it was expected that different aggregates form, the part of larger aggregates, which could be seen in the cryoTEM, was even lower. Impressions of the observations by cryoTEM are shown in Figure 24.

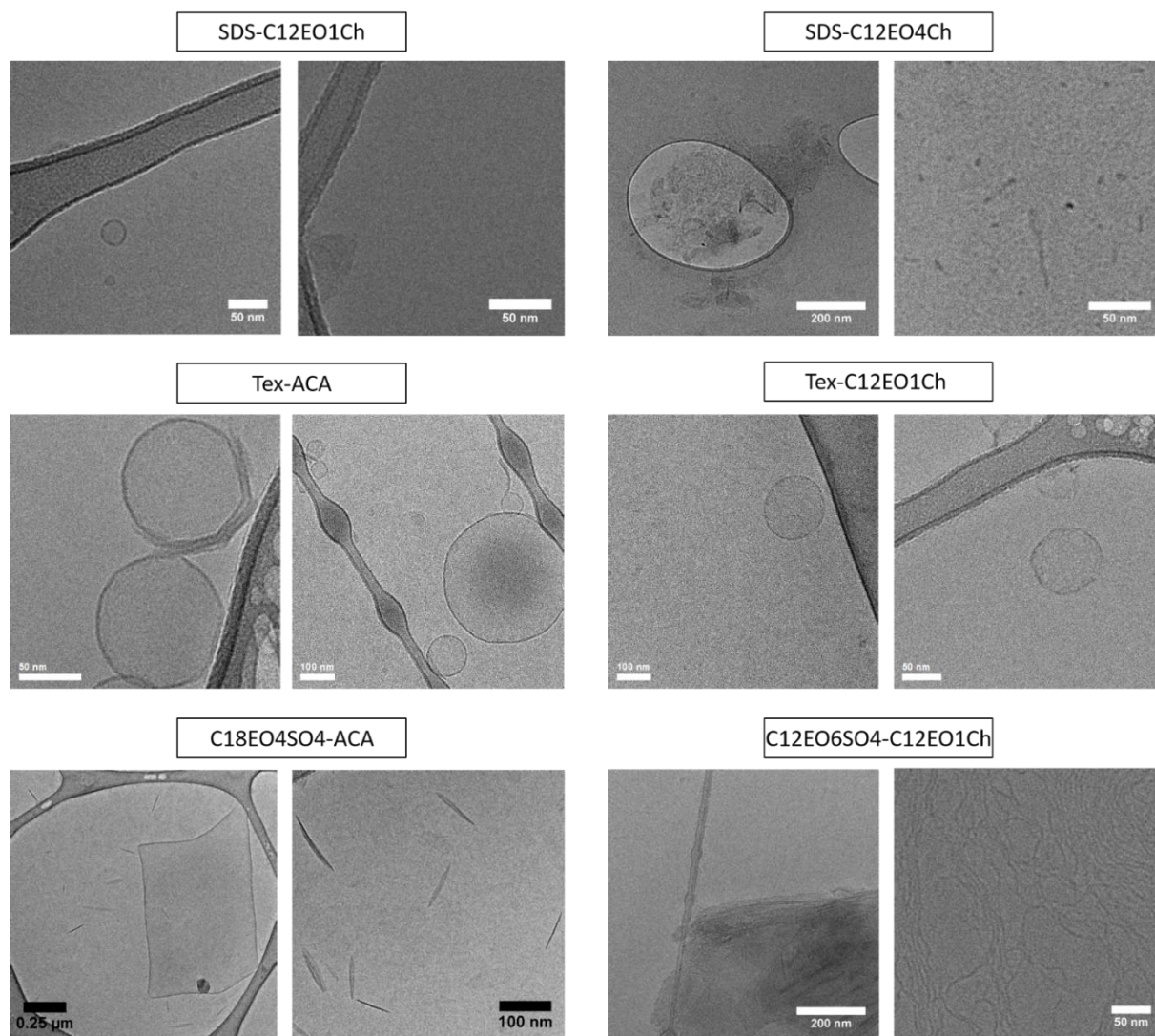


Figure 24: Results of cryoTEM investigations obtained as described in 3.5.2.3 on six catanionic combinations at 1 wt%: SDS-C12EO1Ch (left above), SDS-C12EO4Ch (right above), Tex-ACA (right middle), Tex-C12EO1Ch (right middle), C18EO4SO4-ACA (left below) and C12EO6SO4-C12EO1Ch (right below).

Since only one ratio could be investigated, the pictures could only give a hint towards the aggregation behavior of the catanionic mixtures. Several types of aggregates were observed for all mixtures. The number of visible aggregates was relatively low. In a lot of cases, only undefined widespread aggregates were found. For a defined aggregate to be seen, time-intensive search was necessary. The low concentration was probably responsible for that. For the mixture of SDS and C12EO1Ch, only small amounts of aggregates could be found. Mostly, they were of undefined structure. Several vesicle structures could be found. They were of a size of 20 ± 6 nm and a wall thickness of 2.2 ± 0.2 nm. Under the consideration that only a few aggregates were visible, it was more likely that small micelles that exhibit too little mass to be detected in the cryoTEM were present in the sample. Mostly undefined aggregates were also found for the mixture of SDS and C12EO4Ch. Most likely, they were not the actual structure but artifacts.

Additionally, short worm-like aggregates were present. Again, micelle structures were probably to be present in the solution. Vesicle formation was observed for the combination of Tex and ACA in the cryoTEM. Hints on the multi-lamellar structure were present. The average diameter of the vesicle was 122 ± 60 nm with a wall thickness of 3 ± 0.5 nm. In the cryoTEM for the combination of Tex and C12EO1Ch, very small amounts of vesicles could be seen. But, due to the few numbers, they could not be seen as representative. The average diameter of the vesicles was 81 ± 38 nm with a wall thickness of 3.5 ± 0.8 nm. For the combination of C12EO4SO4 and ACA, 1 wt%, the formation of large and elongated bi-layer phases with a high degree of alignment were visible with an average size up to multiple microns. The aggregate thickness was around 5 nm. For the combination of C12EO6SO4 and C12EO1Ch, very elongated worm-like micelles could be observed. The thickness of them was 3.1 ± 0.5 nm. Similar to SDS-C12EO1Ch and SDS-C12EO4Ch, undefined aggregates were present.

Only six catanionic mixtures out of 150 possible ones were exemplarily investigated. But, already these examples showed a large variety of different structures of different size. Especially, the expected presence of vesicles could be confirmed for most of the mixtures. In most samples, the vesicle appeared together with other structures. In most applications, only one size and shape is

desired for better control. In the case of the cationic mixtures, this seemed not to be the case. An equilibrium between different aggregates could be assumed. It is depicted schematically in Figure 25.

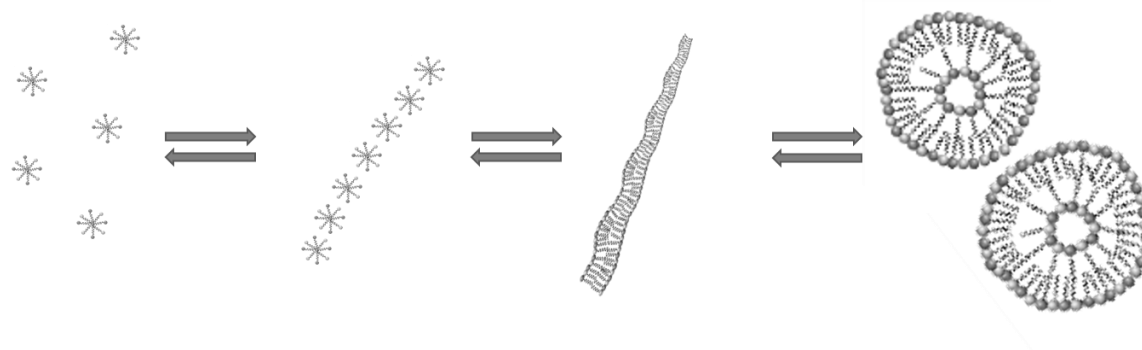


Figure 25: Schematic illustration of the equilibrium state of different aggregates within a cationic mixture.

Micellar structures were likely present in the solution. Due to the packing parameter being close to unity, planar structures were also present in the form of lamellar layers or as vesicles. In the very dynamic cationic systems, all these structures were present. The challenge is to stabilize certain structures while destabilizing undesired ones. This might be possible by tuning the surfactants or the adjustment of external parameters. Deeper investigations on the influence of potential adjustment parameters are necessary. Due to the lack of potential measurement time, this could not be performed within this work, but the presence of a variety of structures can be confirmed.

3.3.7 Cytotoxicity

The toxicity of a compound is a crucial point for any application where human or animals get exposed to it. The tendency of a substance to adsorb onto the investigated organism and to penetrate their cell membranes is found to be the crucial point in the toxic behavior.¹¹⁴ One main advantage of the newly synthesized cationic surfactants is that the choline headgroup for choline is very biocompatible. Normally, cationic surfactants are toxic. The main problem is the hydrophilic part. This leads to the idea to synthesize a cationic surfactant based on a biocompatible headgroup which might have a positive effect. To check this, cytotoxicity tests were performed with the pure cationic surfactants. The determined parameter was the EC50 value, the half maximal effective concentration. It corresponds to the concentration of the investigated substance needed to induce a response halfway between the maximum and the baseline after a certain time, here 24 h.

The measured values with the fitted EC₅₀ values can be seen in Figure 26 (see Experimental 3.5.2.5). As known for cations, the toxicity was high for all three substances compared to anionic or non-ionic surfactants.¹¹⁵ C12EO1Ch was slightly less toxic than the other two cationic surfactants, but all values were in the same range. Comparing the cationic surfactant with the overall same chain length ACA and C12EO1Ch, the influence of the inserted oxygen atoms became visible. C12EO1Ch was slightly less toxic than ACA. But, the difference was not decisive. Especially when compared to biodegradable esterquats where toxicity is a minor problem¹¹⁶, the toxicity of the present cationic surfactants is still high and limit any application.

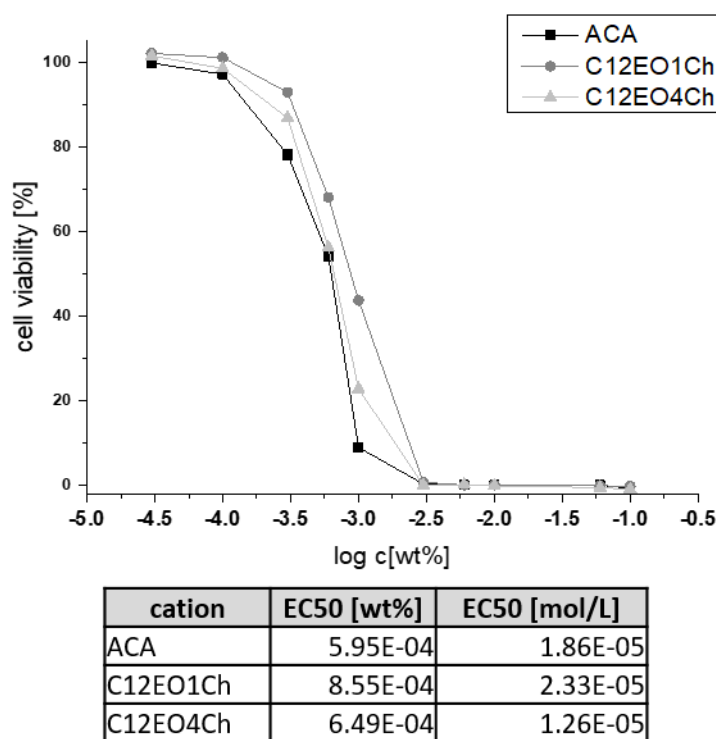


Figure 26: Cytotoxicity tests of the three cationic surfactants ACA (black), C12EO1Ch (dark grey) and C12EO4Ch (light grey) determined with HaCaT cells as described in 3.5.2.5.

The interesting question was the situation of toxicity within the catanionic mixture. Was the toxicity still dominated by the mode of action of the cation or can the interaction with the anionic surfactant reduce the high toxicity of the cationic surfactant? Both cases are reported in the literature. In other cytotoxicity studies, a positive effect could not be shown. Vlachy et al. investigated different combination of quaternary ammonium cations in combination with anionic surfactants with sulfate

and with carboxylate headgroups. A linear trend could not be observed. Already a small amount of cation within the solution gave a significant decrease in the IC₅₀ value.¹¹⁷ The positive effect of the catanionic interaction is considered in the field of pharmaceutical application.¹¹⁸ Their formation of vesicles can enable drug delivery. A catanionic surfactant system was introduced by Isabelle Rico-Lattes and her group, which found industrial application in an eye care product.^{119, 120} They combined a cationic anti-inflammatory active substance with a sugar-based amphiphilic anion. Due to the spontaneous formation of vesicles, the anti-inflammatory activity increases and controlled adsorption into the skin over a longer time scale is possible.

Exemplarily, two catanionic combinations were investigated more intensively. C12EO6SO₄ was set as anionic surfactant. It was combined with C12EO1Ch and C12OE4Ch at different ratios. The toxicity was determined and correlated with the toxicity of the pure cation and the pure anion indicated by a broken line. Figure 27 shows the results.

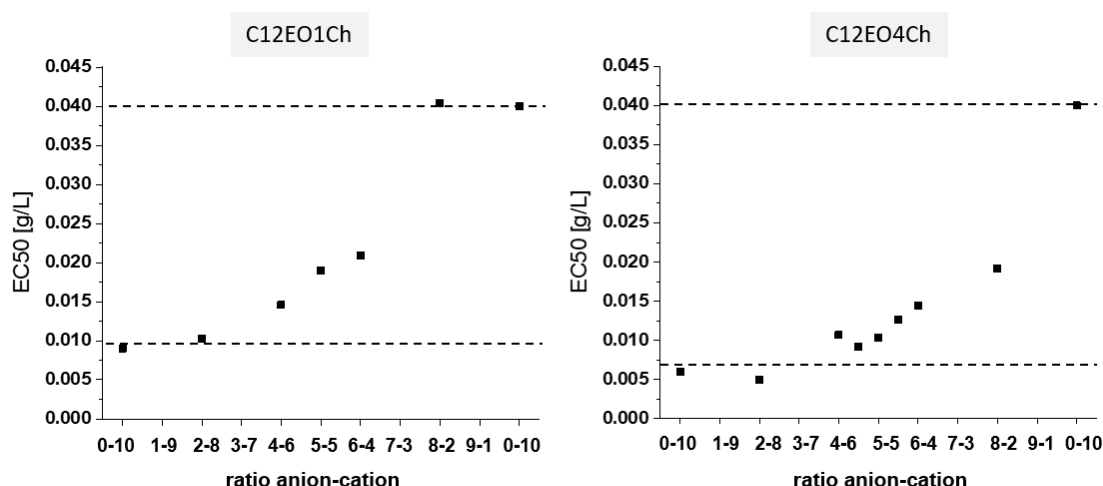


Figure 27: Cytotoxicity measurements as described in 3.5.2.5 of the two catanionic mixtures of the anionic surfactant C12EO6SO₄ and the cationic surfactants C12EO1Ch (left) and C12EO4Ch (right) in comparison with the toxicity of the pure cation (below) and the pure anion (above) indicated by a broken line.

With a value of 0.04 g/L compared to 0.009 g/L for the C12EO1Ch and 0.006 g/L for the C12EO4Ch, the anionic surfactant was by far less toxic. As expected, the toxicity was mainly dominated by the cation. The concentration of the cationic surfactant in the sample of the anion-cation mass ratio 8-2 is already above the determined EC₅₀ value. Thus, in case of maximal toxicity of the cationic surfactant, the EC₅₀ of the mixture should be around the one of the pure cationic surfactants. This

was not observed. A constant “neutralizing” of the cation indicated by a linear increase in toxicity was not measured either. But, the EC50 value increased with increasing amount of C12EOSO4. It did not stay at the EC50-level of the cation. This means that the addition of the anion seemed to have some effect on the cation. The cation did not interact as toxically with the HaCaT cells as it did in pure form. This can be interesting for applications, where contact with cationic surfactant happens.

3.3.8 Statistical analysis

The aim of this chapter was the investigation of the physicochemical properties of the catanionic mixtures and to find any relation between molecular properties and measured the physicochemical properties. Since the volume of data is large, a statistical analysis seems to be an appropriate way for evaluation. For this purpose, the received experimental data have been correlated to molecular properties of the catanionic mixtures with regression analysis, as described in 3.5.2.6. The molecular properties were defined as the following:

- the amount of EO groups in the anion
- the amount of EO groups in the cation
- the alkyl chain length of the anion
- the alkyl chain length of the cation
- the calculated HLB value as described in 3.5.2.6
- the ratio anionic surfactant to cationic surfactant in the catanionic mixture

- the average amount of EO groups in the catanionic mixture
- the average alkyl chain length of the catanionic mixture

The two last points were only considered in the univariate regression analysis. The reason for this is the problem of independence of the molecular properties in the case of multivariate regression analysis. Variables, which are used in the multivariate analysis, must not have any relation to each other. This would be the case since the first four variables are necessary to calculate the last two variables.

Both methods, the univariate and the multivariate analysis, have been performed. Their resulting P-values are calculated. The P-value describes the probability, computed using the test statistics, that measures the support (or lack of support) provided by the sample for the null hypothesis.¹²¹ That means that the smaller the value of P, the more probable it is that the received results are not due to coincidence. If the P-value is below a certain value, the significance level, the test is said to be significant meaning that the correlation of the two variables is not due to coincidence but due to a real connection.

In the present case, the significance value was set to 0.05. The resulting P-values for the univariate regression analysis are shown in Table 1. Green mark indicates values below the significance level meaning the two variables are in direct dependence.

Table 1: Results of the univariate regression analysis between the molecular properties and the determined physicochemical properties of the catanionic mixtures calculated as described in 3.5.2.6.

P-value	molecular property							
Physicochem property	EO anion	EO cation	chain length anion	chain length cation	HLB	molar ratio anion-cation	av. EO number	av. chain length
dyn. surface tension	0.0820	0.1176	0.0085	0.7431	0.0211	0.5165	0.0943	0.0004
solubility	0.0778	0.1389	0.0714	0.1855	0.0563	0.7439	0.0461	0.0878
stat. surface tension	0.2489	0.6845	0.0033	0.0010	0.9991	0.0000	0.0857	0.0041
cmc value	0.0684	0.2045	0.0026	0.0003	0.6643	0.6840	0.2438	0.1666
interfacial tension	0.3143	0.4277	0.4216	0.0135	0.2169	0.1582	0.1581	0.9918
adsorption on SiO ₂	0.0825	0.0056	0.5311	0.7098	0.0449	0.7610	0.0806	0.0392
adsorption on SAM	0.3985	0.1236	0.4351	0.9764	0.6275	0.1977	0.8463	0.6914

Table 1 shows the significance by univariate regression analysis between the molecular properties and the measured physicochemical property. The analysis aimed to point out certain dependencies between these two properties and to give an overall summary of the performed characterization experiments. From those calculations, the following statements can be made:

- The dynamic surface tension depends on the HLB value meaning the ratio of lipophilic and hydrophilic parts in the molecular structure and on the average chain length of the catanionic mixture. From the experimental data in 3.3.5, a higher HLB value and a short alkyl chain correlate to higher dynamics in the solution.
- For the solubility of the catanionic mixture, the average number of EO groups is important. From the experimental data in 3.3.1, the solubility increases with the number of EO groups. This fits to the hypothesis which made EO groups in the molecular structure responsible for the higher solubility of the compound.^{61, 64}
- The reduction of the surface tension depends on the chain length of the anionic as well as on the cationic surfactant. From the experimental data in 3.3.3.1, an optimum of average carbon chain length can be assumed around C14.
- The chain length of the two ionic surfactants also influences the cmc values. As shown in 3.3.2, a longer hydrophobic chain decreases the cmc value. This is known from literature.^{28, 95}
- The interfacial tension against hexadecane depends on the chain length of the cation. If completely dissolved, a long-chain surfactant is more favorable (see 3.3.3.2).
- The adsorption of the catanionic combination on the SiO₂ surface is controlled by the HLB value. For the adsorption on the SAM surface, no dependence can be named. From the experimental data in 3.3.4, no trends can be observed.

Additionally, multivariate regression analysis has been performed for the determined experimental data. Because a dependence between the different independent variables (molecular properties) is not allowed, the two properties 'average EO groups' and 'average chain length' were not considered in the calculation. The resulted P-values are shown in Table 2.

Table 2: Results of the multivariate regression analysis between the molecular properties and the determined physicochemical properties of the catanionic mixtures calculated as described in 3.5.2.6.

P-value	molecular property					
Physicochem. property	EO anion	EO cation	chain length anion	chain length cation	HLB	molar ratio anion:cation
dyn. surface tension	0.0812	0.5743	0.0038	0.8049	0.4263	0.5895
solubility	0.0473	0.3750	0.0266	0.3435	0.9114	0.8061

stat. surface tension	0.0061	0.0127	0.2301	0.0000	0.0000	0.0000
cmc value	0.9267	0.9049	0.0052	0.0001	0.1872	0.7132
interfacial tension	0.8873	0.8257	0.4524	0.0066	0.0352	0.1202
adsorption on SiO ₂	0.0442	0.0139	0.4642	0.9931	0.6619	0.6130
adsorption on SAM	0.0811	0.9403	0.0771	0.8800	0.1402	0.0518

The performed analysis gave the following results:

- The dynamic surface tension depends on the average chain length of the anionic surfactant in the mixture. From the experimental data in 3.3.5, a short alkyl chain is favorable for a higher dynamic in the solution.
- For the solubility of the catanionic mixture, the number of EO groups in the anionic surfactant, as well as its chain length, are the important factors. From the experimental data in 3.3.1, the solubility increases with the number of EO groups and decreases with increasing chain length. A longer carbon chain is known to decrease the solubility^{32, 47}, whereas the insertion of hydrophilic EO groups increases the solubility^{61, 64}.
- The reduction of the surface tension depends strongly on the chain length of the cationic surfactant, the HLB value and the molar ratio of the anionic and the cationic surfactant. From the experimental data in 3.3.3.1, an optimum of surface tension reduction is found around equimolar ratio. Several HLB values seem to be more favorable for a surface tension reduction. Moreover, a longer alkyl chain in the cation, when dissolved, seem to decrease the surface tension.
- The chain length of the two ionic surfactants influences the cmc values. As shown in 3.3.2, a longer hydrophobic chain decreases the cmc value. This is known from literature.^{28, 95}
- The interfacial tension against hexadecane depends on the chain length of the cation and the HLB value. As seen in 3.3.3.2, if completely dissolved, a long-chain surfactant is more favorable. The same counts for a HLB value in the range of 8 to 11.
- The number of EO groups in both ionic surfactants controls the adsorption of the catanionic combination onto the SiO₂ surface. From the experimental data in 3.3.4, a higher number of EO groups correlates with a higher adsorption rate. For the adsorption on the SAM surface, no dependence is observed.

In summary, the two methods of regression analysis give different dependencies for some physicochemical properties. Comparing the results of Table 1 and Table 2, four dependencies match:

- The surface tension of the catanionic mixture depends on the chain length of the cation.
- The cmc value of the catanionic mixture depends on the chain length of the anionic surfactant.
- The cmc value of the catanionic mixture depends on the chain length of the cationic surfactant.
- The interfacial tension of the catanionic mixture depends on the chain length of the cation.

The other significant relationships, which are named in the two analysis (see Table 1 and Table 2) differ. All the named molecular properties will influence the physicochemical property, but the weighting factor is evaluated differently in the two analysis methods. For a concrete statement, the results of the univariate analysis are more suitable. A guarantee that all possible molecular properties are considered in the multivariate analysis cannot be given. Thus, the variables might not be weighted in an appropriate way to each other, leading to a slight divergent result.

3.4 Conclusion

New structures of sulfate-based anionic and quaternary ammonium-based cationic surfactants were synthesized with the focus on the insertion of EO groups into the linear structure of the surfactants. Three cationic surfactants and five anionic surfactants were combined at different ratios and investigated regarding their physicochemical properties at constant conditions (0.1 wt%, 25 °C, millipore water). As reference cation, ACA (trimethyl hexadecyl ammonium chloride) was used. The two newly synthesized cations both consist of an alkyl chain of twelve carbon atoms and a choline headgroup, while they differ in the number of EO groups (one or four EO groups). The reference anionic surfactant was SDS (sodium dodecyl sulfate). Texapon N70 was used as commercially available alkylether sulfate. The three newly synthesized anionic surfactants consist of sulfate as a headgroup and differ in the length of the alkyl chain (twelve and eighteen) and the number of EO groups (four and six).

The solubility of the mixtures was investigated via optical evaluation and via total carbon (TC) measurements. They showed higher solubility than the pure surfactants. Synergistic effects could be confirmed. The additional EO groups in the molecules improved the solubility, especially around equimolar ratio. Higher flexibility in the alkyl chain and higher hydration of the EO groups was named as the reason.

Synergistic effects were also observed during the determination of the cmc. The mixtures showed lower cmc values by at least one order of magnitude. The pseudo-nonionic character of the catanionic combination decreased the cmc. The calculation of the area per headgroups showed the expected decrease in the area per group as the two oppositely charged ions will attract each other by electrostatic interactions. It could be shown that in most cases, a small addition of anionic or cationic surfactant to the oppositely charged one is sufficient. No clear trend regarding the presence of EO groups could be stated.

The same could be observed in the case of interfacial tension against air. A significant decrease in surface tension was found for the mixtures compared to the pure surfactants. Values down to 25 mN/m were detected. This is lower than for commercial nonionic surfactants. Combinations with C12EO4Ch, the cationic surfactant with the highest number of EO groups, were slightly higher in surface tension. Six catanionic combinations were investigated regarding their interfacial tension against hexadecane. A synergistic effect could also be confirmed. For ACA, the lowest values were

received for an excess of the anion. For the other two cationic surfactants, a more symmetric trend was observed with the lowest value around equimolar ratio. The influence of water hardness was tested for one catanionic combination. No significant influence was observed. An increase in temperature slightly decreased the interfacial tension.

Adsorption behavior on two different surfaces, a hydrophilic SiO₂ and a hydrophobic octadecylthiol coated gold surface, were tested for a selection of the catanionic combinations. It could be shown that for the hydrophobic surface the adsorption increases for most mixtures. Nevertheless, the adsorption behavior and especially the amounts remaining on the surface after the washing step depended strongly on the combination. For the hydrophilic SiO₂ surface, the adsorption was higher than on the hydrophobic surface, especially for mixtures of C12EO6SO₄-C12EO1Ch. In average, the adsorption of the mixture only increased for certain combinations. Regarding the adsorbed mass after the washing step, mixtures with ACA seemed to be better than the ones with C12EO1Ch. The presence of water hardness slightly increased the adsorption. Reason for this can be the lower solubility. In the case of adsorbed mass after the washing step, no difference was observed.

The dynamic behavior of the catanionic mixtures depended strongly on the investigated mixture and a general statement is difficult. A longer alkyl chain, at least in the anionic surfactant, leads to a less dynamic system. The presence of EO groups in the anionic surfactant could in some cases compensate the low dynamic of the ACA cation. In mixtures, the combination with a cationic surfactant with fewer EO groups gave best results in most combinations. When an EO group was present in the cationic surfactant, it was not necessary for the anionic surfactant. The determined diffusion coefficients supported most of the statements above. However, especially for C12EO1Ch, the trend for the anionic surfactants did not correspond to the measured dynamic data. Here, the additional influences, like adsorption at the interface, showed their effect.

For the catanionic mixtures, the aggregation behavior was investigated via DLS and cryoTEM for selected combinations. DLS showed an increase in aggregation size around equimolar ratio. In general, the aggregation size was larger than for typical micelles, indicating the presence of larger aggregates. The presence of vesicles, as well as wormlike micelles and larger lamellar undefined aggregates, could be confirmed via cryoTEM. Different aggregates seemed to be present at the same time assuming equilibrium between the structures. For this purpose, under the condition of control over the aggregates, they could be suitable for application, e.g. in drug delivery.

Cytotoxicity tests on HaCaT cells were performed, concentrating on the toxicity of the new synthesized cationic surfactants. The EO groups seemed to have no significant influence. The toxicity of C12EO1Ch was slightly reduced compared to ACA. For C12EO4Ch, the longer chain consisting of the alkyl chain and the EO groups slightly increased the toxicity. Catanionic mixtures were also investigated. Here, the addition of an anionic surfactant to the toxic cationic surfactant lowered the toxicity of the mixture. This indicated an interaction of the anionic surfactant with the cationic one which seemed to prevent the complete effectiveness in toxicity of the cationic surfactant. This is an important aspect when thinking of any application for these catanionic mixtures.

To find general relationships between the molecular properties of the investigated catanionic mixtures and the determined physicochemical properties, a statistical evaluation via linear univariate and multivariate regression analysis was performed. Although the two methods slightly differed, several relations can be stated. The inserted EO groups in the molecule led to a higher solubility and showed positive influence on the adsorption behavior on a SiO₂ surface. The chain length of the surfactants influenced the interfacial properties. A longer alkyl chain correlates to a lower cmc and surface tension value. But, a complete solubility is necessary, which makes the usage of EO groups in the surfactant structure reasonable. The anion-cation ratio is less important regarding the physicochemical properties.

In summary, the newly introduced catanionic mixtures showed synergistic effects regarding several physicochemical properties like cmc value, surface tension reduction, and adsorption behavior. The problem of the low solubility of catanionic mixtures could be solved by the insertion of EO groups into the surfactant structure. In most cases, the addition of a small amount of cationic surfactant to the anionic surfactant was sufficient to achieve high effectiveness. At such low cationic concentrations, the toxicity was still low. This makes the present catanionic mixtures suitable candidates for applications where only small amounts of surfactants and high efficiency are desired.

3.5 Experimentals

3.5.1 Chemicals

SDS ultrapure (purity > 99.9 %) was purchased from AppliChem (Darmstadt, Germany). Hexadecane (purity 98 %) was obtained from Fluka (Switzerland). Texapon N70 (purity 70 %) and the synthesized surfactants are kindly provided by BASF (Ludwigshafen, Germany) from internal synthesis.

Millipore water was used for all experiments, if not mentioned otherwise. All chemicals were used without further purification.

3.5.2 Methods

3.5.2.1 Solubility Measurement

Optical evaluation

Stock solutions with the concentration of 0.1 wt% were prepared for every surfactant. The stock solutions were mixed in the appropriate mass ratio. They were shaken several times and left for equilibration for one week. After that, the samples were evaluated by eye. It was distinguished into four different cases: clear, if the sample was completely transparent; turbid, if the solution was not transparent, but no precipitation could be seen at the bottom of the container; precipitation, if precipitation can be seen at the bottom of the container and bluish, if the solution of the sample was transparent, but has a slightly bluish character.

TC measurement

For the determination of the total carbon content, a TOC-ASI-L from Shimadzu was used. The samples were mixed in the appropriate ratio and left for equilibration for one week. After that, the samples were filtered with a syringe filter with a cut-off at 200 μm . The filtrate was then measured with the named device. The sample was measured three times. If the results were not within the standard deviation, the measurement was repeated until three values were within the deviation range. For calculation of the percentage of solubility, the maximal amount of carbon was calculated based on the results of the pure components and by considering the mass ratio of the sample. The measured value was divided by the calculated value to determine the percentage value.

3.5.2.2 Interfacial tension measurements

Pendant drop measurement

The pendant drop method was used for the determination of the surface tension of the catanionic combinations. A pendant drop tensiometer PAT1M from Sinterface was used for all measurements. The interplay between gravity and surface tension determines the shape of a drop. An analysis of the drop shape according to the Young–Laplace equation (see equation 6) yields the surface tension.

$$\Delta p = \gamma \left(\frac{1}{r_1} + \frac{1}{r_2} \right) \quad (\text{equation 6})$$

Δp : pressure difference, γ : interfacial tension, r_1 and r_2 : radius of the drop

All measurements were performed at 25 °C. All investigated samples were prepared by weighing in the appropriate mass of a stock solution of the pure surfactant. The sample was shaken and then left for equilibration for 24 h. The next day, the sample was measured three times with a washing step before each measurement. The measurement was stopped when a constant value of surface tension was reached. For determination of the value, the average of the last measurement points was taken. Every measurement was performed three times and the average value was taken for evaluation.

Spinning drop measurement

For interfacial tension measurements, a spinning drop tensiometer SVT20 from Dataphysics was used. The capillary was filled with the aqueous phase. A drop of hexadecane was injected into the capillary with a syringe. By applying rotation, a cylindric deformation and thus an increase in interface happens. The interfacial tension counteracts that deformation. The form of the drop at a rotation with the rotational velocity ω can be described approximately by a cylinder. It has rotational energy that decreases with decreasing radius and which counteracts the increasing interfacial energy by the increasing interface. In the equilibrium state, a minimum was reached. The Vonnegut equation was valid and was used for determination of γ :¹²²

$$\gamma = \frac{\Delta \rho R^3 \omega^2}{4} \quad (\text{equation 7})$$

With the density difference of the two phases $\Delta \rho$, the universal gas constant R and the rotational velocity ω .

cmc measurement

A tensiometer (model K100 MK2) from Krüss was used to perform the surface tension measurements. A platinum-iridium plate was used for all measurements. The tensiometer was equipped with a double dosing system (Metrohm Liquino 711). The recording of the surface tension was done automatically as a function of the surfactant concentration. The temperature was kept constant (25 ± 0.5 °C). Every measurement was performed three times and the average value was taken for evaluation.

The surface tension was plotted against the logarithm of the concentration. The cmc was determined by a linear fit of the intersection of the two linear parts of the curve. The surface excess concentration Γ was determined by using the Gibbs adsorption equation for a dilute solution of a completely dissociated surfactant without additional salt:¹²³

$$-d\gamma = RT[\Gamma_A d(\ln c_A) + \Gamma_C d(\ln c_C)] \quad (\text{equation 8})$$

with the anionic surfactant A and the catanionic surfactant C.

Electroneutrality at the surface requires $\Gamma_A = \Gamma_C = \Gamma$ and $c_A = c_C = c$ and equation 8 turns into equation 9. This allows the calculation of the surface excess concentration Γ by taking the slope of the curve at concentrations lower than the cmc.¹²³

$$\Gamma = - \frac{d\gamma}{2RT d\ln c} \quad (\text{equation 9})$$

The area at the surface per molecule A in Å² was calculated from Γ given in mol/m² by the following equation 10, where N_A was Avogadro's number:⁹⁹

$$A = \frac{10^{20}}{\Gamma N_A} \quad (\text{equation 10})$$

Dynamic surface tension

The dynamic surface tension was determined with a bubble pressure tensiometer Sita Science Line T60 from Sita Messtechnik. The investigated solution was prepared the day before, so equilibration was guaranteed. The solution was then filled into a small tube, and the capillary of the device was put into the solution. Before each measurement, the capillary was checked for purity by measuring the

surface tension of pure water. The settings are the same for all measurements. The lifetime of the bubble was set from 0.03 sec to 1 sec. Every measurement was performed twice and the average value was taken for evaluation. The surface tension was given by calculation over the detected pressure. For comparison of the different samples, the value of the decrease of surface tension after a bubble lifetime of 1 sec was taken. The value was determined as it can be seen in Figure 28.

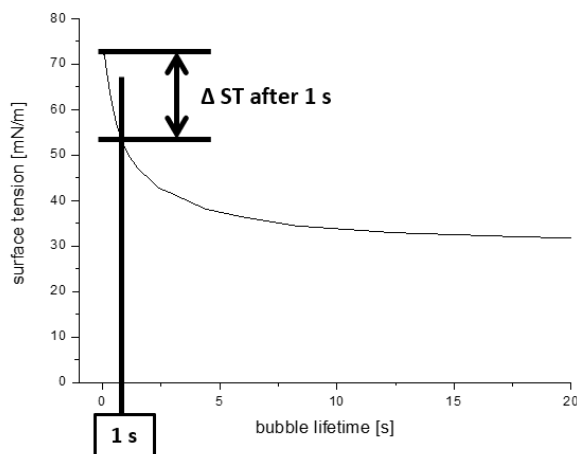


Figure 28: Example of the data evaluation of the maximum bubble pressure tensiometer.

The determination of the effective diffusion coefficient towards the interface was performed as described by Joos and Rillaerts:³⁶

$$\gamma_t = \gamma_0 - 2RTc \left(\frac{D_{\text{eff}} t}{\pi} \right)^{0,5} \quad (\text{equation 4})$$

With the surface tension γ_t at the bubble lifetime t , the surface tension of the pure solvent γ_0 , the universal gas constant R , the absolute temperature T , the surfactant concentration c and the effective diffusion coefficient D_{eff} .

From the measured values, the diffusion coefficient was calculated for each value pair and plotted against the bubble lifetime. For most combinations, no constant value was received. As a comparable value, the maximum of the diffusion coefficient was taken for evaluation.

3.5.2.3 Aggregation measurements

DLS measurement

DLS experiments are performed with a temperature controlled CGS-3 goniometer system from ALV (Langen, Germany) equipped with an ALV-7004/FAST Multiple Tau digital correlator and a vertical-polarized 22 mW HeNe laser (wavelength $\lambda = 632.8$ nm). The samples are measured after 24 h. They are not filtered and used as present in the solution. Measurements are performed at a scattering angle Θ of 90° after thermostating to 25 ± 0.1 °C. Data points were collected for 120 sec. Every measurement was performed three times and the average value was taken for evaluation.

cryoTEM

A Tecnai G2-F20ST microscope from FEI Company, Hillsbroro, USA, with a beam potential of 200 keV at a low dose modus was used for cryoTEM recording. The investigated samples were vitrified with a Plunge Freezer (FEI Vitrobot) with parameters depending on the sample. Then, the samples were examined with the TEM at different magnifications

3.5.2.4 Adsorption measurement

For the determination of the adsorption behavior a quartz microbalance Omega-QCM from QSense was used. The same measurement was performed on two different substrates: SiO₂ quartz and gold quartz covered with 1-Octadecanthiol. Quartz crystals with a silicon dioxide and a gold surface were purchased from QSence and JCM. The investigated gold quartz crystals were put in a 0.001 M solution of 1-octadecanthiol in ethanol overnight. The next day, they were washed with ethanol and dried under nitrogen flow. The pH of the investigated solutions was set to a pH of 6. The procedure of the measurement was the following:

- 30 mins millipore water pH 6
- 60 mins sample solution pH 6
- 60 mins millipore water pH 6

The flow rate of the liquid was 20 μ L/min. Every measurement was performed twice and the average value was taken for evaluation. The fifth frequency was used for the calculation of the mass via

Sauerbrey's equation.¹²⁴ The received mass curves are analyzed towards two parameters. The mass that was absorbed after the step of washing the quartz crystal with the investigated sample solution. It was called $m(\text{ads})$. The second parameter was the mass that remains on the quartz crystal after it was washed with water. It was called $m(\text{rest})$. As an illustration of the parameters, a measured curve with the two parameters was exemplarily shown in Figure 29.

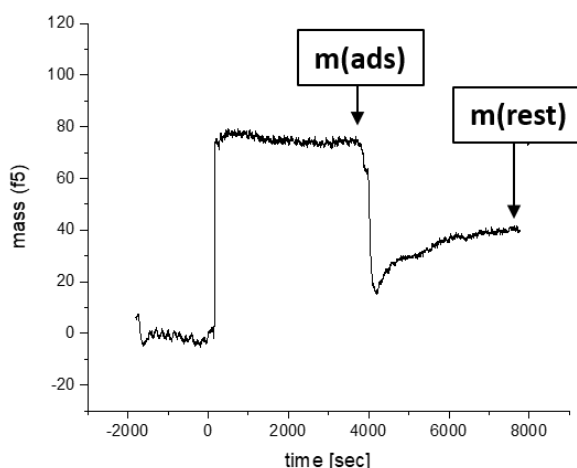


Figure 29: Adsorption curve on a SAM surface of C12EO6SO4-C12EO4Ch, 8-2, as an example of a transformed frequency curve to a mass curve from a QCM adsorption measurement

3.5.2.5 Cytotoxicity

The cytotoxicity of the compounds was determined by a PrestoBlue Assay using human skin keratinocytes (HaCaT cells). The viability of the cells was determined by fluorescence measurements. The cells were seeded in 96 well plates, and each well was incubated with 100 μL of solution (solubilized in cell medium in different concentrations) for 24 hours. Untreated cells are used as negative control. After incubating, sample solutions are removed, 100 μL of the PrestoBlue dyeing solution (1:10 PrestoBlue in PBS⁺⁺ and 0.1 wt% glucose) are added to each well and incubated for approximately 1h. The sample fluorescence was then detected by a microplate reader from Tecan (Männedorf, Switzerland) with an excitation wavelength of 532 nm and an emission wavelength of 600 nm. Every measurement was performed three times and the average value was taken for evaluation.

The EC50 values are determined via a Sigmoidal DoseResponse Fit performed in Origin 2018b.

3.5.2.6 Statistical analysis

For statistical analysis, regression analysis in Excel Office 365 has been used. All experimental data which has been shown in 3.3 were included in the calculation. For the univariate regression analysis, one independent molecular property was correlated with a dependent physicochemical property. For the multivariate analysis, all six independent molecular properties were correlated with one dependent physicochemical property. The P-value was used to evaluate the significance with a significance level of 5 %.

The molecular properties were taken described in 3.3. The molar ratio of anion-cation was determined by dividing the calculated amount anionic surfactant molecules by the calculated amount of cationic surfactant molecules. The HLB value was calculated for each molecule according to equation 1.

4 Towards application: cationics as foaming agents

4.1 Introduction

Walstra defines foam as a dispersion of gas bubbles in a liquid.¹²⁵ They are present in our everyday life in a lot of different situations. Examples are shown in Figure 30. In the kitchen, aqueous foams are present when preparing a mousse, drinking a beer or cleaning the dishes. In the bathroom, we use foaming hair shampoos and setting mousse, and we see foam in our baths. The household is only one example. Foams are also used in a variety of application in industrial sectors. E.g., a fire extinguisher consists of mostly perfluorinated foams.



Figure 30: Examples of foams in our daily life: in the bath, as hair mousse and as cleaning foam for the table tennis racket.

Different from the definition above, the field of foams can be broadened to a variety of different materials.¹²⁶ For example, polymers can be the raw material for solid foams. Their extremely low density is an advantage. Depending on the material and the foam formation, the property of the foam can be adjusted. Polymer foams are used in a lot of different situations: heat isolation of buildings from the outside, noise reduction, sponge for the dish cleaning, and building material for several constructions. Foams made from metals are now also seen as a material with high potential. Due to their excellent stiffness-to-weight ratio, they are used as lightweight structures. Alumina is the preferred material for that, since its foams have ideal preconditions due to their already low density.

Moreover, they allow higher adsorption of kinetic energy. That's why foams are used in the construction of vesicles and machines, e.g. as crash protection in cars.¹²⁷ Foams made of cement are widely used at construction sites for damping. The brick itself can consist of a cement foam, or the cement foam is used at the foundation of the building. In both cases, the damping is increased by the

use of foams compared to homogenous materials.¹²⁸ In the cases mentioned above, foaming is the desired phenomenon. But, there are also situations where foaming is undesired. In some technological processes, foaming is a disadvantage. One example is the pulp and paper industry. Here, foaming of soaps causes problems in the further production process.¹²⁹ Defoaming agents are often used in such cases.

Catanionic mixtures show interesting physicochemical properties which can also be favorable in the topic of foaming. For this purpose, in the following, the investigated catanionic combinations in this work, were investigated towards their foaming behavior. A screening over all combinations was performed as a first step. On that basis, a selection of combinations was exemplarily investigated more deeply with the dynamic foam analyzer.

4.2 Fundamental information

4.2.1 Definition, generation and differentiation

The most commonly known foams are aqueous foams. To produce foam in a liquid, a surface-active material must be present. Surface-active foaming materials in an aqueous medium can be particles, polymers, specifically adsorbed cations or anions from inorganic salts or surfactants. Most times, only very low concentrations are needed to produce foaming.¹³⁰ Foams can be generated by different methods.¹³¹ In general, gas bubbles must be introduced into the solution with low surface tension e.g. by bubbling through a porous frit, shaking or chemical reaction. All methods underlie two basic mechanisms of gas bubble introduction. Either the gas bubbles from the ambient atmosphere are trapped in the solution due to liquid turbulences or the gas bubbles are introduced into the solution by physical or chemical way.¹³²

Foams can be distinguished regarding their geometric structure into 'kugelschaum' and 'polyederschaum'. They differ in the volume fraction ϕ of the gas. If $\phi < 0.74$, the foam is named kugelschaum.¹³³ Small spherical bubbles separated by thick foam lamellas in the aqueous medium are present. They exist mainly in freshly prepared foams. With time, the volume fraction increases to $\phi > 0.74$ due to aging effects. The gas bubbles are no longer completely isolated from each other. A polyhedral foam builds where the bubbles are separated by thin lamellas. Due to capillary forces, the gas bubbles form a structure of equilibrium. This structure is indicated by three polyhedron areas of the gas bubbles connected at a polyhedron border with an angle of 120°. It is called the plateau border.¹³⁰

4.2.2 Stability of foams

All foams show thermodynamic instability. The reason is the high interfacial free energy, which can decrease with rupture. The stability of a foam can be classified into two cases: an unstable foam with a lifetime of seconds and a metastable foam with a lifetime up to hours or days. The crucial point is the used surfactant. Short-chain alcohols and fatty acids show only a short lifetime up to about 20 seconds. A longer lifetime can be achieved with the use of detergents, proteins or long-chain fatty acids. In the case of proteins, the stabilization is due to steric interfacial forces preventing film rupture.

The stability of a liquid foam depends on three different factors: drainage, bubble coarsening and film rupture. Drainage is the crucial factor. The liquid between the bubbles is forced to drain out of the foam by the gravitational force. A separation of the liquid and the foam is the result. Bubble coarsening describes the phenomenon of gas molecules diffusing from smaller gas bubbles to larger gas bubbles due to pressure differences. An average increase in bubble size is the consequence. A higher liquid fraction can slow down the diffusion. Film rupture occurs in dry films when the film thickness is around the average distance between the liquid molecules. If a local void appears due to molecular thermal fluctuation, the film breaks. All three factors are connected. Drainage simplifies coalescence since larger areas of lamellae are in contact. Bubble coarsening increases draining since it concentrates more liquid into a limited number of channels. The growth of bubbles due to film rupture also increases drainage.¹³⁴

If foaming is desired, these factors must be minimized. Several theories about foam stability can be found. A selection of different factors will be presented in the following.¹³⁰

- Bulk viscosity: The bulk viscosity influences the drainage. A higher viscosity of the solution lowers the drainage rate of the foam. An additional solute or an electrolyte can change the viscosity of the solution or form a gel. It decreases drainage.
- Surface viscosity: Increasing the surface viscosity also decreases foam drainage. This can be achieved by a high packing of surfactants or particles in the surface. The addition of high-mass proteins can be an example. Also, using mixed surfactant systems can lead to highly condensed films which stabilize foams. They are therefore called foam builders.
- Adsorbed surfactant: Due to their amphiphilic character, surfactants adsorb at the liquid/gas interface. They control the mechanical-dynamical properties of the monolayer. These are the surface elasticity and the surface viscosity. Surface viscosity describes the speed of the relaxation processes, which restore the equilibrium in the system after imposing stress on it. Surface elasticity is a parameter for the energy stored in the surface layer because of external stress.
- Gibbs/Marangoni effect: An introduced parameter, the Gibbs coefficient of surface elasticity E , describes the increase in surface tension γ for a unit of relative increase in the surface area A in the equilibrium state for thin films:

$$E = 2 \frac{dy}{d\ln A} \quad (\text{equation 11})$$

with the change in surface tension dy and the relative change in surface area $d\ln A$. The factor 2 considers that two film surfaces are enlarged.

E corresponds to the ability of the film to adjust its surface tension if stress is applied. When the surface behavior is described by an elastic and a viscous contribution, E is named surface dilational modulus. It decreases with increasing concentration and increasing film thickness.

- The Marangoni effect considers the situation also for thicker lamellae in dynamic conditions. When a film is exposed to external stress, meaning an increase in surface area, an immediate local decrease in dynamic surface tension occurs. This surface tension gradient leads to a diffusion of molecules from regions of lower surface tension to the region of thinner lamellae. Because of friction resistance, the interlamellae are entrained and therefore 'heals' the disturbance.
- Solid particles: The presence of solid particles in the solution can stabilize the generated foam. According to Pickering, the particles enrich at the interface and prevent coalescence.¹³⁵
- Combination of surfactants: Surfactant mixtures are known to show slower drainage rate and higher foam stability through interfacial cohesion. Reason for this can be the lower cmc values for the mixture, a lowering of the surface tension and/or an increase in surface viscosity.

4.3 Results and discussion

In the following, the foaming behavior of the newly introduced catanionic combinations of this thesis will be investigated. Their structure is based on ethylene oxide (further called EO) groups. A closer description of the anionic and cationic surfactants can be found in 3.3. A screening of all catanionic combinations was performed to select interesting samples for further investigations. The foaming properties of these samples were then analyzed regarding different structural aspects in the surfactant structure.

4.3.1 Pre-screening with the high-throughput robot

In a first step, the foaming behavior of all catanionic components was investigated via a high-throughput robot as described in 4.5.2.1. All combinations were photographed immediately after vigorous shaking for one minute, after two hours and after 24 hours. Also, the effect of water hardness was tested by using 5 °dH water in comparison to millipore water. The pH was adjusted to 6.5 in all measurements. An overview of the pictures is shown in Figure 31. A transparent medium (clear solution or air) led to black color on the picture due to the black background. White color appeared when the light was scattered, either by the turbidity in the solution or the presence of foam. The lighter the whiteness, the denser was the foam. Within each series, the amount of anion decreased from left to right. Due to a large number of different mixtures, a short evaluation based on a general impression will be given in the following.

The evaluation of the foam can be either done by foam stability meaning the foam height over time or by analysis of the foam structure itself. The foam structure can give a hint towards the foam stability since small bubbles and a high density of the foam correlates to higher foam stability.^{126, 131} As for all foams, the foam density was the greatest for the investigated samples right after mixing since over time, each foam will thin out due to several mechanisms described in chapter 4.2.2. Figure 32-A shows this phenomenon for the mixture of SDS and C12EO1Ch, 4-6. Increasing bubble size and lower foam density were detected for the foam density with time. In general, dense foams were observed for the majority of the catanionic mixtures. Especially for the cation C12EO1Ch, the number of mixtures with high-density foams was high. High foam density mostly came along with high foam height. For most mixtures, the maximal measurable foam height was reached. Only, for some mixtures around equimolar ratio, the foam height was lower.



Figure 31: Screening of the foaming behavior of the catanionic combinations via high-throughput robot as described in 4.5.2.1 without water hardness (left) and with 5°dH (right) after 0h (top), after 2h (middle) and after 24h (bottom); the concentration was 0.1wt.% in all samples. The mass ratio of each combination changes from 100 % anionic surfactant on the left to 100 % cationic surfactant on the right.

Low foaming behavior was observed for combinations with the anionic surfactant C18EO4SO4, especially on the anionic surfactant-rich side. The lower solubility, as well as the lower dynamic of the surfactant mixture, could be a reason for that. Although one could argue that lower solubility and the presence of particles in the solution can stabilize the foam¹³⁶, this could not be observed in these cases. With time, all foams thinned out. After two hours, except for combinations with SDS-ACA and Tex-ACA, the foam density was relatively low. This was expected since the bubble size increases and the liquid vanished from the lamellae with time. But, the foam height was nearly the same for the combinations. From the definition, this indicates stable foams. Also after 24 h, several catanionic mixtures showed still maximal foam heights. For the anionic surfactant C18EO4SO4, the foam height after 24 h was very low. All other combinations, at least one ratio had the original foam height. Especially combinations with SDS, Tex, and C12EO4SO4 kept high foam heights.

One point of interest was the influence of the water hardness on the foaming behavior of the catanionic mixtures since in commercial application water hardness is omnipresent. Comparing the pictures on the left side with the right side in Figure 31, the foaming behavior seemed similar and differences were marginal. This was valid for all the three time intervals. The additional presence of ions seemed to have no influence. One reason might be the fact that ions were already present in the solution due to the present counter-ions. A further increase in ionic strength had no influence. The solubility of the mixture was not decreased below the investigated concentration of 0.1 wt%, indicated by no increase of turbidity of the solutions. Consequently, the system itself was not changed significantly and the foaming behavior was the same. It could have been expected that the foaming behavior might be higher with the presence of additional electrolytes in the solution. The addition of salt to a surfactant solution is known to increase the viscosity.¹³⁷ This can have a positive effect on the foam stability. But, in the present case, the concentrations were too low to see such an effect.

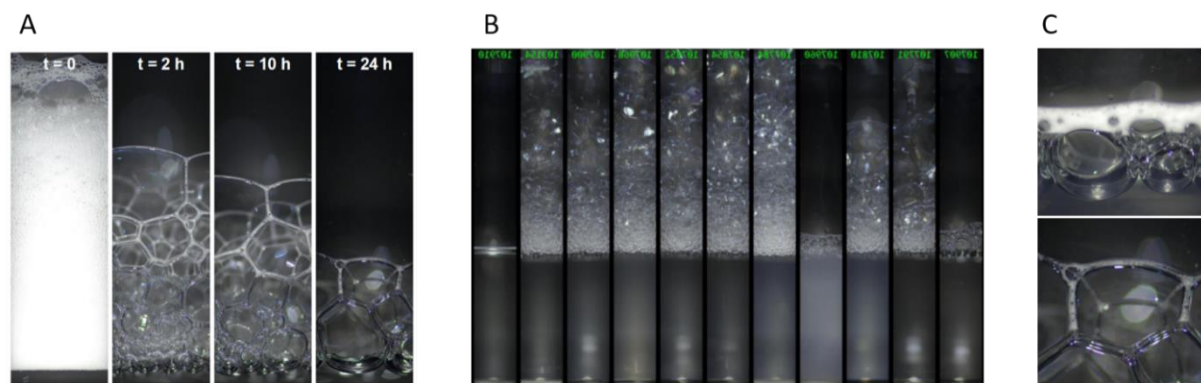


Figure 32: A: time-dependence of the foam structure of SDS-C16EO1Ch, 4-6. B: foam stability of Tex-ACA after 24 h. C: examples for a "foam inside foam" formation from C18EO4SO4-C16EO1Ch 2-8 (above) and SDS-C16EO1Ch 4-6 (below). Pictures were taken from the high-throughput robot as described in 4.5.2.1.

The mixtures of anionic and cationic surfactant showed a higher tendency to form foams than the pure substances. This was the case for all mixtures. Exemplarily, Figure 32-B shows the foaming behavior of the mixture Tex-ACA after 24 h. Here, except for the mass ratio 3-7, the mixtures showed maximal foam height and seemed to be highly stable. The mass ratio 3-7 stuck out of the row. The foaming behavior was significantly lower than for all other ratios. The solution seemed to be slightly more turbid although it was not around equimolar ratio. For some other mixtures, a lower foaming behavior was observed for the ratio around equimolar ratio. In general, the most stable foams were found at the cation- or the anion-rich side. It has been already shown by Varade *et al.* that catanionic mixtures show good foaming behavior. The synergies between oppositely charged amphiphiles can cause higher stability of foams.¹³⁸ Three reasons were named for that: efficient packing at the gas/water interface leading to viscoelastic interfaces, a definite value of the cmc leading to free surfactant molecules, and the formation of vesicles providing bulk viscoelastic properties. All three points were also valid for the investigated systems (see chapter 3.3). Also, Yan *et al.* investigated the foaming behavior of catanionic mixtures. They showed that the combination of a tetradecyltrimethylammonium cation with carboxylates of different chain length had positive effects for several properties, including foaming, compared to a pure anionic surfactant.¹³⁹ A strong interfacial film in water/air interface due to the low surface tension was named as the reason for the good foaming. But, lowering the surface tension and the cmc could not enhance the foaming performance for a carbon chain of more than 10 carbon atoms. They suggested a strong electrostatic

interaction between the cationic and the anionic part, which made a formation of the electric double layer in the interface more difficult.

Moreover, an interesting phenomenon could be observed for some catanionic combinations. Some samples (e.g., C18EO4S-C16EO1Ch 2-8 and SDS-C16EO1Ch 4-6) formed inhomogeneous foams. The lamellae of the larger foam bubbles consisted of very small foam bubbles (see Figure 32-C). It could be described as a “foam inside foam”. An influence on the foam stability was not detected. The foam height decreased with time for the combinations (see Figure 32-A). The foam bubbles seemed to be tightly packed.

Due to a large number of different catanionic mixtures, a selection of mixtures was chosen to perform further investigations for a deeper understanding of their foaming behavior. An overview is shown in Table 3. The selection of catanionic mixtures was made on the basic idea to compare the following different influences:

- the ratio of anionic and cationic surfactant: exemplarily investigated for the mixture SDS-C12EO1Ch. Here, most foams seemed to be stable but differ in foam height and density depending on the anion-cation ratio.
- influence of the structure of the cationic surfactant: for the anion SDS, different cations with the similar ratio were compared.
- influence of the structure of the anionic surfactant: for the cationic surfactant C16EO1Ch, different anions with the similar ratio were compared.
- difference between an unstable and a stable foam with the nearly same catanionic combination: Tex-ACA with the mass ratio 3-7 and 4-6.

The following sections will describe the results of the performed investigations regarding the aspects named above.

Table 3: Overview of the selection of catanionic components for a deeper investigation of the influences on the foaming behavior with the dynamic foam analyzer as described in 4.5.2.2.

anion	cation	ratio	comment
SDS			reference
Tex			reference
C12EO6SO4			reference
	ACA		reference
	C12EO1Ch		reference
	C12EO4Ch		reference
	C16EO1Ch		reference
SDS	ACA	4-6	„worst case“, influence cation
SDS	C12EO1Ch	3-7	influence ratio
SDS	C12EO1Ch	4-6	influence ratio, influence cation
SDS	C12EO1Ch	5-5	influence ratio
SDS	C12EO1Ch	6-4	influence ratio
SDS	C12EO1Ch	7-3	influence ratio
SDS	C12EO1Ch	8-2	influence ratio
SDS	C12EO4Ch	3-7	influence EO, influence cation
SDS	C16EO1Ch	4-6	"foam inside foam", influence cation/anion
Tex	ACA	4-6	stable foam
Tex	ACA	3-7	unstable foam
C12EO4SO4	C16EO1Ch	4-6	stable foam, influence anion
C12EO6SO4	C16EO1Ch	4-6	stable foam, influence anion

4.3.2 Deeper investigations on the foaming behavior of catanionic mixtures

The catanionic combinations, which were selected in the previous chapter 4.3.1, were investigated more closely with a dynamic foam analyzer in the following. For this purpose, the catanionic mixtures were evaluated regarding three characteristics: the total foam height, the liquid volume and the average bubble size of the foam. On the basis of these experimental data, a univariate linear regression analysis was used to determine significant relations between the molecular and physicochemical properties of the catanionic mixtures and the received foam parameters afterward.

4.3.2.1 Foam analysis

Foam analysis was performed with the selected catanionic combinations as described in 4.5.2.2. Three parameters were extracted from the experimental data: the average bubble size of the foam, the liquid volume below the foam and the total height of the foam and the liquid volume. The size of the bubble within a foam over time is a hint towards the tendency for coalescence of the system. The faster the bubbles come together and merge, the faster the foam will be destabilized. The increase in the liquid volume indicates the drainage within the foam lamellae. The faster the liquid flows out of the lamellae, the faster the lamellae thin out. The tendency for coalescence increases. The total height indicates the general foaming behavior of the system. The higher the total height, the more foam was produced. The time-dependent decrease of the total height shows the collapsing of the foam.

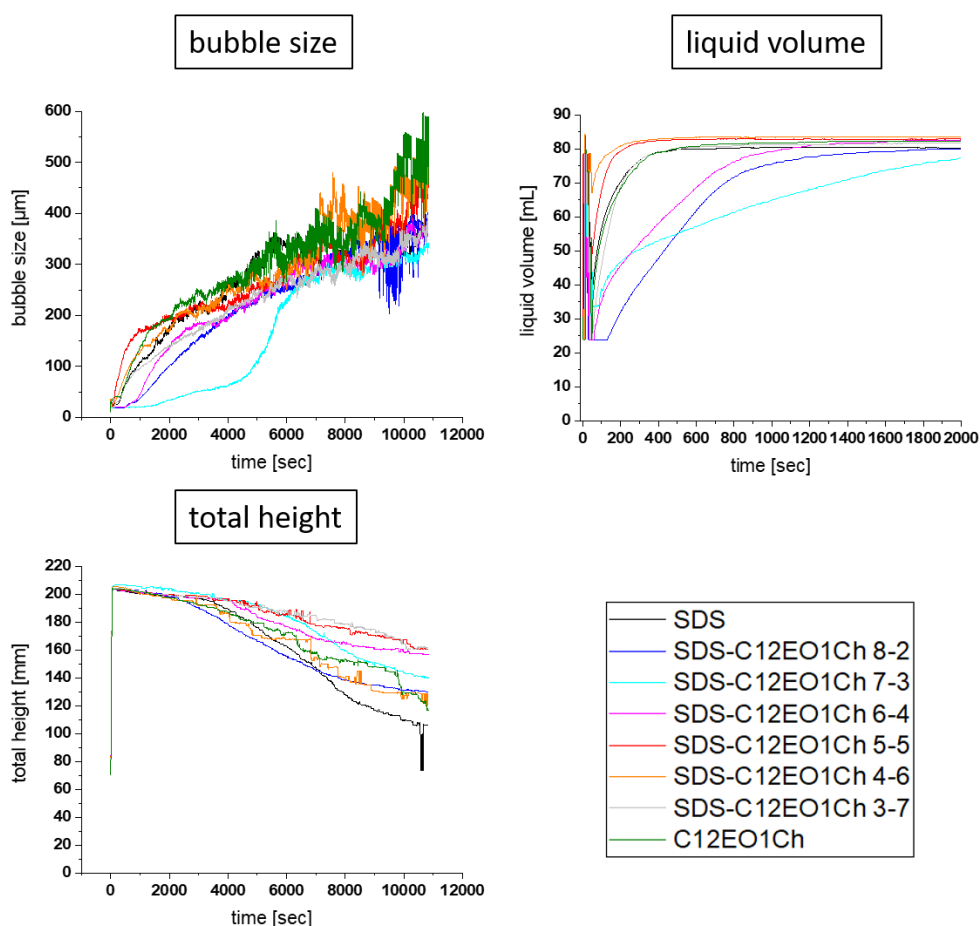


Figure 33: Development of the average bubble size, the liquid volume and the total height of the foam of the catanionic combinations SDS-C12EO1Ch at different ratios measured with the dynamic foam analyzer as described in 4.5.2.2.

Figure 33 shows the measured foaming parameters of the catanionic mixture SDS-C12EO1Ch at different ratios. A pronounced viscoelastic behavior was observed for the two ratios 7-3 and 6-4 by simply swiveling. The total height decreased for all samples, but most intensively for the pure surfactants. The extent of decrease for the samples differed from $\sim 24\%$ for the ratios 3-7, 5-5 and 6-4 to nearly 50 % for the pure anion SDS. The foam stabilizing effect of anion-cation mixtures could be confirmed as it has been already reported in the literature.^{138, 139} No dependence on the anion-cation ratio could be stated for the total foam height. For the bubble size and the liquid volume, three combinations showed outstanding behavior. The combination SDS-C12EO1Ch, 7-3, formed very small bubbles which did not strongly increase for 4000 sec. Also, the liquid volume increased the slowest. A similar, but not as decisive, behavior was observed for the ratios 8-2 and 6-4. Although for the mass ratio 8-2 a pronounced viscoelastic behavior could not be observed with a short swiveling test, this could be the common property, which differentiates the three ratios from the others. Viscoelastic behavior of the bulk phase is known to stabilize foams since the liquid in the lamellae cannot flow down as fast as in a more liquid bulk phase. It hinders the coalescence of the bubbles and thus stabilizes the foam.¹³⁰ Figure 34 depicts the bubble size and the foam structure for this combination. Indicated by a green framing, the pictures of the foam of the three ratios confirmed the measurement data.

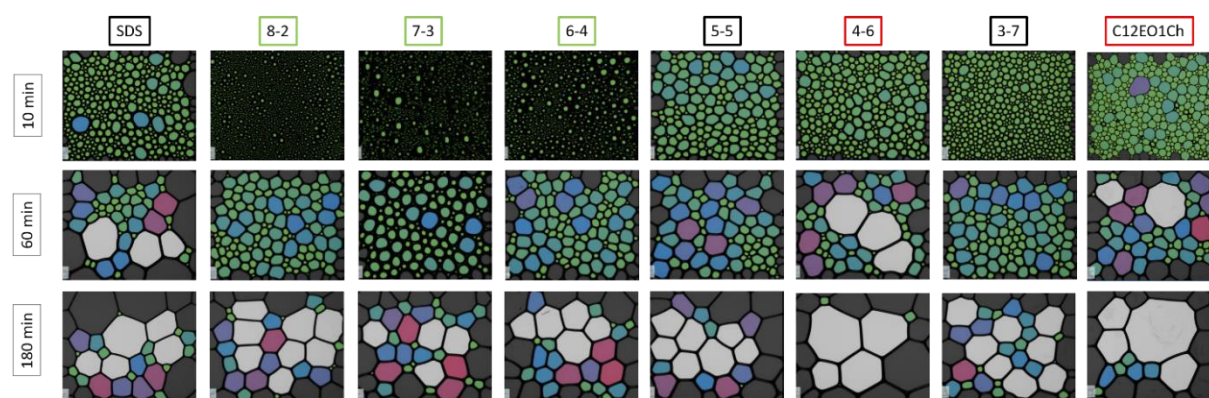


Figure 34: Foam structure and bubble size of the investigated samples of the catanionic mixture of the anion SDS and the cation C12EO1Ch at different ratios detected with the dynamic foam analyzer from Krüss as described in 4.5.2.2.

Very small bubbles were observed, which did not grow significantly within the first hour. Also after 3 hours, the bubbles were smaller than for the other ratios. The importance of the bubble size was also shown for the mass ratio 4-6 (red framing). Here, the bubble size increased quickly. Consequently, the liquid volume increased too, and the total height decreased most. The presented data showed the

viscoelasticity to be one reason for stable foams. As Ferreira *et al.* could show in their research, the bulk self-assembly and the foaming properties can be related to each other. A higher viscosity prevents foam drainage.¹⁴⁰ With a changing ratio, the properties of the bulk solution of the catanionic mixtures can be tuned and either a stable or an unstable foam can be obtained. This was also found by Fauser *et al.* when they investigated the foaming behavior of SDS-CTAB mixtures in relation to the anion-cation ratio.¹⁴¹ They concluded a dominating effect of the stoichiometric catanionic complex on the surface adsorption, which was influenced by an excess of one surfactant of these free molecules.

For investigating the influence of the cationic surfactant, the four cations were combined with the same anion SDS and analyzed regarding their foaming properties in Figure 35. Compared to the pure anionic surfactant, all four mixtures formed a more stable foam.

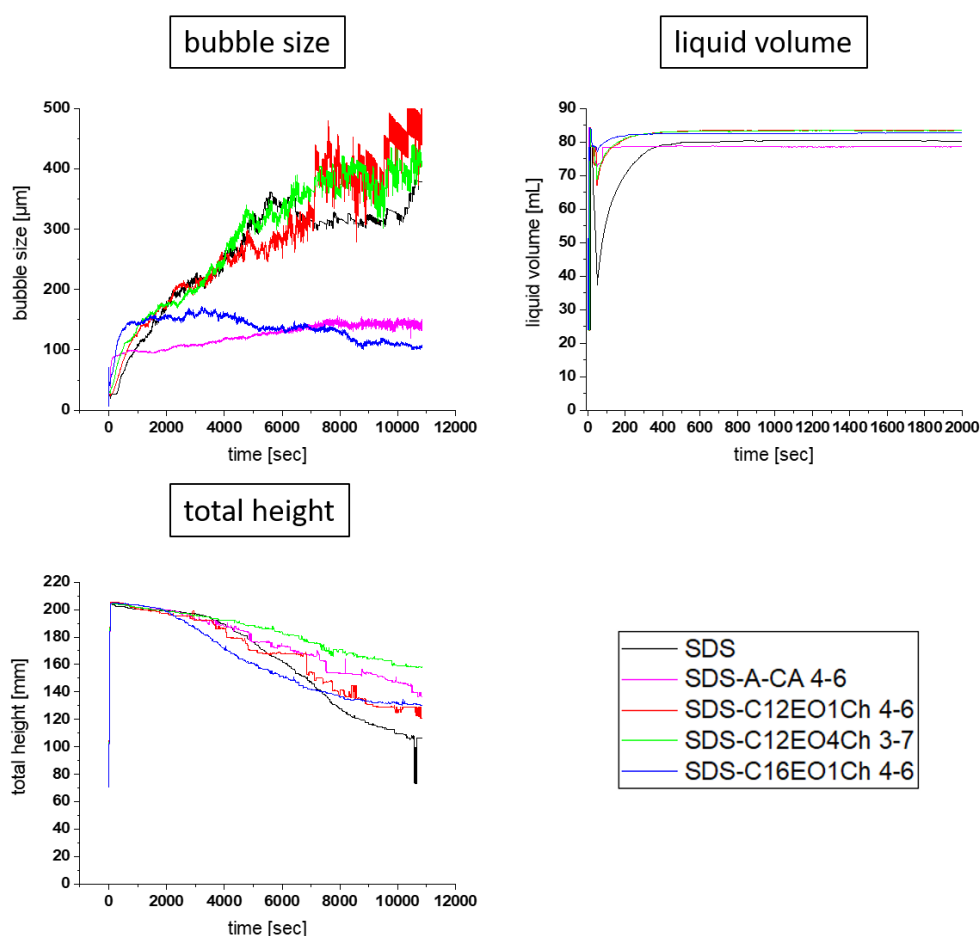


Figure 35: Development of the average bubble size, the liquid volume and the total height of the foam of the catanionic combinations with SDS as anionic surfactant and the four different cationic surfactants ACA (purple),

C12EO1Ch (red), C12EO4Ch (green) and C16EOCh (blue) measured with the dynamic foam analyzer as described in 4.5.2.2.

The development of the liquid volume within the samples did not change much indicating thin lamellae. The total foam height was in a small range of 25-33 % decrease for all samples with SDS-C12EO4Ch having the highest foam level. In the case of the bubble size, the four combinations could be divided into two groups. ACA and C16EO1Ch formed a foam together with SDS with constant bubble size of 100-120 μm , which stayed constant with time whereas the bubble size of SDS with C12EO1Ch and C12EO4Ch increased continually with time. The four samples did not differ in their viscous behavior, but their solubility. The first pair showed lower solubility, indicated by a more turbid solution. Especially for SDS-ACA, the solubility was very low and precipitated particles could be seen. Crystalline particles might have formed and could stabilize the bubbles via a Pickering stabilization.¹⁴² For the combination of SDS and C16EO1Ch, the solubility was higher, but still not in the range of complete solubility. Here, another aspect could come into play. The combination was one of the examples for the foam-inside-foam phenomenon. From the experimental data, no significant difference compared to other samples, where this phenomenon was not observed, could be found. The bubble size stayed in the range of SDS-ACA. But, due to higher solubility of SDS-C16EO1Ch, less solid particles of the combination can be expected in the solution. Thus, foam stabilization due to solid particles according to Pickering cannot be as pronounced as for SDS-ACA. An additional stabilizing factor, the formation of foam between the larger foam bubbles, could support the isolation of the bubbles. This could hinder coalescence. Normally, foam stability can be correlated with a slow increase of the bubble size. This could not be stated here since both, small and large; bubbles seemed to have the same effect. Maybe over a longer timescale, this would become obvious.

The same observation could be made in the case of changing the anionic surfactant with the same cationic surfactant C16EO1Ch (see Figure 36). The cationic surfactant itself had low solubility in water due to its long alkyl chain. The combination with SDS improved the solubility slightly, but it was still low. The two anionic surfactants C12EO4SO₄ and C12EO6SO₄ with EO groups in the molecular structure increased the solubility. Again, for these two combinations, the bubble size increased with time whereas, for the other two samples, it stayed more constant. The lamellae of the foam of all samples were very thin since the liquid volume came back to the original value within a very short time. The total height could, therefore, be directly transferred to the foam height. Here, the mixtures showed a better result than the pure cationic surfactant. The stabilization of the bubbles by the combination SDS-C16EO1Ch could not be seen concerning the foam height. It showed the same trend

as C12EO4SO4. The anionic surfactant C12EO6SO4 decreased the foam height the least. The combination seemed to stabilize the foam and prevented foam collapsing even after merging of the bubbles.

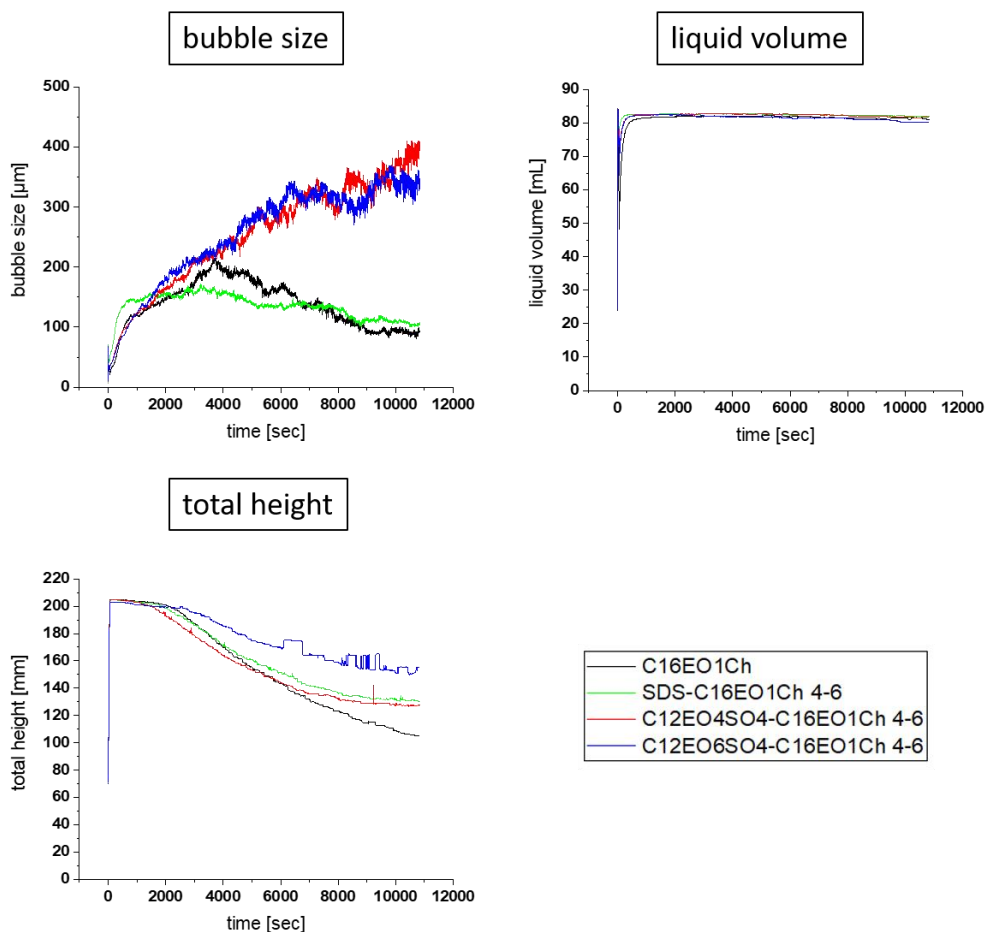


Figure 36: Development of the average bubble size, the liquid volume and the total height of the foam of the catanionic combinations with C16EO1Ch as the cationic surfactant and the three different anionic surfactants SDS (green), C12EO4SO4 (red) and C12EO6SO4 (blue) measured with the dynamic foam analyzer as described in 4.5.2.2.

In Figure 37, two samples with similar composition but different foaming behavior are compared. Again, both catanionic mixtures showed more stable foams than the pure surfactants. In the screening, the mass ratio 3-7 showed significantly lower foaming than the mass ratio 4-6. In the total height in this analysis, the trend was the same. But the difference was not decisive with 5 %. The liquid volume was in the same range for all samples, but the pure surfactants even retained the liquid slightly

better. The bubble size was larger for the pure surfactants. But also, the bubble size could not be correlated to the foam height.

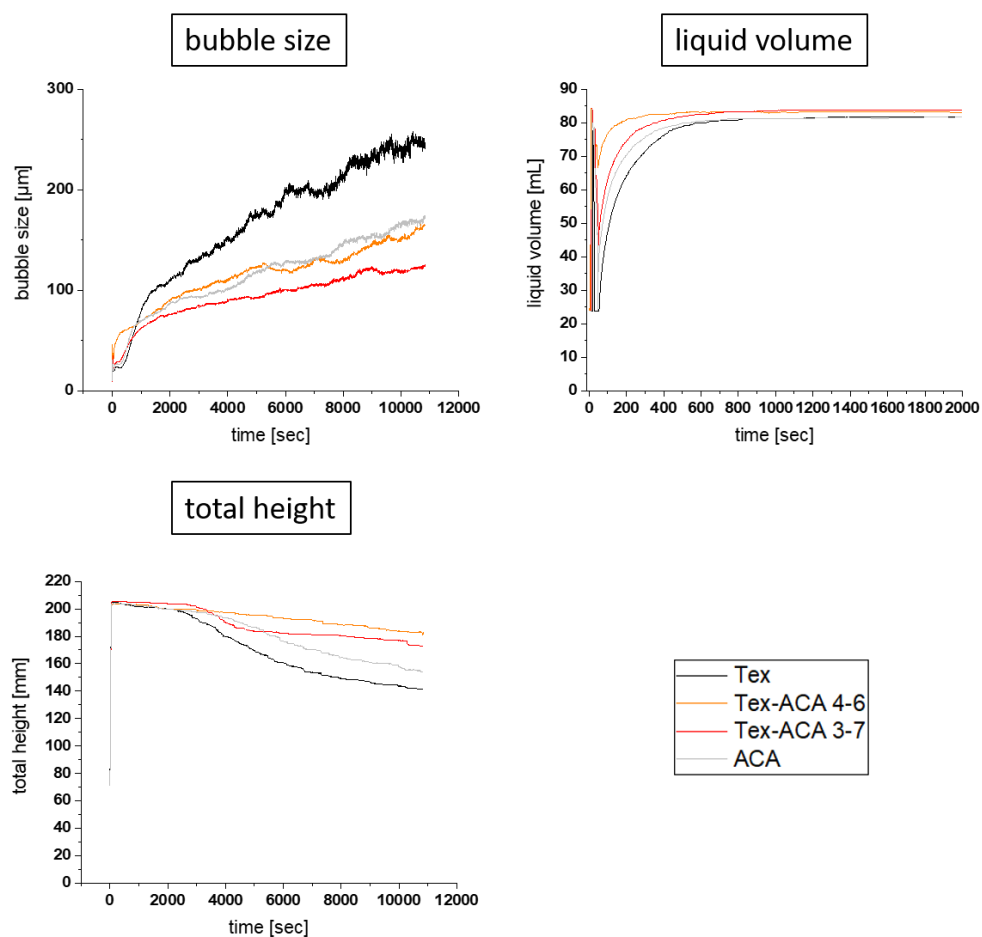


Figure 37: Development of the average bubble size, the liquid volume and the total height of the foam of the catanionic combinations of Tex and ACA at the two anion-cation ratios 4-6 (orange) and 3-7 (red) in comparison to the pure ionic surfactant Tex (grey) and ACA (black) measured with the dynamic foam analyzer as described in 4.5.2.2.

4.3.2.2 Statistical analysis

From the performed measurements with the dynamic foam analyzer, several trends and influences could be summarized with the help of the comparison of different data sets. For a general evaluation, statistical analysis in the form of linear regression analysis as described in 4.5.2.3 was applied to the experimental data. The aim was to find significant relations between the received experimental observations and molecular and physicochemical properties of the catanionic mixtures. For each of

the three parameters (total foam height after 3 h, liquid volume after 5 mins and average bubble size after 2 h), a univariate linear regression was performed. The received P-values were assessed with the significance level of 5 % and marked with green if a significant relation was calculated.

The calculated P-values for the total foam height after 3 h regarding the molecular and physicochemical properties are shown in Table 4. Below a value of 0.05, the relation between the two investigated variables is regarded as significant meaning the received experimental results are not due to coincidence but dependence on each other.¹²¹ For the present case of the total foam height, a significant relation was found only for the physicochemical property of the surface tension. The low surface tension of the solution led to a higher foam level. A high surface activity correlates to an effective packing of the surfactants at the interface.⁹⁵ The energy needed to create larger surfaces depends on the surface tension. A low surface tension facilitates the making of foams.¹⁰⁹ It can be noted that low surface tension is favorable for foamability. But there are also other factors influencing the foamability (see 4.2.2), which were not considered in the calculations.

Table 4: P-value results of the univariate regression analysis between the molecular physicochemical properties and the determined total foam height after 3 h (measured as described in 4.5.2.2) of the catanionic mixtures calculated as described in 4.5.2.3.

P-value	molecular properties		
	EO anion	EO cation	average EO
	0.1509	0.6694	0.4250
P-value	chain length anion	chain length cation	average chain length
	0.1509	0.3339	0.2637
P-value	HLB	molar ratio anion-cation	
	0.1150	0.5062	
P-value	physicochemical properties		
	solubility	surface tension air	dynamic surface tension
	0.5614	0.0207	0.5395
P-value	cmc	interfacial tension	
	0.0762	0.5614	
P-value	adsorption SiO ₂	adsorption SAM	
	0.9862	0.4104	

The same statistical analysis (see 4.5.2.3) was performed for the liquid volume of the foam after 5 min. The calculated P-values are given in Table 5. For this foam characteristic, no significant dependence of any molecular or physicochemical property could be obtained. The liquid volume of the foam is the

result of drainage.^{126, 134} It can be slowed down by several factors, like e.g. increasing viscosity.¹³⁰ But, based on performed experiments, the investigated properties belong not into this group of factors.

Table 5: P-value results of the univariate regression analysis between the molecular physicochemical properties and the determined liquid volume (measured as described in 4.5.2.2) of the catanionic mixtures calculated as described in 4.5.2.3.

P-value	molecular properties		
	EO anion	EO cation	average EO
	0.7090	0.6129	0.1814
	chain length anion	chain length cation	average chain length
	0.7090	0.7090	0.0925
	HLB	molar ratio anion-cation	
	0.6667	0.1505	

P-value	physicochemical properties		
	solubility	surface tension air	dynamic surface tension
	0.6583	0.4366	0.4623
	cmc	interfacial tension	
	0.5361	0.6583	
	adsorption SiO ₂	adsorption SAM	
	0.7411	0.5311	

The statistical evaluation was also done for the average bubble size of the foam after 2 h. As it can be seen in Table 6, three properties were found to be in significant relation to the bubble size: the number of EO groups in the cationic surfactant, the average chain length and the HLB value. The bubble size in the foam indicates the process of destabilization of the foam. The smaller the bubbles in the foam, the more is its resistances against destabilizing process like Ostwald ripening and coalescence.^{125, 126} Regarding the influence of the molecular properties on the bubble size, a lower number of EO groups in the cationic surfactant and a longer average chain length of the surfactants are favorable. The reason can be that under these conditions the solubility is smaller (see 3.3.1). The higher crystalline character can promote the stabilization of the bubbles like it is known for solid particles.^{136, 143} The third significant property is the HLB value. A smaller HLB value correlates with a smaller bubble size. A small HLB value indicates high lipophilicity in the molecule.²⁰ This fits the two parameters. A small number of EO groups and a long chain length leads to a higher HLB value.

Table 6: P-value results of the univariate regression analysis between the molecular physicochemical properties and the determined average bubble size (measured as described in 4.5.2.2) of the catanionic mixtures calculated as described in 4.5.2.3.

P-value	molecular properties		
	EO anion	EO cation	average EO
	0.7152	0.0024	0.0564
	chain length anion	chain length cation	average chain length
	0.7152	0.7152	0.0000
	HLB	molar ratio anion-cation	
	0.0002	0.6242	

P-value	physicochemical properties		
	solubility	surface tension air	dynamic surface tension
	0.8056	0.7730	0.3806
	cmc	interfacial tension	
	0.6893	0.8056	
	adsorption SiO ₂	adsorption SAM	
	0.1316	0.9813	

A multivariate analysis was not performed with the experimental data, since no complete data set was available for all catanionic mixtures. An analysis with fewer properties did not make sense since a comparison would not have been possible.

4.4 Conclusion

The catanionic combinations were tested regarding their foaming behavior. To this purpose, a pre-screening was performed with a high-throughput robot. In general, the samples showed very high foaming behavior and kept the original foam height for at least 24 h. For all samples, an expected thinning of the foams was detected. Combinations with the cation C12EO1Ch showed the highest foam density right after mixing. Low foaming was observed for mixtures with the long-chain anion C18EO4SO₄. For all combinations, a positive effect of the catanionic mixtures compared to the pure surfactants could be observed. In some cases, the foaming was lower around the equimolar ratio. The presence of water hardness had no significant influence on the foaming behavior. For some samples, a phenomenon described as “foam-inside-foam” could be observed.

Deeper investigations were performed with a dynamic foam analyzer. Here, selected catanionic combinations were examined regarding the three parameters: total foam height, liquid volume, and average bubble size. It was focused on four aspects. First, the mixture of SDS and C12EO1Ch was investigated regarding the effect of the anion-cation ratio. A concrete influence could not be found, but it could be stated that the foam stability depended less on the anion-cation ratio but was strongly influenced by the viscoelastic property of the bulk solution as it was present for the ratios 8-2, 7-3 and 6-4. Here, the bubble size, especially at the beginning but also over time, was very small. The viscoelastic property prevented coalescence. Second, the four different cations were compared with the same anion SDS. The samples seemed to behave similarly but showed differences in the average bubble size. ACA and C16EO1Ch kept a constant bubble size whereas C12EO1Ch and C12EO4Ch increased steadily. A stabilization mechanism according to Pickering was suggested as both mixtures show lower solubility.

Additionally, for C16EO1Ch, the foam between the bigger bubbles could stabilize the foam. Third, three different anionic surfactants, SDS, C12EO4SO₄, and C12EO6SO₄, were compared with the same cationic surfactant, C16EO1Ch. Similar observations as for the variation of the anionic surfactant regarding the effect of lower solubility were made. The mixture with SDS showed a constant bubble size. At last, two similar mixtures but with very different foaming behavior were compared: Tex-ACA with the mass ratio 3-7 and 4-6. In the pre-screening, the mass ratio 4-6 showed a high foaming tendency whereas 3-7 did not. The trends could not be confirmed with the dynamic foam analyzer.

Better foaming was observed for both mixtures compared to the pure surfactants. No significant difference could be observed for the two tested catanionic mixtures.

Since at first glance, a statement about the effects of the molecular and physicochemical properties on the foaming properties was difficult, a statistical analysis was performed. Each of the three parameters (total foam height, liquid volume, average bubble size), the significance of the relation to molecular and physicochemical properties were checked. For the total foam height, significant dependence on the surface tension reduction was obtained. The low surface tension of the solution led to a higher foam level. No property could be correlated to the liquid volume of the foam. For the average bubble size, a significant relation to the number of EO groups, the average chain length, and the HLB value was determined. A lower number of EO groups in the cationic surfactant, a longer average chain length of the surfactants as well as a smaller HLB value correlates with a smaller bubble size.

In summary, the catanionic combination showed promising foaming behavior, especially when compared to the pure surfactants. The viscoelastic property could be confirmed to be a crucial factor for foam stability. Also, the lower solubility of the catanionic mixture led to better stabilization of the foam bubble due to Pickering mechanism. The understanding of the foaming behavior is complex and requires deep investigations. Within this chapter, some interesting samples could be pointed out, and some interesting aspects could be shown. But, for a general understanding and the possibility to modify the catanionic mixture for certain applications, further investigation methods are necessary.

4.5 Experimentals

4.5.1 Chemicals

SDS ultrapure (purity > 99.9 %) was purchased from AppliChem (Darmstadt, Germany). Texapon N70 (purity 70 %) and the synthesized surfactants were kindly provided by BASF (Ludwigshafen, Germany) from internal synthesis. Calcium chloride dihydrate (purity >99 %) was bought from Roth (Karlsruhe, Germany). Solutions of 1 M sodium hydroxide and hydrochloric and magnesium chloride hexahydrate (purity 99 %) were from Merck (Darmstadt, Germany).

Millipore water was used for all experiments, if not mentioned otherwise. All chemicals were used without further purification. Water hardness was prepared by weighing appropriate amounts of CaCl_2 and MgCl_2 into millipore water.

4.5.2 Methods

4.5.2.1 High-throughput robot

A high-throughput robot from BASF, Ludwigshafen, was used for all steps. The preparation of the mixtures was done by mixing the appropriate amounts of stock solutions (0.1 wt% in DI-water and 5.0 °dH) prepared from surfactant stock solutions with the concentration of 0.75 wt%. The pH was adjusted to 6.5 with NaOH or HCl solution). Foam generation was done by vigorous shaking of the samples for 1 min. Image analysis was performed in front of a black background after the time of $t = 0$ h, 2 h, 24 h after preparation.

4.5.2.2 Dynamic foam analyzer

A dynamic foam analyzer DFA100 from Krüss was used for the analysis of foaming behavior. For each test, 80 mL of a surfactant solution with a concentration of 0.1 wt% in distilled water, pH 7, was filled into the foam analyzer. All measurements were performed at 23 °C. The foam was generated by putting air through a frit with the pore size of 12-15 μm with a frequency of 0.2 L air per minute. The foaming step was performed until a foam height of 200 mm in total height was reached. Each test lasted three hours in total.

The following parameters were monitored:

- foam height
- liquid height
- average bubble size

4.5.2.3 Statistical analysis

For statistical analysis, regression analysis in Excel Office 365 was used. All experimental data which has been determined in 3.3 as well as the molecular properties, which are closer described in 3.3.8, were included in the calculation. The molar ratio of anion-cation was determined by dividing the calculated amount anionic surfactant molecules by the calculated amount of cationic surfactant molecules. The HLB value was calculated for each molecule according to equation 1. For the univariate regression analysis, one independent molecular property was correlated with a dependent physicochemical property. For the multivariate analysis, all six independent molecular properties were correlated with one dependent physicochemical property. The P-value was used to evaluate the significance with a significance level of 5 %.

5 Towards application: cationics as detergents for fat removal

5.1 Introduction

A turnover of multi-billion US dollars a year indicates the importance of the cleaning market worldwide. Laundry cleaning products contribute the largest part to this market. They are developed for different applications, like the cleaning of clothes or the removal of dirt from dishes (see Figure 38). With a content of 15 to 40 % of total cleaning formulations, surfactants play the main part in this sector of industry, especially anionic surfactants.^{98, 144} The demands on surfactants are high: they must be sufficiently soluble and must not lose their function under all applied conditions. They should be cheap and should have high and flexible performance for the different applications. Due to new environmental regulations, consumer habits or practices, the evolution of anionic surfactants on the cleaning market is an ongoing process.¹⁴⁴



Figure 38: Examples of applications for cleaning products in a typical household.

Carboxylates, commonly called soaps, have been used for thousands of years. They have been the first anionic surfactants used for cleaning.¹⁴⁵ The first sulfates used for cleaning have been natural alcohol sulfates. They were derived from natural oils and first reported in 1932 and distributed as Dreft® in 1933.¹⁴⁶ Alkyl benzene sulfate, ABS, was developed in 1947 based on products from the petroleum industry. ABS was the main component for cleaning formulation until 1961 when environmental legislation stopped its way of success due to its low biodegradability. Based on ABS, a new molecule, the linear alkyl benzene sulfonate (LAS), was produced to fulfill the standards. Methyl ester sulfonates (MES) are another group of surfactants. They are derived from natural resources and were introduced into the market in the 1980s, but could never reach the volumes of LAS and other alcohol sulfates. Linear alcohol ethoxylated sulfates (LES) were the answer to the demand for higher solubility at cold and hard water conditions, which could not be fulfilled with the so far used LAS. But, for the price of better solubility, the surface activity of LES is lower than that of LAS.¹⁴⁴

Nowadays, new demands are challenging the cleaning industry. The awareness of energy and environmental saving in the population is becoming more and more distinctive. Washing laundry is a daily issue in most households. In the German region, 164 washing cycles per year for an average household are typical.¹⁴⁷ Consumption of electricity, water, chemical substances and process time are topics, where research can improve the present situation. Especially in Western Europe, the average washing temperature is very high compared, e.g., to Asia, where washing is normally performed without any heating. In the German region, the lowest possible washing program still has 30 °C. The average washing temperature in Germany is 46 °C.¹⁴⁸ Although, nearly each washing machine sold in Europe is at least of energy label “A”, energy saving due to lower washing temperature is the main issue for the future. The water consumption mainly depends on the technical standard of the washing machine and the habits of the user. Since about 10 % of a household’s water consumption comes from washing clothes, this amount is not negligible. As in our regions, the availability of water is not limited, the reduction of water consumption is mainly a factor of energy saving since all the amount of water has to be heated up in the washing procedure.¹⁴⁹

The efficiency of the washing process can also be improved by the used chemicals. One main aim of today’s research is the investigation of surfactants with higher efficiency at a lower concentration. Nevertheless, the environmental tolerance of the compounds should be guaranteed. There are several strategies towards this: One possibility is to change the complete washing system. However, this can only be realized if the washing performance is several times better than before. Another possibility is to develop and add substances, which can improve the washing results already at small amounts. This would be a more realistic implementation.

This is the basic idea of the present chapter. The newly synthesized catanionic compounds were investigated towards their removal behavior of fats, mainly biskin. The first check of catanionic surfactant combinations was performed with a quartz microbalance. Combinations with high potential were then investigated with an in-house built washing apparatus. It will be the first part of this chapter. The focus of the second part will be on the variation of a standard surfactant mixture due to the addition of a cation regarding a higher efficiency with as little as possible additives. Here, experiments with the quartz microbalance as well as with the in-house built washing apparatus were performed considering several different influences on the surfactant system.

5.2 Fundamental information

5.2.1 The composition of the detergent formulations

Washing mixtures are complex formulations. They contain many different components with different functions.¹⁵⁰ Surfactants and enzymes are the two groups, which are responsible for the soil removal and are therefore of main interest in this thesis.

5.2.1.1 Surfactants

Surfactants are the main components in detergent solutions.¹⁵¹⁻¹⁵³ They have several essential functions in the washing solution like, e.g. the increase of the wetting ability of water. Due to their surface activity, the removal processes, which will be explained in the next section, can occur. Moreover, they are responsible for the solubilization and emulsification of the removed soil.

Mixtures of different surfactants are mostly used to fulfill several demands of different soils since surfactants mixtures are known to show a higher performance than one surfactant alone.¹⁰⁶ Different detergents are known and applied. Anionic surfactants are the main components used for detergency. Anionic surfactants are useful for the removal of oily soils and the suspension of clay soil. A linear carbon chain length of 12-16 is optimal for detergency. Sulfonates, carboxylates, sulfates, and phosphates are commonly used. Due to their negative charge, they are sensitive to the positive charges present in hard water.

Nonionic surfactants are also added to the detergent mixture due to their non-sensibility towards water hardness. They so remove and emulsify oily soils very effectively. Cationic surfactants are normally not used in detergent solutions, but as softeners, since they stick to the negatively charged surface. Zwitterionic surfactants are also rarely found since their production costs are significantly higher than the ones for anionic surfactants. In general, the concentration of surfactants in the washing solution is crucial. It must be higher than the cmc to guarantee micelle formation, which enables the transport of soil through the aqueous medium. But, after a certain concentration, no improvement in washing efficiency can be observed.¹⁵¹

5.2.1.2 Enzymes

One additive, which got more and more interest in the last years, is the group of enzymes. They are effective in the removal of soil made of proteins, starch, and grease from garments and fabrics. They enable the action of surfactants and improve the performance of washing. One problem with enzymes is their sensibility towards several external factors. E.g., the presence of anionic surfactants decreases the activity and the stability under the real washing conditions. Enzyme engineering can be one way to prevent this problem.¹⁵⁴

Proteases are the most commonly used enzymes in detergency.¹⁵⁵ But, another class is also of interest in this industrial field. This is the lipase.¹⁵⁶ With a turnover of 1.5 billion US\$ in 2000 and nowadays even more, the lipases are a more and more used enzyme in the laundry industry. As its name already indicates, it can interact with lipids. The result is the hydrolysis of the ester bonds of the triglycerides into diglycerides, monoglycerides, free fatty acids, and glycerol. This is of main interest since especially the removal of fats from substrates is a challenging task in detergency industry. By converting mostly very hydrophobic substances into more hydrophilic molecules, the removal is facilitated. One characteristic for lipases is their interfacial activation. This means that a significant increase in the activity of the lipases can be detected when an interface, where the formation of an emulsion from the triglyceride substrate happens, is present.¹⁵⁷ So, they fulfill the same functions as surfactants in the washing solution.

But, several factors limit the efficiency of lipases^{156, 158}: the activity of lipase is not at its highest level when the water content is high. This is the situation within the washing procedure in the washing machine. Furthermore, at low temperatures, the activity of the lipase is lowered. This is the case already at room temperature. If the temperature is too high, the lipase gets inactive. An inactivation of lipase in the presence of surfactants can be observed due to concurrent interactions at the oil/water interface. From a global point of view, lipases fulfill the same function as surfactants in the washing solution. They remove the fatty soils from the substrate. Since they are highly effective and only very small amounts are needed, the use of enzyme can decrease the required surfactant concentration, although regarding their problematic sensibility. This needs to be investigated more intensively. New strategies for stabilization of enzymes and therefore the maintenance of their activity is a main task.¹⁵⁸

5.2.1.3 Other ingredients

Complex builders are important to decrease the water hardness by complexation of the corresponding cations. Thus, the inactivation of surfactant due to water hardness is lowered. Colorants are added, especially in the case of blue and white clothes, to intensify the color of the clothes again, which gets lost over several washing procedures.¹⁵¹

Fragrances in the detergent formulation are not important for the cleaning of the clothes itself, but for user-friendliness. A good smell of clothes after the washing process gives the consumer a feeling of the freshness of the clothes. Bleaching agents are added to the formulation for washing of white clothes to re-intensify the shiny white of the clothes.¹⁵¹

5.2.2 Influences on the washing process

Considering all different influences and requests, the process of washing is a very complex one. It can be generally divided into two parts: first, the soil must be removed from the dirty substrate. Secondly, the removed soil must be stabilized in the washing solution. Only then, it can be transported away from the substrate without re-deposition. Several factors influence this process.¹⁵⁹

- Water: Water acts as the solvent and medium of transport in the washing process. With its high surface tension, wetting on a hydrophobic fiber is difficult. For this purpose, surface active compounds must be added to decrease the surface tension and guarantee a fast and effective wetting of the fiber. Depending on the geographic area, the water used for the washing process has a certain amount of water hardness. The metal ions can lead to inactivation of the ingredients due to precipitation, which can deposit on the fibers and leave grey streaks behind. Moreover, they can lead to deposition in the pipes of the washing machine, which over time leads to a non-functioning. Thus, so-called builders, complexing agents, are added to complex these metal ions.¹⁶⁰
- Type of soil: Our clothes are exposed to potential sources of dirt all around the clock if we wear them. We differentiate between sources like mud, marmalade or gravy. But, from a chemical point of view, the distinction due to its solubility and chemical origin is more appropriated. Water-soluble substances can be easily removed by the washing solution

without the need for high mechanical effort. In contrast, for particles like metal oxides or pigments, which do not dissolve in water, the mechanical influence is more important to get the particles into solution. Fats and oils need both, solubilization by active substances and mechanical effort to get removed. They are the most complex soils to get removed since they stick to the textile due to their hydrophobic character. Here, the removal is complex and is therefore of big interest in research.^{153, 160}

- Textile: The interaction of soil and fiber is the main force which must be overcome by detergency. Since most soils have hydrophobic character, the material where it must be removed from, has significant influence. Three types of fibers can generally be distinguished: cellulosic, wool and synthetic. Most commonly known textiles are out of cotton (cellulosic) and polyester (synthetic) materials. With its hydrophilic character and negative charge on the surface, the cotton fiber can more easily get cleared from the soil than the more hydrophobic polyester fibers. Depending on the fiber, the washing conditions and the detergent solutions must be adjusted.¹⁵³
- Washing conditions: Several physical parameters influence the washing result. The mechanical energy put into the washing process by either hand-washing or the washing machine supports the chemical action of the washing solution and improves the removal of the soil. The temperature of the washing process has effects on the aggregation state of the soil. The more liquid the character of the soil, the better it can be removed. Also, a higher temperature improves the kinetics in the washing solution. But, higher temperatures do also mean higher energy consumption, which is not desirable in nowadays understanding of saving resources.¹⁵⁹

5.2.3 Removal mechanisms

As already mentioned above, the washing process can be divided into two parts: the soil removal and the stabilization of the soil in the washing solution. In the case of a water-soluble soil, the solubilization of the soil in pure water and its stabilization in it is not the challenge. It gets more difficult if the soil is an oily-greasy soil. Here, pure water is not enough to solubilize the soil. The

tension between water and soil is too high for any interaction. For this purpose, surfactants must be added to reduce the interfacial tension and allow the wetting of the soil. The efficiency of soil removal is influenced by the surfactant properties and should be optimized for the appropriate washing situation.¹⁵⁷ From the theoretical point of view, it can be distinguished between the mechanism for the removal of a liquid and a solid soil. Both will be discussed in the following.

5.2.3.1 Liquid soil removal

In principle, the process of a non-water-soluble soil removal of a certain liquid substrate can be seen as a process of several different interfaces involved. When a drop of oil lies on a substrate, e.g. a fiber, three interfaces with their interfacial tension γ can be determined: oil-substrate (OS), substrate-gas or liquid (SG) and oil-gas or liquid (OG). This is schematically shown in Figure 39.

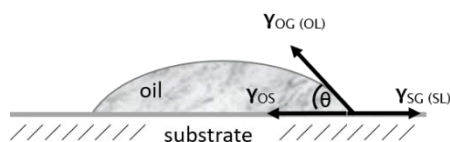


Figure 39: Schematically depiction of a drop of oil on a solid substrate and the corresponding interfaces. The picture is based on reference¹⁶⁰.

An angle θ is formed by the oil drop on the substrate, which can also be described as wetting of the liquid on the solid. Its size depends on the three interfacial forces. γ_{SG} tends to decrease the angle leading to a spreading of the drop to reduce the surface of gas and solid. In contrast, γ_{OS} promotes the formation of the drop on the substrate with the same reason. γ_{OG} is not in direct relation to the substrate. But, it must be taken into consideration to compensate the forces. Young's equation describes these forces under equilibrium conditions as the following¹⁶¹:

$$\gamma(SG) = \gamma(OS) + \gamma(OG) \times \cos \theta \quad (\text{equation 12})$$

In the case of a gas phase or a pure water phase, the contact angle is normally very small because the interfacial tension between oil and substrate is lower than the interfacial tension between substrate and gas/liquid phase. Adding a surfactant to the water, the surfactant molecules will adsorb on the oil-water and the water-substrate interface due to their amphiphilic character. The surfactant

contends with the oil for the contact to the substrate. The consequence is a reduction of the interfacial tension for these two interfaces. This increases in the contact angle. The drop will wet the substrate worse. A little mechanical effort applied to the substrate leads to a removal of the drop. Only a small amount of the soil is left behind. This is called the roll-up mechanism and is schematically shown in Figure 40.^{160, 162}

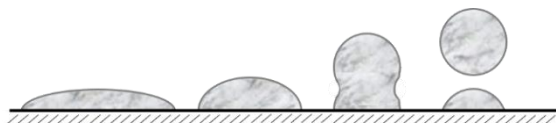


Figure 40: Roll-up mechanism. The picture is taken from reference ¹⁶⁰.

In general, the efficiency of the mechanism depends decisively on the present kinetics. The better the adsorption kinetics of the surfactants on the solid, the better is the detergency performance of a washing solution. The hydrodynamics, the motion of the fluids, does also have a considerable influence since it supports the mechanics to remove the drop. Another crucial point is the substrate itself. The rougher and uneven the substrate, the more difficult it is to remove the oil from the substrate since the area of the potential target is reduced. Considering the changing conditions from one washing process to another, the optimization regarding the substrate and the oil is a crucial point when creating a formulation of washing solution. The mixing of different surfactants can lead to a synergistic effect, which can improve the removal process significantly.¹⁶⁰

After removing the oily soil from the substrate into the solution, it is essential to keep the soil drops in solution and prevent re-deposition.¹⁶³ This can also be promoted by surfactants. Accumulating at the oil-water interface, surfactants serve as thermodynamic support for emulsification by lowering the interfacial tension. The emulsion as a metastable system should exist long enough to fulfill the function of transportation of the soil out of the washing area. Additionally, surfactants prevent coalescence due to steric or, depending on if charged or not, electrostatic barriers between the separated dirt particles and fulfill a kinetic function.

The formation of micelles allows surfactants to get immiscible materials into solution. With reaching the critical micelle value and the Krafft point, no more surfactants will absorb on the surface, but they will form micelles in solution. Consequently, no more reduction of surface tension is possible. On the

other hand, dirt can be stored and transported in the inner hydrophobic cavity of the micelles. Solubilization depends on the total concentration of the surfactant compared to its cmc. At low micelle concentration, solubilization is not dominant, and detergency is mainly based on the roll-up mechanism and the stabilization of the resulting emulsion. At higher micelle concentration (10 to 100 times higher than the cmc), micelles can absorb more and more of the immiscible materials and solubilization is more decisive. All in all, the formation of micelles has no impact on the detergency process itself. But, it can serve as a reservoir for removed dirt from the substrate.^{151, 164}

5.2.3.2 Solid soil removal

Besides removing liquid dirt from a substrate, eliminating solid soil from the fiber is the main purpose in detergency. Comparing the contact area of oily and solid soil, one might conclude that due to the lower contact area the solid soil is easier to remove. But, other interactions like electrostatic ones must be considered in addition to the van der Waal forces. Nevertheless, van der Waal forces are the most attractive forces, which must be broken to relieve the soil from the fiber. Detaching soils from a substrate is the reverse process of coagulation and adhesion. The adhesive bonds between the fiber surface and the particle must be broken and the separated surfaces must be wetted. Because the adhesive bonds are only significant for short distances, the contact area between particle and surface has a significant influence.¹⁶² Consequently, it requires energy to break the bonds, which has to be provided by an external source, like a washing machine. With the addition of detergents, it is possible to reduce the required energy. Hence, it gets easier to remove the soil by improving the wetting ability of the water.

In general, there are two mechanisms induced by surfactants that influence and improve the soil removal^{160, 162}: one is the wetting of the fiber and the particulate soil. The second one is the adsorption of the surfactant at the fiber/water and the soil/water interface. By adsorbing on the surface of the soil and the fiber, the surfactant enhances the repulsion between the two components to be separated. In the case of anionic surfactants at the boundary fiber and soil, an equally charged hydrophilic film is built, which pushes the molecules away from each other. The soil retention is lowered, and the soil is blocked from the fiber. With the help of mechanical movement, the soil can be removed. After that, the soil must be kept in solution. By building a hydrophilic film around the soil and due to the repulsion between the micelles, the soil can be transported within the solution.⁹⁵

The theoretical background of the removal of a solid particle of a fiber is the DLVO theory.^{165, 166} When the potential energy curve reaches its minimum, the closest distance between the particle and the fiber can be assumed. The potential barrier must be overcome to remove the particle from the fiber. In the washing process, one aim is to lower this barrier. But on the other hand, the potential barrier is also an obstacle for the particle to redeposit on the fiber.¹⁶⁰

5.3 Results and discussion

In the following, the fat removal behavior of the newly introduced catanionic combinations of this thesis will be investigated. They are based on ethylene oxide (further called EO) groups. A closer description of the anionic and cationic surfactant can be found in 3.3.

The fat removal behavior was examined via two methods: the quartz microbalance (QCM) (see 5.5.2.2) and an in-house built washing apparatus (see 5.5.2.3). Comparing the two methods, the challenging point of research in detergency can be seen. The washing process consists not only of one mechanism, for which the influences must be considered. But, at least two aspects are important. One is the attraction of the surface-active compounds towards the fat layer. The better the surfactant interacts with the soil, the lower is the interfacial tension and the better it can be removed (see 5.2.3). This was best investigated with the QCM where the interaction with the fat layer can be measured by a change in the frequency. Taking the mechanical influence into account, the emulsification of the soil and prevention of re-deposit is another important part. This was considered with the washing apparatus. Since the washing apparatus is the method which mirrors the situation in real washing machines the best, its results will be the ones to be most meaningful for potential applications.

5.3.1 Pure catanionic combinations

5.3.1.1 Pre-screening of the fat removal performance

5.3.1.1.1 Biskin removal detected with the quartz microbalance

To get a first impression of the fat removal ability of the different pure catanionic combinations, a first screening of the pure cationic combinations was performed with a quartz crystal microbalance (QCM) as described in 5.5.2.2. Here, the fat removal ability of Biskin of each combination was examined. The following parameters were applied to all tests:

- test solution: pure surfactant solution
- water: millipore
- concentration: 0.1 wt%
- pH: 6
- coating solution: biskin:toluol (1:6)
- anion-cation mass ratio: 9-1 and 5-5

- time of the surfactant washing step: 30 mins

Due to the high time consumption for every measurement, only two ratios per combination were investigated. The mass ratio 9-1 was chosen with the idea to see the potential effect of the addition of a cation in small amounts since normally, the washing behavior is based on the anionic character of a surfactant.¹⁶⁷ The mass ratio 5-5 was investigated to see the washing effect around equimolar ratio. The nonionic character within the surfactant solution was high at this anion-cation ratio. The focus was on the question if there was any synergism of anion and cation that can lead to a good or even better washing behavior than the pure anionic surfactant. The QCM measurements were investigated regarding the following four parameters, which are more precisely described in 5.5.2.2:

- peak height describing the adhesion of the surfactant molecules on the fat layer when getting in contact the first time
- maximum of raised fat layer indicating the strength of the interaction between the washing solution and the fat layer
- area below the measured curve describing the overall interaction between the washing solution and the fat layer
- end removal indicating the fat removal efficiency

The four parameters are depicted separately for each ratio. They are given in percentage regarding the maximal possible removal, which was detected after a washing step with acetone. The 'peak height' in the QCM measurement describes the adsorption of the surfactant molecules on the Biskin layer when the surfactant solution gets in first contact with the crystal quartz. The higher the peak, the more surfactants have adsorbed on the fat layer. This corresponds to a stronger interaction with the hydrophobic fat. The tests were also performed with the pure ionic surfactants for comparison. The determined values are given in Table 7.

Table 7: Evaluation of the Biskin removal experiments for the pure anionic and cationic surfactants performed with the QCM as described in 5.5.2.2.

surfactant	peak height [%]	maximum [%]	area [%]	end removal [%]
SDS	1.6 ± 0.4	0.0 ± 0.0	0.0 ± 0.0	0.0 ± 0.0
Tex	0.0 ± 0.0	0.0 ± 0.0	0.0 ± 0.0	0.0 ± 0.0
C12EO4SO4	0.0 ± 0.0	0.0 ± 0.0	0.0 ± 0.0	0.0 ± 0.0
C18EO4SO4	0.0 ± 0.0	0.0 ± 0.0	0.0 ± 0.0	0.0 ± 0.0
C12EO6SO4	2.2 ± 0.6	0.0 ± 0.0	0.0 ± 0.0	0.0 ± 0.0
ACA	7.3 ± 1.1	77.1 ± 4.5	20.0 ± 0.7	0.0 ± 0.0
C12EO1Ch	0.0 ± 0.0	0.0 ± 0.0	0.0 ± 0.0	0.0 ± 0.0
C12EO4Ch	0.4 ± 33.7	95.6 ± 1.1	27.8 ± 0.6	4.2 ± 0.7

For some measurements, the detected values did not give a positive value. In this case, the value was taken as zero since no positive effect regarding fat removal was found. For the anionic surfactants, no influence on the Biskin layer was detected. No interaction with the Biskin layer could be assumed. The same was observed for the cationic surfactant C12EO1Ch. The other two cationic surfactants ACA and C12EO4Ch showed interaction with the Biskin layer in small extent with an area value of 20 %. A raising of the fat layer was detected, but no removal of the fat was found. The potential to remove the Biskin was small for the pure ionic surfactants. The reason could be the only weak interactions between the hydrophilic surfactants and the hydrophobic Biskin layer. Due to that, the same test was performed with the mixtures of the anionic and cationic surfactants.

In Figure 41, the peak height for the catanionic mixtures at two different anion-cation ratios, 9-1 and 5-5, can be seen. For several catanionic combinations, especially with the anion-cation mass ratio 5-5, the obtained values were significantly higher than the ones for the pure ionic surfactants (see Table 7). Comparing the two ratios, stronger adsorption was observed for the mass ratio 5-5. This corresponds to a more nonionic character of the surfactant mixture. A more nonionic surfactant mixture can interact better with the hydrophobic fat layer leading to a higher adsorption rate. Three mixture (SDS-ACA, C18EO4SO4-C12EO1Ch and C18EO4SO4-C12EO4Ch) showed no adsorption on the fat layer. Their low solubility (see 3.3.1) can be the reason for that. If only small amounts of surfactants were soluble in the solution, the ability to adsorb is reduced. Only for three combinations at the mass ratio 9-1 (SDS-C12EO1Ch, SDS-C12EO4Ch and Tex-C12EO1Ch), the adsorption rate was in the same scope than the average for the mass ratio 5-5. Here, the pseudo-nonionic surfactant pairs seemed to have a high tendency to adsorb on the fat layer. Thus, small amounts of the oppositely charged cation formed already enough ion pairs for high adsorption on the Biskin layer.

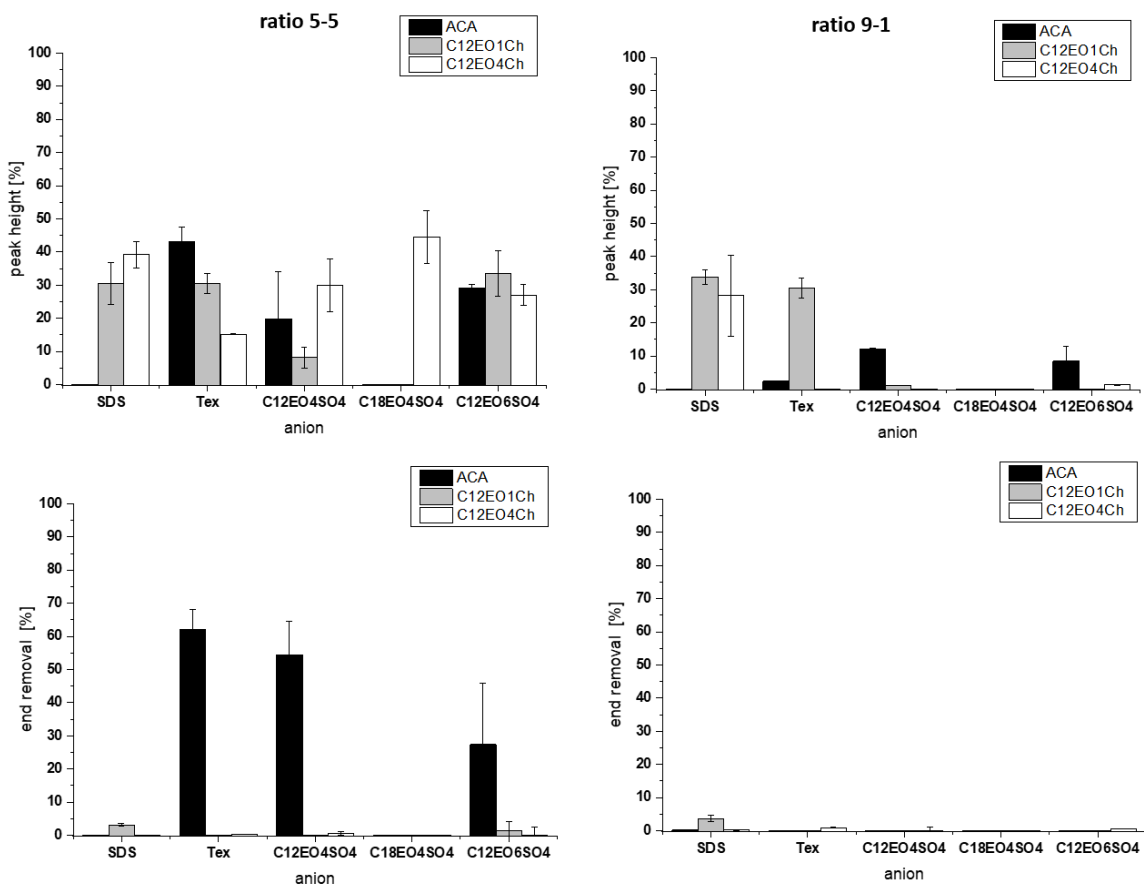


Figure 41: Evaluation of the first QCM scanning for the removal of Biskin by the catanionic mixtures as described in 5.5.2.2 for the anion-cation mass ratio 9-1 (left) and 5-5 (right) by the two parameters peak height (above) and end removal (below).

Additionally, the 'end removal' of the Biskin by the surfactant solution is shown in the same figure. Here, the overall amount of removed Biskin is negligible for most catanionic mixtures as it was already observed for the pure ionic surfactants (see Table 7). Although the surfactant solutions show interaction with the Biskin layer, they were not strong enough to take off parts of the Biskin from the quartz crystals. Three exceptions were observed. Tex-ACA, C12EO4SO4-ACA and C12EO6SO4-ACA at the anion-cation mass ratio 5-5 showed a Biskin removal from 60 % to 25 %. All three have the cation ACA in common. Compared to the other two cationic surfactants, ACA is the most hydrophobic one since no EO groups are present. Thus, the hydrophobic interactions are stronger, which affect the detaching of the fat. From the peak height, an interaction with the Biskin layer was observed. In these three cases, the surfactant mixtures were able to remove parts of the Biskin completely. Again, the nonionic character of the surfactant mixtures seemed to be favorable.

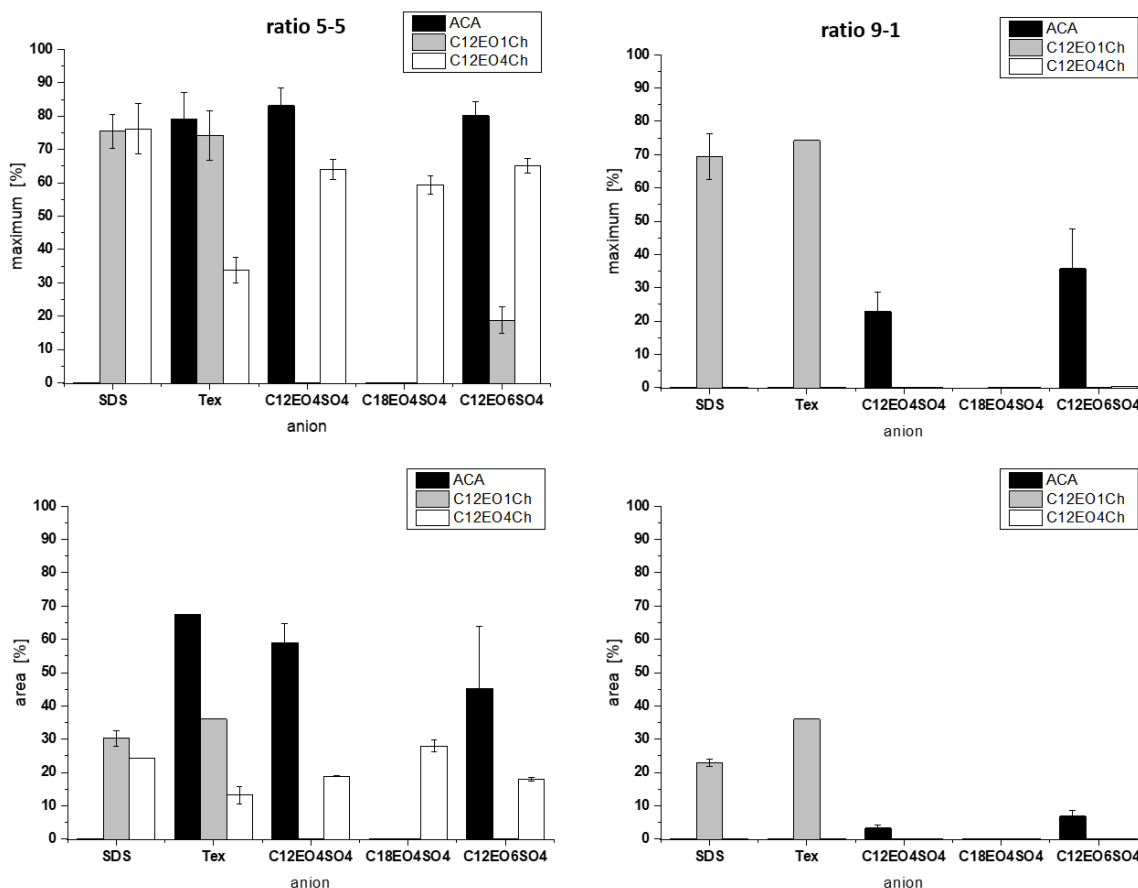


Figure 42: Evaluation of the first QCM scanning for the removal of Biskin by the catanionic mixtures as described in 5.5.2.2 for the anion-cation mass ratio 9-1 (left) and 5-5 (right) by the two parameters area (above) and end removal (below).

In Figure 42, the two parameters 'maximum' and 'area' are shown. Both describe the intensity of the interaction of the surfactant solution with the Biskin layer. The maximum indicates the maximal raising of the fat layer by the washing solution. The maximum value is mostly found at the end of the washing step since the maceration by the surfactant solution is then maximal. As already observed for the peak height, the values for the anion-cation mass ratio 5-5 were significantly higher than the ones for the mass ratio 9-1. Again, the two combinations SDS-C12EO1Ch and Tex-C12EO1Ch showed higher values than the rest. In the case of SDS-C12EO4Ch, which showed high adsorption with the first contact, the further interaction with the fat layer was negligible. The surfactant molecules were washed away with the flow and no interaction was detected. The same trend was obtained for the overall area of the measured curve. It can be seen as a value for the total interaction between the washing solution and the fat layer. The larger the value, the stronger are the interaction and the

raising of the fat layer. The experimental data confirmed stronger interactions of the nonionic character of surfactant mixture (ratio 5-5) compared to the more ionic character (ratio 9-1) with the hydrophobic biskin.

In summary, the catanionic mixtures showed better interactions with the Biskin layer than the pure ionic surfactants. The adhesion of the surfactants at the beginning of the surfactant solution time (= peak height), as well as the interaction of the surfactant solution leading to a slight lift of the fat layer (= area and maximum), were more pronounced for the anion-cation mass ratio 5-5. The more hydrophobic and nonionic character favored the interactions with the hydrophobic fat layer. In contrast, the more anionic 9-1 mass ratio was hindered due to different polarity. In general, there was no real washing effect, no fat removal, observed since all combination seemed only to detach the fat layer a little. The pure catanionic combinations around equimolar mass ratio as well as the ones with anionic excess did not seem to use any synergistic effect leading to a better fat removal than with the pure surfactant solutions. The insertion of a higher amount of EO groups did not improve the results. However, it seemed that a small number of EO groups did have a positive effect. But, the increase in flexibility due to a maximum amount of EO groups was not the decisive factor.

From the received QCM results, it was possible to select four combinations with the highest potential: the combination of SDS with C12EO1Ch, the combination of SDS and C12EO4Ch, the combination of C12EO4SO4 with ACA and the combination of Tex with ACA at the mass ratio 5-5. SDS-C12EO1Ch 5-5 showed an interesting curve with a relatively high value of the area and high adsorption at the beginning of the fat removal process. SDS-C12EO4Ch 5-5 was in the same region and was chosen for comparison of the number of EO groups. The combination of C12EO4SO4 with ACA was the one which showed the highest end fat removal in combination with a high value of area and value of adsorption. Tex-ACA 5-5 also gave high values for all parameters and was the example of a catanionic combination of already commercially available surfactants.

5.3.1.1.2 Statistical analysis

Four different parameters were extracted from the received QCM data and several relationships were identified in the previous chapter. However, due to a large amount of experimental data, an easy correlation of structural effects on fat removal behavior was difficult. For this purpose, a statistical regression analysis (see Experimental 5.5.2.8) was performed to determine the dependencies of the

removal behavior of Biskin on the molecular and physicochemical properties (see 3.3). Two parameters were taken in consideration: the 'area' below the measured curve since it represents the overall interaction of the washing solution with the Biskin layer and the 'end removal' as it indicates the real removal ability of the washing solution. The other two parameters 'peak height' and 'maximum' were skipped because they also describe the interaction of the washing solution with the fat layer. As the area already includes these aspects, it was sufficient to consider only this parameter. For a closer description of the parameter see 5.5.2.2. For all properties, a univariate regression analysis was performed and the significance value of 5 % was applied. The received P-values are shown in Table 8 and Table 9.

Table 8: Results of the univariate regression analysis between the molecular physicochemical properties and the determined parameter 'area' of Biskin in the QCM measurement (see 5.5.2.2) of the catanionic mixtures calculated as described in 5.5.2.8.

P-value	molecular properties		
	EO anion	EO cation	average EO
	0.3146	0.4199	0.1512
	chain length anion	chain length cation	average chain length
	0.3146	0.3703	0.5239
	HLB	molar ratio anion:cation	
	0.0893	0.0085	

P-value	physicochemical properties		
	solubility	surface tension air	dynamic surface tension
	0.6474	0.0035	0.6788
	cmc	interfacial tension	
	0.1246	0.6474	
	adsorption SiO ₂	adsorption SAM	
	0.5247	0.5651	

Table 8 gives the calculated P-values for the univariate regression analysis of the molecular and physicochemical properties determined in 3.3 and the parameter of the area below the curve measured with the QCM as described in 5.5.2.2. The corresponding values are given in 5.3.1.1.1. Only for one property, a significant relation was determined. With a P-value of 0.0035, the surface tension was found to be below the significant level of 5 %. Low surface tension was favorable for the interaction with the Biskin layer. This made sense when considering that the reduction in the surface tension by the surfactant describes its surface activity and its interaction between the water phase and the hydrophobic air phase.⁹⁵ The more surface-active the surfactant, the faster and better it can

also interact with the fat layer resulting in an increased value for the area of the QCM curve. Also, the two parameters HLB value and anion-cation ratio showed low P-values. Although they cannot be named as a significant relation, the following relations can be assumed: an anion-cation ratio around equimolarity promotes the interaction with the Biskin layer. The nonionic character, which interacts more intensely with the hydrophobic fat layer than an ionic surfactant, is the reason. Moreover, a lower HLB value led to a larger area of the QCM curve. A low HLB value correlates to a larger lipophilic part in the surfactant structure.²⁰ With a larger lipophilic part in the molecule structure, the hydrophobic interactions will be increased indicated by a larger area in the QCM curve.

The second investigated parameter was the end removal of Biskin at the end of the QCM measurement. Table 9 gives the calculated P-values for the univariate regression analysis of the molecular and physicochemical properties determined in 3.3 and the parameter of the end removal measured with the QCM as described in 5.5.2.2.

Table 9: Results of the univariate regression analysis between the molecular physicochemical properties and the determined parameter 'end removal' of Biskin in the QCM measurement (see 5.5.2.2) of the catanionic mixtures calculated as described in 5.5.2.8.

P-value	molecular properties		
	EO anion	EO cation	average EO
	0.4433	0.0919	0.3100
	chain length anion	chain length cation	average chain length
	0.4433	0.0163	0.1167
	HLB	molar ratio anion:cation	
	0.0336	0.1838	

P-value	physicochemical properties		
	solubility	surface tension air	dynamic surface tension
	0.6924	0.0772	0.9225
	cmc	interfacial tension	
	0.2227	0.6924	
	adsorption SiO ₂	adsorption SAM	
	0.6986	0.6258	

Two molecular properties were determined to be in a significant relation to the removal of Biskin from the quartz crystal. These were the chain length of the cationic surfactant and the HLB value. For a longer alkyl chain in the cationic surfactant, the removal of the Biskin was higher. A lower HLB also promotes the Biskin removal. In both cases, the hydrophobic proportion in the molecular structure

increases. This makes stronger hydrophobic interactions possible. Since they are the precondition for the removal of the hydrophobic Biskin, they promote the Biskin removal. With a P-value of 0.0772, the surface tension also showed an assuming dependence. Lower surface tension was favorable for the Biskin removal. The same reason as for the area below the QCM curve can be named for that.

In summary, with the statistical analysis, it was possible to determine several significant relations between the fat removal and the properties of the washing solution. An increase in the hydrophobic part of the molecular structure leading to stronger hydrophobic interactions with the fat layer was shown to be a promoting factor. This was indicated by a significant relation with the cationic chain length, the HLB value, the anion-cation ratio, and the surface tension. The QCM measurements only consider the solubilizing ability of the Biskin and not the emulsifying function since the applied flow prevents re-deposition. Thus, further investigations with the washing apparatus are useful, also to consider the mechanical effect. This will be done in the following chapter.

5.3.1.2 Washing tests with the washing apparatus

Based on the results from the QCM measurement (see 5.3.1.1), four catanionic combinations were chosen to investigate their fat removal behavior more realistically in the washing apparatus, as described in 5.5.2.3. First, the combinations in pure millipore water with a concentration of 0.1 wt% and a pH of 10 were used as washing solutions. Second, because a replacement or the use as an additive would be more realistic, the catanionic combinations were used as a replacement for one anionic part in the standard mixture, the Texapon N70. The standard mixture was defined as a combination of the anionic surfactant sodium dodecylbenzylsulfonate (SDBS), the nonionic surfactant Lutensol AO7 (AO7) and the anionic surfactant Texapon N70 (Tex) in the mass ratio 1:1:1 at a total concentration of 0.1 wt%. Since enzymes are often used in detergent formulations, the influence of the interaction of the catanionic solution and an enzyme was examined by adding 2 ppm of lipase to the pure catanionic solution in a third step. All washed fibers were evaluated by measuring the difference in their mass before and after the washing step to determine the mass, which was washed away in the washing process. Moreover, the fibers were examined with a colorimeter detecting the coloriness before and after the washing process. The determined values were correlated to a maximal soil removal of 100 %. The results are depicted in Figure 43.

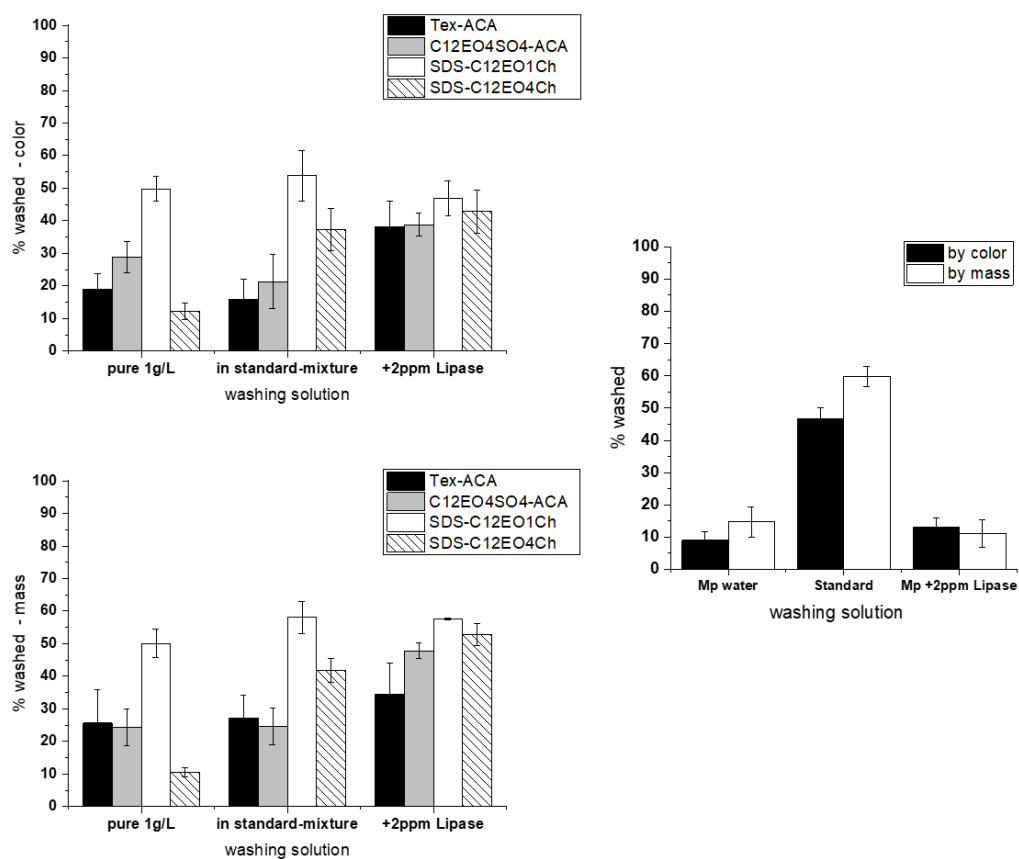


Figure 43: Washing results of the removal of Biskin in % with the in-house built washing apparatus as described in 5.5.2.2 of the pure catanionics combinations Tex-ACA 5-5 (black), C12EO4SO4-ACA 5-5 (grey), SDS-C12EO1Ch 5-5 (white) and SDS-C12EO4Ch 5-5 (whited shaded) in pure form, with the addition of 2 ppm lipase and inserted in the standard mixture of SDBS:AO7:Catanionic (1:1:1) at 25 °C and pH 10 evaluated by color (above left) and by mass (below left) in comparison to the references (right).

Comparing the four pure catanionic combinations in their potential as pure washing solutions, the combination of SDS and C12EO1Ch gave by far the best result. Around 50 % of the soil was removed after the washing process. Inserting more EO groups into the cation seemed to lower the washing efficiency in combination with SDS. Only around 10 % of the Biskin was removed. This correlated to the removal ability of pure millipore water meaning only mechanical effects. The two combinations with ACA as cationic surfactant (Tex-ACA and C12EO4SO4-ACA), which gave the best Biskin removal in the QCM measurements (see 5.3.1.1), could not show the same trend. They were significantly weaker in their fat removal behavior with only 20-30 % of Biskin removal. Comparing the four combinations regarding their number of EO groups, the results gave rise to the suspicion that too many as well as no EO groups could lower the washing efficiency. With more EO groups present, the

flexibility of the chains gets more intensive. But, also the hydration of the hydrophilic part of the surfactants gets more decisive. This might hinder the surfactants to interact effectively with the soil. With no EO groups in the cationic structure, the combination is more hydrophobic and less flexible. The EO groups in the anionic structure were not able to compensate that. One EO group on the cationic side seemed to be most effective for the removal of Biskin.

Including the catanionic combinations into the standard mixture in replacement for Texapon showed superficially the same trend. But here, the combination of SDS and C12EO4Ch seemed to be better in comparison to the two combinations with ACA. The catanionic combinations Tex-ACA and C12EO4SO4-ACA in the standard mixture could not improve their fat removal ability. No synergistic effect was obtained. For the two catanionic combinations containing SDS in the standard mixture, an increase in Biskin removal was observed. Compared to the reference system with only Texapon present, the combination of SDS and C12EO1Ch was the only one which could reach the reference value. From the theoretical view, the nonionic character of the washing solution increased with the presence of the catanionic combination. Nonionic surfactants are known to improve the solubility of ionic surfactants and improve therefore the washing efficiency.¹⁶⁸ But this could not be observed in the present case. A significant improvement of the use of catanionic combination instead of Texapon could not be observed. Since for the washing effect, mostly anionic surfactants are used¹⁶⁹, it might be the case that the amount of SDBS present in the solutions was not high enough or was not enough supported by the nonionic character of the catanionic combination to lead to a removal of the soil.

The addition of the lipase to the pure catanionic solutions gave an increase in washing efficiency for all combinations, except for SDS-C12EO1Ch, which stayed in the same range. Taking the reference of pure lipase into consideration, it got obvious that the combination of catanionics and lipase led to a positive effect in the washing efficiency. Especially for SDS-C12EO4Ch, a three times better fat removal could be measured. Reasons for this can be diverse. It is known from the literature that the activity of the enzyme is generally lowered in the presence of anionic surfactants in most cases.^{170, 171} In the present catanionic case, the interaction of the anionic surfactant could be decreased by the interaction with the cationic surfactant. There are also some examples where the presence of surfactants can also enhance the activity of an enzyme or stabilize the enzyme in the solution. A suggestion is that the surfactants can increase the available surface area for the enzyme due to lowering of the surface tension between the substrate and the liquid.¹⁷² Moreover it has been shown by Magalhães *et al.* that the negative effect of the anionic structure on the lipase activity can be

decreased by the insertion of EO groups.¹⁷³ This could be the case in two of the present catanionic mixtures.

To examine the interaction between the catanionic mixture and the enzyme further, the stability of lipase was exemplarily tested in the presence of a catanionic mixture for the case of SDS as anion and C12EO4Ch as a cation as described in 5.5.2.6. Over one week, the amount of present lipase was detected for the pure anionic surfactant as well as for two catanionic mixtures. The results are shown in Figure 44.

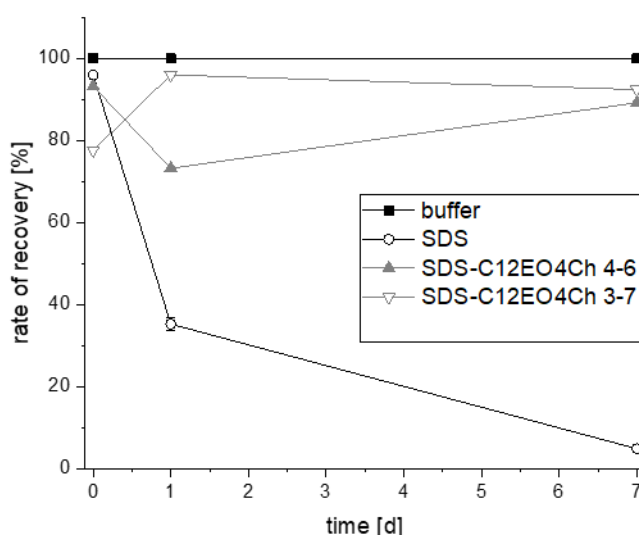


Figure 44. Lipase stability in the presence of the surfactants SDS and C12EO4Ch measured as described in 5.5.2.6.

A significant decrease in detection of lipase could be detected for the pure anionic surfactant. Within one day, only 40 % of the original amount of lipase was detected. The addition of the cationic to the anionic surfactant changed the interaction with the enzyme. The negative effect of the anionic surfactant towards the enzyme could be decreased. About 90% of the enzyme could be measured after one week. The observations of the lipase stability tests fitted to the performed washing tests. In the case of only lipase and the catanionic combination present in the washing solution, a synergistic performance was observable. The negative effect of the anionic surfactant could be decreased by the addition of the cationic surfactant. The same phenomenon in catanionic mixtures was already reported by Mahiuddin *et al.* where the activity of the horseradish peroxidase was investigated in reverse catanionic microemulsions. The enzyme was found to be more stable in catanionic mixtures

than it would have been expected when regarding the presence of a cationic surfactant, which would normally deactivate the enzyme. This was attributed to the strong interaction between the ionic surfactants, which resulted in shielding of the enzyme.¹⁷⁴

5.3.2 Catanionic combinations in complex washing systems

Towards potential commercial application, the concept of catanionic systems was applied to a surfactant combination commonly used in the laundry industry. To this system, it will mainly be referred to in the next sections. It is a combination of three surfactants – two anionic and one nonionic one, which are shown in Figure 45. The surfactants were used at a mass ratio of 1:1:1 and if not mentioned otherwise at a concentration of 0.1 wt%. The system will be named “standard mixture” in the following chapters.

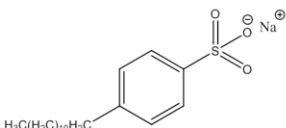
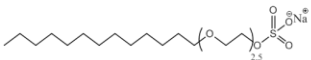

name	Sodiumdodecylbenzylsulfonate	Texapon N70	Lutensol AO7
abbreviation	SDBS	Tex	AO7
structure			

Figure 45: Name and structure of the three surfactants present in the standard mixture.

The fat removal behavior was mainly investigated with the in-house built washing apparatus as described in 5.5.2.3. Additionally, several fat removal tests were performed with the QCM for confirmation (see 5.5.2.2). In the following, different investigated aspects were described. It must be mentioned that the two methods are not completely comparable in their absolute values. The test conditions were different. The QCM only considered the solubilization of the fat by the washing solution. Here, the investigated solution flowed at a constant flow rate over the fat layer. The interaction and the solubilization of the fat by the washing solution were detected. In the washing apparatus, it was possible to additionally consider the mechanical impact due to the turning of the

vessel and the influence of the stainless-steel balls in it. Consequently, the washing apparatus imitated the process of fat removal in a more realistic way than the QCM.

5.3.2.1 Reference systems and the influence of temperature

Water and commercially acquired washing powder of Persil (Persil Universal-Pulver) were tested as reference systems with the in-house built washing apparatus with Biskin as soil under the conditions described in 5.5.2 in a first step. Since water hardness can play a significant role in the washing process^{152, 162}, both washing systems were tested in millipore water and in water with a hardness of 14 °dH adjusted as described in 5.5.1. The amount of Persil was adjusted by the given information on the package of the washing powder for hand wash (10.6 g powder for 1 L). Furthermore, the influence of the temperature was investigated by performing the washing tests at 25 °C and 40 °C.

Pure water indicated the removal of soil only due to the mechanical effort since no ingredients were present in the washing solution, which could influence the interaction of the washing solution with the soil. Persil was used as an example for a commercially washing powder. It is a complex mixture of several components to fulfill the needs of the circumstances in households. For example, building agents are added to complex the metal ions of the present water hardness. As written on the packaging, the major part of the powder is zeolites (15-30 %). Anionic surfactants (5-15 %) and nonionic surfactants together with soaps (<5 %) are declared as amphiphilic substances in the powder. Depending on the water hardness, the amount of powder, which should be used, differs. According to the declaration on the packaging, the washing solution was prepared for soft water (in the present case millipore water) and hard water (in the present case 14 °dH). The results can be seen in Figure 46.

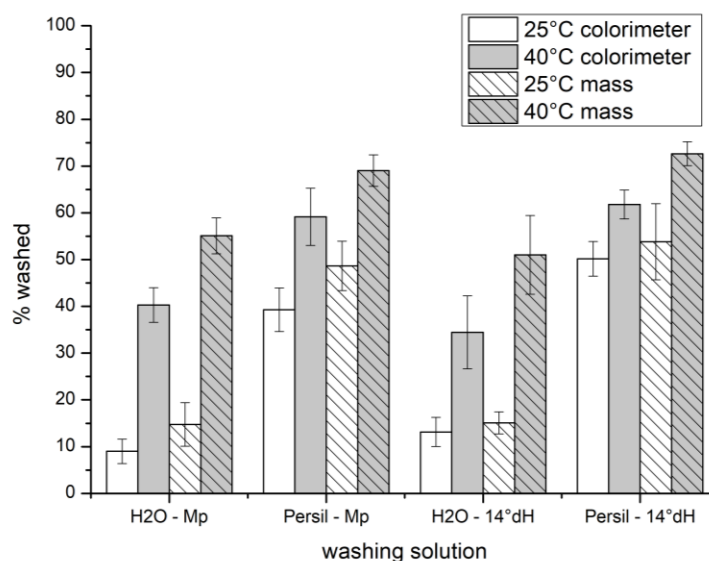


Figure 46: Washing results of the removal of Biskin with the in-house built washing apparatus in % as described in 5.5.2.3 for the references water and commercial Persil at 25°C and 40°C at pH 10 determined by color (not shaded) and by mass (shaded).

The washing result of pure water at 25 °C was very low. This could easily be explained by the fact that no additives were present, which were able to promote fat removal. However, the results showed that the influence of the mechanics with about 10 % fat removal in the washing process was not negligible. The mechanics play an important part of the soil removal. Comparing the influence of water hardness in the case of pure water, no differences were obtained. This was expectable since the present ions Ca^{2+} and Mg^{2+} did not interact in any case with the fat layer. The higher temperature of 40 °C showed more effect. Here, the influence of the aggregation state of the soil on the soil removal got obvious. As it is stated on the packaging, Biskin is a mixture of different vegetable oils and fats. The consequence is a melting range. With increasing temperature in the washing process, the amount of liquid soil increased. Since soil of liquid character is removed more easily, the observed washing results at 40 °C was significantly higher than at 25 °C for all investigated cases.

For the washing solution containing Persil, the washing result at a lower temperature was already significantly higher than with pure water. The surfactants present in the washing solution could decrease the contact angle between water and soil (see 5.2.3). Thus, the removal of the soil was more distinctive. Comparing the results with and without water hardness at 25 °C, the washing efficiency

was higher in the presence of water hardness. This can be explained by the fact that commercial products are always formulated under the aspect that there is a certain amount of water hardness. If no ions are present, like in the case of millipore water, building agents might interact with the active compounds (surfactants) in a way that hinders them to interact with the fat layer in the most efficient way. For this purpose, the washing result might be lowered in a certain way. In the case of higher temperatures, this effect was negligible since the removal was facilitated. But, also in the case of Persil, the effect of increasing temperature got obvious.

Besides water and Persil, a third reference system, the so-called 'standard mixture' was tested. The standard mixture was investigated with the washing apparatus at different concentrations at 25 °C and 40 °C. Results are shown in Figure 47.

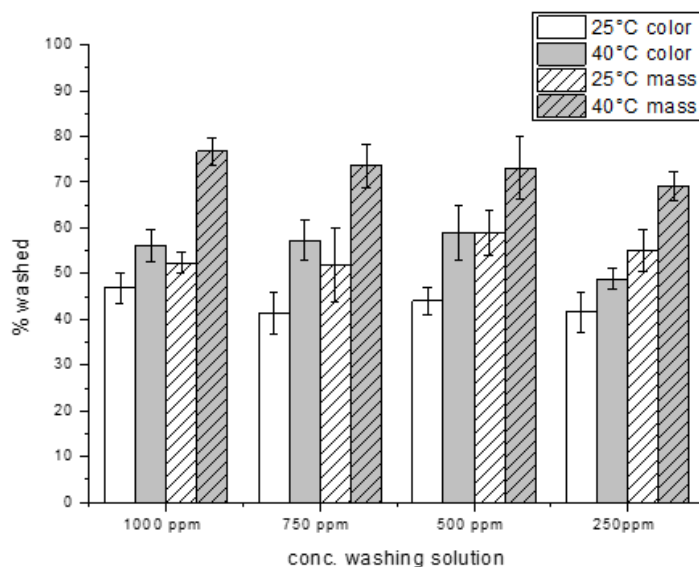


Figure 47: Washing results of the standard mixture of SDS:Tex:AO7 (1:1:1) in % measured as described in 5.5.2.3 at 25 °C as a function of concentration at 25 °C (white) and 40 °C (grey) at 14 °dH evaluated by a colorimeter (blank) and by mass (shaded).

At 25 °C, a fat removal of about 50 % of the Biskin mass was measured. A decrease in concentration down to 0.025 wt% did not reduce the washing efficiency significantly. Since it is the amount of surfactants normally present in the detergent formulation, further investigations will be performed at 0.1 wt%. Regarding the influence of temperature, the same trend as for the two other reference systems was observed. Increasing temperature improved the fat removal for the named reasons

above. Compared to the commercial Persil, the washing performance at higher temperature was slightly better for the standard mixture. Here, a small decrease in washing performance was observed for decreasing concentration

The performed experiments showed the important influence of the mechanics in the washing process. Around 10 % of Biskin was removed without any addition of surfactants. For the commercial Persil, an adjustment to hard water was found. For pure water, no difference was measured. The temperature was shown to affect the efficiency of the fat removal process to a large extent since higher temperatures increase the liquid character of the soil, which facilitates its removal. At lower temperature, the effort of active substances must be much higher than at higher temperatures. It shows the need and challenge for formulation. Since the focus in this work is the improvement of the washing result at lower temperatures due to new cationic combinations in the washing solution, further experiments will be performed at 25 °C, if not mentioned otherwise.

5.3.2.2 The influence of the soil on the washing result

In general, a variety of different soils can be distinguished. For soil removal tests on lab scale, either pure soils like blood or marmalade or mixtures of different substances are used. Since the nature of the soils differs, the efficiency to remove them by the same component also does. Testing different soils is of interest because normal dirt in real life will always consist of a mixture of different substances. Since the focus of this work is on the removal of fat, besides Biskin, two other soils were tested in the washing apparatus for comparison. Both soils were prepared in the lab by mixing different oils and fats as model soils based on the real composition of sebum and beef fat. The sebum model consisted of triolein, cetyl palmitate, squalene, and stearic acid. The beef fat model consisted of triolein, cholesterol, and stearic acid. Their exact composition cannot be named here due to the duty of secrecy with BASF. The standard mixture of SDBS:AO7:Tex (1:1:1) at 0.1 wt% and at a pH 10 as well as the standard mixture with the addition of 100 ppm of C12EO1Ch and also 100 ppm of C12EO4Ch were used as washing solutions in the procedure described in section 5.5.2. The tests were performed with the QCM and with the washing apparatus for comparison. Table 10 shows the results of the QCM measurements. For each combination, the maximal detachment during the measurement, the proportion of area regarding the maximal area of complete removal and the absolute end removal are given. All values were calculated in comparison to the maximum of 100 %

removal. Considering the absolute end removal, sebum showed by far the best results for all combinations. With the addition of 100 ppm of the cationic surfactant C12EO1Ch, nearly a complete removal of the sebum layer was observed. In general, this combination gave the best results in all categories, also for the other soils. A positive effect of the addition of one of the cationic surfactants was significant, especially for sebum and for lard. Biskin showed the smallest removal for all combinations. The end removal was negligible. An effect of the washing solution could be seen regarding the interaction of washing solution and fat layer indicated by the two values: maximal detachment and area. But, the interaction seemed not to be strong enough to lead to observable fat removal.

Table 10: Results of fat removal of three different fat by the standard mixture SDBS:AO7:Tex (1:1:1) with the concentration of 1000 ppm with none, with 100 ppm C12EO1Ch and with 100 ppm C12EO4Ch as additive performed with the QCM as described in 5.5.2.2 at 25 °C.

additives	max. detachment [%]			area [%]			end removal [%]		
	Biskin	sebum	lard	Biskin	sebum	lard	Biskin	sebum	lard
none	88	59	10	29	54	8	2	59	5
100ppm C12EO1Ch	88	96	86	34	91	72	5	95	52
100ppm C12EO4Ch	80	61	74	27	46	52	5	61	17

Figure 48 shows the results of the same samples performed with the washing apparatus. Nearly the same trend as with the QCM measurement could be observed. With around 40 % of removal, Biskin showed the smallest soil removal. The two model soils were in the same range, but the beef fat model showed slightly better soil removal than the sebum model. This was contradicting to the QCM tests. But, the different procedures of the two methods must be considered. Within the QCM, nearly no mechanical effect was simulated, where it was with the washing apparatus. It showed the crucial factor of mechanical work again within the fat removal process. Here, this was shown by the higher values of removal with the washing apparatus. In the case of beef fat, the process of the apparatus gave an even higher value than observed in the QCM.

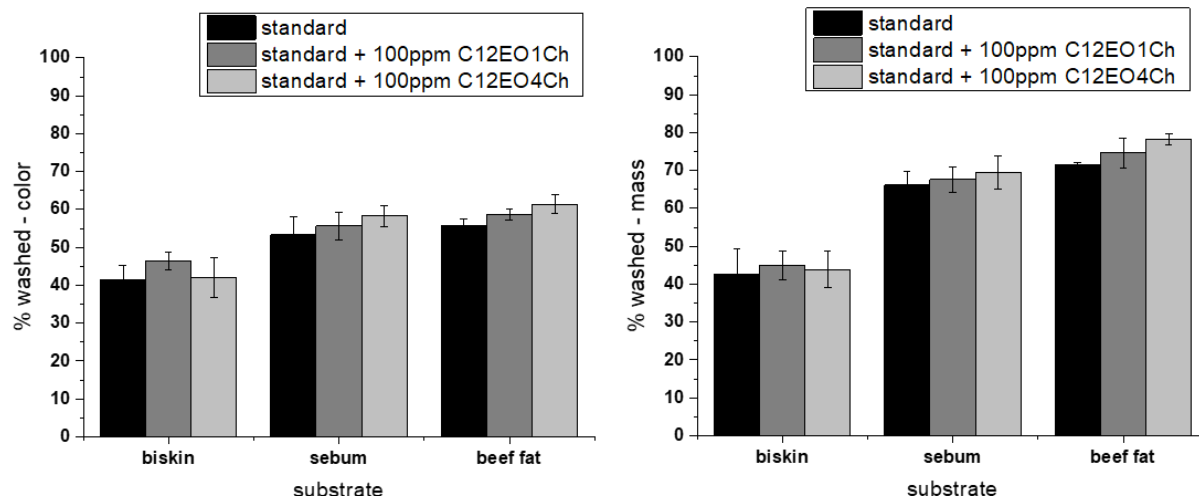


Figure 48: Washing results in % measured as described in 5.5.2.3 at 25 °C of the standard mixture (SDBS:AO7:Tex (1:1:1)) (black), standard mixture + 100ppm C12EO1Ch (dark grey) and the standard mixture + 100 ppm C12EO4Ch (light grey) on three different soils: biskin, sebum and beef fat evaluated by colorimeter (left) and by mass (right).

In general, the composition of soil has a considerable influence on the removal behavior.¹⁷⁵ One important parameter is the melting range of the soil. The more liquid the character of the soil, the more easily it is possible to remove it. In the sebum model, the portion of solid components was higher than in the beef fat model, which can explain the slightly better removal of the beef fat model since the general composition of the two model soils were similar. Another point is the composition of the soil. Since nearly all soils in real life are a mixture of several different oils and fats, the general hydrophobicity of the soil is characteristic. Depending on the structure of the ingredients, the soil attaches stronger to the fiber. Thus, it is more difficult to break these interactions leading to a removal of the soil. Biskin is a mixture of several natural vegetable fats and oils. In average the portion of triglycerides is more than 80 % (details were given on the packaging). The rest consists of saturated and unsaturated fatty acids. All in all, the mixture of Biskin is less hydrophobic than the model soil mixtures with only hydrophobic hydrocarbon functions in the molecules. This can explain the observed soil removal results. On the one hand, the more hydrophilic soil sticks better to the surface of the fiber and is, therefore, more difficult to remove. On the other hand, the melting range of Biskin is higher than the ones of the model soils. This leads to less effective removal of Biskin in comparison to the model soils.

All three soils have been investigated with three different washing solutions distinguishing in the addition of cationic surfactant. For the case of Biskin, no significant difference could be observed. The addition of C12EO1Ch gave a small improvement compared to the other two solutions. A general trend of the addition of a cationic surfactant leading to a more nonionic character in the surfactant solutions and therefore to an improvement of washing solution could not be estimated. In the case of the two model soils, a slight increase with the addition of cationic surfactants could be observed. Here, the more nonionic character had a positive effect. The interaction with the hydrophobic soils can be more distinctive since less rejection between the charged headgroups was present. This led to a stronger interaction of surfactants and soil, meaning better adsorption of the surfactants to the soil. This can have a positive effect on soil removal.¹⁷⁶

In addition to the fat removal measurements, the contact angle of the investigated washing solutions was measured on the three investigated fat layers (see Figure 49). The contact angle describes the interactions between the hydrophobic fat layer and the liquid, which was placed on it.^{177, 178} The better the surfactants in the washing solution reduce the interfacial tension between liquid and solid, the lower will be the observed contact angle. Lower interfacial tension between the fat and the solution will improve the possibility to remove parts of the fat and keep them in the solution.¹⁷⁹ With values of around 45 °, Biskin gave the highest values. On both other substrates, the investigated solutions spread better leading to values of the contact angle of around 30 °. For all solutions and substrates, the trend was the same. The lowest value was observed for sebum followed by lard. The highest contact angle was measured for Biskin. The obtained trend for the contact angles fitted to the results from the fat removal tests. A smaller contact angle correlated to a better fat removal (see Table 10 and Figure 48). Comparing the different washing solutions, the lowest values were measured with the addition of C12EO1Ch on Biskin. For sebum and lard, the addition of a cationic surfactant decreased the contact angle. A slight trend can be suggested: with an increasing number of EOs the contact angle decreased. This fitted the performed fat removal tests. The contact angle measurements confirmed the observation from the fat removal tests that the addition of one of the cationic surfactants lowered the interfacial tension between the two interfaces. This resulted in a lower contact angle and had also influence on the fat removal and emulsification behavior of the fat in the washing solution.

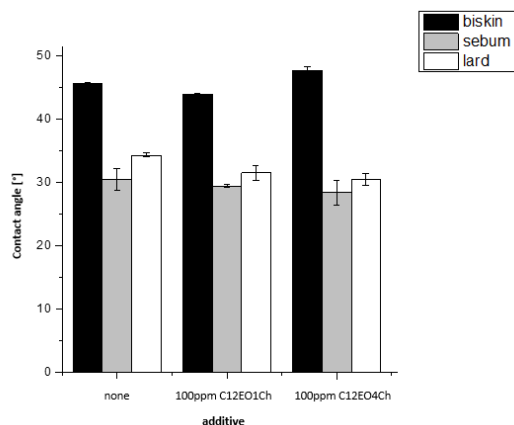


Figure 49: Contact angle measurements measured as described in 5.5.2.7 at 25 °C of the investigated standard solution without additive (left), with 100 ppm C12EO1Ch (middle) and 100 ppm C12EO4Ch (right) on the three different substrates: Biskin (black), sebum (grey) and lard (white).

5.3.2.3 Cationic surfactants as an additive to the standard mixture

The general idea was to investigate the influence of the addition of a cationic surfactant to the anionic standard mixture of the washing solution. With the addition of a cationic surfactant to the solution, the following procedure was suggested: the cationic surfactant will interact with the two anionic surfactants Tex and SDBS due to the electrostatic attraction of the headgroups. This leads to a pseudo-nonionic catanionic surfactant ion pair. Since it is known that these nonionic surfactant pairs adsorb better on hydrophobic surfaces (see also chapter 3.3.4), the surfactant pair should interact better with the soil leading to better soil removal. Moreover, in chapter 3.3 it could be shown that the addition of a cationic to the anionic surfactant leading to a catanionic mixture has a major influence on physicochemical properties, like, e.g. the cmc value. Because the emulsification plays an important part in the washing process¹⁶⁴, a smaller cmc value leads to a potential emulsification possibility at lower surfactant concentrations.

The existing interaction and the influence of the addition of a cationic surfactant on the general situation in the standard mixture were examined with the measurement of the surface tension as described in 5.5.2.4 of the standard mixture and the standard mixture with the addition of 200 ppm of cationic surfactant C12EO1Ch. The two obtained surface tension curves are shown in Figure 50. With the addition of the cationic surfactant, a significant shift of the cmc towards lower concentrations was observed. The explanation for that is the increasing nonionic character due to the

formation of a pseudo-nonionic catanionic ion pair, which leads to a micelle formation at lower concentrations as it is known for nonionic surfactants.⁹⁸ Moreover, a lower value of the final surface tension was measured. This proves the existing interaction of the cationic with the anionic surfactant in the standard mixture.

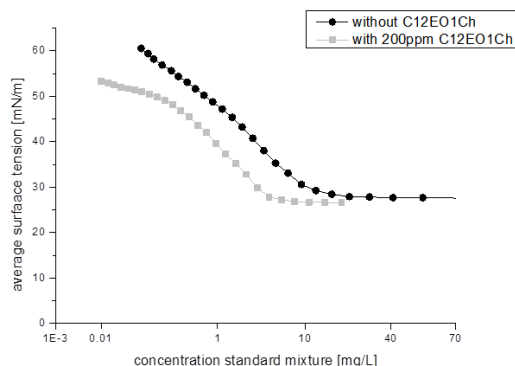


Figure 50: Cmc measurement measured as described in 5.5.2.4 performed at 25 °C of the standard mixture in millipore water (black circles) and the standard mixture with the addition of 200ppm C12EO1Ch (grey squares).

To test this hypothesis in the washing process, several washing experiments were performed with the in-house built washing apparatus as described in 5.5.2.3. The focus was not only on the positive charge of the cationic surfactant but also on the composition of the hydrophilic part in the whole, especially on the insertion of EO groups into the cationic surfactant. For this purpose, three different cations were chosen to be added separately to the standard washing solution: ACA as example for a typical commercially used long-chain alkyl quaternary ammonium surfactant, C12EO1Ch as example for a cation based on the linear structure of ACA, but with the insertion of a flexible EO part in the alkyl chain next to the quaternary ammonium group and C12EO4Ch as example for a long-chain cation with several EO groups in the structure next to the quaternary ammonium group leading to a high flexible alkyl chain. All washing tests were performed as described in 5.5.2. The concentration of the standard washing solution SDBS:AO7:Tex (1:1:1) was varied from 0.1 wt% to 0.025 wt% in a water hardness of 14 °dH. The amount of added cationic surfactant was always 100 ppm. The results can be seen in Figure 51.

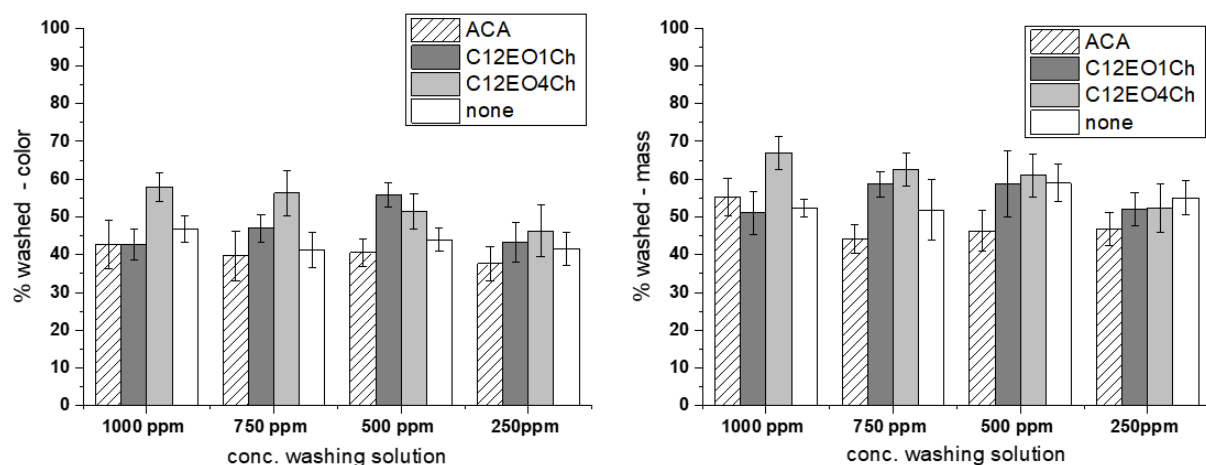


Figure 51: Washing results of Biskin in % measured as described in 5.5.2.3 of the standard mixture SDBS:AO7:Tex = 1:1:1 at different concentrations at 14 °dH and 25 °C with the addition of 100 ppm ACA (white striped), C12EO1Ch (dark grey) and C12EO4Ch (light grey) compared to the pure standard mixture (white) evaluated by colorimeter (left) and by mass (right).

The washing results showed a positive effect of the insertion of EO groups into the cationic surfactant for most of the performed washing tests compared to the pure standard mixture. Both, C12EO1Ch and C12EO4Ch, showed better results than ACA. Compared to the pure standard mixture, the addition of ACA seemed to have a negative effect. The linear alkyl chain with its higher stiffness could interact strongly with the alkyl chain of the anions. This can lead to a hindering of the anions in their washing activity. Since the washing solutions were all clear, the electrostatic interactions were not strong enough to lead to precipitation, which would explain the decreasing washing activity in the washing solution. But, the interactions were distinctive enough to influence the ingredients of the washing solutions. Comparing the different concentrations showed no dependence on the amount of cationic surfactant ACA. Taking the results of C12EO1Ch into considerations, the effect of the hydrophilic EO group into the hydrophobic alkyl chain became clear. The two cations effectively have the same length of the linear alkyl chain. But, the hydrophobicity and the flexibility of the chain differs due to the EO group. By insertion of the EO group, the HLB value increased from 3.1 to 9.2. The interaction with the present surfactants, mainly the anionic SDBS and Tex, differs. Due to the increased flexibility in the chain, the interactions between the anionic and the cationic surfactant might be less distinctive than with the ACA and therefore did not lead to a hindering. From that point of view, the further insertion of EO groups should have an even stronger positive effect on the washing result. But, a linear

dependence on the number of EO groups, in general, could not be stated. It rather seemed that there is an optimum ratio of the amount of cationic surfactant about the concentration of the washing solution for each cationic surfactant. To investigate this assumption, washing tests were performed with a fixed concentration of washing solution of 0.1 wt% and varying concentrations of added cation from 0.005 wt% to 0.025 wt% under the same conditions as described in 5.5.2.3. The results are shown in Figure 52.

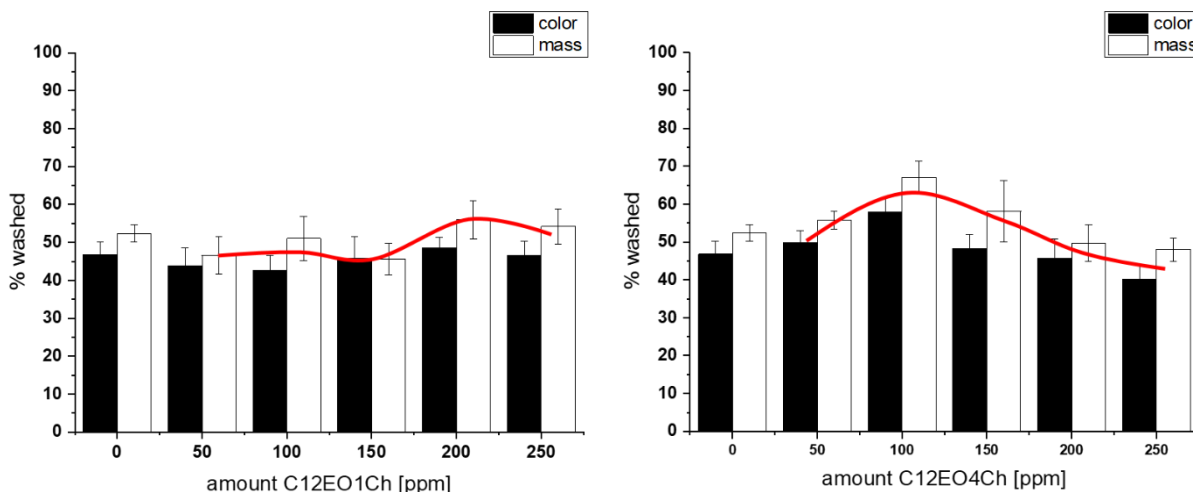


Figure 52: Dependence of the washing results of Biskin in % measured as described in 5.5.2.3 of the standard mixture SDBS:AO7:Tex = 1:1:1 at 0.1 wt% at 14°dH and 25 °C on the addition of different concentrations of C12EO1Ch (left) and C12EO4Ch (right) evaluated by colorimeter (black) and by mass (white).

The washing results changed with changing the amount of added cationic surfactants in both cases. Most results were similar to those of the pure standard mixtures, but a maximum of washing efficiency was found for each cationic surfactant, which was larger than the one of the standard mixtures. For C12EO1Ch, the addition of 200 ppm was most efficient (50 % removal) whereas the best result for C12EO4Ch was obtained with the addition of 100 ppm (60 % removal). Thus, the performed experiments gave a hint towards a dependence of the washing result on the amount of added cationic surfactants and therefore, the dependence on the ratio of added cationic surfactant and the washing solution. More specifically, the ratio of cationic and the anionic surfactant might be the decisive factor, since the nonionic surfactant AO7 will not be influenced by the positively charged additive in the way the anions are. But, the question came up if the crucial point was the positive charge alone or if other factors, in this case mainly the number of EO groups, had any influence on the position of the

maximum of efficiency. For this purpose, the maximum of washing efficiency was considered regarding the molar ratio of the ionic surfactants. The maximum of C12EO1Ch at 200 ppm was two times higher than the one of C12EO4Ch. Thus, a twice as high molar mass of C12EO4Ch would indicate the same molar ratio. The molar mass of the two cationic surfactants did not show that difference. C12EO4Ch has only a 1.4 times higher molar mass than C1EO1Ch. The amounts of present anionic surfactant were the same in all cases. Considering only Tex, the molar ratios of anion and cation were calculated and can be seen in Table 11.

Table 11: Evaluation of the washing results obtained from the washing method as described in 5.5.2.3 regarding the molar amounts of anionic and cationic surfactants at the maximum of washing efficiency.

surfactant	M [g/mol]	ppm at max	n [mol] at max	ratio Tex/cation
C12EO1Ch	366.99	200	0.000545	1.5
C12EO4Ch	515.35	100	0.000194	4.1
Tex	376.48	300	0.000797	

All in all, the performed washing results showed that the positive charge itself was not the crucial point since the two cationic surfactants did not show their maximum at the same molar ratio of anionic and cationic surfactant. Depending on the cationic surfactant, the optimum in washing efficiency changed to different anion-cation ratios. With an increasing amount of EO groups in the cationic surfactant, the number of molecules needed to reach the maximum in washing efficiency decreased. Thus, the necessary amount of cationic additive can be reduced with the insertion of more EO groups.

Additionally to the washing tests, multiple contact angle measurements were performed, as described in 5.5.2.7. With this method, the contact angle of an aqueous solution on a tripalmitin layer surrounded by an oil phase, here triolein, is measured. It gives information about the interaction of the aqueous solution and the two lipophilic phases. The standard solution with a concentration of 800 ppm was measured with the addition of different cationic surfactants. The multiple contact angle, as well as the values of the interfacial tension of the investigated solutions against air and triolein, are given in Figure 53. Significant differences in the interfacial tension measurements could not be detected. This means that the surface activity of the solutions itself was not the decisive factor and

did not change with the addition of the cation. The differences must be in the interaction of additives with the tripalmitin in combination with the triolein. The contact angle values confirmed the trends of the performed washing solutions. A smaller contact angle related to a better interaction of the investigated solution with the solid tripalmitin and the liquid triolein. This can be connected to a better fat removal behavior.

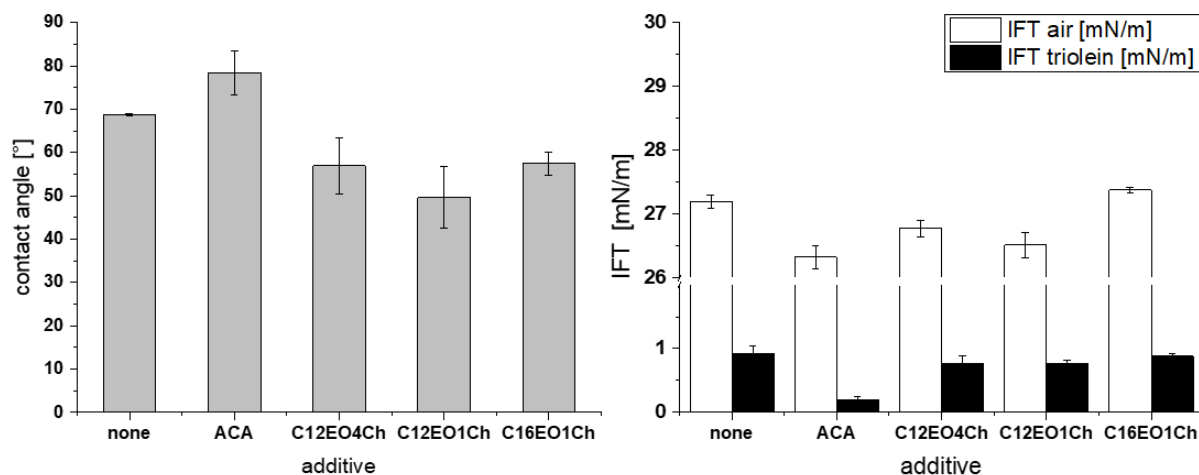


Figure 53: Multiple contact angle measurements (left) and interfacial tension against air (white) and triolein (black) (right) measured as described in 5.5.2.7 at 25 °C of the standard solution (800 ppm) and the addition of 200 ppm of the different cationic additives ACA, C12EO1Ch, C12EO4Ch, and C16EO1Ch.

In comparison to the pure standard mixture as a reference system, the addition of the commercial long-chain cation ACA led to an increase of the multiple contact angle. Surface-active substances, which were promoting the spreading, were disturbed by the cationic surfactant ACA leading to an increase in the contact angle. For the washing efficiency with ACA as additives, no improvement was observed. For the addition of a cationic surfactant, where EO groups are present, a decrease in the multiple contact angle was observed in all cases. The lowest value was obtained for C12EO1Ch with a value of 50 °. Comparing the three different cationic surfactants, the following statement can be made: regarding the multiple contact angle, a certain amount of EO groups seemed to be favorable for decreasing the contact angle between tripalmitin and triolein. But, an increasing number of them did not decrease the value further. Comparing the different chain length, a shorter chain length of 12 carbon atoms was more efficient than 16 carbon atoms. Although it is known that a longer chain length normally increases the surface activity, this seemed to be a hindrance in reducing the multiple contact angle between triolein and tripalmitin.

In summary, the performed washing experiments showed that the addition of a cationic surfactant to the commonly used standard washing solution consisting of the two anionic surfactants Tex and SDBS and the nonionic surfactant AO7 could improve the washing efficiency. But, the presence of EO groups is necessary. A dependence of the optimum of washing efficiency on the added cationic surfactant was found. Depending on the cationic surfactant, which differed in the number of EO groups, the maximum of Biskin removal, which was higher than for the pure standard solution, changed. A trend towards lower amounts of cationic surfactants with a larger number of EO groups in the cationic structure could be assumed. This can be advantageous for washing application. With the addition of small amounts of cationic surfactant, the washing efficiency at room temperature can be improved.

5.3.2.4 Catanionics as compensation for the decrease of AO7 concentration

5.3.2.4.1 Fat removal tests with the in-house built washing apparatus

As already mentioned above, with adding a cationic surfactant as an additive, the overall ionic character of the washing solution was reduced whereas the nonionic influence increased. By behaving as a pseudo-nonionic surfactant, the catanionic ion pair might act as a substitute for the originally present nonionic surfactant AO7. This would make it possible to save surfactant and thus resources. To see if the addition of the cationic surfactant can compensate the decrease of nonionic surfactant AO7, washing tests were performed with changing amount of nonionic surfactant AO7 and added cationic surfactant C12EO1Ch. Four concentrations (0 ppm, 100 ppm, 200 ppm, and 330 ppm) were investigated for each component leading to 16 different washing tests. 330 ppm corresponds to the amount of surfactant which is present in the original standard washing solution. The amount of the anionic components SDBS and Tex was always 330 ppm. Results are shown in Figure 54. The diagrams from left to right show an increase in the amount of nonionic surfactant AO7. The same it is for the cation within one diagram. The broken line indicates the reference system of SDBS:AO7:Tex (1:1:1) with a content of 330 ppm of each component determined via colorimeter.

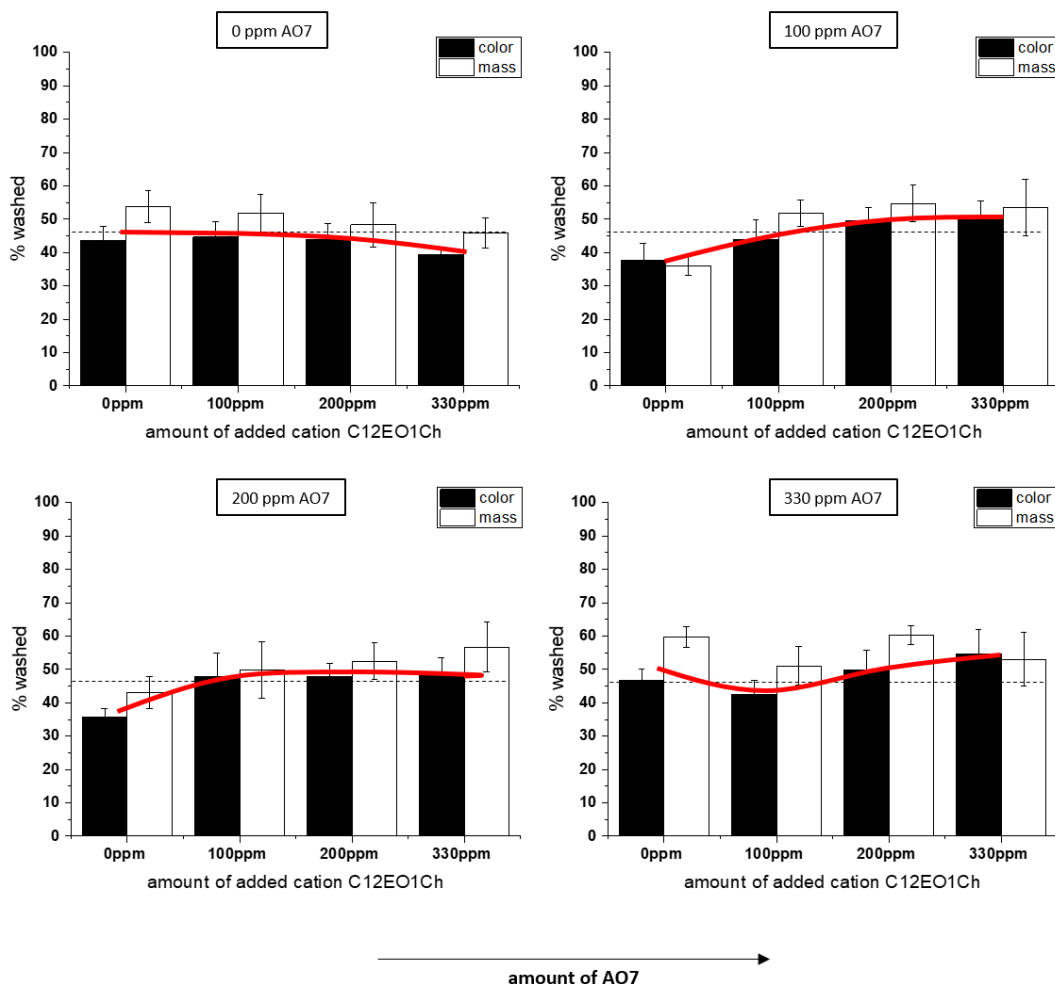


Figure 54: Dependence of the washing results in % measured as described in 5.5.2.3 of the standard mixture SDBS:AO7:Tex = 1:1:1 at 14°dH and 25 °C on the amount of AO7 and the amount of added cation C12EO1Ch evaluated by colorimeter (black) and by mass (white) with constant content of SDBS and Tex of 330 ppm. The broken line indicates the standard mixture.

With no nonionic surfactant present, all washing results were below the standard solution. The washing performance stayed constant with adding the cationic surfactant and even decreased with 330 ppm of cationic surfactant. For the lower AO7 contents of 100 and 200 ppm, the trend was the same for the change in the cationic surfactant concentration. The washing result was below the standard solution when no nonionic surfactant was present. The addition of the cation led to an improvement of the washing result of 35 % reaching a higher washing efficiency than the standard solution for the highest amount of C12EO1Ch. But, it seemed that the amount of additive was not crucial. Already 100 ppm of C12EO1Ch was enough to reach the maximum for the presence of

200 ppm AO7. Saturation could be observed. Also, for the content of 100 ppm of AO7, a saturation in fat removal was observed. For the content of 300 ppm of nonionic surfactant, the smallest amount of C12EO1Ch decreased the washing performance slightly compared to the standard solution. However, with an increasing amount of cationic surfactant, the washing performance improved reaching values for the fat removal of 55 %. This corresponds to an increase in washing efficiency of 22 % compared to the pure standard mixture.

In general, a positive effect of the addition of the cation C12EO1Ch was observed for the three cases, when a certain amount of nonionic surfactant was present. Here, the addition of the cation could compensate the decrease of AO7 content. The additional nonionic character arising from the addition of the cationic surfactant had the same or even a better effect than the AO7 alone. But, the possibility of a complete replacement of the nonionic surfactant could not be proven. In the case of no nonionic surfactant in the washing solution, the washing results were still below the standard solution, indicated by the broken line. The increase of the washing performance showed a higher fat removal efficiency than the original present surfactants, since the effective concentration of surfactants decreased in most samples, when counting the anionic and cationic surfactant as one pseudo-nonionic surfactant.

With the univariate regression analysis as described in 5.5.2.8, the obtained washing results were analyzed regarding the dependence of the washing performance on the nonionic character in the solution. The concentration of nonionic character was calculated as the sum of the concentration of the nonionic surfactant AO7 and the resulted pseudo-nonionic catanionic ion pair. Applying the statistical analysis, a P-value of 0.0049 was obtained. This indicated a significant relation. With higher amounts of nonionic surfactants in the washing solution, the Biskin removal increased. The results fit the observations above, which stated the nonionic surfactants as an important factor for fat removal.

5.3.2.4.2 Fat removal tests with the quartz microbalance

Fat removal tests with the same focus were performed with the QCM as described in 5.5.2.3. To this purpose, a pre-formulated solution of the standard mixture from BASF, called ES1M, was measured with decreasing concentration and the addition of 200 ppm of cationic surfactant C12EO1Ch in each case. It must be mentioned that here some unknown additive could be present in the formulation, meaning an exact comparison to the previously performed measurements with the washing

apparatus was not easily possible. But, the comparison between the QCM curves was reliable. The measured curves were normalized to the value of complete removal determined by removing the complete fat layer with acetone. The curves were analyzed regarding the following parameters: the area of the curve indicating the strength of interaction of the solution with the fat layer and the absolute end removal after the procedure. The measured curves together with the calculated parameters are shown in Figure 55. The broken line indicates the linear decrease in fat removal capacity by lowering the concentration from 800 to 200 ppm.

Adding the cation to the ES1M solution increased the detachment of the fat layer in all cases indicated by a higher shape of the curve. As already seen in previous experiments, the nonionic character induced by the addition of the cation led to a stronger interaction with the fat layer. With the addition of 200 ppm C12EO1Ch to the ES1M mixture, a slight increase in the washing performance was observed, as it was already shown in the previous chapter (see 5.3.2.3). With decreasing concentration of ES1M, the fat removal performance decreased but stabilized to a constant value of around 35 %. Comparing the value to a linear decrease in fat removal performance with the decrease in concentration, the values with the added cationic surfactant C12EO1Ch were higher. Complete compensation of the concentration decrease was not found in this case. But, the addition of a cationic surfactant seemed to have a positive effect. Thus, under certain conditions, the addition of a cation leading to a catanionic surfactant pair with synergistic effects could be seen as a possibility to gain the demanded washing performance at lower surfactant concentrations.

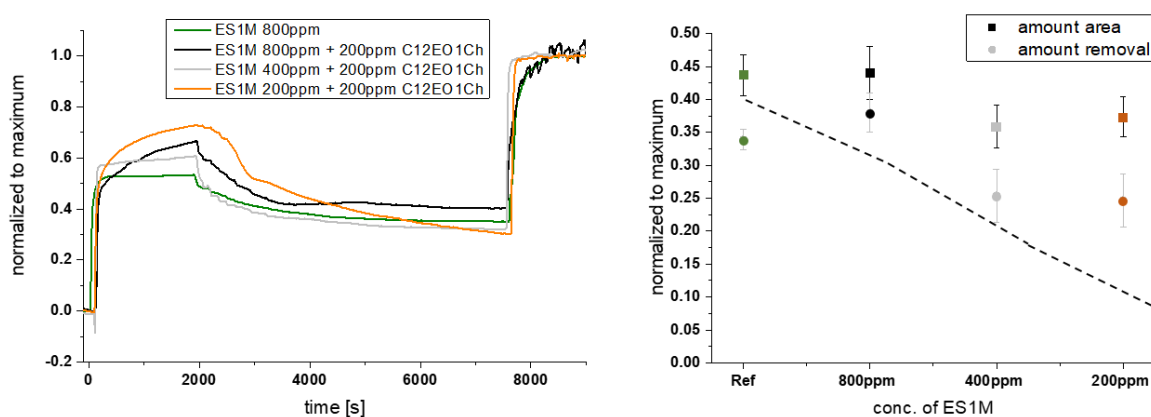


Figure 55: Fat removal results performed via QCM as described in 5.5.2.2 at different concentrations of the pre-formulated standard mixture by BASF at 14°dH with the addition of 200 ppm cation C12EO1Ch. The measured curves are normalized to maximum removal (left), and the evaluated results of the area and end removal are summarized (right). The broken line indicates a linear decrease of the fat removal with the concentration.

Additionally, the multiple contact angle between triolein and tripalmitin was measured for the investigated solutions as described in 5.5.2.7. The interfacial tension (IFT) against air and triolein were also determined. The ES1M solution without any additives was taken as reference (Ref). The results are shown in Figure 56. The addition of 200 ppm of the cationic surfactant C12EO1Ch decreased the multiple contact angle down to 50 °. This was already found in the previous chapter (see Figure 53). The further decrease in ES1M concentration showed no impact. Even at a quarter of the original concentration, the multiple contact angle was in the same range as 800 ppm of the standard solution. The effect of the smaller multiple contact angle can be mainly attributed to the fact that, due to the addition of the cationic surfactant, a catanionic surfactant pair was created. This led to higher efficiency at lower total concentrations. The measurements confirmed the results of the fat removal tests, where the effect of the ES1M concentration decreases did not follow a linear trend. The addition of the cationic surfactant seemed to compensate the decrease of the total surfactant concentration to a certain extent.

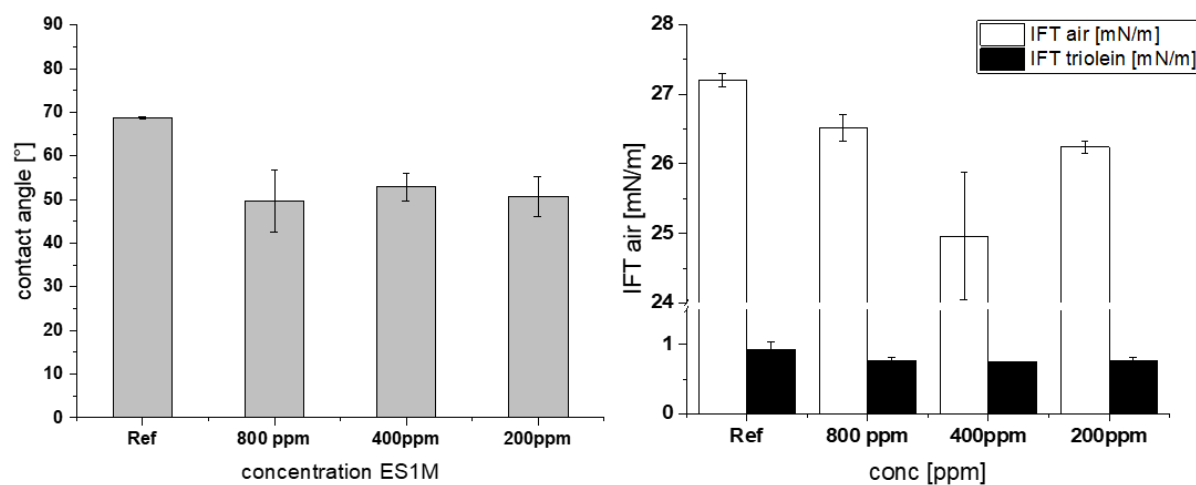


Figure 56: Multiple contact angle measurements (grey) (left), interfacial tension against air (white) and triolein (black) (right) measured, as described in 5.5.2.7 of the standard solution at different concentration (800 ppm, 400 ppm and 200 ppm) with the addition of 200 ppm of the cationic additive C12EO1Ch, in comparison to the standard mixture without additive (Ref).

5.3.2.5 Addition of enzyme

As already done for the addition of the cation to the standard mixture in 5.3.2.3, surface tension measurements were performed to investigate the interaction between the additives and the standard surfactant solution. To this purpose, the influence of the addition of the enzyme alone and in combination with the cationic surfactant to the standard mixture was examined. The obtained surface tension curves are depicted in Figure 57.

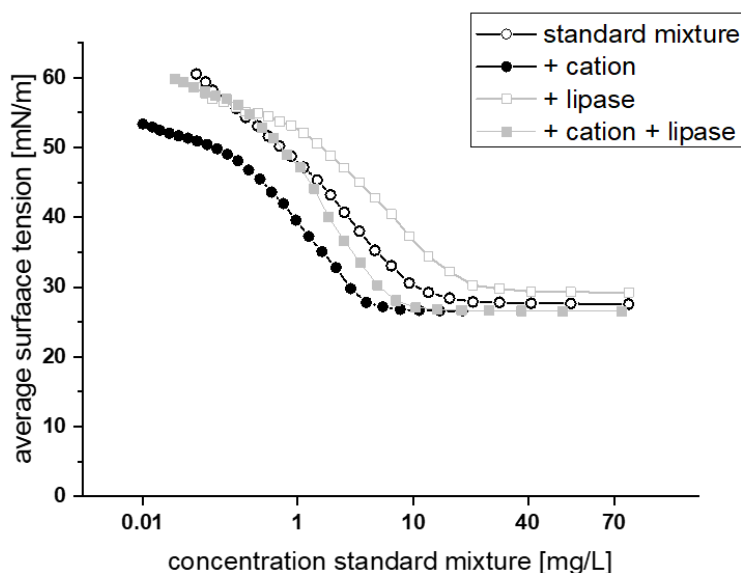


Figure 57: Comparison of the cmc measurement (see 5.5.2.4) of the standard mixture in millipore water (unfilled black circles), the standard mixture with the addition of 200 ppm C12EO1Ch (filled black circles), the standard mixture with the addition of 2 ppm lipase (unfilled grey squares) and the standard mixture with the addition of both, 200 ppm C12EO1Ch and 2 ppm lipase (filled grey squares) at 25 °C.

The cmc curve can be evaluated by two parameters: the efficiency and the efficacy. Both parameters are interesting, since they described the tendency to build aggregates and the surface activity. For the investigated samples, both values showed the same trend. The addition of the enzyme alone gave a higher value for the cmc and also for the finale surface tension. The lipase seemed to interact with the surfactants in a way that hindered them to act in full extent regarding their interfacial behavior. For the addition of the cationic surfactant, a decrease of both values was found (see 5.3.2.3). Adding the cationic surfactant C12EO1Ch to the standard mixture containing the enzyme, the positive effect of the cationic surfactant alone was inhibited. The cmc value was shifted to higher values but did not

reach the value of the pure standard mixture. The interaction of the enzyme with the surface in competition with the present surfactants is reason for that. Moreover, the presence of the enzyme seemed to disturb the interaction between the both oppositely charged surfactants. This resulted in less nonionic ion pairs, which were less surface active. The two additives seem to be inhibited by each other.

5.3.2.5.1 Fat removal tests with the in-house built washing apparatus

Since enzymes gain more and more importance in the detergency industry by now¹⁸⁰, the interaction of surfactant with enzymes is of great interest. The compatibility of pure cationic surfactant mixtures was already shown in 5.3.1.2 exemplarily for the combination of SDS and C12EO4Ch (see Figure 44). But, the situation can change with the presence of different surfactants as it is the case in the washing solution. Furthermore, the compatibility of the substances in solution does not necessarily mean that fat removal performance is the same.

For this purpose, the addition of an enzyme, here a lipase from the *Thermomyces lanuginosus*, to the washing solution was investigated. Since enzymes are normally very sensitive to the pH¹⁸¹, the washing efficiency as a function of the pH was checked to make sure that the performed experiments are reliable and do not take place at minimum enzyme efficiency.

For this, 2 ppm of the enzyme were added to the standard mixture and the pH was set to three different values: pH 10 was chosen, since all other experiments until now have been performed at that value; pH 7 was set to see the effect of neutral surroundings; pH 4.3 indicates the isoelectric point of the enzyme¹⁸², meaning that the enzyme has a net of zero charge. The pH values below that value have not been examined, since washing at such low pH values is not realistic. As it can be seen in Figure 58, the influence of the pH on the washing results obtained from the washing apparatus was small. The washing efficiency slightly decreased at neutral pH compared to the other two investigated points. Thus, changing the pH in experiments with the enzyme was not justified and the following washing tests were performed at a pH of 10.

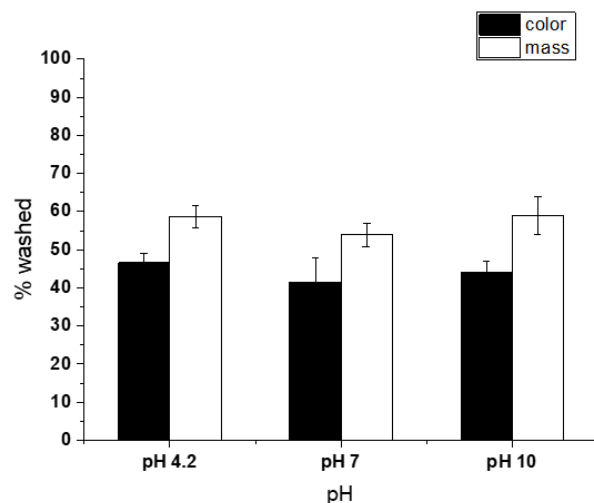


Figure 58: Dependence of the washing results on the pH in % measured as described in 5.5.2.3 of the standard mixture SDBS:AO7:Tex (1:1:1) 0.1 wt% + 2 ppm lipase at 25°C evaluated by color (black) and mass (white).

The investigations of the effect of enzyme were performed with the in-house built washing apparatus, as described in 5.5.2.3 with two different washing systems. One was the standard mixture and the second one was the standard mixture with 100 ppm of the cationic surfactant C12EO1Ch added to the solution leading to a catanionic combination. To both systems at four different concentrations (250, 500, 750 and 1000 ppm), 2 ppm of the enzyme was given. A blank value without any surfactant addition was measured additionally. The results are shown in Figure 59.

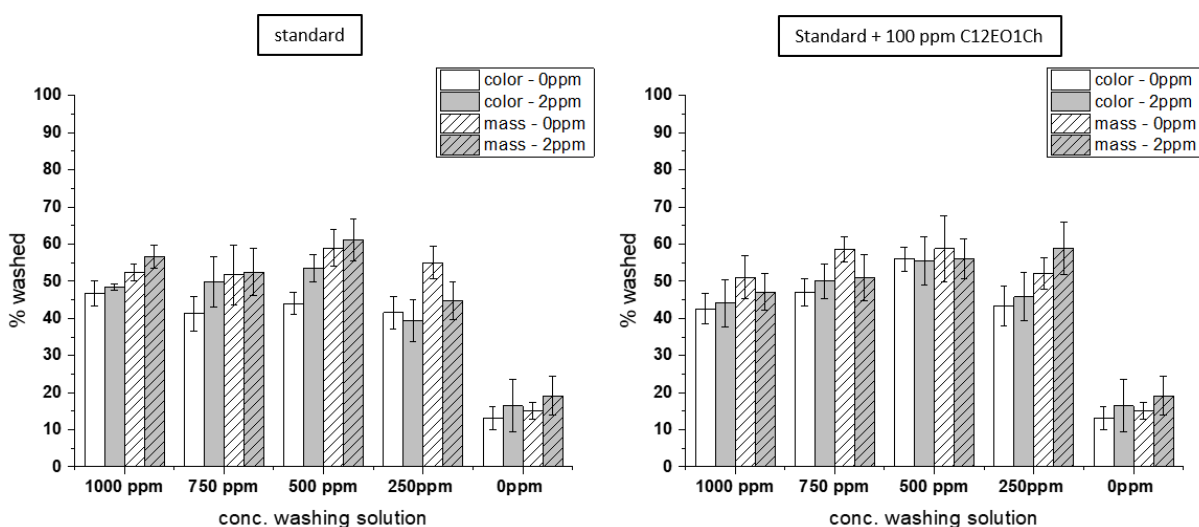


Figure 59: Influence of the addition of 2 ppm of lipase on the standard mixture (left) and the standard mixture with 100 ppm added C12EO1Ch (right) on the washing results in %, depending on the concentration, at 25°C and pH 10 evaluated by color (blank) and by mass (shaded) as described in 5.5.2.3.

The left diagram shows the washing efficiency of the pure standard mixture. The addition of the enzyme increased the washing efficiency – slightly at higher concentrations and with a larger effect at a concentration of 500 ppm. When decreasing the concentration of the standard solution further, no positive effect was found for the added enzyme. The positive effect of the addition of an enzyme to the washing solution is known and thus commonly found in detergent formulations.^{156, 183} An added enzyme in the washing solution could support the fat removal of the surfactants. The fatty stains of the triglycerides in the Biskin were decomposed into more hydrophilic compounds. Compared to their non-hydrolyzed stains, they can be removed more easily.¹⁸⁴ With smaller amounts of surfactants in the solution, this effect becomes more significant. Then, more space is available for the enzyme to act at the interface which was occupied by the surfactants. This was shown by a higher difference in the washing efficiency of both solutions at a lower concentration of 500 ppm of the standard mixture. An increase of 10 % could be observed.

In the case of the standard solution combined with the cationic surfactant C12EO1Ch, the situation was different. The difference between adding and not adding the enzyme was marginal. The values were in the same range. Especially at higher concentrations, the addition of the enzyme was contra productive. The presence of the cationic surfactant, which already led to an improvement of the washing results (see 5.3.2.3), in combination with the enzyme does not show a synergistic effect of both additives. They even seemed to hinder each other. An exception was found for low surfactant concentration of 250 ppm. Here, the addition of the enzyme increased the washing performance by more than 10 %. The interaction between the cationic surfactant and the enzyme must be reduced in this case.

Both additives showed an improved fat removal performance, when used as the only additive. The question arose which additive was more effective since the combination of both did not lead to an improvement of the washing result. For a better comparison of this thematic, the two cases are compared in Figure 60.

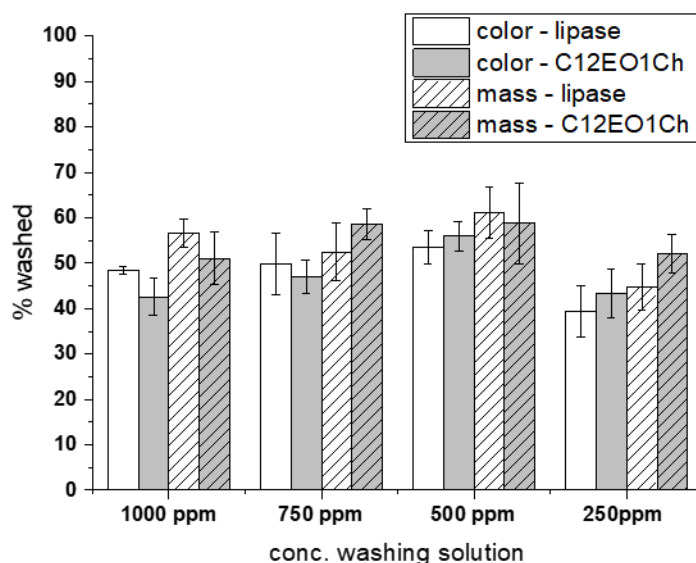


Figure 60: Comparison of the washing results in % of the standard mixture with the addition of 2ppm lipase (white) and 100ppm C12EO1Ch (grey) evaluated by color (blank) and by mass (shaded) at 25°C and pH 10 as described in 5.5.2.3.

For this purpose, the addition of 100 ppm C12EO1Ch or 2 ppm lipase were compared at four different concentrations of the standard mixture SDBS:AO7:Tex (1:1:1). For the highest concentration of 1000 ppm, the washing results were better in case of the addition of the enzyme. For all lower concentrations, the fat removal was equal or better with the addition of the cationic surfactant. Especially for the lowest concentration of 250 ppm, the difference was significant. Here, the effect of increasing the nonionic character was more effective than the effect of additional hydrolysis of the triglycerides from the enzyme. Since the problem of stabilization of enzymes in solution over longer time is still not completely solved, the use of a cation instead of an enzyme is a promising alternative, which can lead to an even better fat removal result.

5.3.2.5.2 Fat removal tests with the quartz microbalance

The same aspect was also investigated with the QCM. As already described more precisely in 5.3.2.4.2, the ES1M solution was used as standard mixtures. The Biskin removal performance from the quartz crystal was measured for the standard solution alone, with the addition of 2 ppm enzyme, with the addition of 100 ppm cationic surfactant C12EO1Ch and with the addition of both. The received curves were analyzed regarding the three parameters: maximum, area and end removal with regard to the

maximal removal by acetone, as described in 5.5.2.2. The curves are shown in Figure 61 and the resulting parameters are given in Table 12.

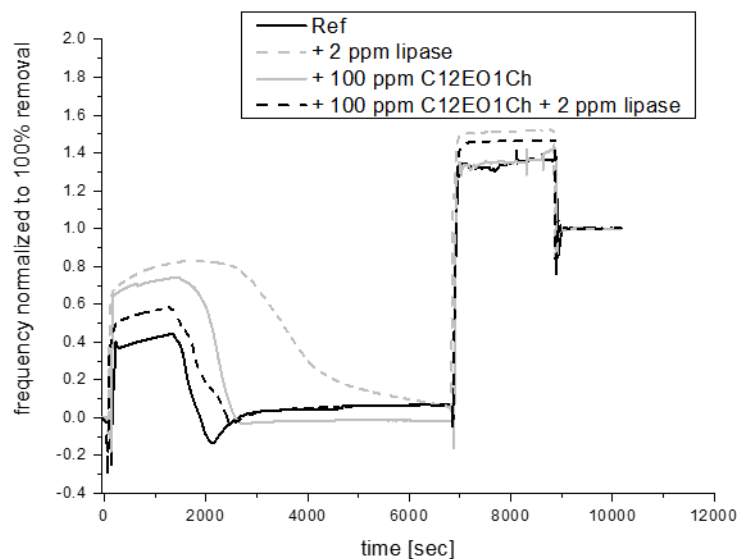


Figure 61: Comparison of the influence of the addition of the cationic surfactant C12EO1Ch and lipase to the washing formulation ES1M (pre-formulated standard mixture by BASF) via QCM measurement as described in 5.5.2.2 in 14°dH at pH 6. The measured frequency was normalized to the value of complete removal of the Biskin layer by acetone at the end of the measurement.

Table 12: Resulting parameter maximum, area and end removal in % in regard to the complete removal by acetone from the QCM measurement as described in 5.5.2.2 in 14°dH at pH 6 for the washing formulation ES1M (pre-formulated standard mixture by BASF) and the influence of the addition of the cationic surfactant C12EO1Ch and lipase.

additive	maximum [%]	area [%]	end removal [%]
none	44	30	6
+ 2ppm lipase	82	47	6
+ 100ppm C12EO1Ch	74	20	1
+ 100ppm C12EO1Ch + 2ppm lipase	58	18	6

The end removal of all combinations was nearly the same and negligible with only some percentages. But, a difference in the area and also in the maximum of the curves was measured. This showed a difference in the direct interaction of the washing solution with the fat layer. In contrast to the washing apparatus (see 5.3.2.5.1), the enzyme as the only additive gave the best values in the case of

the QCM. This means that considering only the influence of the interaction of the washing solution with the fat layer without any external influences, the enzyme seemed to interact with the fat layer the best. But, no reaction with the Biskin layer could be assumed since no significant removal was observed, which would be probable if more hydrophilic substances would have been formed. The pure solution of ES1M gave the worst result, whereas the addition of the cationic surfactant C12EO1Ch improved the interaction with the fat layer. So, the interaction with the fat layer could be improved by either the enzyme or the cationic surfactant. But, the combination of both additives did not result in any synergistic effects. This fits the results obtained with the washing apparatus (see 5.3.2.5.1).

Until now, the fat removal from the quartz crystals was only detected by measuring the frequency. Here, only an overall value was obtained and no impression of the microscopic view on the quartzes was possible. For this purpose, the investigated quartz crystals were checked with the white light interferometer (WLI) and the scanning electron microscope (SEM), as described in 5.5.2.5. The different quartzes can be seen in Figure 62.

For comparison, a coated but unwashed quartz crystal was analyzed as a reference. For the unwashed sample (left), a homogenous fat layer was observed. With surface-active substances in the washing solution, removal of the fat could be seen. For the presence of a lipase, an attack over the complete fat layer at different points could be observed. For the pure ES1M solution, it seemed that the removal of the fat starts more from the edges and not from the overall area. More removed areas in-between the fat layer were present in the case of the enzyme. This fitted to the fact that the lipase can stick to the fat surface due to its amphiphilic character and could catalyze the hydrolysis of the triglycerides.¹⁵⁸ This results in easier removal of the fats. The addition of the cationic surfactant showed the same trends, but they were less decisive. The increased nonionic character could be the reason for a better sticking to the nonpolar fat layer. When attached there, the surfactants could support the fat removal by emulsification.

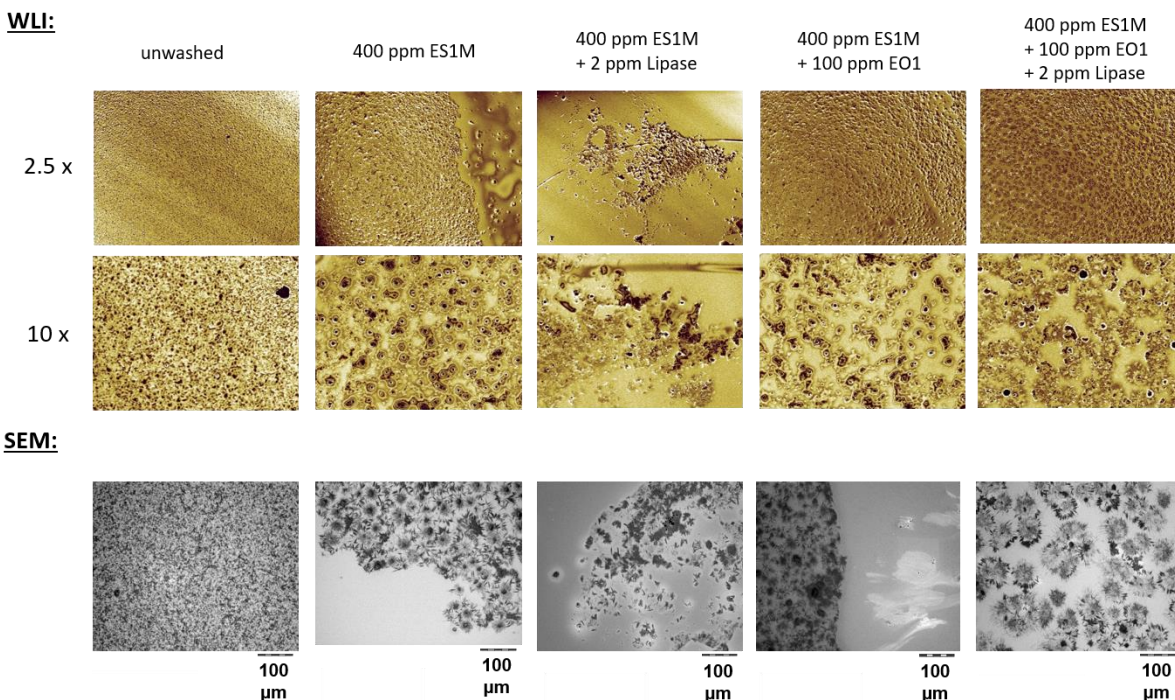


Figure 62: Pictures of the surface of the quartz crystals from the comparison of the influence of the addition of C12EO1Ch and lipase to the washing formulation ES1M performed with a WLI (above) and a SEM (below).

In summary, the previous experiments with the washing apparatus as well as the QCM showed similar results. The addition of the cationic surfactant C12EO1Ch improved the fat removal of the standard washing solution. The same was observed for the lipase as an additive. Comparing both additives showed a better washing performance for lower concentrations of the standard solution. Combining both additives showed negative effects. The fat removal was less. Since several complications with the lipase in solution are known^{156, 158}, the use of a cationic surfactant instead of an enzyme is a promising alternative, which can lead to an even better fat removal result at lower surfactant concentration. This is of main interest, especially when considering the saving of resources.

5.4 Conclusion

The catanionic combinations were investigated regarding their potential for fat removal. This was performed via two different methods: the QCM and the washing process with an in-house built apparatus. The main intention was to investigate the influence of the presence of a catanionic surfactant pair by the addition of a newly synthesized EO group-based cationic surfactant to the anionic washing solution.

For this purpose, the pure catanionic mixtures were scanned with the QCM at the ratios 5-5 and 9-1, in a first step. The four parameters peak height, maximum detachment, area, and end removal were used for analysis. The combinations around equimolar ratio (5-5) showed better fat removal results in nearly all cases due to their more nonionic character in the washing solution. With univariate regression analysis, an increase in the hydrophobic part of the molecular structure leading to stronger hydrophobic interactions with the fat layer was shown to be a promoting factor. This was indicated by a significant relation with the cationic chain length, the HLB value, the anion-cation ratio, and the surface tension. From the QCM measurements, four promising combinations (SDS with C12EO1Ch, SDS with C12EO4Ch, C12EO4SO4 with ACA and Tex with ACA at the anion-cation mass ratio 5-5) were chosen to be investigated with the washing apparatus. Here, the pure combinations, the combinations with the addition of 2 ppm of lipase and the combinations inserted in the standard mixture as a replacement for Tex were tested. For all cases, the combination of SDS and C12EO1Ch gave the best results. The washing result was similar to the reference. The pure catanionic combinations with the addition of the enzyme lipase showed promising results compared to both components alone. In an enzyme stability tests, the negative effect of the cationic surfactant was shown to be reduced with the addition of the anionic surfactant.

Complex washing systems based on the three surfactants sodium dodecylbenzylsulfonate, Lutensol AO7, and Texapon N70 were tested regarding several different parameters concerning the catanionic systems. The temperature was shown to be a crucial factor for all investigated systems. Reason for this was the melting state of the soil, which could lead to easier removal with higher liquid character. Since the focus was on the challenge to perform fat removal efficiently at a lower temperature, all experiments were performed at room temperature. By comparing Biskin, sebum model and beef fat model, the type of soil was shown to be another important point. Most effort was necessary to remove Biskin, whereas the other two soils were removed more easily. The observations could be

correlated to the contact angle measured between the washing solution and the investigated fats. With decreasing contact angle, the fat was removed more efficiently. The influence of the addition of a cationic surfactant to the standard mixture was examined. The presence of an EO group in the cationic structure was observed to be a crucial factor for a positive effect in the fat removal performance. Depending on the number of EO groups in the cation, the maximum of the positive effect was found at different ratios regarding the amount of anionic surfactant present in the solution. The increasing nonionic character of the washing solution seemed to promote fat removal. Moreover, the higher flexibility due to the EO groups led to a higher solubility in solution and out of it to higher effectiveness.

The effectiveness of the addition of a cationic surfactant leading to a pseudo-nonionic surfactant pair was compared to the effectiveness of the non-ion surfactant AO7. It was shown that it was possible to reach a significantly higher fat removal with the addition of the cation C12EO1Ch, if the concentration of AO7 was decreased. But, a certain amount of AO7 seemed to be necessary for good removal. With the QCM, the same trends were confirmed. The use of a cationic surfactant as an additive instead of the typical amount of the nonionic surfactant like AO7 is an elegant way to reach a better washing result at lower overall surfactant concentration.

Furthermore, the effect of the addition of an enzyme, the lipase, was examined. No synergistic effect could be observed for the two additives, lipase and the cationic surfactant C12EO1Ch. The washing results of the two additives alone were similar. For low surfactant concentration, the washing performance was increased with the cationic surfactant to a larger extent than with the enzyme. This can be interesting. Especially, when regarding the still present disadvantages like the sensitiveness and stability of the enzymes, a cationic surfactant can be a promising alternative to the enzyme for improving the washing result through an additive.

In summary, an improvement of the fat removal performance with the addition of a cationic surfactant to the standard washing solution was shown. The formation of a pseudo-nonionic catanionic surfactant pair seemed to increase the washing behavior. Also, when comparing the washing performance to enzymes as additives, the use of catanionic combinations in detergent formulations seems a promising way to achieve high efficiency at low surfactant concentrations at low temperatures. However, it is not excluded that enzymes can be found that are compatible with catanionic EO-surfactants and then can lead to the desired synergism to improve fat removal.

5.5 Experimentals

5.5.1 Chemicals

The lipase from *Thermomyces lanuginosus* (>100 U/g), sodium dodecyl sulfate (purity >99 %), glyceryl trioleate (purity >99 %), squalene (purity >98 %), stearyl palmitate (purity >99 %), cholesterol (purity >99 %), stearic acid (purity >98 %), sodium dodecylbenzene sulfonate (purity 81.7 %), squalene (purity >99 %), cholesterol (purity >99 %), toluol (purity 99.8 %), acetone (purity 99.5 %) and Sudan black B were purchased from Sigma-Aldrich (Taufkirchen, Germany). Texapon N70 (purity 70 %), Lutensol AO7 (purity 99 %) and all other newly synthesized anionic and cationic surfactants and cetyl palmitate were kindly provided by BASF (Ludwigshafen, Germany). Calcium chloride dihydrate (purity >99 %) was bought from Roth (Karlsruhe, Germany). Solutions of 1 M sodium hydroxide and hydrochloric acid and magnesium chloride hexahydrate (purity 99 %) were from Merck (Darmstadt, Germany).

ES1M describes a pre-formulated mixture of the three surfactants Texapon N70, SDBS, and Lutensol AO7 prepared by BASF. To some extent, there can be some unknown further additives present in the solution.

Biskin was bought as commercially available vegetable fat from Peter Kölln KGaA in the supermarket. For the model fat layers of sebum and beef fat, the oils and fats were weighed in and homogenized by heating up to 60 °C for 15 mins.

Millipore water was used for all experiments, if not mentioned otherwise. All chemicals were used without further purification.

5.5.2 Methods

5.5.2.1 Preparation of the washing solution

Millipore water was used in all experiments, if not mentioned otherwise. For experiments with hard water (14 °dH), appropriate amounts of $\text{CaCl}_2 \cdot 2\text{H}_2\text{O}$ and $\text{MgCl}_2 \cdot 6\text{H}_2\text{O}$ were weighed into millipore water and stirred until complete dissolution. The molar ratio of Ca^{2+} to Mg^{2+} was always 2:1.

For the pure cationic solutions, the appropriate amounts of cation and anion were weighed in into a glass bottle and filled up with Millipore water. For the complex systems, stock solutions of Texapon N70, SDBS and AO7 with 10 wt% were prepared to be used for all washing solutions. For the washing solutions, the appropriate mass of stock solution was weighed in a glass bottle. The volume of needed additives was added to the solution via pipette. Then, the prepared hard water was filled into the bottle, until the final volume was reached. The pH was adjusted with solutions of different concentrations of NaOH and HCl. The solution was then stirred overnight for equilibration and used the next day.

5.5.2.2 Quartz microbalance

The quartz crystal microbalance QSense Pro from Biolin Scientific was used for several first experiments before testing promising combinations and more complex systems in more realistic ways like a washing apparatus. Here a quartz crystal was coated with a fat, here biskin, and its frequency was detected while solutions flow above it with a defined rate and time. With the change of mass, the frequency changes, either by adhesion on the fat layer leading to a decrease in frequency or by removing mass from the fat layer leading to an increase in frequency. Every measurement was performed twice and the average value was taken for evaluation.

The determined curves were normalized to the complete removal of the fat layer. The analysis of the resulted curve was done by determination of three parameters. An example of a measured curve and an illustration of the determined parameters can be seen in Figure 63. The four parameters are the following:

- The absolute end removal describes the amount of fat removed by the surfactant solution after the complete washing procedure – read off by the end frequency value in comparison to the potential removal of 100 %.
- The peak height at the beginning of the surfactant solution describes the absorption of the surfactants on the fat layer, when the surfactant solution gets in the first contact with the fat layer.
- The maximum of the curve describes the lifting of the fat layer by the surfactants.

- The area under the measured frequency curve was a measure of the interaction of the surfactants with the fat layer. Due to this, a light hoisting of the fat layer, reflected in an increase in frequency, can be observed. The relative size of this area in comparison to the whole possible area was determined.

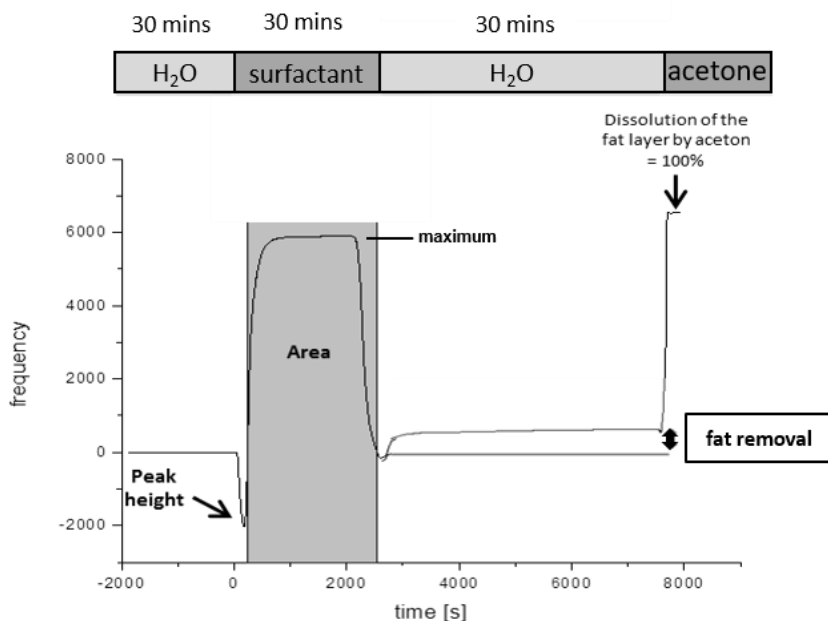


Figure 63: Example of a QCM measurement with the determined parameter illustrated.

Procedure

The quartz crystals were prepared the day before. First, the quartz crystals were treated with plasma for 15 mins in a femto plasma oven from electronic Diener Plasma-Surface-Technology. After that, the crystals were spin-coated with a Spincoater LapSpin6 from Süss Microtec. A solution of dissolved Biskin in toluol (1:6) was used for that. The parameters of the spin-coating procedure were always the following: 30 μ Ls of Biskin solution, 30 seconds, 3000 rpm. After that, the crystals were put in the refrigerator to cure overnight.

The next day the quartz crystals were measured. For the pure catanionic combinations, the method was the following: 30 mins of millipore water, 30 mins washing solution (catanionic solution), 90 mins millipore water, 20 mins acetone. For the fat removal tests of more complex systems, the method was the following: 10mins hard water, 30 or 40 mins formulation, 30 mins hard water, 20 mins EtOH/acetone and 20 mins hard water. All tests were performed at a pH of 6.

5.5.2.3 The in-house-built washing apparatus

Washing tests were performed with an in-house built washing apparatus (see Figure 64). Here, 15 sample vessels of stainless steel were rotated with 40 rpm in a tempered water bath. Each vessel has a volume of 100 mLs and can tightly be sealed. It was filled with 50 mLs of investigated washing solution. Five stainless steel balls ($r = 0.35$ cm, $m = 2$ g) were added to the solution to imitate the mechanics present in a usually used washing machine filled with clothes. One washing procedure was defined as a time of 30 mins.



Figure 64: In-house built washing apparatus.

Procedure

For the investigated textile stripes, unsoiled cotton was purchased from Swissatest and cut in pieces of 2 x 8 cm. The investigated soil was colored with 0.5 wt% Sudan black B. Sudan black B is a lysochromic and fat-soluble azo dye (see Figure 65). It is commonly used as a staining agent for lipids or triglycerides.

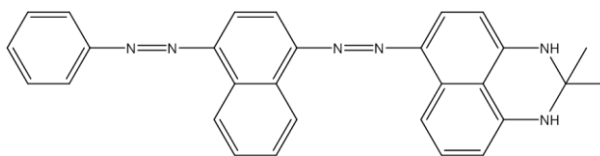


Figure 65: Molecular structure of the azo dye Sudan black B.

The mixture of soil and color was heated to 65 °C to get liquefied. The liquid soil was mixed with chloroform in the mass ratio 1:5. The fibers were dipped into the solution for several seconds and were dried overnight at ambient conditions. The mass of the stripes was measured the next day before the washing test. After the washing procedure, the washed fibers were dried again overnight and weighed again the day after. Besides the evaluation by mass, the fibers were measured with a spectrophotometer Elrepho SE 071 from Lorentzen & Wettre. For each stripe, ten different positions

on the stripe were measured. Here, the difference of E before and after the washing process was compared. The ΔE value was calculated as the following:

$$\Delta E = \sqrt{L^{*2} + a^{*2} + b^{*2}} \quad (\text{equation 13})$$

where a^* , b^* and L^* are the coordinates of a color system (depicted in Figure 66), in which a^* and b^* correspond to the colorfulness and L^* to the brightness. The larger the ΔE value, the larger the color difference and the better the detergency performance of the respective surfactant solution.

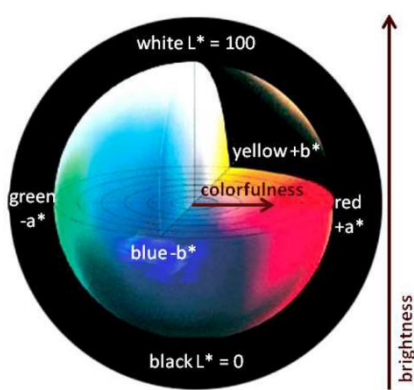


Figure 66: The L, a and b color system, in which a^* and b^* correspond to the colorfulness and L^* to the brightness. The picture was taken from reference ¹⁸⁵.

5.5.2.4 Determination of the cmc

Surface tension measurements were performed with a force tensiometer – K100 (model K100 MK2) from KRÜSS using a platinum-iridium plate. The tensiometer was equipped with a double dosing system (Metrohm Liquino 711), and the recording of the surface tension was done automatically as a function of the surfactant concentration. The temperature was monitored and kept constant at 25 °C. The surface tension was plotted against the logarithm of the concentration. The cmc was determined by a linear fit of the intersection of the two linear parts of the curve. Every measurement was performed three times and the average value was taken for evaluation.

5.5.2.5 White light interferometry and scanning electron microscope

For optical illustration, a white light interferometer (WLI) Wyko NT9300 from Bruker was used. The investigated quartz crystal was checked for dryness and placed under the interferometer to depict the surface of it at two different magnifications (2.5x and 10x). Additionally, a scanning electron microscope (SEM) Phenom Pro-X from PhenomWorld – Thermo Fisher Scientific was used to image the surface of the quartz crystal.

5.5.2.6 Enzyme stability tests

For the enzyme stability tests, the surfactant solutions were used at a concentration of 20 wt% in millipore water. 50 ppm of lipase was added to the solutions. Samples were taken right after mixing and after 1 and 7 days. The enzyme activity was determined with a lipase assay as described in reference ¹⁸⁶.

5.5.2.7 Contact angle measurements

Contact angle on substrates against air

The preparation of the substrate was done in the following way: for each soil, a solution of 10 wt% of soil in toluene was prepared. A quartz crystal was then spin-coated as described in 5.5.2.2 two times with this solution. The coated quartz crystals were cured overnight and measured the next day. For the measurement of the contact angle, a drop shape analyzer - DSA100 from KRÜSS was used. With this device, a small droplet of the investigated solution was put onto the prepared fat layer. The contact angle was measured five times in intervals of 5 secs, 30 secs after the drop hits the fat layer. The measurement was repeated three times, and the average value was taken.

Multiple contact angle

The procedure of the measurement of the multiple contact angle was the same as for the contact angle measurement against air described above. The preparation was the following: tripalmitin was melted and put on a microscopic slide. It was put overnight in the refrigerator to cure. The tripalmitin slide was put onto a small metal ring into a measurement chamber so it can be easily removed after

that. The chamber was filled with triolein so that the tripalmitin slide was spaciouly covered. Then, a drop of the sample was put onto the tripalmitin surface with the drop shape analyzer - DSA100 from KRÜSS and was measured five times in intervals of 5 secs 30 secs after the drop hits the fat layer. The measurement was repeated three times, and an average value was taken.

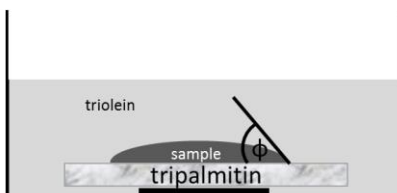


Figure 67: Construction of the multiple contact angle measurement chamber

5.5.2.8 Statistical analysis

For statistical analysis, regression analysis in Excel Office 365 has been used. All experimental data, which has been shown in 3.3 was included in the calculation. For the univariate regression analysis, one independent molecular property was correlated with a dependent physicochemical property. The P-value was used to evaluate the significance with a significance level of 5 %.

6 Towards application: catanionics as spreading agents

6.1 Introduction

The phenomena of a drop spreading on a certain surface is an observation, which is done by everyone in everyday life. The picture of dew on a leaf is in everyone's mind and is symbol when talking about this topic (see Figure 68). For some applications, exactly this phenomenon is desired. For example, more and more glass surfaces like in showers are coated to assure that the water flows down fast without any unpleasant deposit of calcium carbonate.¹⁸⁷ In this context, the most known term in the field of spreading is probably the term "lotus-effect"¹⁸⁸, which has been gaining fame due to the advertising of outdoor clothes of several companies. The term indicates the runoff of drops on very hydrophobic surfaces and is, therefore, the opposite of spreading. Preventing spreading on a surface is also of interest in several processes in industry and for the consumer. For example, road pavements should not be wetted easily, since water in the cracks destroys the surface when crystallizing in the winter.¹⁸⁹



Figure 68: The lotus-effect on a leave after rain.

The control and understanding of the spreading phenomena are still not completely explained.¹⁹⁰ But, the investigations are ongoing. Great interest is the investigation of different aqueous surfactant solutions and their wetting behavior towards complete wetting. For example, Dutschk *et al.* examined the wetting dynamics of surfactant solutions on different hydrophobic polymer surfaces. They found that ionic surfactant solutions do not spread on low energy surfaces. Nonionic surfactants did show different behavior and enhanced the wetting of all tested hydrophobic surfaces. In the area of pest control in agriculture, the aspect of wetting is crucial. Since the plant leaves are normally water-repellent (hydrophobic), the speed and efficiency of wetting these surfaces are of great interest. The

situation of a drop spreading on hydrophobic surfaces, which is present in such applications, was investigated, e.g. by Rafai *et al.* They compared the spreading speed to silicone oil. They showed that certain surfactants based on trisiloxane speed up the spreading whereas the anionic surfactant did not.¹⁹¹ In oil recovery, the topic of spreading is also a decisive factor. The oil that has to be removed from the reservoir is simplified by decreasing the spreading of the oil in the rock. The determination of the transport properties such as capillary pressure, relative permeability and oil recovery is significantly influenced by the wetting conditions of a reservoir rock. Several investigations on this topic have already been done.¹⁹² The aim is not always to increase the spreading of aqueous solutions, but also to inhibit it. For this purpose, liquid coatings of superhydrophobic layers are performed since reactions through water can be reduced by that. By using such coatings, the friction drag of water can be decreased significantly.¹⁹³ Printing is another field, where the topic of spreading is important. If the ink is sprayed on a surface, it should not spread. This would lead to blurred signs. Several investigations on this topic have been done. Perelaer *et al.* for example introduced a new process on polymer substrates for direct fabrication of conductive features. The best spreading agents investigated there were the group of surfactants based on trisiloxanes, and are therefore called “super-spreader”.¹⁹⁴ The process behind this behavior is still not completely understood. They do have some disadvantages. Over a longer period, they are unstable in an aqueous environment and even more unstable in basic or acidic medium. A splitting of the Si-O bonds in the silicone backbone happens. This is a problem, since a lot of processes are based on aqueous media.¹⁹⁵

The ideal spreading agent is not yet found, and thus, investigations are of high importance. For this purpose, the new combinations of catanionics are tested towards their spreading behavior in the following. On a polyethylene surface, the contact angle was measured. Combinations with promising results were investigated further. For three combinations, high-speed camera recording of the wetting process was performed. Other physicochemical properties of the surfactant combinations like surface tension and adsorption behavior were considered as influencing effects on the spreading behavior.

6.2 Fundamental information

6.2.1 Spreading and wetting

If a liquid is put onto a solid surface, a drop forms. The shape of the drop is determined by the intermolecular interactions - more precisely: by the three participating interfacial tensions. Thomas Young was the first who described the relation of these interfacial tensions with the introduction of the contact angle θ by the Young equation (see (equation 12)).¹⁶¹

It is defined as the angle between the intersection of the solid-liquid interface and the liquid-vapor interface. Two cases can be distinguished and are shown in Figure 69. If the contact angle is smaller than 90° , the liquid favors wetting on the surface. The spreading of the liquid over a certain area of the surface occurs. It is called wetting. A contact angle greater than 90° indicates that the liquid does not favor spreading on the surface. It is called non-wetting.¹⁹⁶ If the contact angle of water on the surface is larger than 150° , the surface is called super hydrophobic.¹⁷⁸

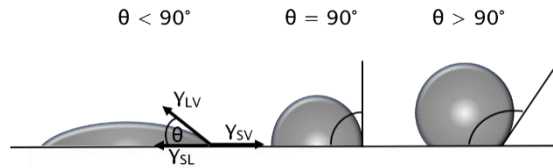


Figure 69: Schematical picture of the three possible ways of the formation of a droplet on a homogenous solid surface. The picture was taken from reference ¹⁷⁸.

For the description of the different wetting states, a parameter was introduced by de Gennes in 1985.¹⁹⁷ It is called the spreading coefficient. It describes the surface free energy $\gamma(SV)$ relative to its value for complete wetting. Mathematically it is described as:

$$S_{sp}(LS) = \gamma(VS) - \gamma(LS) - \gamma(VL) \quad (\text{equation 14})$$

where S_{sp} is the spreading coefficient and γ is the interfacial tension between the vapor phase (V), the liquid phase (L) and the solid (S). If $S_{sp}(LS)$ is positive, the liquid spreads completely. If $S_{sp}(LS)$ is 0 or smaller, the drop does not spread completely. It will reach an equilibrium contact angle.¹⁹⁸

As described above, the interfacial properties of the liquid have a crucial effect on the spreading behavior. Another important aspect is the surface itself. Differentiation is done between two different kinds of surfaces: high-energy and low-energy surfaces. As the names already describe, they differ in their solid/vacuum surface energies. Hard solids, which are held together via covalent, ionic and metallic bonds, have high-energy surfaces meaning that high energy is needed to break the bonds. Soft solids are bound through weaker bonds like van der Waals forces or in certain cases hydrogen bonds. Here, less energy is necessary to break the bonds. In general, for high-energy surfaces, a complete wetting is observed for the most solutions. This is not the case for low-energy surfaces. Here, the situation is more difficult, and the number of components which spread on the surfaces is limited.¹⁹⁷

Additionally, Wenzel proposed an equation where the roughness of a surface was considered.¹⁹⁹ He included a roughness factor into the Young equation, which is defined as the ratio of the actual surfaces and the geometric surface. Wenzel's equation is not completely applicable since it does not consider the air as a surface in very rough surfaces. Thus, the Cassie equation was implemented, which is used to describe such heterogeneous surfaces with the Cassie contact angle defined as:

$$\cos \theta (C) = f_1 \cos \theta (1) + f_2 \cos \theta (2) \quad (\text{equation 15})$$

where f_1 and f_2 are the fractions of material 1 and 2 on the surface and $\theta(1)$ and $\theta(2)$ are the intrinsic contact angle of the liquid with material 1 and 2.²⁰⁰

6.2.2 Surfactant-enhanced spreading

To increase the wetting of a hydrophilic liquid, most times water, on a hydrophobic surface, the easiest way is to add some surfactants to the solution. By adding a surfactant, the process of wetting gets more complex.²⁰¹ The diffusion of the surfactant in solution is time-dependent as well as the adsorption on the interfaces. But, these processes are very fast. Consequently, the interfacial tension between the solid-liquid and the liquid-vapor phase will not change over time compared to the initial state when the drop hits the surface. The only interfacial tension that can vary is the one between the solid and vapor phase. The reason for this is the slow adsorption of surfactant molecules in the front of the droplet on the bare hydrophobic surface. The surface free energy Φ_F of a drop on a solid surface can be described with the following equation:^{187, 196}

$$\Phi_F = \gamma (LV) S + PV + \pi R^2(\gamma (SL) - \gamma (SV)) \quad (\text{equation 16})$$

where S is the area of the liquid-vapor interface. $P = P_a - P_1$ is the excess pressure inside the liquid. P_a is the ambient air pressure, and P_1 is the pressure inside the liquid, respectively. R is the radius of the drop and γ is the interfacial tension between the phases vapor (V), liquid (L) and solid (S).

Regarding the possible surfactant-enhanced spreading processes with the addition of a surfactant, the following can be concluded: the adsorption of the surfactant on the solid-liquid interface decreases its interfacial tension. The same it is for the liquid-vapor interface. The adsorption of surfactant molecules onto the bare hydrophobic surface will increase the interfacial tension between the solid and vapor phase. So, all of the three processes decrease the surface free energy of the droplet. Spreading on the surface is more favorable with an added surfactant.¹⁸⁷

Several investigations on this topic have been done where partially the Young equation was adapted. But, the overall interplay of the influences on the process is still not completely understood. Von Bahr *et al.* investigated the dynamic of spreading of surfactant solutions on partially wettable hydrophobic surfaces. They concluded that it can be distinguished between two steps in wetting of a surfactant solution of low concentration. The first wetting step, which is short and rapid, occurs at the beginning. The second step is a longer period where the spreading is slow. The adsorption of the surfactant molecules from the bulk to the increasing liquid-vapor interface was proposed as the rate-limiting factor in the spreading process. The adsorption of surfactant molecules behind the expanding solid-liquid interface was suggested for the initial spreading step.²⁰² Dutschk *et al.* made measurements of the wetting behavior of ionic and nonionic surfactant solutions. They found that there was a difference in the wetting behavior depending on the headgroup if different surfaces are regarded. Nonionic surfactants enhance the spreading on hydrophobic surfaces whereas ionic surfactants do not. Moreover, they discussed that the adsorption of surfactants at the solid-liquid interface was slower than the diffusion. Thus, the long period suggested by von Bahr was predicted to be even longer.²⁰³ In contrast, Starov *et al.* suggested a different spreading mechanism.²⁰⁴ A slow transfer of the surfactant molecules onto the bare hydrophobic surface in the front of the moving liquid-vapor interface was described. Both suggested mechanisms are shown in Figure 70.

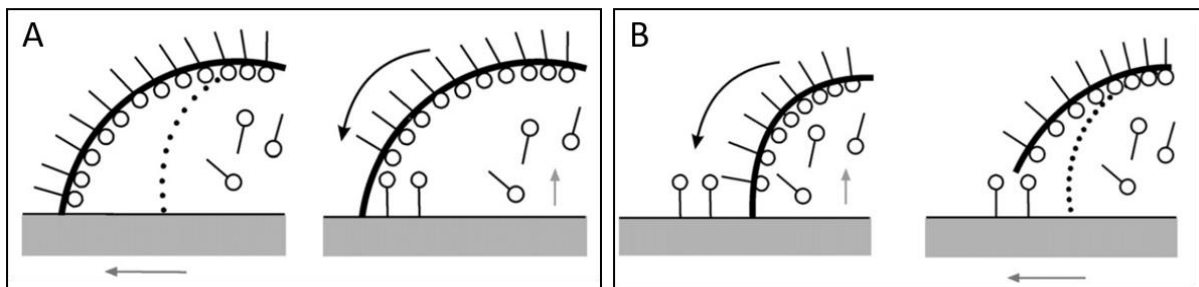


Figure 70: Spreading mechanisms of an aqueous surfactant solution on a hydrophobic surface according to von Bahr *et al.* (A) and according to Starov *et al.* (B). Pictures are taken from reference¹⁸⁷.

6.2.3 Spreading of catanionic combinations

The investigations of the combination of an anionic surfactant together with a cationic surfactant are rarely discussed in the literature. From a theoretical point, there are several aspects which should favor suitability of catanionics as good wetting agents. The superspreading behavior of trisiloxanes is explained by their molecular geometry as hammer-shaped. They aggregate in bilayer structures and vesicles. Moreover, they show very low surface tensions down to ~ 20 mN/m.²⁰⁵ Their high affinity to substrates in combination with high adsorption kinetics is another aspect. Catanionic combinations are known to have synergistic effects in several physicochemical properties, which often results in areas where nonionic surfactants are found. But, one big disadvantage is hindering the application of catanionics: their limit of solubility.²⁰⁶⁻²⁰⁸ Due to their possible precipitation, investigations could only be performed when the mixing of the two surfactants was happening directly prior to the measurement. This procedure is called a two-step procedure by Wu *et al.* since the two surfactants have to be added separately.²⁰⁶ They showed that at certain ratios the combination of anion and cation increased the spreading on highly hydrophobic surface significantly and investigated it further. An increase of the spreading behavior of a factor of 400 could be observed. But, the procedure of mixing could not be performed by preparing the solution some time before the measurement. They put first a drop of the aqueous cationic surfactant solution on the measurement plate and added the aqueous anionic surfactant solution afterwards. Right after that, the spreading was examined and found to be high. A mechanism based on the high adsorption behavior of the catanionic combination was suggested. Compared to the pure ionic surfactant, the adsorption at the solid-liquid interface was enhanced. This resulted in a decrease of surface concentration in the precursor film next to the interface. This difference in surface tension between the precursor film and the other surface of the

drop was suggested as the force of the fast spreading. Kovalchuk *et al.* were faced with the same problem. They observed a significant impact of the age of the solution. The crystal growth within the solution reduced the surfactant concentration in the solution. It reduced the spreading behavior over time. So, after some seconds the spreading decreased, and the contact angle increased again.²⁰⁷ They then used surfactant combinations where no immediate precipitation below the cmc was observed and investigated at such concentrations. Here, the synergistic effect could be proven, and high spreading could be observed under the precipitation concentration.²⁰⁸

6.3 Results and discussion

Although catanionic mixtures are promising candidates as spreading agents²⁰⁸, the problem of the low solubility of them was a limiting factor in any application.^{206, 207} With the newly introduced catanionic mixtures in this thesis, this problem could be solved (see 3.3.1). Due to this, their spreading behavior was a factor of interest. In the following, the catanionic mixtures, which are closer described in 3.3, will be examined regarding their spreading behavior on hydrophobic surfaces.

6.3.1 Contact angle on hydrophobic surfaces

6.3.1.1 Polyethylene

Several combinations of anions and cations were tested towards their spreading on a hydrophobic surface. The contact angle is a characteristic value describing the spreading behavior on a solid.¹⁷⁷ Thus, the contact angle of the solutions was measured on a polyethylene surface as described in Experimental 6.5.2.1. For each investigated cation, at least two different anions were tested and compared to each other regarding their dynamic spreading behavior and their absolute value of contact angle after 10 secs.

The commercial ACA was combined with two ethoxylated sulfates, C12EO4SO4 with four EO groups and a chain length of C12 and C18EO4SO4 with four EO groups and a chain length of C18. A measurement of the combination with SDS would not have made sense, since the solution starts to precipitate immediately, like it is known from the literature for other catanionic combinations.²⁰⁷ The other two combinations, C12EO4SO4-ACA and C18EO4SO4-ACA, did also partly show some turbidity, but clear precipitation was not observed. As it can be seen in Figure 71, a trend in the dynamic behavior becomes obvious for C12EO4SO4. Getting closer to the equimolar ratio, the absolute values decreased. The spreading of the drop was speeded up. The increasing nonionic character could be the reason for this. A different observation was made with the longer chain anion. The dynamic behavior was much slower for all other combinations. Only for high anionic content, a small decrease was observed in the curve. The change in ratio did not influence the dynamic behavior. ACA is not very flexible in its structure, and as already observed in previous chapters, the combination of cation and anion hinders the dynamic properties due to the strong interaction of the two ions. This became even

more distinctive, when ACA was combined with longer chain anions, since here the solubility of the anion itself was already low.

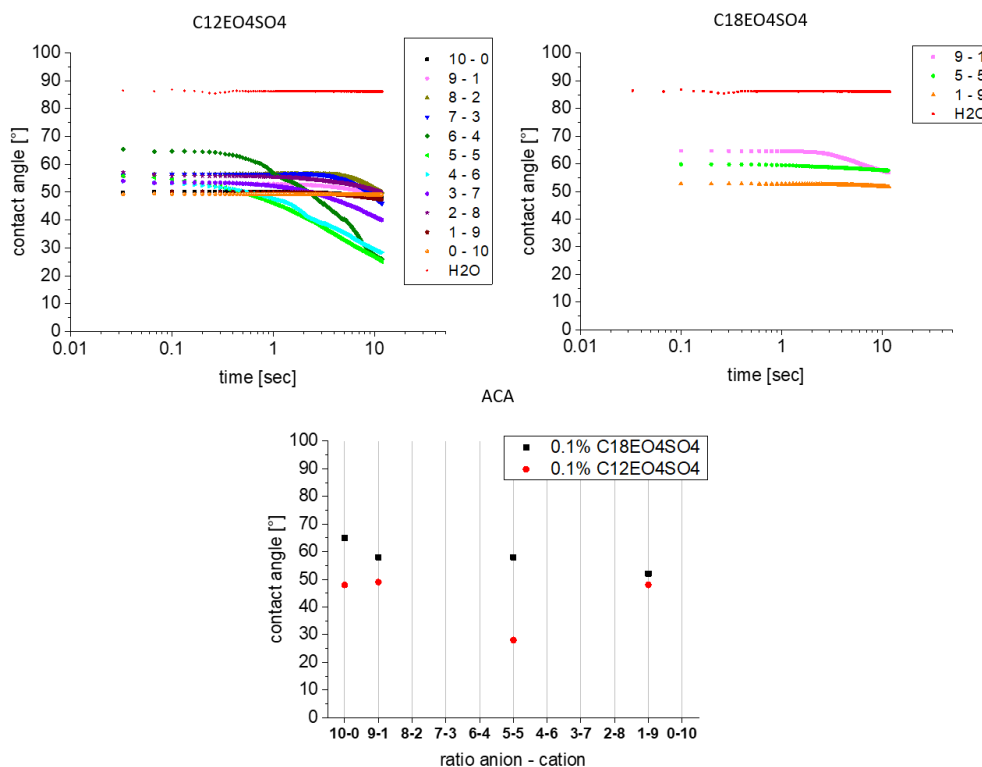


Figure 71: Contact angle on a polyethylene surface measured for the different ratios of the catanionic combination of the cation ACA with the anion C12EO4SO4 (above left) and C18EO4SO4 (above right) at pH 7 in millipore water and a concentration of 0.1 wt% as described in 6.5.2.1. A comparison of both anions is shown on the bottom.

Moreover, the cation C12EO1Ch was combined with the three anions SDS, C12EO4SO4, and C18EO4SO4 (see Figure 72). In comparison to ACA, the combinations with C12EO1Ch showed a higher dynamic. Also, the absolute values were significantly lower than without an EO group present. Consequently, a short alkyl chain in the anionic surfactant led to even higher dynamic behavior. But, in the case of C12EO1Ch, the higher solubility of the catanionic ion pair of C18EO4SO4 got obvious. Compared to Figure 71, for the combination of C18EO4SO4 and C12EO1Ch, a trend in the dynamic behavior was observed. The combination with the anion-cation mass ratio 5-5 was by far the one with the lowest contact angle.

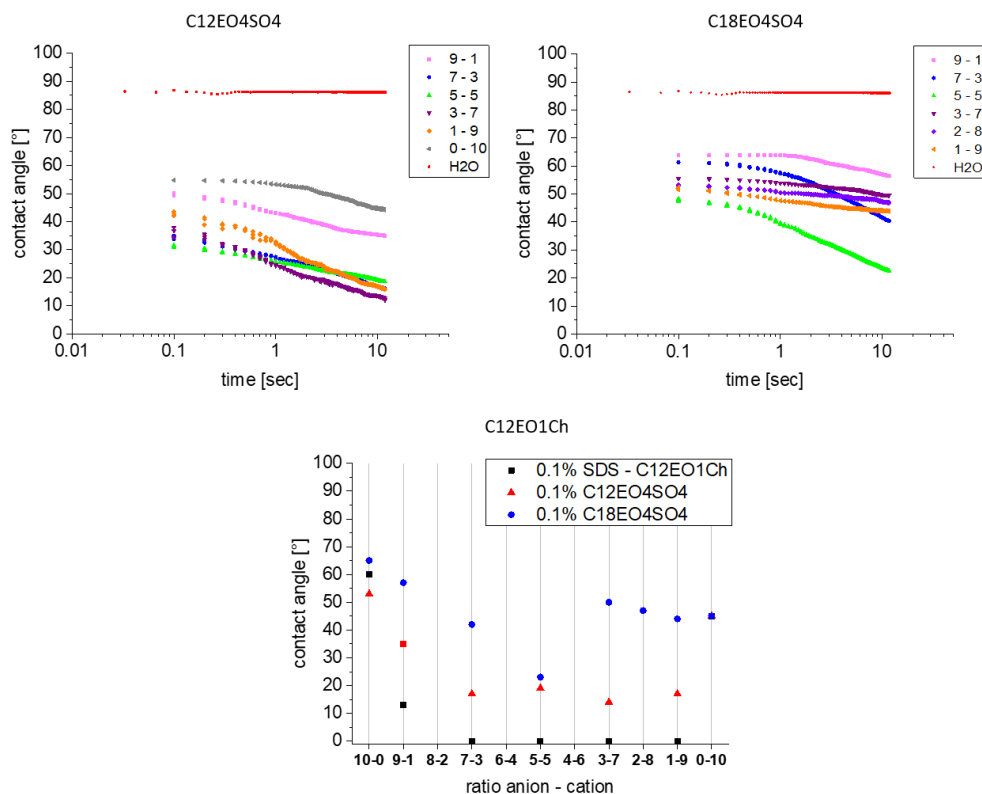


Figure 72: Contact angle on a polyethylene measured with different ratios of the catanionic combination of the cation C12EO1Ch with the anion C12EO4SO4 (above left) and C18EO4SO4 (above right) at pH7 in millipore water and a concentration of 0.1 wt% as described in 6.5.2.1. A comparison of the anions with the data from SDS added was shown on the bottom.

Also, the dynamic behavior was the fastest. When the long-chain anion got dissolved, and the interactions between the ion pair were not strong enough to lead to precipitate, the increasing effect of the nonionic character of the ion pair could be seen. But, a shorter chain length seemed to be favorable regarding the spreading behavior. In combination with C12EO4SO4, the dynamic behavior as well as the absolute contact angle values after 10 secs were more efficient than with C18. Although a longer alkyl chain leads to several positive aspects, e.g. in the aggregation of micelles at lower surfactant concentration. This could not be transferred to the spreading behavior. The dynamic behavior is not shown for SDS in Figure 72 since nearly all combinations showed immediate spreading so no process with time could be measured. This means that the combination of these two ions led to a spreading on the hydrophobic surface of polyethylene within a very short time. This is a phenomenon which has not been observed so far. EO groups seemed not to be necessary for a great spreading behavior. The presence of one EO group in the cation seemed to be the decisive factor. Otherwise, the EO group in the anions would have had a larger effect in the case of ACA.

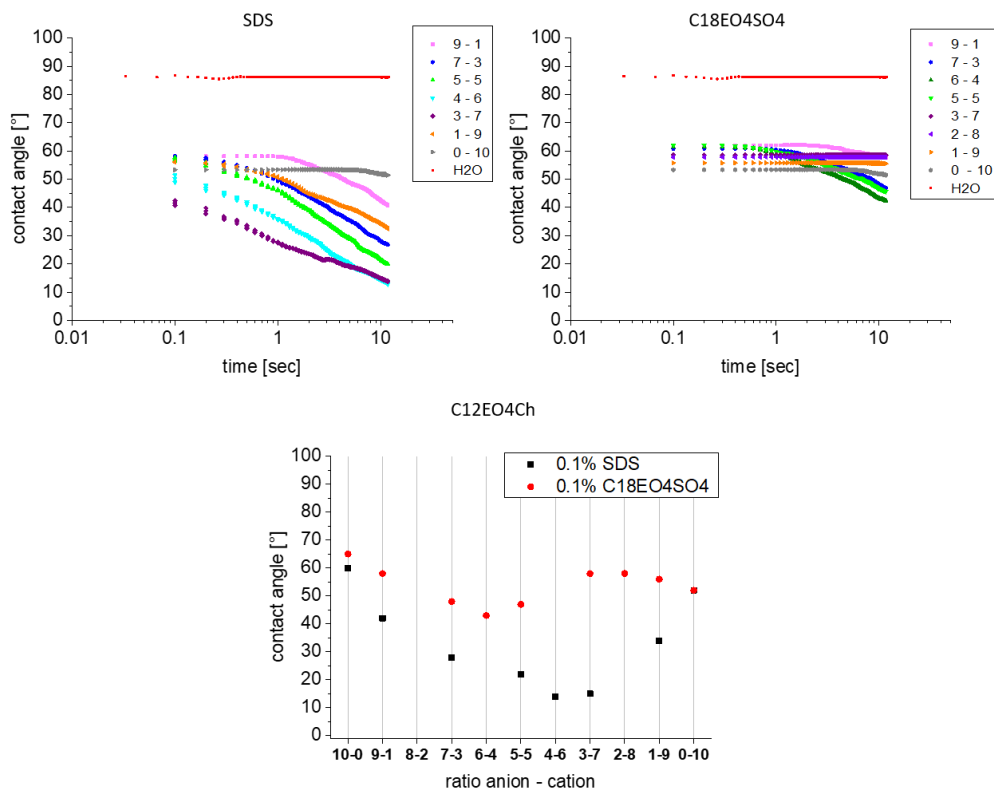


Figure 73: Contact angle on polyethylene of different ratios of the catanionic combination of the cation C12EO4Ch with the anion SDS (above left) and C18EO4SO4 (above right) at pH7 in millipore water and a concentration of 0.1 wt% as described in 6.5.2.1. A comparison of both anions was shown on the bottom.

To investigate the influence of the EO groups in the cation, the choline-based cation with four EO groups was also checked for its spreading behavior in combination with different anions as it can be seen in Figure 73. For the combination with SDS, a spreading dynamic dependent on the ratio was observed. An excess of cation had positive effects until the amount of the cation got too high. Then, the positive influence regressed. For the combination with C18EO4SO4, an excess of anion was favorable. But, the overall result was not as good as with SDS. Here again, the long-chain of the anion hindered the high dynamic behavior leading to fast wetting. With SDS, contact angle values down to nearly 10° were possible within 10 secs. For C18EO4SO4, the contact angle never reached 40°. Compared to the cation with only one EO group, it got obvious that more EO groups in the molecule suggesting more flexibility did not lead to a better result. There is an optimum. This optimum was found for a smaller number of EO groups. Here, the dynamic behavior was better, especially for anions with a shorter alkyl chain of 12 carbon atoms. For the longer alkyl chain, the trend was not that pronounced since the absolute values were in the same range.

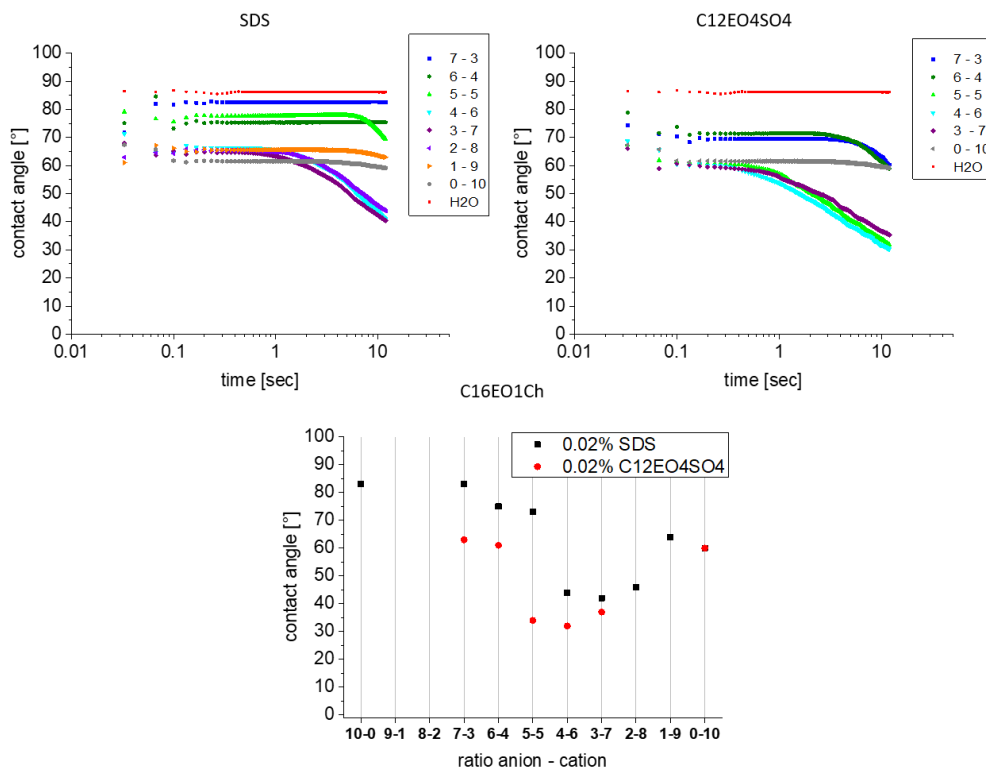


Figure 74: Contact angle on polyethylene of different ratios of the catanionic combination of the cation C16EO1Ch with the anion SDS (above left) and C12EO4SO4 (above right) at pH7 in millipore water and a concentration of 0.02 wt% as described in 6.5.2.1. A comparison of both anions was shown on the bottom.

Figure 74 shows the contact angle measurements for the cation C16EO1Ch. Since a longer chain length had a negative effect on the spreading behavior, the C16EO1Ch cation was only combined with the short-chain anions. Both combinations gave only contact angle values of higher than 30 °. So, a longer alkyl chain in the cation did not seem to have a positive effect. For the combination with SDS, an excess of cation was favorable. With a portion of 20 wt% of the anion, the contact angle was in the lowest possible range. Also for the combination with C12EO4SO4, an addition of the anion below 50 wt% was already enough to reach low contact angle values compared to the pure cationic surfactant. Compared to the cations with the shorter alkyl chain, the trend within the combined anions was reversed. SDS gave higher contact angle values than C12EO4SO4. For the long-chain cation, the insertion of EO groups into the anion structure improved the spreading behavior. The higher flexibility and the more distinctive hydrophilic part in the anion kept the cation more soluble in the solution. SDS was not sufficient enough in this case.

For all performed measurements, the positive effect of mixing the anionic and the cationic surfactant became obvious. The contact angle decreased most for mixtures around equimolar ratio. The increasing nonionic character can be named as the reason for this observation. Long alkyl chain in the anionic structure reduced the spreading efficiency compared to shorter alkyl chains. The combination of SDS and C12EO1Ch showed the best spreading behavior. At the investigated concentration of 0.1 wt%, spreading on the polyethylene surface was observed for several anion-cation ratios. Also, the dynamic of the spreading process was fast. The presence of an EO group within the cationic structure had a positive effect on the spreading behavior. This makes the combination a promising candidate for application where fast wetting is desired (see chapter 6.1). Most other catanionics showed intermediate spreading behavior resulting in contact angles between 30 and 60 °. Only a few catanionic mixtures showed a worse spreading behavior than the pure surfactants. The worst combination was SDS and C16EO1Ch at the anion-cation mass ratio 7-3. For a closer investigation regarding the influences on the spreading behavior, three combinations are examined in further sections: SDS-C12EO1Ch, mass ratio 5-5, as an example for a good wetting performance, SDS-C16EO1Ch, mass ratio 3-7, as an example for an intermediate wetting performance, and SDS-C16EO1Ch, mass ratio 7-3, as an example for a bad wetting performance.

6.3.1.1.1 Influence of the chemical structure of the cationic surfactant

One main question regarding the spreading behavior of the various cations was the understanding of the influences of the structural parts. For this purpose, a comparison of the two different cations with one EO group but different chain length, as well as a comparison of two different cations with the same chain length but different number of EO groups was done with the same anions as counterions (see Figure 75). Since for SDS and C12EO1Ch, the values of the contact angle at 0.1 wt% were too small to measure, the plotted points were measured at a concentration of 0.02 wt% (see Experimental 6.5.2.1). The anion for both combinations was SDS. The contact angle values for the combination with only 12 carbon atoms in the alkyl chain of the cation were significantly lower than the ones with the longer alkyl chain of 16 carbon atoms. The pure anion spread to a contact angle of 83 °. With only 10 wt% of C12EO1Ch in the mixture, the value decreased to 62 °. For the mass ratio 5-5, the minimum of 11 ° was measured. The same trend could not be observed for C16EO1Ch. Here, the values stayed constant until 30 wt% of the cation and decreased slowly to a minimum at the anion-cation mass ratio 3-7 with a value of 42 °. The chain length in the cation seemed to have a crucial effect. Since the

hydrophilic part of the cation was the same, the increase of the hydrophobic part of the molecule changed the molecular interactions. For the C16EO1Ch, the portion of the hydrophilic part in the cation, the EO group, and the headgroup was smaller than within the C12 cation. The impact of the EO group on the contact angle value was relatively small for C16EO1Ch. The increase of the hydrophobic part due to the increase of the alkyl chain in the cation compensated the effect of the EO group. So, SDS in combination with the cation was not as mobile as it was with the C12EO1Ch since the dynamic behavior was lowered.

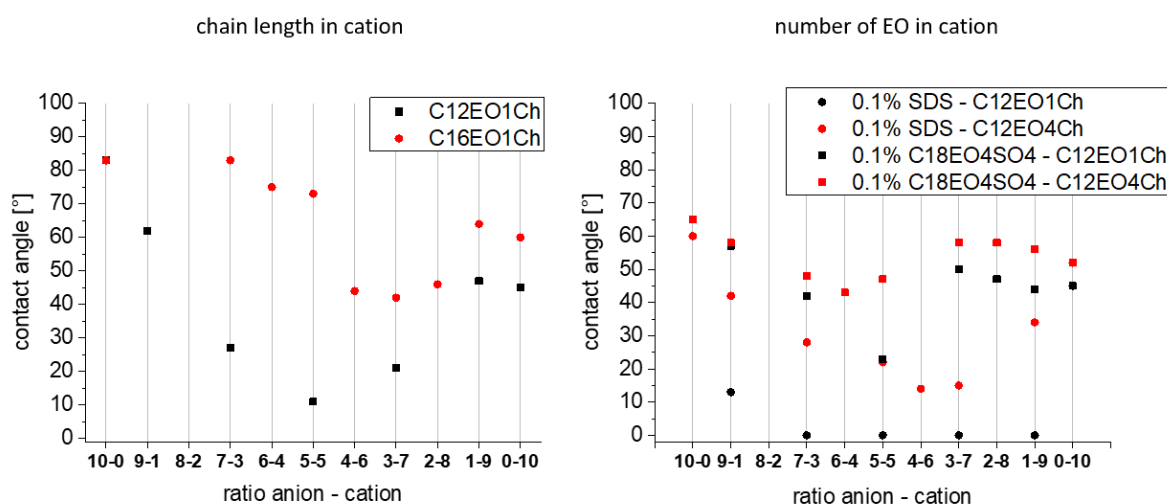


Figure 75: Comparison of the influence of the chain length (C12EO1Ch (black squares) and C16EO1Ch (red circles)) of the cation for the anion SDS at a cationic concentration of 0.02 wt% (left) and the comparison of the influence of the number of EO groups (1EO (black) and 4EO (red)) for the anions SDS and C18EO4SO4 at a cationic concentration of 0.1 wt% (right) in regard to the contact angle on polyethylene at pH 7 in millipore water measured as described in 6.5.2.1.

Regarding the number of EO groups present in the cation, for both anions SDS and C18EO4SO4, the same trend could be observed. With the higher number of EO groups, the contact angle increased, meaning the wetting was worse. For SDS the difference between one and four EO groups was larger than for C18EO4SO4. Only around the anion-cation mass ratio 5-5, the difference was more than 50 %. The long alkyl chain in the anion hindered the mode of action in a way that cannot be compensated with the cation. More EO groups in the molecule increased the hydrophilic part. Moreover, the molecule itself became more flexible in the area of the EO groups. EO groups are also more hydrated

due to their chemical structure. This could lead to weaker interactions with the anion. The synergistic effect is based on the attractive interaction of anion and cation until to the point where the interactions are too strong, and precipitation occurs. But as already seen in previous chapters, the linear relation of a larger amount of EO groups with an increasing effectiveness was not observed. An optimum with only a few EO groups, in the present case only one EO group, can be assumed.

6.3.1.1.2 Influence of water hardness

All combinations so far were only tested in millipore water and without any potential disturbing ions in it. In a realistic application, mostly additionally ions due to water hardness are present. Salts can influence the contact angle.²⁰⁹ For this purpose, the contact angle values of different combinations were also measured in water with a hardness of 5 °dH and compared to the measurement without water hardness (compare Experimental 6.5.2.1). This investigation is important regarding a potential subsequent application in realistic conditions. Three examples are shown in Figure 76 with their dynamic behavior and the contact angle value after 10 secs.

As a reference, pure millipore water or water with 5 °dH was used. The references are indicated in red in the diagram. A contact angle value of 85 ° was determined for millipore water and of 78 ° for 5 °dH. In general, the difference in water hardness was not very decisive. The values were in the same range and also the dynamic behavior was similar. However, the addition of ions to the aqueous surfactant solution changed the ionic situation. In the present case, calcium and magnesium ions were added. Chloride was already present due to the counterions of the cationic surfactants, and its amount increased. The added cations can interact with the anionic surfactant in the solution. Depending on the strength of the interaction, this can lead to an inhibition of the anion. Inhibition of the synergistic effect of the catanionic combination can be the result, since the amount of “free” anionic surfactant will be very small. But, this was not the case in the performed experiments.

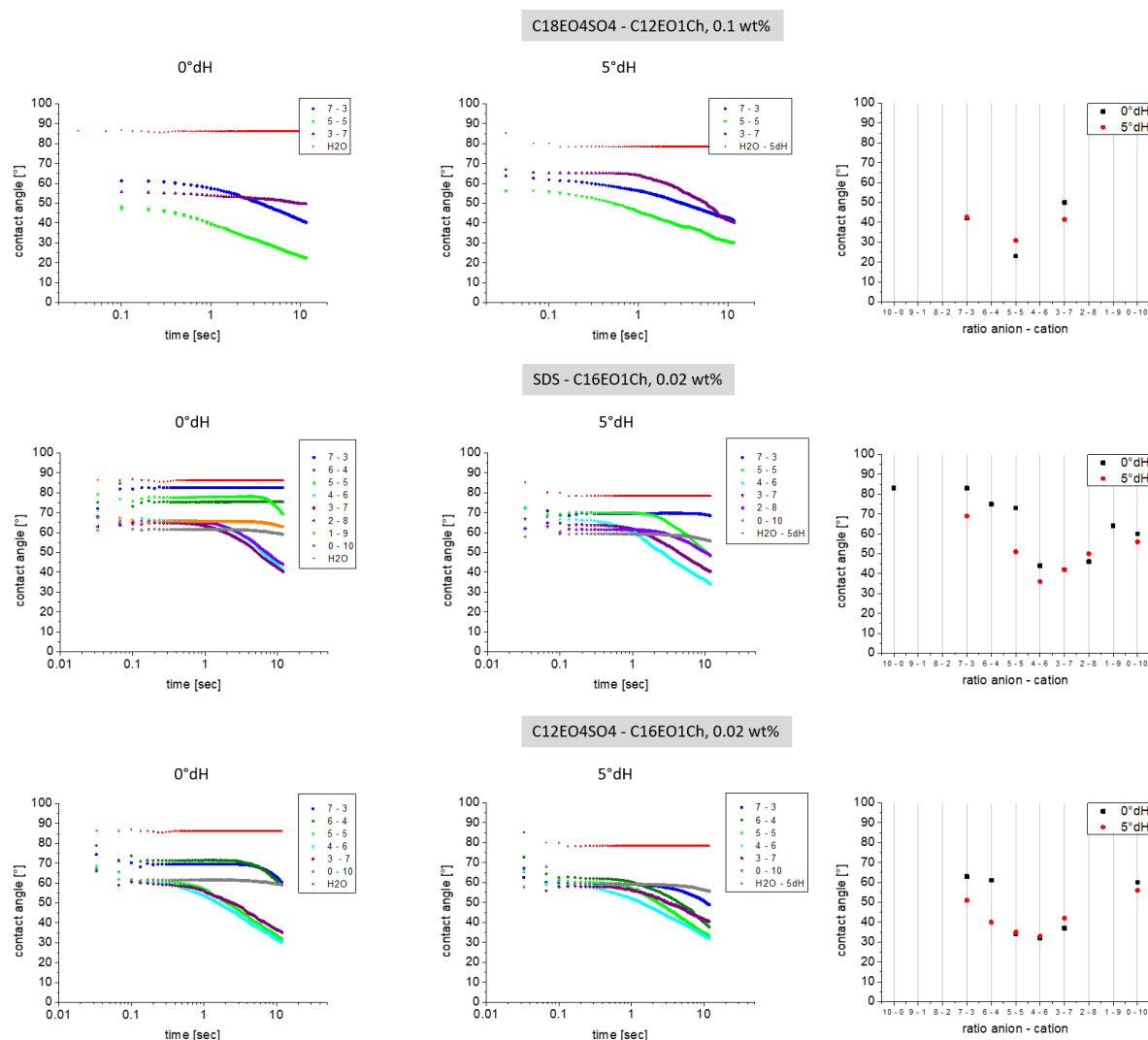


Figure 76: Comparison of the influence of water hardness 0°dH (left) and 5°dH (middle) in regard to the contact angle after 10 secs for different ratios of the catanionic combination C18EO4SO4 - C12EO1Ch at 0.1 wt% (above), SDS - C16EO1Ch 0.02 wt% (middle) and C12EO4SO4-C16EO1Ch 0.02 wt% (below) at pH 7 measured as described in 6.5.2.1. A comparison is shown on the right.

A more specific comparison of the results showed a slight trend towards smaller contact angles with the presence of water hardness. The added ions seemed not to have a negative influence on the spreading behavior. This was also summarized by Sghaier *et al.* who found only a small influence of the NaCl concentration on the contact angle on hydrophobic surfaces for a NaCl-water solution.²¹⁰ Moreover, the presence of the ethoxylated cation compensates the tendency for precipitation of SDS

in combination with the present cations. The sensibility towards water hardness was reduced in this way. This result supports the potential of catanionic systems in various applications.

6.3.1.2 Plant leaves

All plants have hydrophobic surfaces to prevent evaporation of water from the epidermal surface and also to prevent contamination of plant tissue with external water, dirt, and microorganism. In the theory of contact angle, this means that the contact angle of water is very small. In case of gravitation forces and a not complete horizontal surface, the drop will run off the leave. This is of advantage for plants regarding their protection. But, it is a challenge in plant treatment since the chemical spray, if not formulated correctly, will also run off and will not have its desired effect of pesticide. The spreading behavior was tested on real plant leaves to simulate the situation of practical application of chemical sprays on e.g. fields. The leaves are taken from the houseplants money tree (*Crassula ovata*) and benjamin fig (*Ficus benjamina*) and red cabbage. To investigate the contact angles, the aqueous solutions of various catanionic combinations were put onto the leave surface with a pipette and photos were taken after 30 secs. The combination with the best spreading behavior so far, the combination of SDS and C12EO1Ch at the mass ratio 5-5, was used on all plants. In Figure 77, the spreading behavior at the concentration of 0.1 wt% is shown in comparison to a drop of millipore water. For all surfaces, the contact angle of water was higher than 90 ° indicating a hydrophobic surface. The catanionic combination showed wetting in all cases indicating a contact angle less than 90 °. But, a difference in the leaves could be observed. Complete wetting occurred at the red cabbage leave, and on the money tree leave. The wetting area increased by several factors. In contrast to the money tree leave, the leave of the red cabbage was rougher. On the benjamin fig leave, a contact angle was present. But, the wetting area had at least doubled in relation to right after putting the drop on the leave.

The tests were performed with a concentration of 0.1 wt% since this concentration was used in all other experiments. Because complete wetting was partially observed, the concentration was lowered to check the spreading behavior further. The two room plant leaves were tested with the concentration of 0.02 wt% and 0.002 wt%. For the lowest concentration, a decrease in contact angle was observed. It decreased further with increasing concentration. But, already a very low concentration was sufficient to observe a more pronounced wetting.

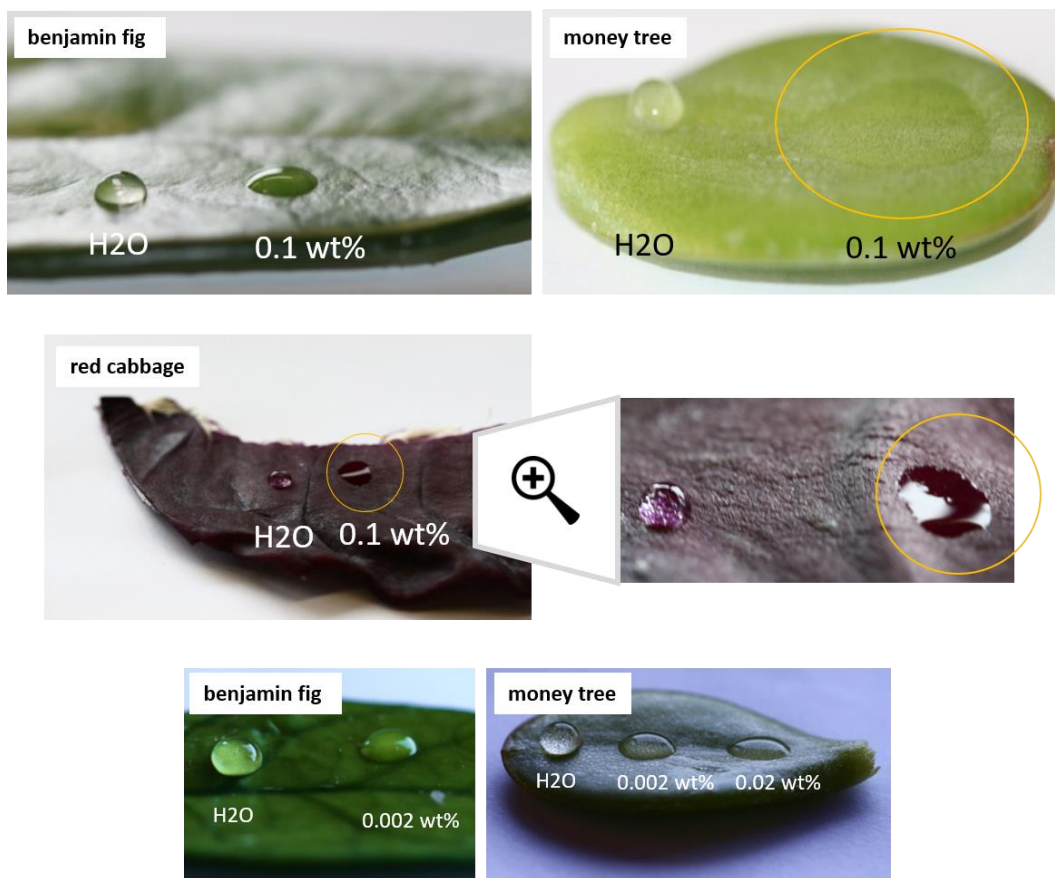


Figure 77: Spreading behavior of the catanionic combination SDS-C12EO1Ch at the mass ratio 5-5 and a concentration of 0.1 wt% investigated on the leave of the benjamin fig (left above), the money tree (right above) and red cabbage (middle) in comparison to water. Below: spreading behavior of the catanionic combination SDS-C12EO1ch at the mass ratio 5-5 and a concentration of 0.002 and 0.02 wt% on the leave of the benjamin fig (left below) and on the money tree (right below).

6.3.2 Spreading behavior investigated with a high-speed camera

Fast wetting, which is desired in an application like pesticide sprays on the fields, happens within seconds and can nearly be observed with the human eye. However, differences between various samples can only be evaluated by the eye after a certain time when no big changes occur anymore. To detect the process of a drop attaching a surface from the first moment on, a high-speed camera was used to depict the spreading behavior within the first moments of contact of the drop on the surface. Three combinations were chosen to be investigated this way. One was the combination of

SDS and C12EO1Ch 5-5 as an example for the best investigated catanionic spreading behavior. The combination of SDS and C16EO1Ch at two different ratios, 3-7 and 7-3, was exemplarily taken for an intermediate wetting behavior and a bad one. Two references were used to compare the catanionic samples: pure millipore water and Plurafac LF 300 (LF300). LF300 is a low foaming nonionic surfactant consisting of alkoxylated, predominantly unbranched fatty alcohols, and higher alkene oxides alongside EO. Due to its nonionic character, it is a very good spreading agent.²¹¹ Each sample was investigated in the same way (see Experimental 6.5.2.2). Pictures of the process of wetting with time are depicted in Figure 78.

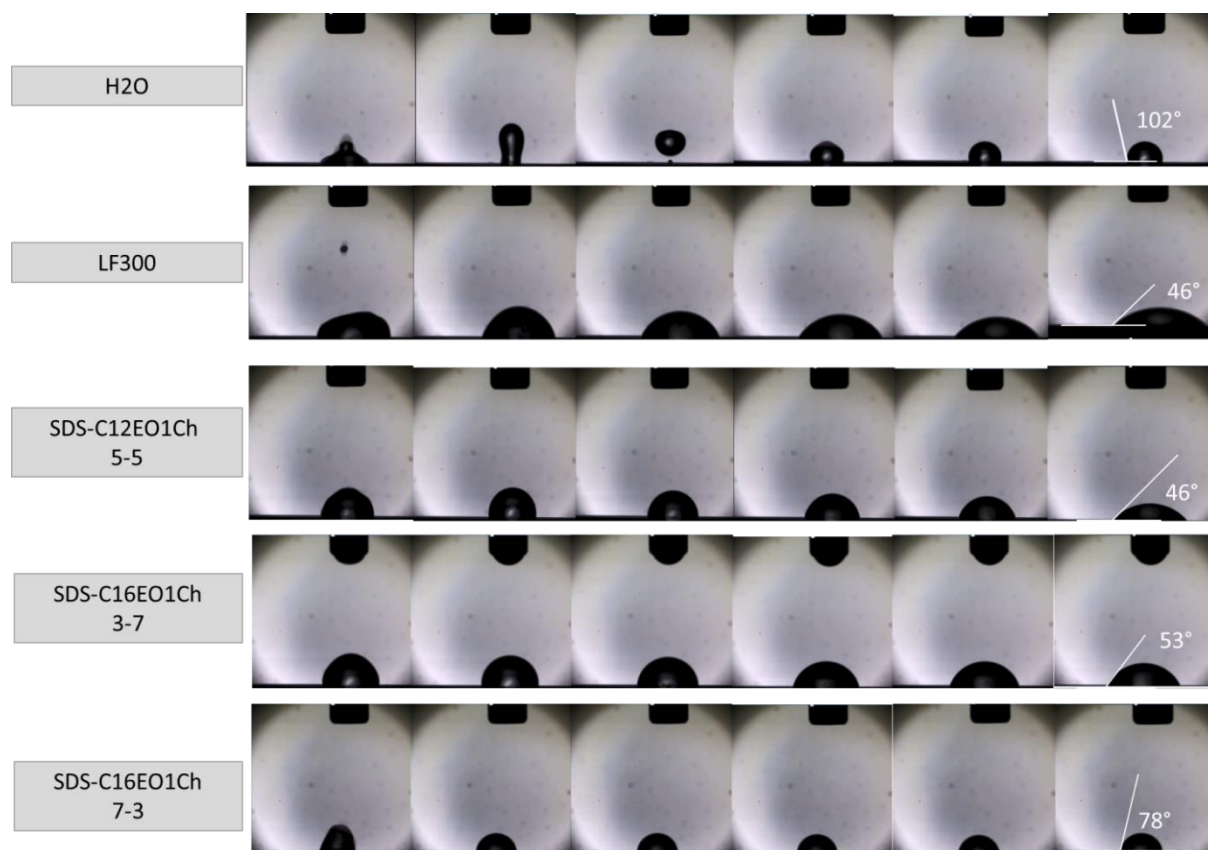


Figure 78: Observations of the spreading behavior on a polyethylene film of water and LF300 as a reference and the three catanionic samples SDS-C12EO1Ch 5-5, SDS-C16EO1Ch, and SDS-C12EO1Ch 7-3 at a concentration of 0.02 wt% recorded with a high-speed camera as described in 6.5.2.2.

To investigate the efficiency of the catanionic combinations, the compounds were compared with the nonionic surfactant LF300 from BASF, which is commercially used in detergents and housecleaning products. The contact angle measurement was carried out by the recording procedure as it is

described in Experimental 6.5.2.2. For both substances, a contact angle of 46° was measured. This means that the static wetting value was the same for the compounds. Also, the change of the contact angle until this value was very similar for both substances. With LF300, it seemed to reach the absolute value a little bit earlier, and the wetting started a short time before that of the catanionic combination. The reason for this could be the lower nonionic character. The catanionic combination has only a pseudo-nonionic character, and there are still ionic parts in the solution. The nonionic surfactant seemed to adsorb better on the hydrophobic surface of the polyethylene and led therefore to a faster wetting.

For both other samples, SDS-C16EO1Ch with the ratios 3-7 and 7-3, a higher contact angle and a slower spreading behavior were observed. As it can be seen above, the increase of the chain length made the wetting worse (see Figure 78). For the combination of SDS and C16EO1Ch with the mass ratio 3-7, the contact angle increased by 15 % to 53° compared to SDS-C12EO1Ch, 5-5. For the mass ratio 7-3, it increased by 70 % to a value of 78° . The slower dynamic in the solution may be reasonable for this. In the sample SDS-C16EO1Ch, 7-3, the anionic part is dominant. In the sample SDS-C16EO1Ch, 3-7, the cationic part is dominant. Both led to a worse wetting. But, the cationic part hindered the adsorption on the polyethylene surface less than the anionic excess. Reason for this can be the fact that the cation has a longer chain length than the anion and has, therefore, a more distinctive hydrophobic part than the anion. The adsorption on the hydrophobic surface was here more favorable.

6.3.3 Correlation with other chemical properties

For a deeper understanding of the spreading process, the relation of spreading behavior and the physicochemical properties of the substances is of high interest. So, the three examples of a good, an intermediate and a bad wetting agent from the high-speed camera tests (see 6.3.2) were compared in the following three properties: the surface tension and its dynamics, the interfacial tension towards a hydrophobic substance, here hexadecane, and the adsorption on a hydrophobic substrate, here a gold surface coated with 1-octadecane thiol. All three properties can be related to the spreading process which is described in the following. For the three investigated substances, the measured properties can be seen in Figure 79 and Table 13.

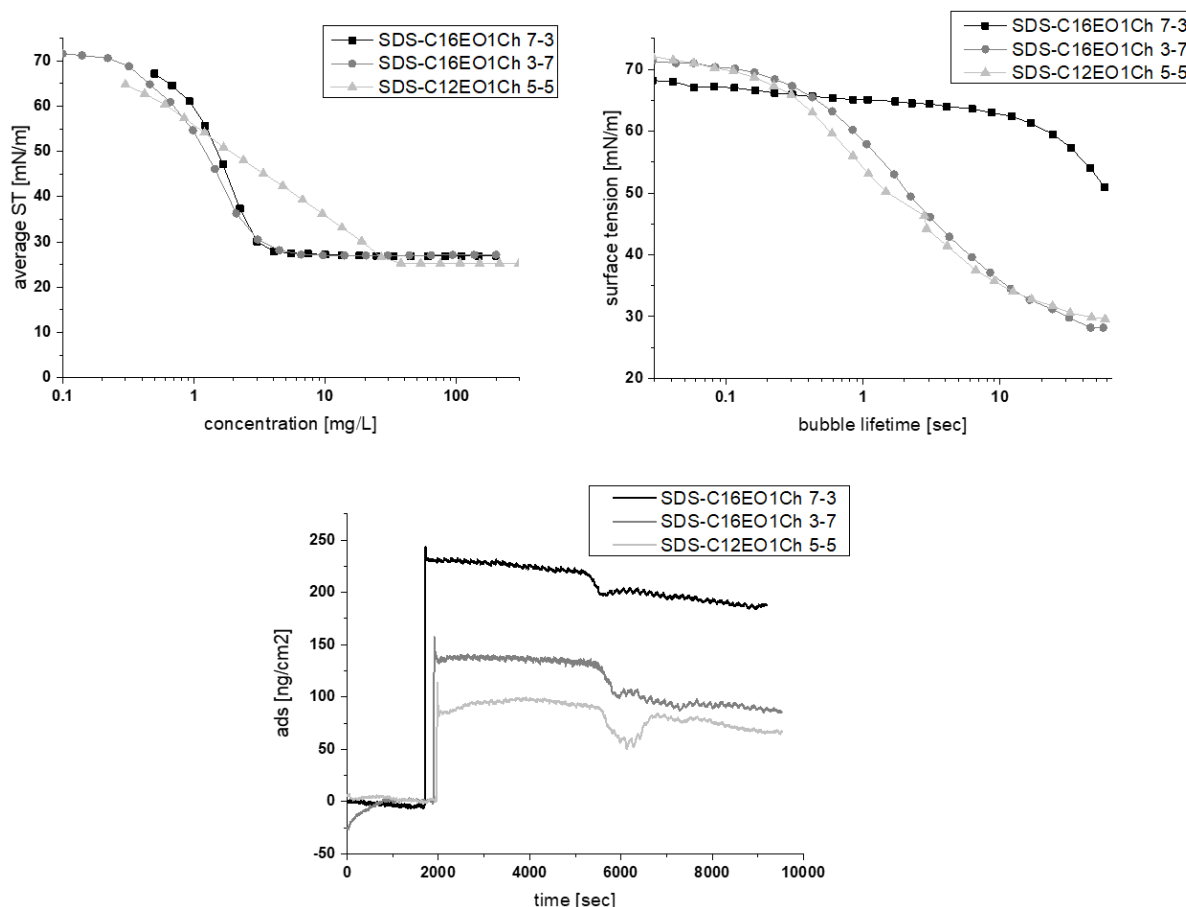


Figure 79: Determination of the critical micelle concentration (cmc) (top left) obtained by tensiometer (see 6.5.2.5), the dynamic surface tension (ST) (top right) obtained by bubble pressure tensiometer (see 6.5.2.4) and the adsorption behavior on a hydrophobic gold-coated surface with 1-octadecane thiol (below) obtained by QCM (see 6.5.2.6), of the three investigated catanionic combinations SDS-C16EO1Ch 7-3 (black), SDS-C16EO1Ch 3-7 (dark grey) and SDS-C12EO1Ch 5-5 (light grey) at 0.1 wt% and pH 7 obtained by tensiometer.

The dynamics of the surface tension describes the velocity of the molecule in bulk to move to the air-water interface. The faster the molecule moves to the interface, the faster it can compensate the disappearance of molecules absorbing on the surface and leading to the spreading process. For the same reason, the adsorption on hydrophobic surfaces is interesting. If the molecules adsorb on the hydrophobic surface, they leave the aqueous phase. This step is crucial for the spreading process, according to the theory described in chapter 6.2.2. The more and the faster the molecules adsorb, the more accelerated is the spreading process. The interfacial tension describes the interface of the aqueous phase and the hydrophobic liquid phase.^{95, 212} It can be transferred to the interface of the surfactant solution on the hydrophobic substrate. For this purpose, it can give information about the drop on the hydrophobic surface.

For simplification the three catanionic combinations will be abbreviated by the following letters: A: the bad wetting combination SDS-C16EO1Ch, 7-3; B: the intermediate wetting combination SDS-C16EO1Ch, 7-3; C: the good wetting combination SDS-C12EO1Ch, 5-5.

Table 13: Values of physicochemical properties of the three investigated catanionic combinations SDS-C16EO1Ch 7-3, SDS-C16EO1Ch 3-7 and SDS-C12EO1Ch 5-5 at 0.1 wt% and pH 7 obtained by tensiometer (see 6.5.2.5), bubble pressure tensiometer (see 6.5.2.4) and QCM (see 6.5.2.6).

	cmc [mg/L]	ST [mN/m]	dyn. ST after 1sec [mN/m]	abs max [ng/cm ²]	abs after [ng/cm ²]	IFT after 60min [mN/m]
sample A	3.27 ± 0.03	26.8 ± 0.04	3.40 ± 0.05	216 ± 6	184 ± 17	0.51
sample B	3.45 ± 0.24	27.0 ± 0.17	13.93 ± 0.41	120 ± 2	78 ± 11	0.55
sample C	34.66 ± 0.84	25.2 ± 0.14	19.00 ± 0.40	90 ± 4	60 ± 6	0.21

From the concentration-dependent surface tension measurements, the cmc values were determined via the intersection of the two linear parts of the curve (see 6.5.2.5). The surface tension curves of the three samples A, B and C showed a different shape of the curve. The two combinations A and B with a longer chain length of C16 gave smaller cmc values by one magnitude. This behavior could be expected, since an increase in the alkyl chain is known to decrease the cmc value. From the cmc curves, the final value of the surface tension for each sample after the cmc could be determined. Only small differences could be seen. With a value of 25.2 mN/m, combination C gave the smallest value, followed by combination A with 26.8 mN/m and combination B with 27.0 mN/m. From the experimental data, the cmc value is not a decisive factor since the trend of cmc values was contradictory to the trend in spreading behavior. Of course, a low cmc value is positive for the effectiveness of a surfactant. But, with the tested catanionic combinations, the cmc value was already very low for all combinations. Small differences did not change the situation significantly. Also, because the concentration was far above the cmc when the combinations were investigated. So, the micellar situation was the same for all three combinations.

The dynamic surface tension was measured with a bubble pressure tensiometer for the three samples A, B and C as described in 6.5.2.4. The results are shown in Figure 79. A significant difference between the bad wetting combination A and the two other samples B and C was observed. For the maximum

of bubble lifetime of nearly 60 seconds, the dynamic surface tension was nearly twice as high for combination A compared combination B and C. The dynamic behavior itself was less intense for A and showed no steep decrease with increasing bubble lifetime. It started to decrease only at higher bubble lifetimes. Between the other two combinations, there could not be observed a large difference in surface tension. For combination C, the dynamic behavior was slightly faster indicated by a higher value of 5 mN/m for the surface difference after a bubble lifetime of 1 sec. The measurements agreed with the observations in spreading behavior. This confirmed the assumption that the dynamic behavior of the solution is of high importance for the spreading process. High dynamics means that the molecules in solution can move very fast from the bulk to the interface. This is favorable since a new interface is created by further wetting of the droplet on the surface. If the molecules within the solution can compensate the concentration decrease at the interface within a short time, the spreading process can go on.

The adsorption behavior of the three combinations A, B and C on a hydrophobic surface was measured with the QCM as described in 6.5.2.6. Two values were analyzed from the received curve: the maximum amount of the surfactant combinations that adsorbed on the surface and the amount of surfactant that stays on the surface after it was washed for 60 mins with millipore water. The results are shown in Figure 79 and Table 13. The same trend was observed for both values. Combination A, which was the worst wetting combination, gave the highest values for adsorption followed by combination B and combinations C with the smallest adsorption. More than twice of the mass of combination A adsorbed and stayed on the hydrophobic surface compared to combination C. Both combinations A and B have a longer alkyl chain in the cation. With a longer alkyl chain in the cation, the combination gets more hydrophobic. This could cause stronger interaction with the hydrophobic surface. But, in case of combination A, the ratio of anion and cation was far on the anion side. So, this could not be the crucial point. The trends of the experimental data of adsorption were not in accordance with the observed spreading behavior. The adsorption behavior on a hydrophobic surface seems to be not a crucial factor for the spreading process as other properties, like e.g. the dynamics in the solution.

Furthermore, the interfacial tension of the catanionic combinations was measured against hexadecane with the spinning drop tensiometer (compare Experimental 6.5.2.3). The values were taken after 60 mins. Here, combination C gave a significantly lower value than the other two combinations. In contrast to A and B with values around 0.5 mN/m, combination C had only half of

the interfacial tension with a value of 0.21 mN/m. The trend of interfacial tension agrees with the trend observed for the surface tension measurements. For combination C, a highly dynamic behavior at the interface against hexadecane as well as against air was observed. It seems to be a promoting factor for the spreading process.

From the theoretical point as described in 6.2, three properties were assigned to an efficient spreading process on a hydrophobic surface. A high dynamics in the surfactant solution, high adsorption on a hydrophobic surface and low interfacial tension of the surfactant solution against a hydrophobic phase enhances wetting.²⁰²⁻²⁰⁴ For this purpose, the influences of these properties on the spreading behavior of the present catanionic mixtures were investigated. The order of the efficiency in wetting was compared to the order of efficiency in the corresponding property for three catanionic examples. An overview of the observations can be seen in Figure 80. For the investigated catanionic samples, the following statement regarding the effect of the physicochemical properties on the spreading behavior can be made:

- The dynamics within the bulk solution enhanced wetting. The corresponding value of dynamic surface tension determined with the bubble pressure tensiometer showed the same trend for the two behaviors.
- A high interfacial activity of the surfactants in the aqueous solution led to a better wetting performance. Lower interfacial tension values against the hydrophobic hexadecane phase corresponded to a better wetting performance.
- The adsorption of the surfactant molecules on the hydrophobic surface played only a minor role. Experimental data of the adsorption behavior determined with the QCM showed contradictory trends compared to the spreading behavior. Another effect, like the ones mentioned above, seemed to dominate the effect of adsorption on the hydrophobic surface.

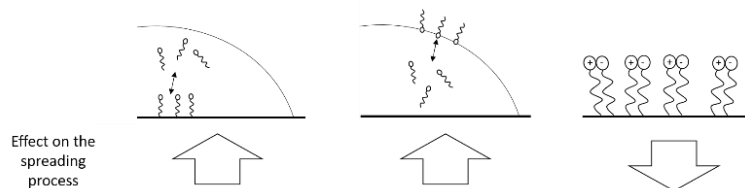


Figure 80: Schematic illustration of the influence of different physicochemical properties on the spreading behavior of the catanionic combinations.

6.3.4 Statistical analysis

In the previous chapter 6.3.3, the spreading results from 6.3.1 and 6.3.2 were correlated with three physicochemical properties to evaluate the weighting of them regarding the spreading behavior of the investigated substances. Here, only a small number of results were considered. For this purpose, a statistical regression analysis (see Experimental 6.5.2.7) was performed to determine the dependencies of the spreading behavior on the polyethylene surface on the molecular and physicochemical properties (see 3.3). For all properties, a univariate regression analysis was done and the significance value of 5 % was applied. The received P-values are shown in Table 14.

Table 14: Results of the univariate regression analysis between the molecular physicochemical properties and the determined spreading performance on the polyethylene surface of the catanionic mixtures calculated as described in 6.5.2.7.

P-value	molecular properties		
	EO anion	EO cation	average EO
	0.0000	0.4380	0.0008
	chain length anion	chain length cation	average chain length
	0.0000	0.1412	0.0001
	HLB	molar ratio anion:cation	
	0.3656	0.0607	

P-value	physicochemical properties		
	solubility	surface tension air	dynamic surface tension
	0.0038	0.0000	0.0000
	cmc	interfacial tension	
	0.2152	0.0038	
	adsorption SiO ₂	adsorption SAM	
	0.2030	0.1171	

From the performed regression analysis, four significant relationships were found for the molecular as well as physicochemical properties. The following statements can be made regarding the influences towards a small contact angle on the hydrophobic polyethylene surface:

- Smaller number of EO groups in the anion and also in average is favorable.
- Lower chain length in the anion and also in average promotes wetting.
- Solubility is necessary for wetting.
- High dynamic in the solution favors the spreading behavior.
- Low surface tension and low interfacial tension increase the wetting of the surfactant solution.

To apply the multivariate regression analysis was only possible for a selection of the physicochemical properties, since not all properties have been determined for all investigated combinations. The results are shown in Table 15.

Table 15: Results for the P-value of the multivariate regression analysis between the molecular physicochemical properties and the determined spreading performance on the polyethylene surface of the catanionic mixtures calculated as described in 6.5.2.7.

molecular properties		physicochemical properties	
EO anion	EO cation	solubility	surface tension air
0.2983	0.0321	0.1962	0.3153
chain length anion	chain length cation	cmc	interfacial tension
0.0051	0.0292	0.3068	0.2729
HLB	molar ratio anion:cation		
0.9399	0.0741		

The multivariate analysis supports the results from the univariate analysis regarding the molecular properties. The number of EO groups, as well as the chain length, seem to be a decisive factor for the spreading of the catanionic solution. For the physicochemical properties, a significant relation towards the spreading behavior could not be found with the multivariate analysis. But, since not all possible properties could be considered within this analysis, the result is not completely reliable. The results of the univariate analysis have a higher informative value.

6.4 Conclusion

The newly synthesized catanionic combinations were tested towards their spreading behavior on hydrophobic surfaces. A screening of several ratios of these combinations with the concentration of 0.1 wt% on a polyethylene film was performed regarding their dynamic spreading behavior and the absolute value of contact angle after 10 secs. For all combinations, a synergistic effect was observed in comparison to the pure anion or cation. Getting closer to equimolar ratio, the effect became more intense. Especially for the combination of SDS and C12EO1Ch, a complete spreading behavior within a very short time could be found for the concentration of 0.1 wt%. The dynamic behavior was unobservably high. A decrease in concentration down to 0.02 wt% did still result in a contact angle decreases down to 10 °.

With the performed measurements, the structural impact of the surfactants regarding the spreading behavior was analyzed. Longer alkyl chains in the anion as well as in the cation led to a reduction of the dynamics of the spreading behavior and a higher contact angle. Considering the EO group as a component in the surfactant structure of the cation, a significant improvement could be observed with the insertion of it. But, the further insertion of more EO groups did not lead to further improvement. It became clear that an optimum of the number of EO groups was probable. Combinations with C12EO1Ch gave better results than C12EO4Ch. Regarding the impact of EO groups in the anion structure, the trends were not evident. For the C16EO1Ch cation, EO groups in the anion are favorable. But, the C12EO1Ch cation combinations with SDS, meaning no EO groups present, gave better wetting results. The influence of the structure of the cation seemed to be more decisive regarding the received contact angle measurements.

The spreading behavior of the best combination, SDS and C12EO1Ch 5-5, was tested on different plant leaves: a benjamin fig leave, a money tree leave and a red cabbage leave. For all leaves, a spreading was observed. Especially for the money tree and the red cabbage leave, fast spreading was seen within seconds. The decrease in concentration down to 0.02 and 0.002 wt% still showed a significant decrease in contact angle.

Three combinations exemplarily for a good (SDS-C12EO1Ch 5-5), an intermediate (SDS-C16EO1Ch 7-3) and a bad (SDS-C16EO1Ch 3-7) catanionic combination were investigated on a polyethylene film with a high-speed camera and were compared to a commercial wetting agent Plurafac LF300. The combination SDS-C12EO1Ch 5-5 could compete with commercial wetting agents. The dynamics was

similar, and the same contact angle of 46° was measured. The two other combinations confirmed the measurements before and showed higher contact angles and slower dynamic behaviors.

Three different physicochemical properties were determined for the three combinations of different wetting ability to gain knowledge about the importance of them regarding the spreading process. It could be shown that the adsorption capacity on a hydrophobic surface had less effect than the dynamic behavior in solution. The dynamic behavior measured with bubble tensiometer and spinning drop tensiometer confirmed the trend observed in the wetting behavior. In both cases, the good wetting combination of SDS-C12EO1Ch, mass ratio 5-5, was most efficient and had the lowest values. In contrast, the QCM measurements gave a different trend. Here, the good wetting combination had the lowest adsorption capacity on the hydrophobic surface. But, this seemed to be dominated by the dynamic behavior. Out of these measurements, the importance of the dynamic in the solutions got obvious. A schematic illustration of the influences is shown in Figure 80.

Statistical analysis was used to evaluate the influence of the molecular and physicochemical properties on the spreading behavior on a polyethylene surface. Several significant relations were found with the univariate regression analysis. A lower number of EO groups, as well as a shorter chain length, promotes the wetting. Additionally, high solubility and dynamic behavior in the bulk solution together with high surface activity is favorable for wetting of hydrophobic surfaces.

In the literature, a problem of precipitation is reported regarding the investigations on spreading behavior. With the newly introduced catanionic combinations, the big disadvantage of crystal growing in the aqueous solution was not observed. For certain combinations containing SDS and C12EO1Ch, a superspreading behavior could be observed. Consequently, there is no practical reason for not using catanionic combinations in different situations of application. This offers the use of catanionic combinations as commercial wetting agents in several applications, especially if only small amounts of surfactants are desired.

6.5 Experimentals

6.5.1 Chemicals

SDS ultrapure (purity > 99.9 %) was purchased from AppliChem (Darmstadt, Germany). Hexadecane (purity 98 %) was obtained from Fluka (Switzerland). Texapon N70 (purity 70%) and Plurafac LF 300 (purity 99 %) and the synthesized surfactants were kindly provided by BASF (Ludwigshafen, Germany) from internal synthesis for this research. 1-Octadecanethiol (purity 98 %) and ethanol (purity 99.8 %) were obtained from Sigma-Aldrich (Taufkirchen, Germany). The gold quartz crystals are purchased from JCM (Frankfurt am Main, Germany).

Millipore water was used for all experiments, if not mentioned otherwise. All chemicals were used without further purification.

6.5.2 Methods

6.5.2.1 Contact angle measurement

For contact angle measurements, an OCA H 150 from DataPhysics was used. The contact angle on the right and the left side of the drop was measured over a certain period. The average value of these two contact angles after 10 secs was taken for evaluation. All samples are set to pH 7. The measurements were all performed at 25 °C.

6.5.2.2 High-speed camera recording

A high-speed camera construction from BASF was used for the sharply focused filming of the impact of a drop with a certain speed on variable surfaces. The construction of the device is shown in Figure 81. On the bent metal surface, different surfaces like e.g. a polyethylene film or a leaf can be fixed. With the pressure control and the setting of the volume, the drop outlet can be controlled. The film recording starts with the droplet being pushed out of the cannula.

The recording was performed with the same speed and the same settings for all samples: The solution was pressed out of the cannula with a pressure of 0.15 bar. The pulse duration was set to 0.950 msec. For the drop formation, 15 pulses were used.

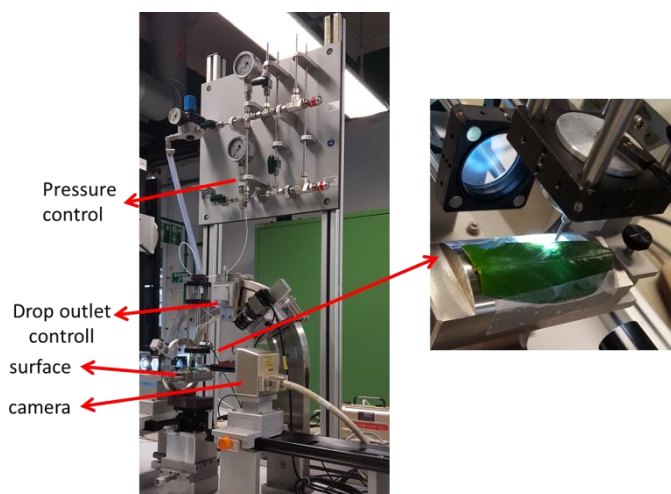


Figure 81: Construction of the high-speed camera apparatus

6.5.2.3 Interfacial tension measurement

The measurements were performed as described in chapter 3.5.2.2.

6.5.2.4 Dynamic surface tension measurement

The measurements were performed as described in chapter 3.5.2.2.

6.5.2.5 Cmc measurements

The measurements were performed as described in chapter 3.5.2.2.

6.5.2.6 Adsorption behavior

The adsorption measurements were performed with an Omega-QCM from QSense. The investigated gold quartz crystals were put in a 0.001 M solution of 1-octadecanethiol in ethanol overnight. The next day, they were washed with ethanol and dried under nitrogen flow. The pH of the investigated solutions was 6. The procedure of the measurement was performed as described in 3.5.2.4 with the following parameter:

- 30 mins millipore water pH 6
- 60 mins sample solution
- 60 mins millipore water pH 6

The flow rate of liquid was 20 $\mu\text{L}/\text{min}$. Every measurement was performed twice and the average value was taken for evaluation. The fifth frequency was used for the calculation of the mass via Sauerbrey's equation.¹²⁴ The evaluation is more precisely explained in chapter 3.5.2.4.

6.5.2.7 Statistical analysis

For statistical analysis, regression analysis in Excel Office 365 was used. All experimental data which has been determined in 3.3 as well as the molecular properties, which are closer described in 3.3.8, were included in the calculation. For the univariate regression analysis, one independent molecular property was correlated with a dependent physicochemical property. For the multivariate analysis, all six independent molecular properties were correlated with one dependent physicochemical property. The P-value was used to evaluate the significance with a significance level of 5 %.

7 Towards application: catanionics as an emulsifier

7.1 Introduction

An emulsion is the mixture of two immiscible phases where one phase is dispersed in the other phase. The two phases are mostly a water and an oil phase.⁹⁷ Emulsions are present in our everyday life in many different situations – from drinking a glass of milk in the morning to several cleaning products and the use of an anti-aging night-cream in the evening (see Figure 82). Various emulsions can be found in diverse industrial sectors. One reason for that is the possibility to transport hydrophobic substances in an aqueous phase. Due to that fact, emulsions are favorable and useful transport agents in several industrial processes but they are also found in household products. A lot of end products on the market are emulsions. In cosmetics, a lot of products consist of an emulsion, e.g., the daily face-cream or the after-sun lotion. Especially in the food sector, emulsions are present in a variety of products.²¹³ Here, emulsions are used because of their rheological behavior. An example is a classical mayonnaise. In medicine and pest control, they are used as drug carriers in several applications.²¹⁴



Figure 82: Examples of emulsions in our daily life: face cream (left), mayonnaise (middle) and milk (right).

In most cases when emulsions are produced, the aim is to create a long-lasting emulsion system, which is independent of different external influences like temperature. E.g., we do not want our cosmetic product to be split into two phases after some weeks. This is a problem in a lot of situations, since an emulsion is only kinetically stable and will separate into two phase within a certain time. A lot of research has been done in this direction.²¹⁵⁻²¹⁷ But, the point of interest is also the other way around: to control the stability of an emulsion in a way that offers the possibility to stabilize and to destabilize the emulsion with changing certain parameters like the electric field²¹⁸ or the pH²¹⁹. E.g. macroscopic phase segregation can be useful to expose substances which have been transported within an emulsion at certain circumstances like applied in drug delivery.²²⁰

The following chapter focuses on emulsions based on the catanionic mixtures introduced in chapter 3. The main idea was to use the catanionic combinations as emulsifiers. Due to their interfacial properties (see 3.3.3), they might be efficient emulsifying agents. One main advantage of catanionic mixtures is the possibility to change their physicochemical properties by changing the anion-cation ratio.^{72, 221} The properties of the catanionic combination can also be changed by external parameters. E.g., the crystallization state of the catanionic surfactant layers can be changed by changing the temperature. For catanionic mixtures, a separation of the solubility temperature from the crystallization temperature is reported.^{222, 223} A gel-phasic state between these two temperatures can be found, which can stabilize emulsion very efficiently. Thus, the emulsifying efficiency can be decreased by exceeding the crystallization temperature.²²⁴

To get an overview of the emulsification ability of the catanionic mixtures, a general screening was performed regarding their stabilization of an aqueous phase with different oil phases in the first part of this chapter. Then, an interesting catanionic combination, the combination of Tex and ACA at the anion-cation mass ratio 5-5, was investigated closer with the focus on emulsion stability behavior by changing different parameters like pH, the addition of salt and temperature.

7.2 Fundamental information

7.2.1 Definition and classification of an emulsion

Whenever two immiscible liquid phases are dispersed, an emulsion is formed. It consists of droplets of the dispersed phase in a continuous outer phase. A third component is needed to reach a longer-lasting dispersed emulsion: an emulsifier.^{225, 226} The emulsifier is a surface-active molecule, which can accumulate at the interface of the two immiscible phases. This leads to a stabilization of the dispersed droplets in the second liquid phase due to several factors described in the following.

Depending on the outer and inner phase, different classes of emulsions can be distinguished. An emulsion is called oil-in-water (O/W) emulsion when the oil droplets are dispersed in an aqueous phase. A water-in-oil (W/O) emulsion is defined as a dispersion of water droplets in an oil phase. An oil-in-oil (O/O) emulsion describes oil droplets of one oil dispersed in another oil of different density and polarity.²²⁷

The size and the structure of the droplets within an emulsion can be used to subdivide the term emulsion further.¹ For typically O/W or W/O emulsions they size range differs from 0.1-5 μm . They are called “macroemulsions” and are only kinetically stable. The size range of 20-100 nm for emulsion droplets is described by the term “nanoemulsions”. They are only kinetically stable, too. “Microemulsions” are in the size range of 5-50 nm.²²⁸ They are clear, stable and isotropic mixtures, which are thermodynamically stable. Their formation happens spontaneously. Due to their stability and variety in their formation, they find many applications and the research interest is high.^{229, 230} “Multiple emulsions” are defined as emulsions in emulsions, either O/W/O or W/O/W. Their drop size and stability can vary.

An emulsifier is essential for a stable emulsion.²²⁷ Most efficient are nonionic surfactants. It is also possible to use ionic surfactants as emulsifiers for O/W emulsions. But, their sensitivity against electrolytes is disadvantageous. For compensating the sensitivity, mixtures of different surfactants are often used. Also, nonionic polymers are used as efficient emulsifiers. But, high energy is needed to emulsify the emulsion.

7.2.1.1 Emulsion from the thermodynamical point of view

From the thermodynamical point of view, an emulsion can be described as two different phases building up a planar interface, which is described by the Gibbs-Duhem equation (equation 17). Here, a drop size larger than 10 nm is assumed. For a constant temperature and a constant composition at the interface, the interfacial tension γ can be written as seen in equation 18.²²⁸

$$dG^\sigma = -S^\sigma dT + A d\gamma + \sum n_i d\mu_i \quad (\text{equation 17})$$

$$\gamma = \left(\frac{dG^\sigma}{dA} \right)_{T, n_i} \quad (\text{equation 18})$$

with the surface free energy G^σ , entropy S^σ , temperature T , area A , interfacial tension γ , number of moles of component n_i , chemical potential μ_i .

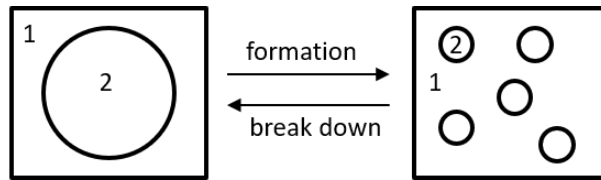


Figure 83: Schematic presentation of the formation and break down of an emulsion. The picture is taken from reference ²²⁸.

Schematically, the formation of an emulsion can be described by the formation of small droplets out of a bigger droplet (see Figure 83). After the emulsion formation, the overall area of the interface A_{12} is larger than before. A positive surface energy term equal to $\Delta A\gamma_{12}$ and a positive entropy of dispersion term equal to $T\Delta S^{\text{conf}}$ contribute to the change in free energy within the emulsion formation process. From the second law of thermodynamics, equation 19 can be set up since in most cases $\Delta A\gamma_{12} \gg -T\Delta S^{\text{conf}}$, ΔG^{form} is positive.

$$\Delta G^{\text{form}} = \Delta A\gamma_{12} - T\Delta S^{\text{conf}} \quad (\text{equation 19})$$

This means that the formation of an emulsion is not spontaneous. The system is thermodynamically unstable, and without any stabilization, the emulsion will break down. An energy barrier is necessary to prevent a continuous breakdown process. This can be done by the addition of an emulsifier. Due to this, the emulsion system gets kinetically stable. An energy barrier must be overcome before destabilization of the emulsion occurs.

7.2.1.2 Interaction energy forces

Interaction forces between the droplets are the reason why droplets within an emulsion come together and assemble or keep a certain distance. Three different interaction forces can be distinguished: van der Waals attraction, electrostatic repulsion, and steric repulsion. Their appearance and their strength depend on the outer layer of the droplets.⁹⁷

Van der Waals interactions are the interaction forces, which power the destabilization of the emulsion and can be differentiated further in Dipole-dipole (Keesom), dipole-induced dipole (Debye) and dispersion (London) interactions. The first two named interactions forces are vectors and can balance each other due to the different orientations of the dipoles. The London forces are the most decisive ones since they originate from charge fluctuation resulting in a temporary dipole within the molecule. This induces another dipole in the nearby molecule. The attraction forces can be described as in the following²²⁸:

$$G_a = - \frac{\beta}{h_{sep}^6} \quad (\text{equation 20})$$

with the London dispersion constant β determined by the polarizability of the molecule and the separation distance h_{sep} .

From the equation mentioned above, an inverse proportional to the power of sixth of the separation distance r between the atoms gets obvious. These forces G_a between the molecules are of short range. For close distances between the molecules, the van der Waal attraction is large since the interaction forces between the molecules in macroscopic bodies, like the emulsion droplets, can be summed up. This was suggested by Hamaker by inventing a new parameter, the Hamaker constant.²³¹ The relations are given in the following:

$$G_a = - \frac{A_H R_{eq}}{12h} \quad (\text{equation 21})$$

with the effective Hamaker constant $A_H = (A_{11}^{\frac{1}{2}} - A_{22}^{\frac{1}{2}})^2$ and the Hamaker constants of the droplets A_{11} and A_{22} , the equal radii R_{eq} and the separation distance h .

The Hamaker constant A_H is defined by the number of molecules per unit volume q and β , the London dispersion constant, shown in the following equation:

$$A_H = \pi^2 q^2 \beta \quad (\text{equation 22})$$

Due to the situation described above, flocculation can lead to large agglomerates within a short time. For this purpose, repulsion forces in opposition to the attraction of the molecules are necessary.

One main repulsion force is the electrostatic repulsion.^{97, 228} It appears when ionic surfactants adsorb at the interface of the droplet and the outer medium of the emulsion. By this, the droplet layer gets charged and a double layer according to Gouy-Chapman and Stern arises. The surface potential increases with coming closer to the double layer. A linear increase up to the Stern potential is observed. With lowering the distance h as it is shown in Figure 84, the surface potential increases exponentially. Electrolytes in the solution have a crucial impact. The higher the concentration and the higher the valency of the electrolytes, the lower extended is the double layer. When two charged bodies, here the emulsion droplets, come closer and the double layers start to overlap, the repulsion interaction G_{el} between them occurs. Combining the repulsion interactions with the interaction of attraction gives the total energy of interaction G_T :

$$G_T = G_{el} + G_a \quad (\text{equation 23})$$

The second main repulsion force is the steric repulsion. This is observed for nonionic surfactants or polymers. Repulsion of the hydrophilic chains has two contributions. In the presence of a good solvent, meaning low temperatures and low electrolyte concentration, the hydrophilic chains favor a non-mixing of themselves. The mixing free energy of interaction G_{mix} is positive in this case. Second, an overlap of the hydrophilic chains results in a loss of configurational entropy G_{el} of the chains. This means a positive value for G_{el} , which is not favorable. Combining the three parameters gives the total energy of interaction G_T :

$$G_T = G_{mix} + G_{el} + G_a \quad (\text{equation 24})$$

The situation of electrostatic repulsion and van der Waals attraction can also be described with the Derjaguin, Landau, Verwey, and Overbeek (DLVO) theory (see Figure 84).^{165, 166}

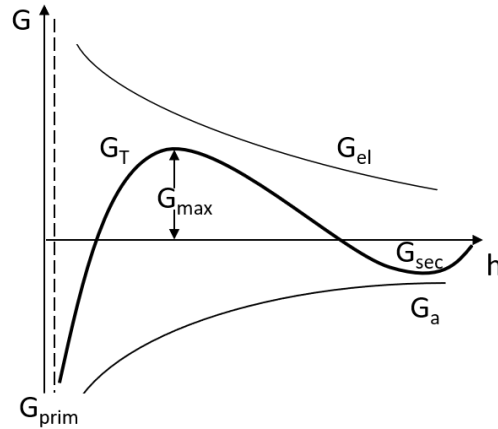


Figure 84: Schematic illustration of the total energy-distance curve of two emulsion droplets according to the DLVO theory.

Here, the two independent potentials of repulsion G_{el} and attraction G_a are combined. At high h values, the attraction leads to a minimum G_{sec} . With decreasing distance, the energy barrier increases. The height of G_{max} depends on the electrolyte concentration and the repulsion energy of the two droplets. After overcoming this energy barrier, the attraction interactions result in another minimum G_{prim} . The result is agglomeration and coalescence.²²⁸

7.2.1.3 Stability of emulsions

7.2.1.3.1 Destabilization of an emulsion

The main challenge in most applications regarding emulsions is to adapt their instability within a certain period. There are several processes which lead to a separation of the two mixed phases. They can be concurrent.^{232, 233} A schematically overview is given in Figure 85. Reasons for these processes are complex and are based on several surface forces which are described below.

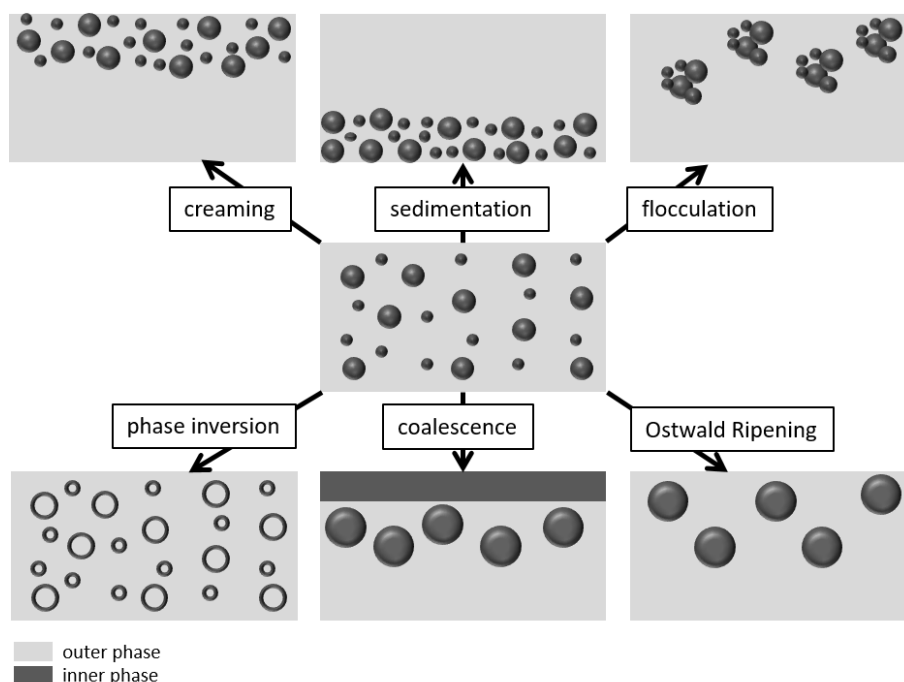


Figure 85: Schematic illustration of the different breakdown processes of an emulsion. Figure is taken from reference ²²⁸.

The droplets in the emulsion are driven by thermal motion (Brownian motion) leading to a constant movement of the drops in the medium. External forces like gravitational force affect the droplets and pull the heavier phase downwards. If the external forces are beyond the thermal motion, a gradient of concentration builds up within the emulsion system. Depending on the density of the droplets, they will shift to the bottom or the top. The action is described as sedimentation or creaming. For preventing this, several aspects can be considered. The decrease of the droplet size has a significant influence on the stability. The increase of the viscosity of the emulsion is another point for increasing emulsion stability. Thus, the motion of the droplets is hampered. Consequently, an opposite force to the gravitational force is present, which leads to a slowdown of the creaming or the sedimentation.⁹⁷

When the droplets aggregate to larger units without changing the initial size of the droplet, it is named flocculation. Van der Waals attractions are the reason for this. If they are stronger than the repulsion between the droplets, agglomeration is observed, c.f. G_{sec} in Figure 84. Then, the energy barrier of repulsion has been overcome. For the prevention of flocculation, repulsion forces, like electrostatic or steric ones, must be increased. This can e.g. be done by changing the emulsifier from nonionic to ionic or to increase the bulkiness of the hydrophobic part of the surfactant.

If an exchange of the dispersed phase and the outer phase happens, phase inversion occurs. Most times, a transition state of multiple emulsions is observed. Reason for this is mostly the change in the characteristics of the surfactant due to change in conditions like e.g. the pH value or the temperature. The phase inversion point (PIT) defines the critical temperature where phase inversion is observed.²²⁵ The interest on the phase inversion in the emulsion system has grown the last years and is a popular method to create stable emulsions.

If several droplets connect by forming a larger droplet, coalescence is observed. The thinning and disruption of the liquid film between the droplets by surface fluctuation is a reason for this. The presence of strong van der Waals interactions leads to the close up of the droplets. Fluctuations and the rupture of the droplet surface are kinetic processes, which result in the coalescence of the droplets.

Ostwald Ripening describes the phenomena of the disappearance of smaller droplets by the growth of large droplets. Reason for this phenomenon is the difference in pressure between the small and the large droplets. For small droplets, the Laplace pressure, which is described in equation 6 with the surface tension γ and the radius of the bubble r , has a higher value.

Molecules in the small droplets tend more to dissolve in the outer phase. They diffuse to the larger droplets. The higher the difference in the radius of the two droplets, the faster is the rate of Ostwald ripening. Small interfacial tension γ by, e.g. the addition of a surfactant can reduce the Ostwald ripening.²³⁴

7.2.1.3.2 Stabilization of an emulsion

The addition of a surfactant can delay or even prevent the breakdown of an emulsion. Due to the adsorption at the interface of the two phases, the interfacial tension γ is lowered. This leads to a smaller size of the droplets. The extent of the surfactant effect depends on its structure and its amount. Depending on the activity of the surfactant in bulk, the necessary amount varies to produce the smallest droplet size and to reduce γ the most. The emulsification process increases the interfacial area. A decrease in the surface excess concentration is the result. Depending on the activity of the surfactant, it can compensate the gradient by fast adsorption on the interface and stabilize the

created droplets. The usage of a mixture of surfactants with differences in their properties can partly compensate the situation by having the maximum of efficiency in different properties.²²⁸

An emulsion can also be stabilized without the presence of surfactants, but with solid particle instead. The phenomenon is named after S.U. Pickering, who reported about the stabilization of an O/W emulsion of paraffin oil with solid particles.²³⁵ No surfactant is present in the formulation. This is desired in several applications, like e.g. pharmaceuticals or food. The emulsion systems show a high resistance against coalescence. Solid particles smaller than the droplets are necessary for the adsorption at the emulsion interface. The adsorption of the particle is the crucial point. The way they adsorb at the interface is determined by their wettability. So, the main precondition for the particles is that they allow the partial wetting by water and oil. The hydrophobicity of the particle about the used oil is decisive. For an optimum in emulsion stability, a contact angle of 90° is desired. The rule of Bancroft can also be applied for solid particles. It states that the continuous phase of an emulsion is the phase in which the emulsifier is more soluble. Thus, it gives a hint towards their favored continuous medium and therefore their favored emulsion type.²³⁶ The extent of hydrophobicity can be easily adjusted with the suitable components or coating. A lot of different types of particles are known.^{237, 238} The most common material used is silica. The adsorbed particles build up a rigid shell around the droplets, which hold together due to attractive forces between the particles. This mechanical barrier prevents the droplets to merge.²³⁹

7.2.1.4 Catanionics systems in emulsions

The structure and properties of catanionic combinations suggest themselves to be good emulsifiers due to the combinations of two emulsion supporting features. One is their amphiphilic structure, which leads to adsorption at the interface and decrease of the interfacial tension as it is known for all surface-active compounds.⁹⁵ The second point is the fact that in certain ratios of anion and cation, the catanionic combination has more or less intense crystalline-like character around equimolar ratio. This results in crystalline particles, which can stabilize an emulsion according to the principle of the Pickering emulsion.²⁴⁰

Several approaches for the stabilization of emulsions with catanionic surfactant combinations have been reported, but the field of research on this topic is still not very intensely explored. It was May-

Alert in 1985 who investigated several preparation ways to form emulsions stabilized by a crystallized catanionic combination at an equimolar ratio. She mixed two immiscible phases with the anionic surfactant in one phase and the cationic surfactant in the other phase. When the two phases met, precipitation of neutral aggregates at the water-oil-interface occurred. This led to a stabilization of the prepared emulsion.²⁴¹ Based on that work, Schelero investigated further on emulsions with catanionic surfactant combinations. She performed scattering experiments for the determination of size and shape in a water-tetradecane emulsion system with hexadecyltrimethylammonium hydroxide in combination with myristic acid. She found crystalline discs surrounding the oil droplets.²⁴² The preparation and the high stability of the stacks of crystalline nanodiscs was reported. The possibility of adjusting the surface charge of the discs by changing the anion-cation ratio was examined in a further paper. High resistance against creaming and coalescence was found in combination with nearly no salt sensitivity.²⁴³ Margulis-Goshen investigated the catanionic system of hexadecyltrimethylammonium bromide and sodium octyl sulfonate in the emulsion system heptane and water as templates for the design of size-controlled, water-dispersible nanoparticles of butylated hydroxytoluene. Several advantages of a catanionic system such as the stable droplet size in the microemulsion could be stated.²⁴⁴ Tetradecyltrimethyl ammonium laurate was tested as a catanionic emulsifier for the paraffin oil-water system from Zhang *et al.* A polydisperse system of droplets with interesting viscosity properties was found. In another paper, they expanded their research to more head-to-tail structured catanionic combinations. Emulsions with high stability were found. The influence of the excess of one ion leads to a change in stability and polydispersity.²⁴⁵

7.2.2 Specific ion effects

The investigations of the interactions of ions with the surrounding system are of great interest in many different sectors since a salt-free system is hardly present in real life. They play an important role in biology and chemistry. Specific ion effects can help to explain these interactions. More than 100 years ago, in 1888, Franz Hofmeister was the first scientist who studied the influence of salts on different phenomena, such as the precipitation behavior of protein and minerals oxides systematically.²⁴⁶ He created an order of salts according to their water withdrawing capability, which was the basis of his argumentation for precipitation of proteins in solution. The order of salts was changed into an order of ions later. It is now named the Hofmeister series²⁴⁷, see Figure 86.

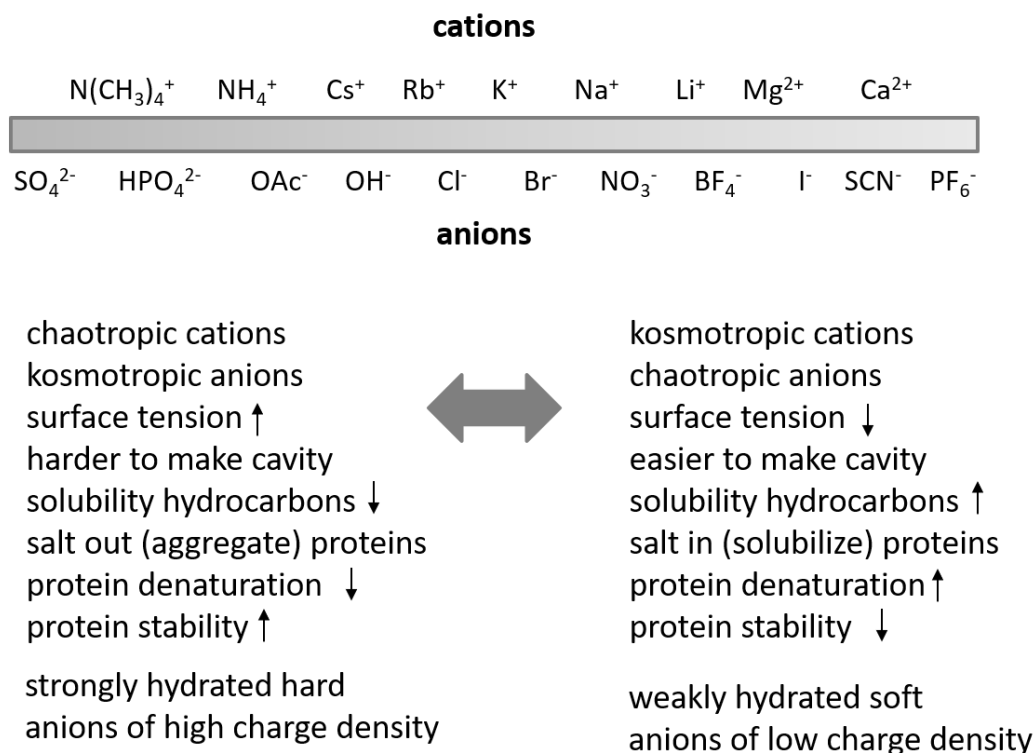


Figure 86: A typical ordering of anions and cations in the Hofmeister series. The figure is based on reference ²⁴⁸.

The order can change dramatically when the properties of the systems are changed. The order of hard and soft ions is set oppositely for anions and cations. This agrees in many biological systems. But, when a system without charges is considered, the situation is different. Then, only the charge density is decisive. Small and highly charged ions will be salting-out and larger and polarizable ions will be salting-in. The Hofmeister series gives a good basic rule about the interactions of ions. But, it may differ for a system with uncommon salts.²⁴⁷

In 2004, Collins described the so-called “Collins’ concept” to explain the specific ion interactions in a general way.¹⁰⁵ It is called the “concept of matching water affinities”. It orders the ions regarding the relative strength of the ion-water interactions compared to water-water interactions (see Figure 87). Ions are considered as spheres with a point charge in the center. Small ions are tightly bound by water molecules. They are known as hard ions and kosmotropes. For larger ions, the hydration shell is only loosely bound. They are called soft ions and chaotropes. Two kosmotropes will form an ion pair by

breaking down the hydration shell since the interaction between the two ions is larger than the interaction between the ions and water. Two chaotropes will also form an ion pair since the hydration shells will break because the interaction between the water molecules is stronger than the interaction between the large ions and the water molecules. Due to their different interaction with the water molecules, a kosmotropic and a chaotropic ion will not interact strongly with each other and will not form an ion pair. Only simple ions are considered in this concept.

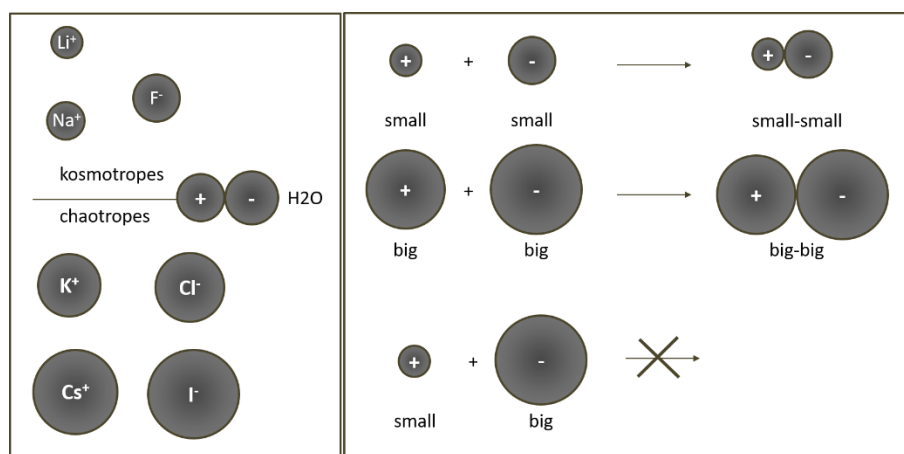


Figure 87: Left: Division of alkali ions and halide ions into strongly hydrated kosmotropes (above the line) and weakly hydrated chaotropes (below the line). The medium-sized zwitterion in the left illustration represents a water molecule. Ion sizes are drawn true to scale. Right: It is shown that ions have to be similar in size to form inner sphere ion pairs. This figure is based on reference ¹⁰⁵.

Thus, Jungwirth *et al.* performed some simulation and delivered experimental data²⁴⁹ and Harrison *et al.* collected some experimental data from chromatography tests²⁵⁰ to enable the extension to a series of cationic and anion headgroups. This new series was published by Vlachy in 2009 who made studies on the transition from micelles to vesicles by the addition of salts in the aqueous solution of dodecyl trimethyl ammonium bromide (DTAB) and an excess of sodium dodecyl carboxylate (SL).²⁵¹ From this, the anionic alkyl sulfate headgroup was considered as a soft ion and as chaotrope, in contrast to the hard sulfate ion. A trimethyl alkylammonium cation was also considered as a soft ion.

Considering the catanionic mixtures in this thesis, four ions are present in the solution: sulfate and trimethylammonium as the two headgroups and chloride and sodium as the two counter-ions. From the discussion above, it follows that the two headgroups interact strongly with each other since they

are both considered as soft ions. Sodium is defined as a small and hard ion. It will not interact intensively with the sulfate headgroup. Chloride is regarded as an intermediate case. According to Collins, it will interact with the ammonium headgroup only slightly. But, since sodium does not interact with the sulfate headgroup intensively, it will interact with the chloride. Consequently, a strong ion pair due to the same water affinities can be assumed for the two surfactants, which will be disturbed by the counter-ions only in a moderate way.

7.3 Results and discussion

In the following, the different catanionic mixtures based on ethylene oxide (further called EO) groups, which are described more precisely in chapter 3.3, are outlined regarding their ability to act as an efficient emulsifier. First, the stability of all catanionic mixtures was checked in a screening over ten different oils. From that screening, the most interesting mixture was investigated more deeply with respect to an external parameter which could influence the emulsion stability. For this purpose, the influence of the change in the temperature, the pH value, the salt content and the addition of alcohol was investigated for this system via optical observation, DLS and viscosity measurements.

7.3.1 Emulsion screening

For a general overview regarding the potential of the different catanionic combinations with four different anion-cation ratios (see chapter 3.3) as emulsifiers, a screening over all combinations with ten different oils was performed. Most experiments were performed within the bachelor thesis of Silva Kronawitter in June 2018.²⁵² The investigated mass ratios of anion to cation were the following: four to six, five to five, six to four and equimolar. The concentration was 1 wt%. The investigated oils were divided into three different classes: plant oils, alkanes, and glycerides. Rape oil and sunflower oil were taken as examples for commercial plant oils with hydrophobic character. Biodiesel was also classed into this group since it is based on plant (or animal) fats and oils, which are esterified. The three implemented oils in the glyceride-based group (Miglyol 812, diisostearyl malate and triolein) differ in the number of chains connected to the glyceride from two to three and also in their chain length. Pentaerythrityl tetraisoostearate is added to this group as fourth component. It has four alkyl chains connected via ester bonds to a glyceride-similar backbone. Octane, dodecane, and hexadecane were tested as examples of typical linear alkanes with different chain lengths. For better comprehensiveness, a letter was assigned to each of the oils. An overview of the different oils is shown in Figure 88.

oils	alkanes	A octane	B dodecane	C hexadecane
	plant oils	D rape oil	E sunflower oil	F biodiesel
	glycerides	G Miglyol 812	H diisostearyl malate	
		I triolein	J pentaerythrityl tetraisoostearate	

Figure 88: Overview of the ten oils used for the emulsion stability screening of the different catanionic combinations.

The stability evaluation of the samples was done macroscopically as described in 7.5.2.1. If a phase separation was observed to start, the sample was named to be unstable and marked with the corresponding number. An overview of the stability tests for each cation is shown in Figure 89 – Figure 91. The summarized results of the evaluation of the emulsion stability are shown in Figure 92. As a reference, the pure cationic or anionic surfactant solutions were also tested. However, they showed no emulsification behavior. They were all part of the group of lowest emulsion stability. So, only the catanionic combinations are shown in the figures.

For the catanionic mixtures with the cationic surfactant ACA, a phase separation was observed after 1 hour in most samples as it can be seen in Figure 89 and Figure 92. A creaming phase on the top of the sample was observed indicating large droplets, which are sensitive to density difference and raise (see 7.2.1.3.1). Several samples showed a complete demixing indicated by a clear aqueous solution on the downside of the tube. For the combination of ACA and SDS, it has to be noted that the

surfactant solution alone was already turbid. So, a complete separation was not indicated by a clear aqueous solution. In general, the samples with the equimolar ratio showed the lowest stability. Especially the combination with C12EO6SO₄ showed very fast separation. The solubility of the combination, which was very high for C12EO6SO₄, had no positive effect in comparison to the other cationic surfactants.

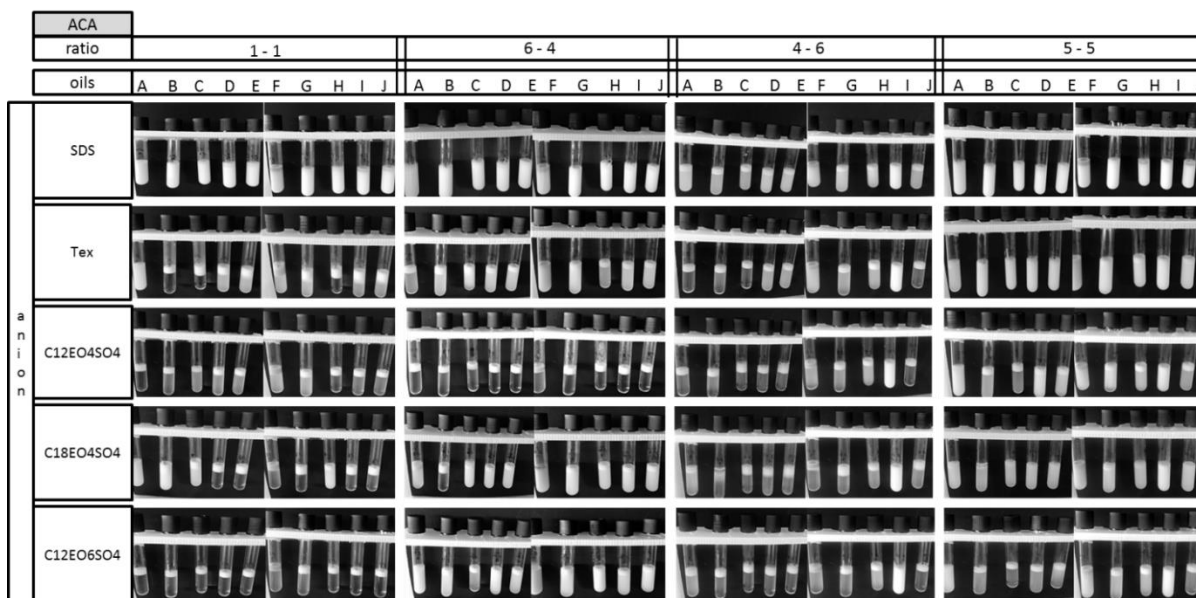


Figure 89: Pictures of the emulsion stability tests after 1 hour for the catanionic combinations with ACA as cation and the five different anions SDS, Tex, C12EO4SO₄, C18EO4SO₄ and C12EO6SO₄ with an anion-cation molar ratio 1-1 and mass ratios 6-4, 5-5 and 4-6 at 1 wt% with ten different oils: A (octane), B (dodecane), C (hexadecane), D (rape oil), E (sunflower oil), F (biodiesel), G (Miglyol 812), H (diisostearyl malate), I (triolein) and J (pentaerythrityl tetraisoostearate) at room temperature evaluated as described in 7.5.2.1.

The increasing nonionic character of the surfactant did not promote the emulsification ability as it might be expected from literature. There, it is described that with increasing nonionic character, the repulsion of the emulsion droplets depends more strongly on the steric hindrance than on electrostatic repulsion.¹⁰⁰ The steric hindrance is not efficient enough to stabilize the emulsion systems. The headgroup of the pseudo-nonionic ion pair has only small bulkiness. The EO groups can enhance the flexibility and thus the steric hindrance.^{9,31} But, this hindrance is not enough as it can be seen in the corresponding figures regarding the repulsion of the emulsion droplets. The highest stability after 1 hour could be determined for the anion-cation mass ratio 5-5. On the molar scale, this

means a small excess of the anionic surfactant. Comparing the influence of a higher excess of one surfactant showed small differences. Except for C12EO4SO₄, an excess of the anion (mass ratio 6-4) gave slightly better results than an excess of the cation (mass ratio 4-6).

Consequently, a small excess of charges stabilizes the emulsion. Only small differences in the structure are assumed when the amount of anionic and cationic surfactant is changed. The main difference is the charge of the droplets in the emulsion. In these cases, the electrostatic repulsion seems to be more efficient than the steric one. Regarding the different oils, triolein was the oil which got emulsified the best. Comparing the triglycerides with each other showed that the triglyceride bone was not the decisive factor since Miglyol 812 did not give the same result than triolein. Also, the number of chains mattered. Two as well as four alkyl chains were less effective to be emulsified than the long-chain triglyceride triolein. Tex-ACA at the mass ratio 5-5 showed one of the best emulsion results compared to the other combinations, also when compared with the other cations. For this purpose, the combination is suitable for a closer investigation regarding parameters for changing the catanionic system, which is discussed in chapter 7.3.2.2.

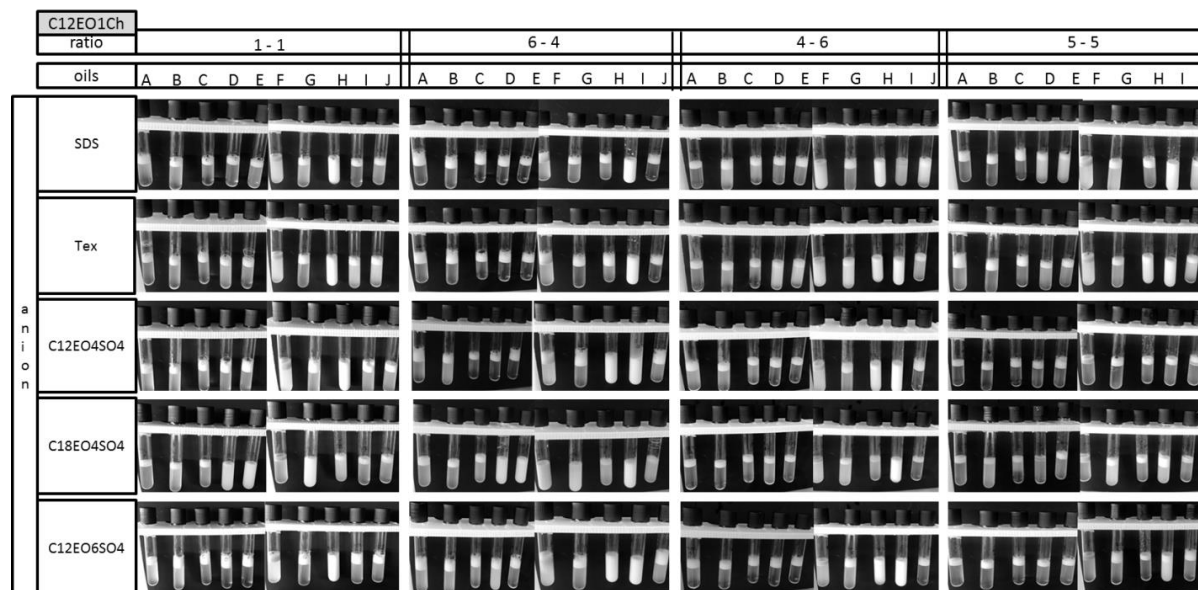


Figure 90: Pictures of the emulsion stability tests after 1 hour for the catanionic combinations with C12EO1Ch as cation and the five different anions SDS, Tex, C12EO4SO₄, C18EO4SO₄ and C12EO6SO₄ at the anion-cation molar ratio 1-1 and mass ratios 6-4, 5-5 and 4-6 at 1 wt% with ten different oils: A (octane), B (dodecane), C (hexadecane), D (rape oil), E (sunflower oil), F (biodiesel), G (Miglyol 812), H (diisostearyl malate), I (triolein) and J (pentaerythrityl tetraistearate) at room temperature evaluated as described in 7.5.2.1.

For the cation C12EO1Ch, the situation was similar, as it can be seen in Figure 90 and Figure 92. The largest difference compared to ACA regarding the solubility was the combination with SDS as an anion. Here, the catanionic combinations were by far more soluble than with ACA. But, in the performed tests, the emulsification behavior was already low after 1 hour. All in all, the triglycerides gave the best results. Especially, triolein and diisostearyl malate showed more stable emulsions. Plant oils were hardly emulsified for a longer time. Also, the alkanes showed no stable emulsion after 1 hour in most cases. For C12EO1Ch as cation, the mass ratio of 4-6, meaning a small excess of cation, gave the best results in average. Here, in contrast to ACA, the cation had a more positive effect on the emulsification behavior. Since the length of the alkyl chain was the same with 16 carbon atoms, the difference must have been in the present EO group. Two different contributions come into account. The HLB value increases with the insertion of the polar EO group, which should make the surfactant more suitable for O/W emulsions.²¹ This should normally enhance the emulsion stability. Additionally, the additional EO group in the cationic structure increases the polarity in the hydrophilic part of the surfactant. Stronger polar interactions between the surfactant molecules are the result, which reduces the volume of the molecule and thus its bulkiness. The flexibility of the chain counteracts these interactions, which increases the bulkiness and thus promotes emulsion stability. In the present case with C12EO1Ch, the steric aspect seems to be dominated by the interaction aspect.

Regarding the cation with the highest number of EO groups, C12EO4Ch, a lot of emulsions showed already phase separation after 1 hour (see Figure 91 and Figure 92). No significant difference could be observed compared to the cation with only one EO group, C12EO1Ch. Again, the catanionic combination with a small excess of cation showed the best results. They were even slightly better than with C12EO1Ch. Noticeable was the catanionic combination of the cation C12EO4Ch with the long-chain anion C18EO4SO4. Compared to the two other cations, the results in emulsion stability were significantly better. Several emulsions were stable after 1 hour. Especially at the mass ratio 6-4, meaning a small excess of anion, homogenous emulsions, except for octane and biodiesel, could be observed. One important aspect must be mentioned at this point. This catanionic combination showed significantly higher viscosity than the surfactants alone and also in comparison to all the other combinations. Higher viscosity could prevent the fast separation of phases since the droplets cannot move as fast as at lower viscosities.

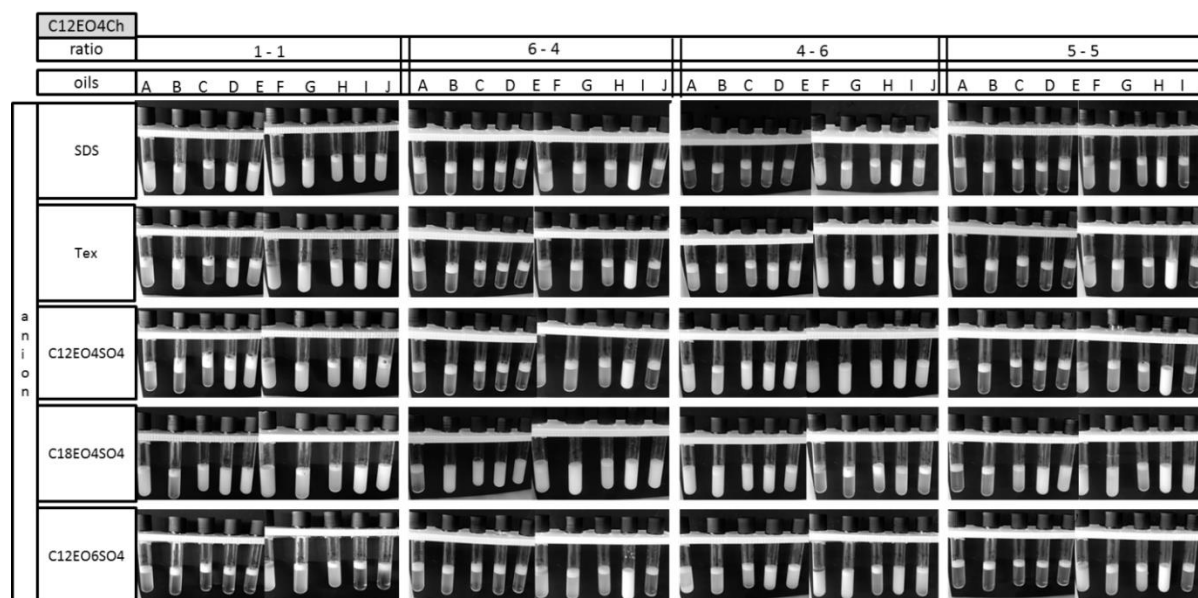


Figure 91: Pictures of the emulsion stability tests after 1 hour for the catanionic combinations with C12EO4Ch as cation and the five different anions SDS, Tex, C12EO4SO4, C18EO4SO4 and C12EO6SO4 at the anion-cation molar ratio 1-1 and mass ratios 6-4, 5-5 and 4-6 at 1 wt% with ten different oils: A (octane), B (dodecane), C (hexadecane), D (rape oil), E (sunflower oil), F (biodiesel), G (Miglyol 812), H (diisostearyl malate), I (triolein) and J (pentaerythrityl tetraistearate) at room temperature evaluated as described in 7.5.2.1.

In general, the emulsion capacity of the catanionic combinations was lower as expected (see Figure 92). From the theoretical background, a good emulsifier should connect the two immiscible phases.²²⁵ This is done best when the emulsifier can interact with both phases. A similar chemical structure and polarity of molecules promote this. From that thinking, the alkanes, whose chemical structure is similar to the linear alkyl chain of the investigated surfactants, should have been emulsified in a good way. But, this was not the case. Independently of the chain length, the alkanes were not good to be emulsified with the catanionic combinations. Consequently, these interactions cannot be the decisive factor. Emulsions with plant oils were not stable either. Sunflower oil consists mostly of fatty acids, especially linoleic acid (67 %) and oleic acid (19 %). Rape oil has a broader distribution of fatty acids. The main components are oleic acid (34 %), erucic acid (26 %) and linoleic acid (17 %).²⁵³ Because of their hydrophobicity, they are difficult to emulsify. Except for Tex-ACA 5-5 and some combinations with the anion C18EO4SO4, they were not emulsified satisfactorily. The worst oil was biodiesel. Biodiesel consists of a mixture of different fatty acid methyl esters from rape oil mostly with double bonds present.²⁵⁴ The interaction of the surfactants with the substances must be low considering the observed emulsion samples. Regarding the different glycerides, triolein was by far the oil which was

emulsifiable the best. Comparing the different glycerides, different structural aspects can be interpreted. The glyceride backbone itself was not the decisive factor since all other glycerides did not give the same results. Also, the triglyceride structure could not be the crucial point since a significant difference between triolein and Miglyol 812 was observed, although they only differ in the chain length. The reason must be specific interactions between the oil and the surfactant molecules which are not visible at first glance.

		ratio	1 - 1										6 - 4										4 - 6										5 - 5													
		oil	A	B	C	D	E	F	G	H	I	J	A	B	C	D	E	F	G	H	I	J	A	B	C	D	E	F	G	H	I	J	A	B	C	D	E	F	G	H	I	J				
cation	anion																																													
ACA	SDS		3	2	2	2	1	0	3	2	2	1	1	1	1	2	2	2	2	2	2	2	1	1	1	1	1	2	2	2	4	1	1	3	5	2	2	1	4	0	4	0				
ACA	Tex		4	0	1	1	1	0	1	1	1	1	1	2	2	1	1	1	3	2	1	1	1	1	1	1	1	2	2	2	4	0	1	4	5	4	4	2	3	2	4	2				
ACA	C12EO4SO4		0	0	0	0	1	0	0	0	0	0	0	0	0	0	0	0	0	0	0	0	1	1	1	1	1	1	1	2	3	1	2	1	0	1	1	2	1	2	3	1				
ACA	C18EO4SO4		2	2	2	0	0	0	0	0	1	0	0	1	0	2	1	1	2	1	1	2	2	1	1	1	1	1	2	2	3	1	1	1	2	2	2	2	2	1	3	2				
ACA	C12EO6SO4		0	0	0	0	0	0	0	0	0	0	0	1	1	1	1	4	1	1	1	1	1	1	1	1	1	2	2	1	1	1	2	3	1	1	1	1	2	2	2	4	2			
C12EO1Ch	SDS		2	2	2	1	1	1	1	4	1	1	1	1	1	1	1	1	1	1	1	6	1	1	2	2	1	1	2	1	1	2	1	6	1	2	1	1	3	3	1	1	2	6	2	
C12EO1Ch	Tex		1	1	1	1	1	1	1	4	1	1	1	1	1	1	1	1	1	1	1	6	1	1	1	1	1	1	2	2	3	3	1	1	1	1	1	1	1	1	1	2	4	2		
C12EO1Ch	C12EO4SO4		1	1	1	1	1	1	1	5	2	2	1	1	1	1	1	1	1	1	4	4	1	1	1	2	1	1	1	1	1	2	4	0	0	0	0	0	0	0	0	0	0			
C12EO1Ch	C18EO4SO4		2	2	2	4	4	2	2	2	2	2	1	2	2	3	1	4	4	2	4	2	1	1	1	1	1	1	1	0	5	0	2	2	0	0	0	0	0	0	0	1	0			
C12EO1Ch	C12EO6SO4		1	1	1	1	1	1	2	5	2	2	2	1	1	1	1	1	2	4	5	2	1	1	1	1	1	1	2	1	2	6	0	0	0	0	0	0	0	0	0	0	1	0		
C12EO4Ch	SDS		1	1	1	1	1	1	1	1	1	1	1	1	1	1	1	1	1	1	6	0	1	1	2	1	1	2	2	0	5	0	1	1	1	1	1	1	1	1	1	1	3	0		
C12EO4Ch	Tex		1	1	1	2	2	1	1	1	2	2	1	1	1	0	0	1	1	1	6	1	1	1	1	1	2	1	2	2	4	2	1	1	1	0	0	1	1	1	1	6	0			
C12EO4Ch	C12EO4SO4		1	1	1	2	2	1	2	2	1	1	1	1	1	1	1	1	1	1	6	0	1	1	2	2	2	2	1	1	1	1	1	1	1	1	1	1	1	1	2	1	6	0		
C12EO4Ch	C18EO4SO4		2	2	2	4	4	2	2	4	4	1	2	3	2	2	4	1	2	2	3	2	2	3	2	1	1	0	0	0	0	0	1	2	2	4	4	2	4	2	3	1				
C12EO4Ch	C12EO6SO4		1	1	1	1	1	1	1	1	1	1	1	1	1	1	1	1	1	1	6	1	1	1	1	1	1	1	2	0	0	0	0	1	1	1	1	1	1	2	2	2	4	1		

Figure 92: Summary of the macroscopic evaluation of the emulsion stability evaluated as described in 7.5.2.1 of the different catanionic combinations at the anion-cation molar ratio 1-1 and mass ratios 6-4, 5-5 and 4-6 at 1 wt% with ten different oils: A (octane), B (dodecane), C (hexadecane), D (rape oil), E (sunflower oil), F (biodiesel), G (Miglyol 812), H (diisostearyl malate), I (triolein) and J (pentaerythrityl tetraistearate) at room temperature. The evaluation parameters are the following: 0 (immediate separation), 1 (separation after 10min), 2 (separation after 1h), 3 (separation after 2h), 4 (separation overnight), 5 (separation after 24h) and 6 (stable after 24h).

From the screening tests, several statements can be made: The efficiency of stabilizing an emulsion with the investigated catanionic mixtures seemed to be an interplay of several factors: the viscosity had a positive effect on the emulsion stability. The higher solubility of the catanionic combination principally did not lead to a better emulsifier. A partly crystalline character indicated by slight turbidity was a positive aspect on the emulsion stability, like in the case of Tex-ACA. The individual interaction of the catanionic combination was not flexible for all different structures of the oil. There were certain combinations where the interactions were strong enough to connect the two phases. Together with this, the orientation of the surfactants at the interface was in a way that prevents coalescence due to the repulsion of the droplets. For the catanionic system Tex-ACA, mass ratio 5-5, the best stability

tests could be achieved regarding the different oils. Especially for dodecane, hexadecane, rape oil, sunflower oil, and triolein, emulsion stability over more than several hours was observed. For this purpose, this system will be investigated more deeply in the following chapter. Additionally, the catanionic combination C18EO4SO4-C12EO4Ch, mass ratio 5-5, showed good emulsifying properties. A higher viscosity of the sample was noticed, which can be the reason for that.

7.3.1.1 Correlations to the interfacial tension of the catanionic mixtures

As already mentioned in chapter 7.2.1.3, one main parameter, which has a significant influence on the emulsion behavior of the two immiscible phases, is the interfacial tension (IFT) between the aqueous and the oil phases. A small interfacial tension enhances the generation of small droplets²⁵⁵ and helps to preserve the surface area to prevent phase separation.²⁵⁶ For this reason, several examples of the investigated emulsion were also investigated regarding their interfacial tension. Since for catanionic combinations, a synergism in several interfacial properties is known⁷², small values of interfacial tension are expected. For this purpose, the spinning drop method (described in 7.5.2.2) was the method of choice since the pendant drop method and the Wilhelmy plate method are not precise enough. Four oils (biodiesel, triolein, octane, and dodecane) were exemplarily measured against two surfactant combinations (C18EO4SO4-C12EO4SO4 and SDS-C12EO1Ch) with the anion-cation mass ratio 5-5. For the best combination in the previous screening (see 7.3.1), Tex-ACA 5-5, all ten different oils (octane, dodecane, hexadecane, rape oil, sunflower oil, biodiesel, Miglyol 812, diisostearyl malate, triolein, and pentaerythryl tetraisoostearate) were investigated to see any correlation of the interfacial tension with the stability of the emulsion. The interfacial tension describes the work per area which is necessary to expand the interface between the two phases.²⁵⁷ A small interfacial tension corresponds to low energy needed to create large interfaces like it is the case in creating droplets in an emulsion. Thus, a small IFT is desirable for the emulsification process. Unbalanced forces of the two phases at the interface are the reason for the interfacial tension. The interaction between the two phases is low since the molecules (water and oil) differ significantly in their molecular structure. In the case of adding a surfactant, the interfacial tension is affected by the surfactants, which adsorb at the interface. The repulsive interactions between the two immiscible phases are reduced since the amphiphilic structure balances the different nature of the two phases. Consequently, the interfacial tension decreases significantly.⁹⁵

The results of the performed interfacial tension measured as described in 7.5.2.2 are shown in Figure 93. The corresponding values from the screening in 7.3.1 are included above the graphs. The determined IFT values were extremely low, especially for the combination Tex-ACA where IFT values below 1 mN/m were measured. The IFT values for C18EO4SO4-C12EO4Ch were in the range of 2-8 mN/m, whereas for SDS-C12EO1Ch all values were below 3 mN/m. Comparing the measured IFT values with the emulsion stability for each catanionic mixture, the trend of lower interfacial tension between two immiscible phases resulting in a more stabilized emulsion was confirmed. If the surfactant can interact efficiently with both phases, the energy differences are low, and the creation of an emulsion needs less energy. Consequently, it is easier to form an emulsion.²⁵⁷ All combinations with higher emulsion stability showed smaller values of interfacial tension. Thus, a different preference for the different oils could be concluded. Although, it got obvious that the interfacial tension is not the only factor. A clear ranking according to the value of interfacial tension was not possible. Within one combination, the trend of interfacial tension against the different oils fitted to the macroscopic observations. But, no comparison of the different combinations with each other was possible. The interactions due to the structure and nature of the catanionic surfactants seemed to be individually different.

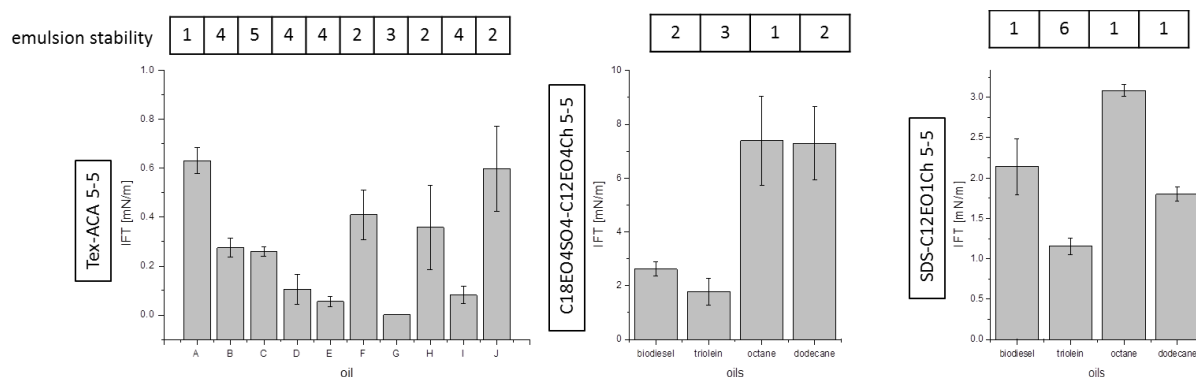


Figure 93: Results of the spinning drop measurements of the aqueous catanionic combinations against several investigated oils: A (octane), B (dodecane), C (hexadecane), D (rape oil), E (sunflower oil), F (biodiesel), G (Miglyol 812), H (diisostearyl malate), I (triolein) and J (pentaerythrityl tetraistearate) at 25 °C as described in 7.5.2.2.

7.3.1.2 Microscopic investigations with the CLSM

As closer described in 7.2.1.3, the size of droplets in an emulsion indicates the process of the emulsion destabilization.²²⁸ To get a closer look into the samples, a confocal light scanning microscope (CLSM) can be used to depict the microscopic situation in an emulsion. Nonpolar hydrophobic areas can be visualized by coloring. The addition of a hydrophobic dye, in the present case Nile Red, the hydrophobic areas (mostly oil) can be differentiated from the hydrophilic surrounding. For this, three examples for a stable, an intermediate and an unstable emulsion of the investigated samples of the catanionic combinations were investigated as described in 7.5.2.5 for comparing the aggregation situation and the droplet size. The pictures are shown in Figure 95.

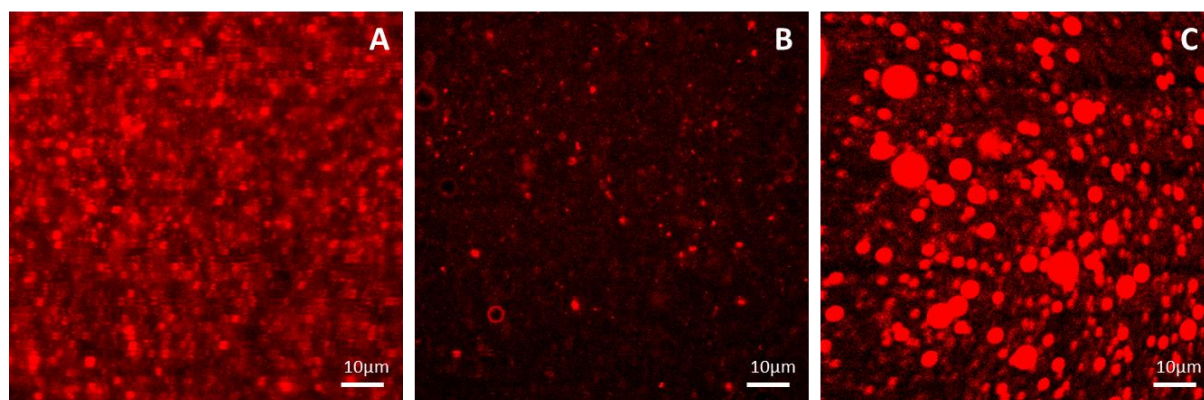


Figure 94: Pictures of three different emulsions of catanionic systems taken with the CLSM as described in 7.5.2.5: A: SDS-C12EO1Ch, 5-5, triolein, 2 h after preparation; B: Tex-ACA, 5-5, rape oil, 2 h after preparation; C: C12EO6SO4-C12EO4Ch, 5-5, biodiesel, 2 mins after preparation.

In Figure 95-A, the stable emulsion of the combination SDS-C12EO1Ch, 5-5, with triolein as oil can be seen. The emulsion was evaluated as stable over more than 24 h (see Figure 92). The precondition for a stable emulsion is the fact that the droplets do not form larger aggregates. In the optimal case, the droplets should be of the same small size. This situation is depicted in the corresponding figure. A homogeneous sample with an average droplet size of around 1 μm was observed. It indicates prevention of coalescence.²²⁶ This confirms that the catanionic system of SDS-C12EO1Ch, 5-5, can form an optimal emulsion by repelling the droplet from each other for several hours.

The emulsion of the catanionic combination of Tex-ACA, mass ratio 5-5, together with rape oil, is shown in Figure 95-B. The emulsion system was also evaluated as relatively stable (see Figure 92), although it was presumed as intermediate. As in the case before, small droplets could be seen. The size differed in a small range from less than 1 μm to 2 μm . Interesting was the appearance of different structures in the system. Especially, vesicle-like structures were present. Their size was several μm . Since the vesicles showed only thin walls, only very small amounts of oil could be present in the hydrophobic shell of the vesicles. The oil was found in small spherical droplets. This indicates the catanionic system Tex-ACA, 5-5, as suitable emulsifier since it can prevent the attraction of the droplets, which would lead to the destabilization of the emulsion.

A different situation was found in the case of the catanionic system of C12EO6SO4-C12EO4Ch, anion-cation mass ratio 5-5, with biodiesel as oil. The sample was only stable for minutes. Phase separation was observed within only a few minutes (see Figure 92). The reason for this can be seen in Figure 95-C. Here, a variety of different droplet sizes were observed already after 2 min. In the background, smaller droplets were still present. This led to the assumption that the droplets coagulated and rose up to build a creaming layer. The repulsion between the droplets was not strong enough to prevent the attraction between them. This led to fast phase separation (compare 7.2.1.3).

From the investigations with the CLSM, a reliable insight view into the emulsion system of three catanionic examples was possible. The pictures confirmed the theoretical approaches of emulsion stability depending on the drop size. For an unstable emulsion, larger droplets could be seen after several minutes whereas the stable emulsions still formed small droplet after 2 h. The microscopic situation strongly depended on the investigated system. The pictures from the CLSM confirmed the statements from 7.3.1. Stable emulsions can be formed with the catanionic systems, but the used surfactants must be chosen with care and adjusted to the oil, which is desired to be emulsified.

7.3.2 Deeper investigation of the system Tex-ACA, 5-5, 1 wt%

From the macroscopic investigations in the previous chapter 7.3.1, the catanionic system with Tex as an anionic surfactant and with ACA as a cationic surfactant with the anion-cation mass ratio 5-5 was one of few combinations with a high potential as an emulsifier. Several emulsions with this combination were regarded as stable over several hours. For this purpose, this system was

investigated in more detail. The results of this chapter were part of the research report of Chantal Walser in January 2018.²⁵⁸

7.3.2.1 Basic characterization of the catanionic system

To be able to evaluate potential changes in the present catanionic system, the system itself needed to be investigated as a reference. For this purpose, the system was examined via DLS and CLSM as it is described in 7.5.2.6 and 7.5.2.5. The results are shown in Figure 95. The optical appearance of the catanionic mixtures at a concentration of 1 wt% showed no complete transparency, but slight turbidity. This points to larger aggregates in the solution. DLS measurements of the sample at different concentrations confirmed this assumption. A monomodal fit gave a value of 150 nm as the average radius for the aggregates. The correlation curve did not change until a concentration of 2 wt%. Here, a shift towards larger aggregates could be seen (see Figure 95 - left). But, as known from the literature, catanionic systems often show a variety of different structures, especially based on double layers.⁸² So, the calculated size of aggregates from the DLS can only be seen as an average value over several different sized aggregates.

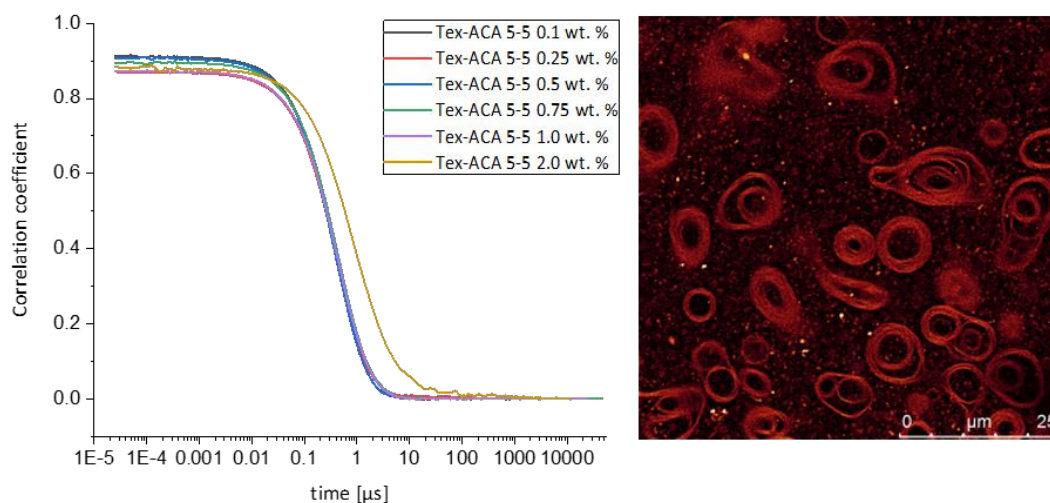


Figure 95: Concentration-dependent DLS curves measured as described in 7.5.2.6 of the catanionic system Tex-ACA, mass ratio 5-5 (left); pictures of the CLSM from the catanionic system Tex-ACA, 5-5, 1 wt%, (right) performed as described in 7.5.2.5.

The assumption could be confirmed with pictures taken with the confocal light scanning microscope (CLSM) described in 7.5.2.5. As it is shown in see Figure 95, a variety of different structures were present at a temperature of 25 °C. Vesicle-like structures could be seen in different size and shape. Even multiple vesicles within each other were present. They were very flexible and moved fast through the medium. Additionally, the viscosity was measured as it is described in 7.5.2.4 for the system with the concentration of 1 wt%. A value of 1.5 mPas was obtained. The viscosity is slightly higher than the one from pure water.²⁵⁹ The aggregation structures of the catanionic surfactant molecules increase the viscosity of the solution since they disperse in the aqueous phase.

Although the CLSM picture shows a variety of structures, a clear DLS curve was detected for the catanionic system Tex-ACA, 5-5. This enables the comparison of the DLS curve from the reference system to the ones with changed parameters. Thus, in the following, the received experimental data will be compared to the data of the present section.

7.3.2.2 External influences on the Tex-ACA system

One of the main ideas behind the investigation of the catanionic combination with regard to the emulsion stability was the possibility to control the stability of the emulsion by changing external parameters. A change of the pH value, the addition of salt or alcohol or the change in temperature may change the catanionic system, which has the consequence of a change in the emulsion system. For this purpose, the influence of the external parameters on the catanionic mixture was studied by comparing macroscopic appearance, DLS and viscosity data according to 7.5.2.6 and 7.5.2.4. For all samples, the parameters were changed in the original system (Tex-ACA, mass ratio 5-5, 1 wt%), and the effect was investigated the next day.

7.3.2.2.1 Addition of salt

Four different salts were added to the catanionic system to investigate the influence on the catanionic system: CaCl_2 , NaCl , Na_2SO_4 , and NaSCN . CaCl_2 was used as an example for a divalent salt. The other three salts are monovalent, and each salt represents a group of salts according to Hofmeister.¹⁰⁵ NaCl is a neutral salt whose ions were already present in the system due to the counterions of the

surfactants. Na_2SO_4 is an example for a salting-out salt. NaSCN is an example for a salting-in salt. For the tests, different amounts of salt (5–100 mmol/L) were added to the catanionic system Tex-ACA 5-5 (1 wt%). The samples were mixed and let equilibrated overnight. The samples were investigated by macroscopic observation. Furthermore, DLS and viscosity measurements were carried out the next day.

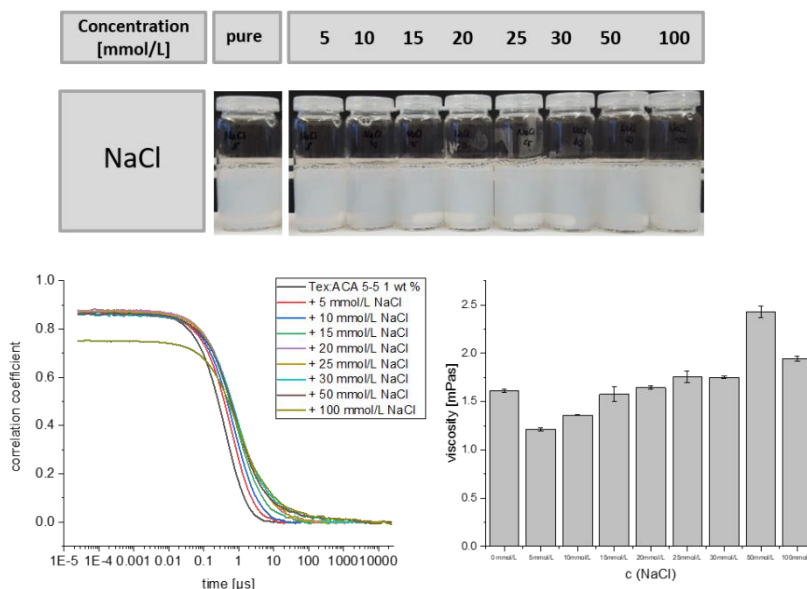


Figure 96: Influence of the addition of the salt NaCl in different concentrations on the catanionic system Tex-ACA, 5-5, 1 wt% evaluated by optical appearance (above), DLS measurement (left below) and viscosity (right below) as described in 7.5.2.

As it can be seen in Figure 96, the addition of NaCl to the catanionic system led to no significant changes in all three properties. No change in the optical appearance was observed, except for slightly higher turbidity at the highest concentration (100 mmol/L). The samples showed the same correlation function measured via DLS. That means no change in the average size of the aggregate structure of the catanionic system. An exception was the highest concentration of 100 mmol/L where the correlation function slightly decreased but did not change in the fitted size. That means that the intensity of aggregates was smaller than in the other samples. Viscosity measurements, which can give hints towards the aggregation shape, gave only small changes to the reference system with a value of 1.5 mPas. At a low salt concentration, the viscosity decreased by ~25 % compared to the reference sample. With increasing NaCl concentration, the viscosity increased to the value of the pure system. For the concentration of 50 mmol/L, an increase of viscosity of ~ 50 % could be observed. But,

all observations were only in small extent compared to known viscosity increases due to the addition in salts with higher surfactant content where the formation of wormlike and branched micelles increases the viscosity by several factors.¹³⁷ So here, a constant system could be assumed without any change in stability with increasing salt addition. However, from the theoretical point of view, the addition of NaCl changes the situation in the system in the way that a lot of water molecules will be needed to hydrate the added ions. This would lead to a decrease of hydration of the solute, here the catanionic surfactants. Since Na^+ and Cl^- can be found in the middle of the Hofmeister series, the effects will not be that strong and will therefore not be observed at low concentrations. The investigated concentrations seemed to be in that range. So, no external influence of the addition of the 'neutral' salt was observed.

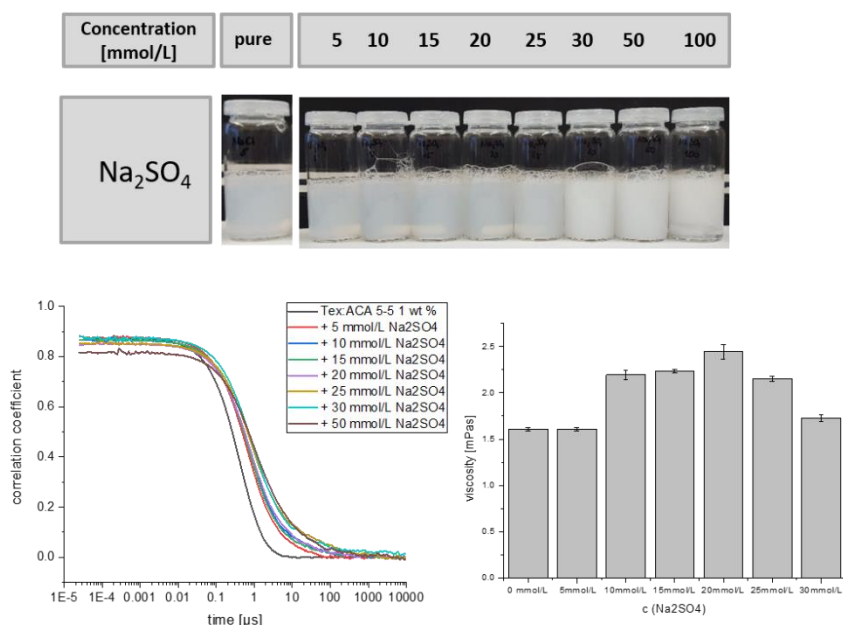


Figure 97: Influence of the addition of the salt Na_2SO_4 different salts in different concentrations on the catanionic system Tex-ACA, 5-5, 1 wt% evaluated by optical appearance (above), DLS measurement (left below) and viscosity (right below) as described in 7.5.2.

The sulfate anion is known to be very salting-out.¹⁰⁵ For this purpose, Na_2SO_4 was used as a typical example of a salting-out salt. The addition of Na_2SO_4 changed the optical appearance of the catanionic system as it can be seen in Figure 97. With a higher salt concentration (50 mmol/L), phase separation occurred. The homogenous samples below 50 mmol/L were measured via DLS. With increasing the salt concentration, the correlations function increased slightly pointing to marginally larger

aggregates in the solution. The viscosity increased by $\sim 50\%$ to 2.5 mPas up to a salt concentration of 20 mmol/L until it decreased to the original value of 1.6 mPas compared to the reference sample without salt addition. The same optical observations were done with the addition of CaCl_2 as it can be seen in Figure 98. Here, clear phase separation was observed for the highest concentration of 100 mmol/L as well. The other samples with lower salt concentration were stable despite the addition of CaCl_2 . With DLS, a slight increase of the correlation function to larger aggregates was measured, which indicated no significant changes in the average aggregation size. The viscosity was in the same range for all concentration ranges, which showed no changes in the catanionic system. This fitted to the observations from the DLS measurements.

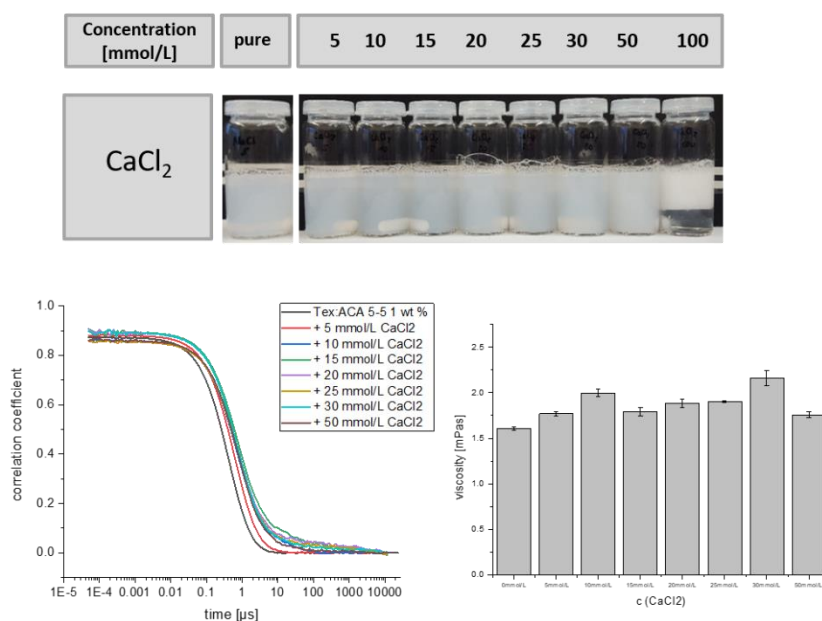


Figure 98: Influence of the addition of the salt CaCl_2 different salts in different concentrations on the catanionic system Tex-ACA, 5-5, 1 wt% evaluated by optical appearance (above), DLS measurement (left below) and viscosity (right below) as described in 7.5.2.

Comparing the two salts to the neutral NaCl , the anion was changed to sulfate for Na_2SO_4 , and the cation was changed to calcium for CaCl_2 . Both ions, SO_4^{2-} and Ca^{2+} , were ions with salting-out properties.¹⁰⁵ They bind a close hydration shell around them. This can lead to less intense hydration of the catanionic surfactants. If the surfactant molecules are less hydrated, they are less soluble. If surfactant molecules come together, the interaction is increased. Consequently, larger aggregates are built. Unless enough water molecules are present to hydrate the surfactants in a sufficient way, the

catanionic surfactants precipitate, and phase separation occurs – one aqueous phase with high salt content and another phase with high surfactant concentration (upper white phase). This phase separation is observed for both salts Na_2SO_4 and CaCl_2 (see Figure 97 and Figure 98) and confirms the salting-out character of both salts in the case of the present catanionic system Tex-ACA, 5-5, 1 wt%.

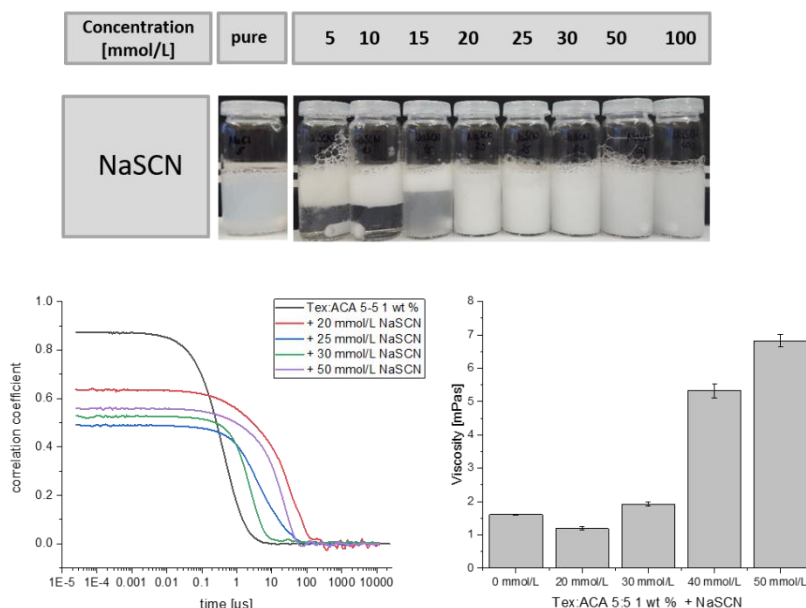


Figure 99: Influence of the addition of the salt NaSCN different salts in different concentrations on the catanionic system Tex-ACA, 5-5, 1 wt% evaluated by optical appearance (above), DLS measurement (left below) and viscosity (right below) as described in 7.5.2.

According to Hofmeister, the salt NaSCN can be categorized as a salting-in salt.¹⁰⁵ The SCN^- anion has only a low charge density regarding the large size of the molecule. Due to this, the ion can easily be polarized. When only small amounts of the salt are added, the ions get hydrated by the water molecules. This effect could also be observed by adding SCN to the catanionic system Tex-ACA, 5-5. The hydration of the ions led to a phase separation as it can be seen in Figure 99. A salting-out character was observed. With still higher amounts of added NaSCN, the solution became one-phasic again at a NaSCN concentration of 20 mmol/L with increasing turbidity. The DLS measurement showed a change in the correlation function towards larger aggregates. With this, also the viscosity increased by a factor of four at a concentration of 50 mmol/L. These observations gave a hint towards a potential switchability factor of the catanionic surfactant system by the addition of NaSCN and changing the respective concentration change in NaSCN concentration. At low concentrations, the

solution was phase-separated. At higher salt concentrations, one-phasic samples with higher viscosity were present. This can improve the emulsion stability. The influence of the NaSCN concentration was only observed in the pure aqueous catanionic system. To check the relevance of this external parameter, the observations must be tested within an emulsion system. For this purpose, switchability tests were performed, which are described later in 7.3.3.

7.3.2.2.2 Addition of alcohol

To investigate the potential to switch a catanionic-based emulsion due to external parameters, the pure catanionic system Tex-ACA, mass ratio 5-5, 1 wt%, was examined first on its reaction against them. Also, the addition of alcohol as external influences was measured. Depending on their hydrophilicity alcohols are known to act differently in micellar solution. Alcohols with higher hydrophilicity like methanol, ethanol, and propanol, are known to act as “co-solvent”. They can dissolve in the solvent, most times water, and change the character of the aqueous phase. More hydrophobic alcohols, like pentanol and higher homologs, interact with the micelles. In more detail, they become part of the micelles and are known as “co-surfactants”. Depending on the amphiphilic character, they can orientate towards the hydrophilic part of the micelle or the palisade layer.²⁶⁰

The addition of ethanol and butanol was tested to check its influences on the catanionic system. For this purpose, different concentrations from 0.1 to 5 wt% of alcohol were added to a 1 wt% solution of Tex-ACA, 5-5. The results can be seen in Figure 100. For the addition of ethanol, no differences in the optical appearance of the samples could be observed. Also, the DLS measurements gave no change in the measured average size of the structure in the solution. For the viscosity, the addition of ethanol led to no change as well. In fact, this would be assumed since the ethanol molecules dissolve in the water due to their high hydrophilicity. In the investigated concentration range, the ethanol molecules are not interacting with the surfactants, they only interact as co-solvent. Thus, no influence on the catanionic system was observed macroscopically as well as on microscopic level by the addition of ethanol.

The addition of butanol promoted the transparency of the catanionic mixture of Tex-ACA, 5-5, 1 wt%. By the addition of 5 wt% BuOH, the sample was less turbid than at lower concentrations. This hints towards smaller aggregates in solution. But, with DLS measurements, no change in the average aggregate size could be seen for lower concentrations. At 5 wt%, the correlation function increased

slightly. The viscosity decreased with the increase of butanol concentration until it started to increase at a concentration of 0.5 wt%. Adding butanol in small amounts dilutes the solution since the butanol molecules act as co-solvent. A dilution of the solution results in a decrease in the viscosity.

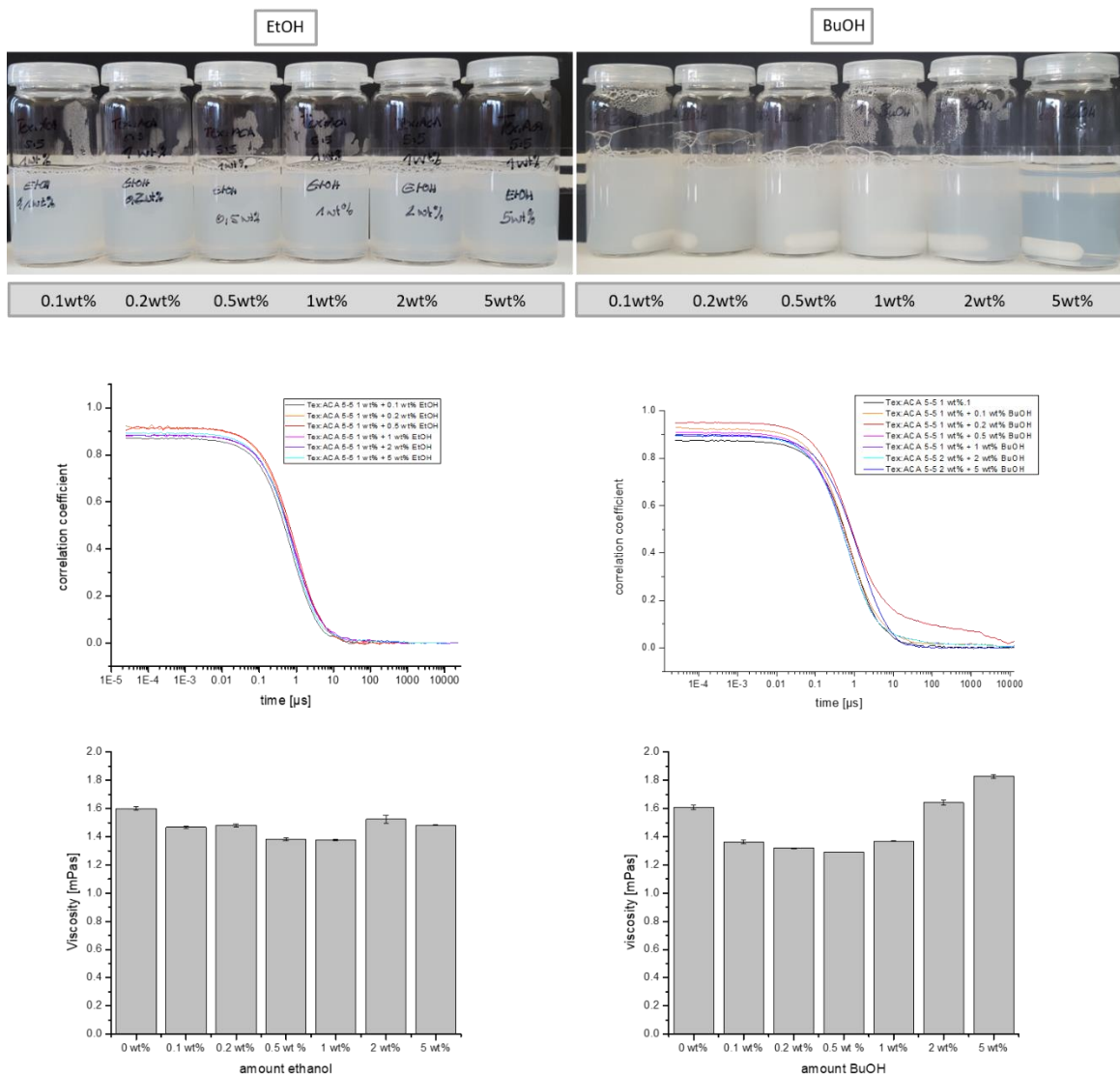


Figure 100: Influence of the addition of ethanol (left) and butanol (right) on the catanionic system Tex-ACA, 5-5, 1 wt% evaluated by optical appearance (above), DLS measurement (middle) and viscosity measurements (below) measured after one day after preparation as described in 7.5.2.6 and 7.5.2.4.

Butanol has a solubility in water of 79 g/L at room temperature.²⁶¹ That means that all samples were still in the range of complete solubility. Butanol molecules are more hydrophobic compared to ethanol molecules. For this purpose, their tendency to interact with hydrophobic parts in the aggregations of

the catanionic surfactants is higher. Their tendency to act as the solvent is less. As they interact with the aggregates in solution, the aggregate shape and size can influence the viscosity. All in all, the changes in the catanionic system were small by the addition of an alcohol. No significant influences were observed. Thus, the addition of alcohol has no decisive effects as a potential control parameter.

7.3.2.2.3 Changing the pH value

The value of pH is another external parameter, which might be useful to change the catanionic system. For this purpose, the pH of the catanionic solution of Tex-ACA, mass ratio 5-5, 1 wt%, was adapted to five different values: 3, 5, 7, 9 and 12. This was done by the addition of aqueous HCl or NaOH solutions meaning that the same ions were added as already present due to the counter ions of the surfactants. According to the concept of Hofmeister, the sodium cation, as well as the chloride anion, has only a negligible effect when added.¹⁰⁵ The choline headgroup in the cationic surfactant is weakly hydrated by water molecules. In contrast, the sulfate group in the headgroup of the anionic surfactant is strongly hydrated by water. Increasing the pH value means adding hydroxide ions to the solution. Hydroxide ions are defined as kosmotropes. No strong interaction between the hydroxide ion with the ammonium cation can be assumed. The electrostatic interactions between the sulfate group and the ammonium group will dominate.

To test this consideration, the samples of various pH values were prepared and equilibrated for 24 h. The next day, the samples were investigated via optical evaluation, DLS and viscosity measurements as described in 7.5.2.6 and 7.5.2.4. The results are shown in Figure 101. From the macroscopic point of view, no significant differences could be observed. No phase separation occurred. All samples looked slightly turbid (see Figure 101-A). However, the DLS curves showed differences. With increasing pH, the correlation function got wider and its intensity decreased. This gave a hint towards larger aggregates in solution. Regarding the viscosity measurements, no significant differences could be found. The viscosity of the pure system of Tex-ACA, 5-5, at 1 wt% did not change with changing the pH value. It was in the range of 1.5 mPas for all samples. For the pH value of 9, the sample was investigated via CLSM as it is described in 7.5.2.5. As it can be seen in Figure 101-D, the size of the aggregates decreased in comparison to the species at lower pH (see Figure 95-right). This is contradictory to the results observed with the DLS. But, it must be considered that larger lamellar aggregates, which might be taken into account in the DLS, were not visible in the CLSM. The change

in pH showed small changes in the structuring via DLS, but from the optical view as well as from the viscosity measurements no significant differences, which could give a hint towards a control parameter, could be found. Thus, changing the pH value was stated as not relevant for a possibility to influence the system Tex-ACA to change its emulsifying behavior.

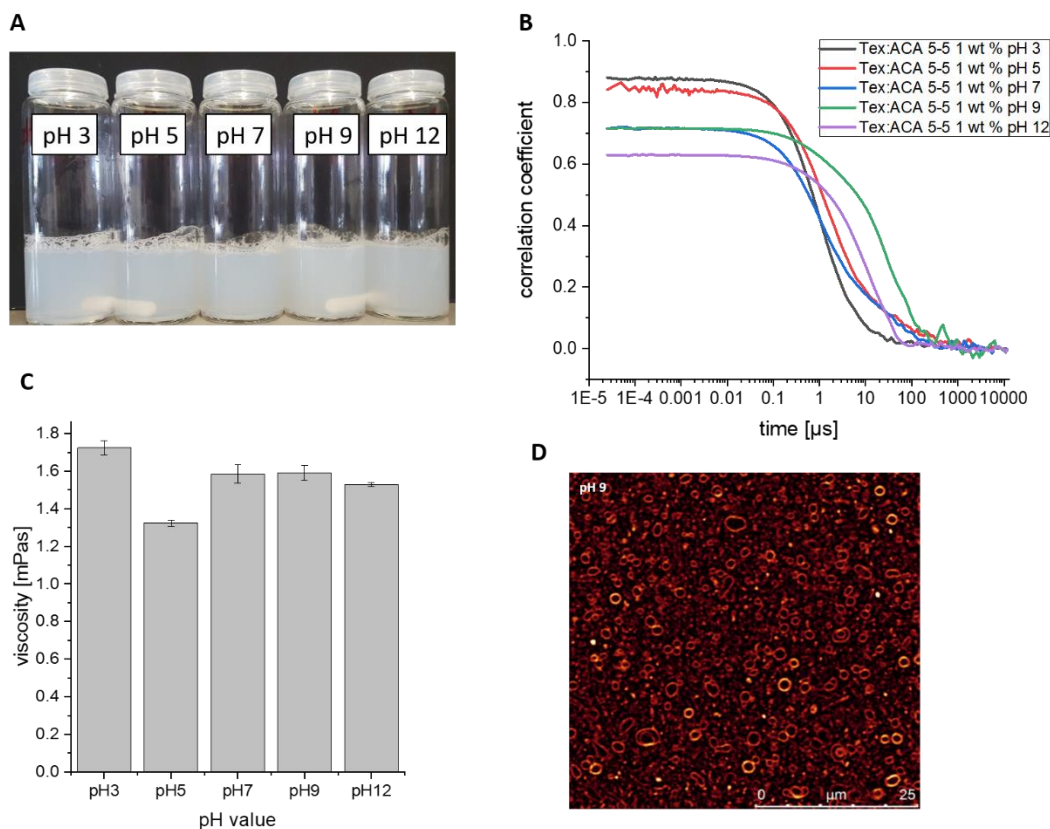


Figure 101: Influence of the pH value on the catanionic system Tex-ACA, 5-5, 1 wt% evaluated by optical appearance (A), DLS measurement (B), viscosity (C) and CLSM for the sample of pH 9 (D) as described in 7.5.2.

7.3.2.2.4 Changing the temperature

The idea that the change in temperature can have a significant effect on the stability of the system Tex-ACA, mass ratio 5-5, 1 wt%, was based on the following idea: When the cation and the anion are combined, the ions will interact, and an ion pair will form. If the interactions between the ion pair are strong, the ion pair will precipitate. Due to the present EO groups in the system, the interactions are weakened, and the ion pair will not precipitate but stay in solution (see 3.3.1). If a surfactant is dissolved by the formation of micelles at a certain temperature, the surfactant is above its Krafft point.

Normally, the Krafft temperature corresponds to the temperature at which the surfactant is in a molten state. In the case of catanionic surfactant, the situation in double layer aggregates can be different. Here, a crystalline-like state can be present within the double layer of aggregated catanionics, whereas the aggregates are dissolved at the same time. Consequently, the Krafft temperature is not the same temperature value as the melting point of the surfactants in the double layer. Vautrin *et al.* reported a decoupling of the temperature of solubilization from the crystallization temperature, above which the surfactant layers melt.²²² The catanionics can be crystallized on the surface of oil droplets to stabilize the oil-in-water emulsion by Pickering between these two temperatures. With increasing the temperature, this crystalline-like state can vanish. The chains melt. For this purpose, the stabilization ability should decrease. A faster separation of the immiscible phases should be observed due to the change in the structure and the aggregation state of the catanionics. Thus, heating or cooling can then be used to destabilize the emulsion at will.²²⁴

For this purpose, the catanionic system was investigated regarding the influence of the temperature via turbidity measurement, SAXS measurement and confocal light scanning microscope (CLSM). The macroscopical change of the system by changing the temperature was measured with the in-house built turbidity apparatus as described in 7.5.2.3. The obtained curve is depicted in Figure 102.

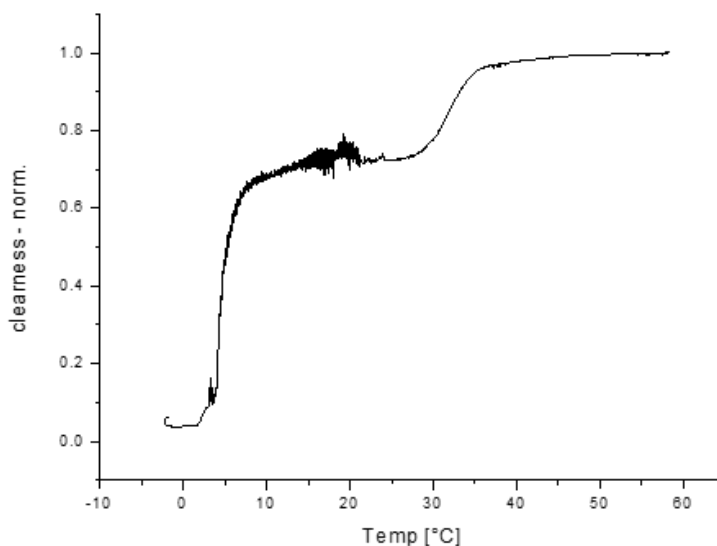


Figure 102: Measurement of turbidity with the in-house built apparatus of the catanionic system Tex-ACA, 5-5, 1 wt%, with a heating rate of 2 K/h depending on the temperature as described in 7.5.2.3.

Starting from below 0 °C, where the sample was completely turbid due to the crystallization of water, the system got clearer until reaching a plateau at 5 °C. At a temperature of 35 °C, the sample cleared up to complete transparency. A change in the structure of the catanionic system is a probable reason for that. The observation supports the introduced idea that with increasing temperature the catanionic system can be changed and the solubility is increased. Based on the hypothesis of Vautrin *et al.*, the temperature of 35 °C can be regarded as the melting point of the catanionic surfactants in the double layer of the aggregates. At room temperature, a crystalline-like state is present, but the surfactants are soluble as no precipitation was observed. With increasing temperature, the crystalline-like state vanished. At the same time, the solubility increased indicated by higher transparency of the solution. But, proof of crystallinity in the system below 35 °C could not be made with this method.

A possible crystalline character in the catanionic system Tex-ACA, 5-5, 1 wt%, at lower temperatures, was investigated with SAXS as described in 7.5.2.7. The catanionic combinations were measured at a temperature of 20 °C and 40 °C. The two curves are shown in Figure 103.

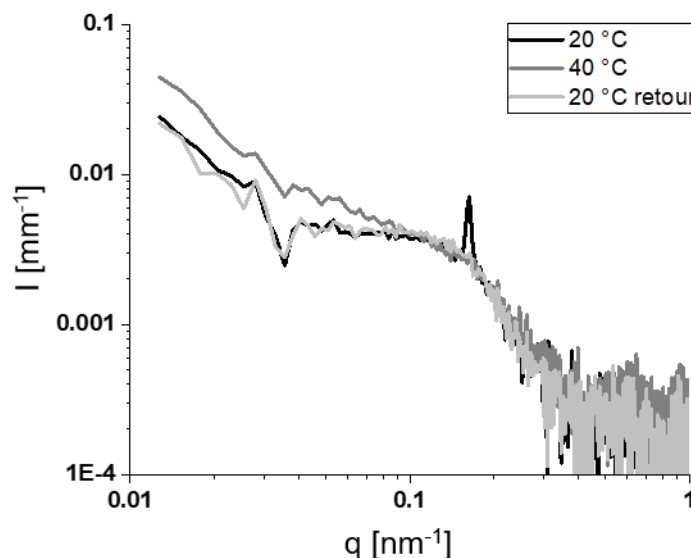


Figure 103: SAXS measurement of the catanionic sample Tex-ACA at the anion-cation mass ratio 5-5 and a concentration of 1 wt% at 20 °C (black), after heating up to 40 °C (dark grey) and after re-cooling to 20 °C (light grey) measured as described in 7.5.2.7.

The two SAXS curves for the two temperatures 20 °C and 40 °C showed similar shape. At lower q -range, a q^{-2} -dependence was observed for both temperatures, which can give a hint towards larger disks. This is probable for catanionic mixtures.⁸¹ For the sample measured at 20 °C, a sharp peak was detected at 0.163 \AA^{-1} . The peak corresponded to a distance of 3.85 nm, which might arise from bilayer structures potentially consisting of lamellar crystals. At a higher temperature of 40 °C, this peak was not found. This would confirm the presented theory of the change in the aggregation state. However, after re-cooling the sample to 20 °C, the peak was not detected. Thus, quick reversibility could not be assumed. But, the measurement was performed right after re-cooling. When assuming a longer time necessary for the “re-crystallization”, the peak should be visible after a longer time of equilibration.

The influence of the temperature change was also investigated microscopically. With the CLSM, the sample of Tex-ACA, mass ratio 5-5, at 1 wt% was observed while heating up to 37 °C and cooled down to room temperature (25 °C) again as described in 7.5.2.3. As shown in Figure 104, a significant change in the aggregation shape and size could be observed with increasing temperature. The shape of the vesicles changed. With a higher temperature, they became more elongated by several factors. Less multiple vesicles were found. Also, the motion of vesicles was faster than before. With decreasing the temperature, the original structure was rebuilding. The vesicle became more spherical and smaller in size. Evidence for the crystalline character could not be detected with this method, but the CLSM measurements confirmed the change of the catanionic system on a microscopic level.

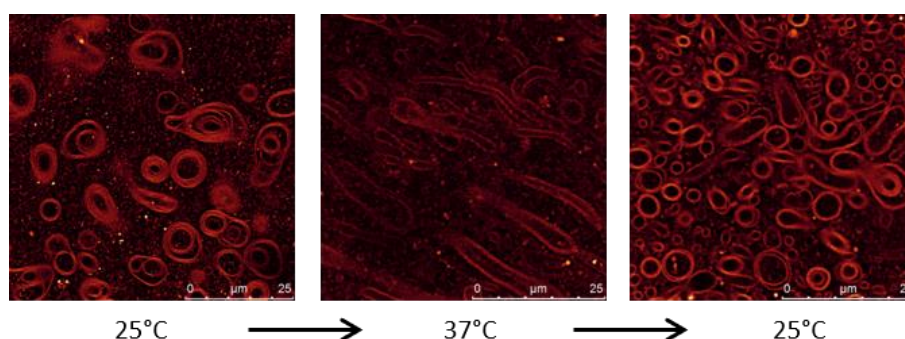


Figure 104: Influence of temperature increase from 25 °C to 37 °C on the structure of the catanionic system Tex-ACA, 5-5, 1wt%, observed with CLSM as described in 7.5.2.5.

The performed experiments showed a change in the catanionic system with a change in temperature. From the optical appearance, the samples looked more transparent above a temperature of 35 °C, which could also be detected quantitatively with the turbidity apparatus. Also, with SAXS, a change in

the system could be detected. A peak, which can be assumed to a potential crystalline state in the sample was found for lower temperatures. CLSM confirmed the system change by depicting elongated micelles at higher temperature instead of multi spherical micelles at lower temperatures.

With the performed experiments, a statement about the crystalline state of the structures could not be made. But, some changes are probably, as it is suggested in the literature.²²⁴ The influence of the parameter temperature could clearly be shown. Thus, the temperature seems to be suitable as another control parameter besides the NaSCN concentration, which is interesting to be tested in an emulsion system. This will be done in the following chapter 7.3.3.

7.3.3 Tests on the switchability of emulsions

In the previous chapter 7.3.2.2, tests were performed to check the realistic possibility in using the external parameters addition of salt, addition of alcohol, pH value, and change in temperature to change the state of the catanionic system of Tex-ACA, 5-5, 1 wt%. Based on these experiments, two promising parameters could be found to check their influence in emulsion systems. One was the addition of salt in varying concentration, which was found to influence the stability of the catanionic solution. Especially the addition of NaSCN could change the state of the emulsion (see chapter 7.3.2.2.1). One reason for this was the change in the viscosity with increasing salt concentration. Second, for small salt concentrations, phase separation was observed whereas for higher concentration it was not. This might also be a parameter to switch the state of an emulsion.

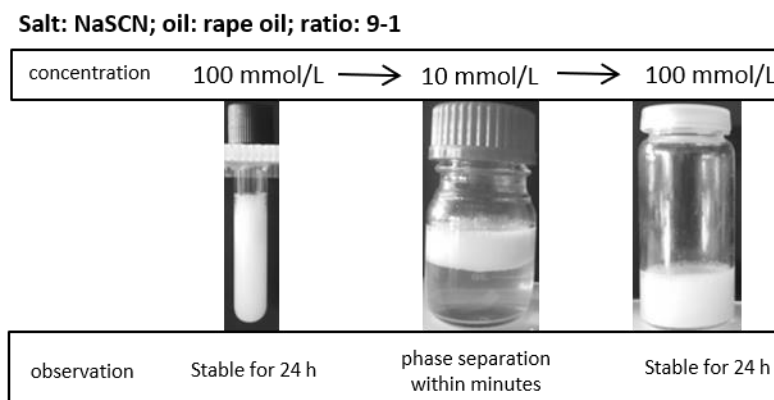


Figure 105: Switchability test due to changing the concentration of NaSCN of the emulsion combination Tec-ACA, 5-5, 1 wt% with rape oil.

For this purpose, an emulsion system was tested on the effect of different concentrations of NaSCN. The following test concerning the emulsion stability was performed: an emulsion of Tex-ACA, 5-5, 1 wt%, with a NaSCN content of 100 mmol/L was prepared with rape oil in the mass ratio 9:1 by vortexing for 1 min. The stability of the emulsion was tested for 24 h. At this time, the emulsion system was completely homogenous and did not change within time. The emulsion was then diluted by a factor of 10 with the aqueous catanionic solution to receive a concentration of 10 mmol/L. Phase separation was observed within a short time. The sample was then again homogenized with the vortexer, and a part of the solution was taken. To this new sample, NaSCN was added to reach again a salt content of 100 mmol/L. Then, the solution was homogenized again, and the stability of the emulsion was evaluated. Stability of more than 24 h was observed. The different states of the experiment are shown in Figure 105. The performed test confirmed the suggestion that the stability of an emulsion with the catanionic system Tex-ACA as emulsifier can be changed by changing the salt content within the emulsion. With lowering the NaSCN concentration from 100 to 10 mmol/L, the emulsion could be broken. The reversibility was confirmed by increasing the NaSCN concentration again up to 100 mmol/L.

The second parameter, which was found to be a potential switching-factor for the emulsion stability, was the temperature (see chapter 7.3.2.2.4). A change in the structure of the catanionic system Tex-ACA indicated by a change in turbidity as well as in the microscopic view with the CLSM could be seen with the increase of temperature. The idea was to switch from an emulsion state stabilized by a pseudo-Pickering principle to a state where the catanionic combination has less crystalline character and may, therefore, destabilize the emulsion. To check the temperature influence on the emulsion system, three different samples were prepared consisting of the catanionic system and hexadecane in the mass ratio 9-1. The samples were observed regarding their emulsion stability over a time of 24 h.

One sample was prepared and stored at room temperature (25 °C) (sample 1). It was the reference catanionic system when no temperature effect was present, and the crystalline character of the surfactant double layers should have been present. A second sample was prepared at room temperature and stored at a higher temperature of 50 °C in an oil bath for the time of the experiment (sample 2). It represented the catanionic system when a temperature effect was present, and the crystalline character of the surfactant double layers should have vanished. And, for a third sample, the pure catanionic solution was heated up to 50 °C for 15 mins and cooled down to 25 °C again. After

that, the oil was added, the emulsion was prepared, and stored at room temperature (sample 3). It indicates the catanionic system when the temperature effect had affected the system but was not present anymore. The increasing temperature should have led to a melting of the surfactant double layers. But as the temperature has been cooled down again, the crystalline character should have rebuilt. Depending on the time needed for that process, the emulsion should be more stable than the heated sample, but less stable than the not heated one. With these three different cases, the situation and the influence of the temperature within the catanionic combination could be investigated in more details.

Tex-ACA, ratio 5-5, 1wt%

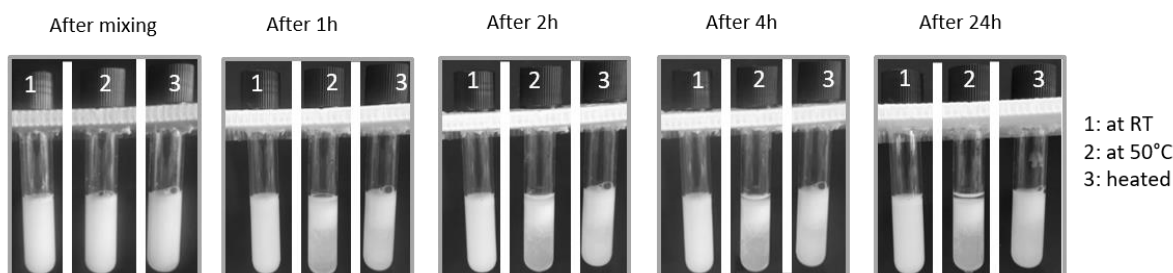


Figure 106: Switchability tests due to the change of temperature of the emulsion combination Tec-ACA, 5-5, 1 wt% with hexadecane as oil over time. Number 1 indicates the sample where the emulsion was prepared and stored at room temperature. Number 2 indicates the sample where the emulsion was prepared at room temperature and stored at 50°C. Number 3 indicates the sample where the surfactant solution has been heated up to 50°C for 15 mins before preparation and storage at room temperature.

The observations for the catanionic system Tex-ACA, 5-5, 1 wt%, with hexadecane in the water-oil mass ratio 9-1 are shown in Figure 106 above. Phase separation was observed for samples 2 and 3 whereas sample 1 looked still homogenous after 24 h. For sample 2, the phase separation was already more pronounced compared to sample 3. Sample 2 was stored at a temperature of 50 °C. At this temperature, the catanionic surfactants should have no crystalline character and thus no stabilizing effect. This was confirmed by fast phase separation of sample 2 after 1 h. Sample 3 was the system, which has been heated before the preparation of the emulsion. Here, the lastingness of the temperature increase on the catanionic system got obvious. If the system had shown the same behavior as sample 1, the time to equilibrate into the system originally found for room temperature

would be within several minutes. This was not the case. Thus, the system needed a longer time to get back into the original state, which could stabilize the emulsion. This stabilizing effect appeared only delayed since the emulsion stability was between the two extrema, sample 1 and sample 2. Consequently, reversibility of the catanionic system was not possible within a short time. For the investigated system, a destabilization of the emulsion system with increasing temperature was observed, but the reversibility of the process seemed not to be possible since the equilibration process of the catanionic system seemed to take at least several hours. An investigation of the sample after 1 or more days could give information about the time necessary to reach again equilibrium.

A second catanionic system was checked under the same conditions as described above: the system C18EO4SO4-C12EO4Ch, mass ratio 5-5, 1 wt%. The observations are shown in Figure 107. The combination was chosen because an increased viscosity was observed for the aqueous catanionic system. With increasing temperature, the viscosity decreased, and a lamellar-like solution with the slightly bluish character was observed. From the theoretical point of view, a higher viscosity can be a stabilizing factor for an emulsion since the velocity of the droplets is lowered.²⁶² So, the time for the droplets to meet will be longer and destabilization processes are hindered. The observations for the catanionic system are shown in Figure 107.

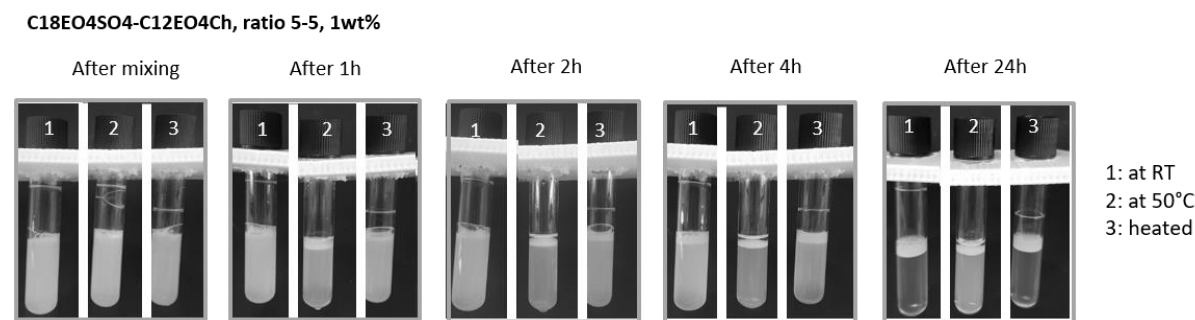


Figure 107: Switchability tests due to the change of temperature of the emulsion combination C18EO4SO4-C12EO4Ch, 5-5, 1 wt% with hexadecane as oil over time. Number 1 indicates the sample where the emulsion was prepared and stored at room temperature. Number 2 indicates the sample where the emulsion was prepared at room temperature and stored at 50°C. Number 3 indicates the sample where the surfactant solution has been heated up to 50°C for 15 mins before preparation and storage at room temperature.

The general observation was the same as for the first catanionic system Tex-ACA. But, the emulsion was less stable compared to the one formed with Tex-ACA, which fits the results from 7.3.1. After 24 h, complete phase separation was observed for all three samples. However, the influence of the

temperature was also decisive in this system. Fast phase separation occurred for sample 2, which was stored at a higher temperature of 50 °C. Sample 3 behaved similarly to samples 1, but showed an earlier phase separation. After 4h, the difference was maximal. Only a small creaming phase was observed for sample 1 at this time. This supports the theory of emulsion destabilization with increasing temperature. As it was for the first system Tex-ACA, the change in temperature affected the emulsion system, but the fast reversibility of the catanionic system was also not present.

The experiments showed that changing certain external parameters changed the catanionic system. In the case of Tex-ACA, mass ratio 5-5, 1 wt%, the change in the salt content of NaSCN and the temperature led to a change of the emulsion stability. The basic idea to change the stability of an emulsion due to changing the catanionic system could be confirmed. For the salt content, it was possible to stabilize the emulsion again by returning to the original condition. For the temperature, the tests showed difficulties with the reversibility of the emulsion system. The catanionic system needed a too long time to set back the original behavior. The performed tests confirmed the possibility to change the emulsion system by changing external parameters, but the potential catanionic combinations have to be chosen with care. A general procedure for all catanionic combinations could not be introduced. A hint towards the desired possibility to switch the stability of a catanionic system could be shown here, but further experiments towards a deeper understanding of the interactions and structural changes are still necessary. Nevertheless, one could imagine an application for the corresponding system under the described conditions. If only the destabilization of the emulsion is desired, this can be done by the described procedure. This could be the case, for example, when it comes to the controlled release of substances from an emulsion.

7.4 Conclusion

The newly synthesized catanionic combinations based on EO groups were investigated towards their ability to emulsify different oils. To this purpose, a macroscopic screening over ten different oils of different structure and origin was performed with all catanionic combinations at four different ratios. The screening was supported by spinning drop measurements and CLSM investigations exemplarily for some systems. In general, the emulsification ability was lower as expected for the investigated emulsion systems. The anion-cation mass ratio of 5-5 was the one with the highest emulsification potential. Triolein was the oil which could be emulsified the best. It could be shown that low interfacial tension was a supporting factor for a stable emulsion. Moreover, higher viscosity extends the stability of the emulsion, which is in accordance with the literature.

Concerning the potential use of the catanionics as an emulsifier with the property of switching the stability of the emulsion by changing external parameters, the influence of the different parameters (addition of salt, addition of alcohol, salt content and temperature) was tested on the pure aqueous catanionic combination of Tex-ACA, 5-5, 1 wt%. The samples were examined via optical observation, DLS and viscosity measurements. The pH of the system was varied from 3 to 12 but showed no effect on the system. Two alcohols, ethanol and butanol, were added to the system in varying concentrations. The addition of the short chain alcohol ethanol did not influence the system in any way. For the addition of butanol, increasing transparency and a slight increase in the structure was observed at higher butanol concentration. The addition of four different salts (NaCl, Na₂SO₄, CaCl₂, and NaSCN) showed different influences. Whereas for NaCl, no influence was observed, the two salting-out salts Na₂SO₄ and CaCl₂ led to phase separation at higher salt contents. A slight increase in the size of aggregates was observed until phase separation occurred. Moreover, the addition of NaSCN resulted in a phase separation at low salt contents. For a higher NaSCN content, a homogenous solution was observed with increasing viscosity. Only the observations with NaSCN showed potential in sufficiently changing an emulsion from stable to unstable by changing the salt content in the system. The influence of temperature was also investigated. The turbidity measurement showed a rise in transparency at 35 °C. With SAXS measurements, a peak indicating a potential crystalline character in the catanionic solution was found at 20 °C, which disappeared at 40 °C. CLSM measurements showed a change in structure from spherical vesicles with partly onion structure to elongated vesicles without onion structure. The observations gave a hint towards a potential change in the structure of the catanionics due to a change in temperature.

The two potential control parameters, temperature, and NaSCN content were tested in an emulsion system towards their switchability of the corresponding stability. The change in the salt content from 100 to 10 mmol/L showed a fast way to destroy the stability of the emulsion. With increasing the salt content, the emulsion could be stabilized again. Stability of more than 24 h could be reached. The destabilized emulsion system could be re-stabilized by setting the original experimental conditions of higher salt content. Reversibility and thus a switchability of the emulsion stability was obtained. The influence of temperature was examined for three different cases for the two catanionic systems Tex-ACA, 5-5, 1 wt%, and C18EO4SO4-C12EO4Ch, 5-5, 1 wt%: 1: the emulsion was prepared and stored at 25 °C; 2: the emulsion was prepared at 25 °C and stored at 50 °C and 3: the emulsion stored at 25 °C but the aqueous catanionic solution was heated to 50 °C for 15min before preparation at 25 °C. Influence of the temperature on the emulsion stability was observed. Higher temperature led to an earlier phase separation compared to 25 °C. From sample 3, the lasting effect of the temperature effect on the nature of the catanionic system became obvious. The emulsion stability was between the other two samples. No quick reversibility of the system was observed. This limits the application when a switchability is desired.

For the emulsifying potential, a detailed structural correlation could not be given until now, but the optical observations showed clear results. In general, a change of the stability of an emulsion emulsified with the catanionic surfactant system by changing certain external parameters was possible, which led to a change in the structure of the catanionics. Within this work, the basic idea could be confirmed. But, several different aspects are interesting to be investigated in the future: can the sensitivity of a catanionic system be tuned to certain parameters? For this purpose, more combinations of anion and cations have to be tested, especially regarding a higher variety of cations with different chain lengths. Was a certain observed turbidity a hint towards a higher crystalline character in the catanionic system and therefore a precondition for that application? A deeper analysis of the structure of the different combinations with the help of scattering experiments at different temperature would be interesting. If the concept can be enforced with the help of further research, applications in various fields are conceivable. It would be useful in medicine where controlled drug delivery is an important aspect. Likewise in the field of extractions, a controlled destabilization of the emulsion can be used to dissolve substances on the transport medium.

7.5 Experimentals

7.5.1 Chemicals

Octane (purity 98 %), dodecane (purity > 99 %), triolein (purity 65 %), Nile Red (purity 100 %), sodium chloride (purity > 99 %), sodium thiocyanate (purity > 99.9 %), calcium chloride (purity 99 %), sodium sulfate (purity > 99 %), ethanol (purity < 99 %) and butanol (purity < 99.9 %) were purchased from Sigma-Aldrich (Taufkirchen, Germany). SDS ultrapure (purity > 99.9 %) was obtained from AppliChem (Darmstadt, Germany). Hexadecane (purity 98 %) was purchased from Fluka (Switzerland). Texapon N70 (purity 70 %) was obtained from BASF (Ludwigshafen, Germany). The synthesized surfactants were kindly provided by BASF from internal synthesis. Rape oil and sunflower oil were bought in a commercial supermarket. Miglyol 812 was provided by Sasol (Hamburg, Germany). Diisostearyl malate and pentaerythrityl tetraisostearate were kindly provided by L'Oreal (Paris, France). Biodiesel was purchased from Syntharo Fine Chemicals (Troisdorf, Germany).

Millipore water was used for all experiments, if not mentioned otherwise. All chemicals were used without further purification.

7.5.2 Methods

7.5.2.1 Emulsion stability

Preparation of the emulsion

Stock solutions of cationic and anionic surfactants with the concentration of 1 wt% were used to prepare the emulsion solution. Four different ratios of cationic and anionic surfactant were investigated: the molar ratio one to one and the weight ratios four to six, six to four and five to five. All samples were prepared by weighing-in the appropriate amount of anion and cation into a glass tube. The catanionic mixture was mixed with a vortexer for 1 min at room temperature. To each catanionic solution, the appropriate oil was added, and the sample was homogenized for 1 min with the vortexer at maximum. The ratio of aqueous surfactant solution and oil was always nine to one.

Evaluation of the emulsion

The emulsions were analyzed visually regarding their stability after a certain time. The emulsion was named as unstable when a start of phase separation could be observed when holding the glass tube in front of a black background. A classification of different time intervals was created, which is described in the following.

0:	immediately
1:	separation after 10 mins
2:	separation after 1 hour
3:	separation after 2 hours
4:	separation overnight
5:	separation after 24 hours
6:	stable after 24 hours

Pictures were taken after 1 hour for each system.

7.5.2.2 Spinning drop tensiometer

A spinning drop tensiometer SITE from KRÜSS with a thermostat was used for interfacial tension measurements. The aqueous surfactant solution was put into the measurement chamber. 1-3 µL of the oil, the lighter phase, was injected with a syringe into the chamber at a revolution of 200 rpm. The speed of revolution was increased until the drop was approximately three times longer than it was thick. An equilibration time of 15min was set before the oil droplet was focused and the droplet diameter was determined. The respective values were inserted in the following formula of equation 25 to determine the interfacial tension. Every measurement was carried out three times and the average values were taken for evaluation.

$$\sigma = e (vd)^3 n_r^2 \Delta\rho \quad (\text{equation 25})$$

with σ : surface tension,

e : unit factor with the value $3.427 \cdot 10^{-7} \frac{\text{mN cm}^3 \text{min}^2}{\text{m g mm}^3}$,

v : magnification, d : droplet diameter, n : number of rotations, $\Delta\rho$: density difference

7.5.2.3 Turbidity measurement

For turbidity measurements, an in-house built apparatus was used. The apparatus is described more precisely in reference ¹⁷⁵. It consists of a measuring chamber, which is connected to a thermostat that controls the temperature. In the measurement chamber, six sample tubes can be put into a metal block where each tube is set between a photodiode and a light source. The amount of light, which is detected, can be correlated to the turbidity of the solution.

Each time, 2.5 mL of the investigated samples were put into a tube with a magnetic stirrer inside. The samples were cooled down to -20 °C overnight. The next day, the measurement was started with a heating rate of 2 K/min from 0 to 65 °C. The measurements were repeated twice.

For evaluation, the measured voltage was plotted against the temperature. If present, the point of clearness was determined by the intersection of the two linear fits of the measured curve before and after the point of clearness.

7.5.2.4 Viscosity and density measurement

The automated micro falling ball viscometer (according to Höppler) AMVn from Anton-Paar was used for measuring the viscosity of the catanionic system Tex-ACA. The viscometer was connected to a thermostat and the measurements were performed at 25 °C. The tube within the apparatus, which was filled with the sample, was angled to a slope of 70 ° when the falling time was measured. The falling time started when the ball reached the starting point 1 and ended at the endpoint 2. The viscosity η can be calculated with the law of Stokes:

$$\eta = k (\rho(B) - \rho(S)) t \quad (\text{equation 26})$$

With $\rho(B)$: density of the ball, $\rho(S)$: density of the investigated solution, t : falling time, k : experimental apparatus constant.

The necessary density to determine the viscosity was measured with a density measurement device DMA 500M from Anton Paar.

7.5.2.5 Confocal light scanning microscope

A confocal light scanning microscope SP8 from Leica was used together with the software Leica Application Suite X (LAS X). Nile Red was used as a fluorescent dye. The investigated surfactant solution and emulsion samples were mixed with 100 ppm Nile Red and were stirred overnight for complete dissolution of the dye. Via DLS measurements, the samples were checked to ensure that no significant change in structure occurred due to the dye. The samples were put on a microscopic slide and put under the microscope for observations (fluorescence modus, magnification factor 50) to see the microscopic aggregation behavior.

To examine the influence of the temperature on the aggregation behavior of the catanionic system Tex-ACA, heating experiments were performed with a heating chair within the microscope. Here, the temperature was set to 37 °C, and it was heated up within less than a minute while the picture was recorded.

7.5.2.6 DLS measurement

2.5 mL of the investigated samples were filled into appropriate glass tubes, which were cleaned with acetone and nitrogen. The latter was then placed in a temperature-controlled bath of toluene of a CGS-3 goniometer system from ALV (Langen, Germany) equipped with an ALV-7004/FAST Multiple Tau digital correlator and a vertical-polarized 22-mW HeNe laser (wavelength $\lambda = 632.8$ nm). The homodyne correlation functions were recorded at 25 °C and an angle of 90 ° for 120 sec. The size of the particles was determined by fitting the experimental intensity autocorrelation function using a monomodal equation with the TableCurve 2D v5.01 software. The measurements were repeated three times and the average value was taken for evaluation.

7.5.2.7 SAXS measurement

Small-angle-X-ray scattering (SAXS) data were collected by Pierre Bauduin. The homemade setup was the following: X-ray patterns were collected with a Pilatus 300 K (Dectris, Baden, Switzerland), mounted on a microsource X-ray generator GeniX 3D (Xenocs, Sassenage, France) operating at 30 W. The monochromatic $\text{CuK}\alpha$ radiation was of $\lambda = 1.541$ Å. The diffraction patterns were therefore

recorded for reciprocal spacing $q = 4\pi \sin \theta / \lambda$ in a range of repetitive distances from 0.015 \AA^{-1} (418 \AA) and 0.77 \AA^{-1} (8 \AA).

8 General summary and outlook

The topic of this work was the investigation of new catanionic mixtures with the focus on the potential application in foaming, spreading, washing and as emulsifiers. A new group of catanionic mixtures was introduced. These anionic and cationic surfactants, newly synthesized by BASF, were combined and investigated regarding their physicochemical properties. The surfactants consist of a linear molecular structure with ethylene oxide (EO) group(s) between the alkyl chain of different lengths and the ionic headgroup, a sulfate group for the anions and a choline group for the cations. The intention of the insertion of the EO groups in the surfactant structure was the reduction of the known precipitation behavior for such mixtures.^{72, 263} With this, the fields of application can be increased and the positive effects for catanionic mixtures^{10, 89, 264} can be used in a maximal extent.

In the first part of the thesis, the concept of the insertion of the EO groups into a linear cationic surfactant structure was introduced. The focus was on the characterization of the catanionic mixtures at different anion-cation ratios from 9-1 to 1-9 regarding different physicochemical properties like the solubility behavior, the interfacial properties, the adsorption behavior, and the toxicity. An improved solubility, which could be led back to the present EO groups, could be confirmed. This precondition enabled the investigation of further properties. Synergistic effects for the interfacial activity were observed. For the cmc, as well as the surface tension reduction, small amounts of the oppositely charged surfactant were sufficient to reach the highest efficiency. Regarding the dynamics of the surfactants in the bulk solution, the efficiency to decrease the surface tension within 1 sec differed with the anion-cation ratio and the used surfactants. High dynamics was found in combination with the anionic surfactant SDS. For the adsorption on a hydrophobic and a hydrophilic surface, synergistic effects for the mixtures compared to the pure ionic surfactants became again obvious. As expected^{79, 81, 265}, a large variety of different aggregation structures was found for the catanionic mixtures with cryoTEM, which can be useful in different applications as transport systems. Regarding the cytotoxicity on HaCaT cells, the addition of the anionic to the cationic surfactant decreased the toxicity compared to the cationic surfactant alone. With the help of statistical analysis, several relations between the molecular and the observed physicochemical properties could be quantified. Especially for the solubility, the presence of EO groups is favorable. The chain length influences the interfacial properties.

Based on the results from the physicochemical characterization, the following chapters dealt with tests regarding the potential application of the catanionic mixtures in the four industrial fields of foaming, washing, spreading and emulsification.

A pre-screening of all catanionic mixtures regarding their foaming behavior was performed with a high-throughput robot. Based on these results, a selection of catanionic mixtures was chosen to make further investigations with a dynamic foam analyzer. Here, the total foam height, the liquid volume of the foam and the average bubble size were detected over time and compared regarding different structural aspects. The anion-cation ratio itself did not show a trend. But, for combinations with viscoelastic behavior, increasing foam stability was found. Moreover, the influence of the different anionic and cationic surfactants was examined. It was observed that a lower solubility of the surfactant solution was also favorable. A stabilization according to Pickering is probable. Both methods, high-throughput robot and dynamic foam analyzer, showed the complexity of foams, which is reported in the literature.^{126, 130} By statistical analysis, the properties of the catanionic systems were correlated to the foaming behavior. Only a few relations were found. The low surface tension of the surfactant solution favors foamability. The bubble size can be kept small, which correlates to high foam stability, by a small number of EO groups in the cationic surfactant, a small HLB value and a long average chain length of the surfactants.

The catanionic mixtures were investigated regarding their ability to remove fat by two methods: the quartz crystal microbalance (QCM) and the in-house built washing apparatus. In a first screening, the pure catanionic mixtures were tested in the QCM regarding their ability to remove biskin from the quartz crystals. Four catanionic mixtures were then further investigated in the washing apparatus. The combination of SDS and C12EO1Ch gave the best results. In a second step, the effect of a catanionic combination in a more complex washing system based on the three surfactants sodium dodecylbenzylsulfonate, Lutensol AO7, and Texapon N70 was investigated. By adding a cationic surfactant, a catanionic system was built. The addition of a cationic surfactant had positive effects, but only if EO groups were present in the cationic surfactant. The increasing nonionic character of the washing solution seemed to promote fat removal. Furthermore, the presence of the catanionic combination was tested for the compensation of decreasing the concentration of the nonionic surfactant. A significant influence of the nonionic character in the washing solution was observed. But, the nonionic surfactant was not necessary for full extent if the cationic surfactant C12EO1Ch was added. It could compensate for the decrease of the nonionic surfactant. Moreover, the addition of an

enzyme, a lipase, was investigated. No positive effect of the enzyme could be observed together with the cationic surfactant compared to when only cationic surfactant or enzyme was in the washing solution. Both seemed to hinder each other. With the use of the cationic surfactant, the enzyme was not necessary. The same washing result was observed. Consequently, the catanionic combination is an appropriate substitute for the commonly used lipase. But, it may be that other enzymes are more compatible to catanionic systems.

The wetting ability of the catanionic mixtures was tested on a hydrophobic polyethylene surface where the contact angle of the surfactant solution was detected. A synergistic effect of the mixtures was observed. Around equimolar ratio, the contact angle was lowest for most mixtures. The combination of SDS and C12EO1Ch was found to wet the surface completely at several ratios. For a deeper insight, three catanionic mixtures were chosen as examples for a good, an intermediate and a bad wetting. They were investigated via high-speed camera and compared to the wetting agent Plurafac LF300. The combination SDS-C12EO1Ch, mass ratio 5-5, gave the same good result as the wetting agent. The catanionic combination was also checked for their spreading on real plant leaves (red cabbage, benjamin fig, and money tree). A good spreading behavior was confirmed. Moreover, the three catanionic combinations were used to find a correlation to their physicochemical properties. The importance of the dynamics in the surfactant solutions and its surface activity got obvious. The same conclusion could be done by statistical analysis. For a good spreading behavior, EO groups are necessary to guarantee high solubility. Moreover, a shorter chain length promotes wetting as well as high dynamics in the surfactant solution. With the investigated catanionic mixtures, the problem of precipitation, as it is often described in the literature^{72, 207}, can be solved by the insertion of the EO groups. Thus, the maximal efficiency of them can be used, and super-spreaders can be tuned.

The emulsification behavior of the catanionic combinations was investigated via a screening over ten different oils. Compared to the pure ionic surfactants, a lot of mixtures showed higher emulsion stability. But, in general, the emulsification performance of the catanionic mixtures was lower than expected. Highest emulsion stability was obtained for the anion-cation mass ratio 5-5. Triolein was the oil which could be emulsified the best. A low interfacial tension was shown to be a supporting factor for a stable emulsion. The combination of Tex and ACA, mass ratio 5-5, gave the best results on average. Thus, it was investigated further regarding the potential to switch the stability of the catanionic emulsion system. For this purpose, the pure catanionic system was examined on external influences like changing the pH, the addition of salt and alcohol and changing the temperature.

Increasing temperature led to a clearing up of the solution and a change of the aggregates towards more elongated structures was observed. The addition of NaSCN led to phase separation at lower concentration and increased the viscosity of the monophasic system at higher concentrations. Both parameters were checked in an emulsion system with triolein. Influence of the NaSCN content and the temperature was found, which could be used to destabilize the emulsion system. The principle concept could be confirmed, but further investigations are necessary to get a deeper insight into the influences and the emulsion capacity of the catanionic mixtures.

Within this work, the potential of the catanionic mixtures for the application could be shown. Catanionic mixtures have high potential especially due to their high efficiency at low concentrations. Their synergistic effects can enhance their performance. But, also another point got obvious. Their advantage of changing different parameters like ratio, number of EO groups or chain length, makes the subject very complex and multifaceted. Small changes in the catanionic system influence several properties. Depending on the desired impact, the catanionic system must be tuned. To do this, the influences and effects of structural properties must be completely understood. A step towards this could be done in this work. But, some interesting points remain to be investigated. As a solubilizing hydrophilic group in the surfactant structure, only ethylene oxide groups were investigated. Their positive effect, especially regarding the solubility, could be proven. Another additional structural group is the propylene oxide group. It would be interesting to investigate the difference between ethylene and propylene oxide within in the surfactant structure. The general trend of increasing the solubility should be similar, but differences in the physicochemical properties should be observable. A difference in the degradability process is reported.²⁶⁶ Moreover, the influence of the alkyl chain length has been regarded in this work with two different chain length for the anionic and the cationic surfactant side. But for complete understanding, an expansion to a larger variety of chain lengths would be necessary. Especially, the investigation of shorter chain lengths would be of interest for higher dynamics. Until now, a clear and general trend regarding the influence of the ethylene oxide groups in the surfactant structure could not be provided. Depending on the property, an optimum of the number of used ethylene oxide groups is probable. For its determination, a broader collection of surfactants would be necessary.

All in all, catanionic mixtures are rightly a growing field of research. Due to their extraordinary properties, they enable an improved performance combined with higher efficiency for several desired applications. The toxicity of the cationic surfactants is often a problem. This problem could be

overcome by the use of only small amounts of cationic surfactant (~ 10 %) where already maximal synergistic effects are found. But for a concrete application, all possible variables and influences in the catanionic system must be understood and controlled. This requests intense research wherefore this thesis could hopefully contribute.

9 Appendix

9.1 List of figures

Figure 1. Classification of surfactants	6
Figure 2. Effect of the packing parameter on the packing shape and the assembled structure. The figure is based on reference ²⁴	8
Figure 3: Schematic illustration of the dependence of different physicochemical properties of aqueous surfactant solutions on the surfactant concentration. The broken lines indicate the cmc range.....	9
Figure 4: Temperature-dependence of the cmc, monomer solubility and total solubility of a surfactant. The intersection of the surfactant monomer solubility curve and the cmc curve defines the Krafft temperature (T_{kr}). The figure is based on reference ³²	11
Figure 5: Chemical structure of an ethylene oxide (EO) group in a surfactant structure.	16
Figure 6: Formation of an ion pair of two oppositely charged ionic surfactants as it is the case for catanionic surfactants.	23
Figure 7: A schematic triangular phase diagram of the symmetric catanionic mixture at constant temperature and pressure. The dashed line denotes the equimolar line dividing the diagram into the cationic-rich and the anionic-rich region. Close to the charge neutrality line, a solid precipitate (P) is usually formed, but excess charge in the system usually leads to vesicle stabilization (denoted as $V+$ and $V-$). Mixed micelles (denoted as $M+$ and $M-$) are usually formed at the highest excess of the mixture components. Multiphase regions (multi- Φ) often involve a lamellar phase occurring at higher concentrations (denoted as $L+$ and $L-$). The figure is taken from reference ⁶⁸	24
Figure 8: A schematic explanation for the nomenclature of the investigated compounds.	27
Figure 9: Chemical structure of choline (left), the basic structure of the choline derivatives (middle) and the SDS derivatives (right).	28
Figure 10: Overview of the investigated anionic surfactants and cationic surfactants. Cations are depicted on the horizontal line, and anions are shown on the vertical line.....	29
Figure 11: Optical evaluation of the solubility of the catanionic mixtures at a total surfactant concentration of 1 g/L in the anion-cation mass ratio 9-1 to 1-9 wt% after one week evaluated by eye; distinction was made into a clear solution with bluish glimmer (light blue), complete clear solution (green), turbid solution without precipitation (orange) and precipitation in the solution (red); the equimolar ratio is given in the yellow box respectively.....	31
Figure 12: Results of the solubility measurements via Total Carbon determination as described in 3.5.2.1 in percentage of the catanionic combinations of the five anionic surfactants (SDS (black), Tex (red), C12EO4SO4 (blue), C18EO4SO4 (purple) and C12EO6SO4 (green)) and the cationic surfactants ACA (A), C12EO1Ch (B) and C12EO4Ch (C) at a total surfactant concentration of 1 g/L.	33
Figure 13: Results of the cmc determination as described in 3.5.2.2 in percentage of the catanionic combinations of the five anionic surfactants (SDS (black), Tex (red), C12EO4SO4 (blue), C18EO4SO4 (purple) and C12EO6SO4 (green)) and the cationic surfactants ACA (A), C12EO1Ch (B) and C12EO4Ch (C) at 25°.	34
Figure 14: Area A per molecule at the surface A in Å ² calculated from the cmc data as described in 3.5.2.2 in percentage of the catanionic combinations of five anionic surfactants (SDS (black), Tex (red), C12EO4SO4 (blue),	

C18EO4SO4 (purple) and C12EO6SO4 (green)) and the cationic surfactants ACA (A), C12EO1Ch (B) and C12EO4Ch (C) at 25°C and a total surfactant concentration of 1 g/L.....	36
Figure 15: Results of surface tension via pendant drop measurements of the catanionic combinations of five anionic surfactants (SDS (black), Tex (red), C12EO4SO4 (blue), C18EO4SO4 (purple) and C12EO6SO4 (green)) and the cationic surfactants ACA (A), C12EO1Ch (B) and C12EO4Ch (C) at a total surfactant concentration of 1 g/L.	38
Figure 16: Interfacial tension results of six catanionic combinations of the three different cations (ACA (left), C12EO1Ch (middle) and C12EO4Ch (right)) at different mass ratios from 9-1 to 1-9 at 25 °C and a total surfactant concentration of 1 g/L measured as described in 3.5.2.2.	40
Figure 17: Comparison of the interfacial tension values for the influence of water hardness (0 °dH (black squares) and 5 °dH (grey circles)) for the catanionic combination of the anion C12EO4SO4 and the cation C16EO1Ch (left) and comparison of the influence of three different temperatures (25 °C (black squares), 40 °C (dark grey circles) and 50 °C (light grey triangles)) for the catanionic combination of the anion Tex and the cation C16EO1Ch (right). Experimental data is measured as described in 3.5.2.2 at a total surfactant concentration of 1 g/L.....	42
Figure 18: Results of the adsorbed mass after the surfactant step (left) and after the washing step (right) of the catanionic combinations with the cation ACA (above) and C12EO4Ch (below) at a total surfactant concentration of 1 g/L determined via QCM measurements on a SAM surface, as described in 3.5.2.4.	44
Figure 19: Results of the adsorbed mass after the surfactant step (left) and after the washing step (right) of catanionic combinations with the cationic surfactant ACA (above) and C12EO4Ch (below) at a total surfactant concentration of 1 g/L determined via QCM measurements on a SiO ₂ surface, as described in 3.5.2.4.....	46
Figure 20: Investigation of the influence of water hardness on the adsorption behavior of the catanionic combination SDS-C12EO1Ch at a total surfactant concentration of 1 g/L on a SiO ₂ quartz crystal determined via QCM measurement, as described in 3.5.2.4. On the left: adsorbed mass after the first step of washing with the surfactant solution; on the right: adsorbed mass after the second step of washing with water; below: the optical appearance of the investigated samples.....	47
Figure 21: Dynamic surface tension measurements performed with a bubble tensiometer as described in 3.5.2.2 for the catanionic combinations consisting of the anionic surfactants SDS (A), Tex (B), C12EO4SO4 (C), C18EO4SO4 (D) and C12EO6SO4 (E) and the cationic surfactants ACA (black), C12EO1Ch (dark grey) and C12EO4ch (light grey); The evaluated value is the decrease in surface tension (ST) after a bubble lifetime of 1 sec.	50
Figure 22: Calculated values for the effective diffusion coefficient from the dynamic surface tension measurement as described in 3.5.2.2 of the catanionic combinations of the five anionic surfactants (SDS (black), Tex (red), C12EO4SO4 (blue), C18EO4SO4 (purple) and C12EO6SO4 (green)) and the three cationic surfactants ACA (A), C12EO1Ch (B) and C12EO4Ch (C).	52
Figure 23: Radii, determined via monomodal fit of the corresponding DLS curves, as described in 3.5.2.3 of the catanionic combinations of five anionic surfactants (SDS (black), Tex (red), C12EO4SO4 (blue), C18EO4SO4 (purple) and C12EO6SO4 (green)) and the cationic surfactants ACA (A), C12EO1Ch (B) and C12EO4Ch (C) at 25°C and a total surfactant concentration of 1 g/L.....	54
Figure 24: Results of cryoTEM investigations obtained as described in 3.5.2.3 on six catanionic combinations at 1 wt%: SDS-C12EO1Ch (left above), SDS-C12EO4Ch (right above), Tex-ACA (right middle), Tex-C12EO1Ch (right middle), C18EO4SO4-ACA (left below) and C12EO6SO4-C12EO1Ch (right below).	56
Figure 25: Schematic illustration of the equilibrium state of different aggregates within a catanionic mixture.	58

Figure 26: Cytotoxicity tests of the three cationic surfactants ACA (black), C12EO1Ch (dark grey) and C12EO4Ch (light grey) determined with HaCaT cells as described in 3.5.2.5.....	59
Figure 27: Cytotoxicity measurements as described in 3.5.2.5 of the two catanionic mixtures of the anionic surfactant C12EO6SO4 and the cationic surfactants C12EO1Ch (left) and C12EO4Ch (right) in comparison with the toxicity of the pure cation (below) and the pure anion (above) indicated by a broken line.....	60
Figure 28: Example of the data evaluation of the maximum bubble pressure tensiometer.....	72
Figure 29: Adsorption curve on a SAM surface of C12EO6SO4-C12EO4Ch, 8-2, as an example of a transformed frequency curve to a mass curve from a QCM adsorption measurement	74
Figure 30: Examples of foams in our daily life: in the bath, as hair mousse and as cleaning foam for the table tennis racket.	76
Figure 31: Screening of the foaming behavior of the catanionic combinations via high-throughput robot as described in 4.5.2.1 without water hardness (left) and with 5°dH (right) after 0h (top), after 2h (middle) and after 24h (bottom); the concentration was 0.1wt.% in all samples. The mass ratio of each combination changes from 100 % anionic surfactant on the left to 100 % cationic surfactant on the right.	82
Figure 32: A: time-dependence of the foam structure of SDS-C16EO1Ch, 4-6. B: foam stability of Tex-ACA after 24 h. C: examples for a "foam inside foam" formation from C18EO4SO4-C16EO1Ch 2-8 (above) and SDS-C16EO1Ch 4-6 (below). Pictures were taken from the high-throughput robot as described in 4.5.2.1.....	84
Figure 33: Development of the average bubble size, the liquid volume and the total height of the foam of the catanionic combinations SDS-C12EO1Ch at different ratios measured with the dynamic foam analyzer as described in 4.5.2.2.	87
Figure 34: Foam structure and bubble size of the investigated samples of the catanionic mixture of the anion SDS and the cation C12EO1Ch at different ratios detected with the dynamic foam analyzer from Krüss as described in 4.5.2.2.	88
Figure 35: Development of the average bubble size, the liquid volume and the total height of the foam of the catanionic combinations with SDS as anionic surfactant and the four different cationic surfactants ACA (purple), C12EO1Ch (red), C12EO4Ch (green) and C16EOCh (blue) measured with the dynamic foam analyzer as described in 4.5.2.2.	89
Figure 36: Development of the average bubble size, the liquid volume and the total height of the foam of the catanionic combinations with C16EO1Ch as the cationic surfactant and the three different anionic surfactants SDS (green), C12EO4SO4 (red) and C12EO6SO4 (blue) measured with the dynamic foam analyzer as described in 4.5.2.2.	91
Figure 37: Development of the average bubble size, the liquid volume and the total height of the foam of the catanionic combinations of Tex and ACA at the two anion-cation ratios 4-6 (orange) and 3-7 (red) in comparison to the pure ionic surfactant Tex (grey) and ACA (black) measured with the dynamic foam analyzer as described in 4.5.2.2.	92
Figure 38: Examples of applications for cleaning products in a typical household.	100
Figure 39: Schematically depiction of a drop of oil on a solid substrate and the corresponding interfaces. The picture is based on reference ¹⁵⁹	106
Figure 40: Roll-up mechanism. The picture is taken from reference ¹⁵⁹	107
Figure 41: Evaluation of the first QCM scanning for the removal of Biskin by the catanionic mixtures as described in 5.5.2.2 for the anion-cation mass ratio 9-1 (left) and 5-5 (right) by the two parameters peak height (above) and end removal (below).....	113

Figure 42: Evaluation of the first QCM scanning for the removal of Biskin by the catanionic mixtures as described in 5.5.2.2 for the anion-cation mass ratio 9-1 (left) and 5-5 (right) by the two parameters area (above) and end removal (below).	114
Figure 43: Washing results of the removal of Biskin in % with the in-house built washing apparatus as described in 5.5.2.2 of the pure catanionics combinations Tex-ACA 5-5 (black), C12EO4SO4-ACA 5-5 (grey), SDS-C12EO1Ch 5-5 (white) and SDS-C12EO4Ch 5-5 (whited shaded) in pure form, with the addition of 2 ppm lipase and inserted in the standard mixture of SDBS:AO7:Catanionic (1:1:1) at 25 °C and pH 10 evaluated by color (above left) and by mass (below left) in comparison to the references (right).	119
Figure 44: Lipase stability in the presence of the surfactants SDS and C12EO4Ch measured as described in 5.5.2.6.	121
Figure 45: Name and structure of the three surfactants present in the standard mixture.	122
Figure 46: Washing results of the removal of Biskin with the in-house built washing apparatus in % as described in 5.5.2.3 for the references water and commercial Persil at 25°C and 40°C at pH 10 determined by color (not shaded) and by mass (shaded).	124
Figure 47: Washing results of the standard mixture of SDS:Tex:AO7 (1:1:1) in % measured as described in 5.5.2.3 at 25 °C as a function of concentration at 25 °C (white) and 40 °C (grey) at 14 °dH evaluated by a colorimeter (blank) and by mass (shaded).	125
Figure 48: Washing results in % measured as described in 5.5.2.3 at 25 °C of the standard mixture (SDBS:AO7:Tex (1:1:1)) (black), standard mixture + 100ppm C12EO1Ch (dark grey) and the standard mixture + 100 ppm C12EO4Ch (light grey) on three different soils: biskin, sebum and beef fat evaluated by colorimeter (left) and by mass (right).	128
Figure 49: Contact angle measurements measured as described in 5.5.2.7 at 25 °C of the investigated standard solution without additive (left), with 100 ppm C12EO1Ch (middle) and 100 ppm C12EO4Ch (right) on the three different substrates: Biskin (black), sebum (grey) and lard (white).	130
Figure 50: Cmc measurement measured as described in 5.5.2.4 performed at 25 °C of the standard mixture in millipore water (black circles) and the standard mixture with the addition of 200ppm C12EO1Ch (grey squares).	131
Figure 51: Washing results of Biskin in % measured as described in 5.5.2.3 of the standard mixture SDBS:AO7:Tex = 1:1:1 at different concentrations at 14 °dH and 25 °C with the addition of 100 ppm ACA (white striped), C12EO1Ch (dark grey) and C12EO4Ch (light grey) compared to the pure standard mixture (white) evaluated by colorimeter (left) and by mass (right).	132
Figure 52: Dependence of the washing results of Biskin in % measured as described in 5.5.2.3 of the standard mixture SDBS:AO7:Tex = 1:1:1 at 0.1 wt% at 14°dH and 25 °C on the addition of different concentrations of C12EO1Ch (left) and C12EO4Ch (right) evaluated by colorimeter (black) and by mass (white).	133
Figure 53: Multiple contact angle measurements (left) and interfacial tension against air (white) and triolein (black) (right) measured as described in 5.5.2.7 at 25 °C of the standard solution (800 ppm) and the addition of 200 ppm of the different cationic additives ACA, C12EO1Ch, C12EO4Ch, and C16EO1Ch.	135
Figure 54: Dependence of the washing results in % measured as described in 5.5.2.3 of the standard mixture SDBS:AO7:Tex = 1:1:1 at 14°dH and 25 °C on the amount of AO7 and the amount of added cation C12EO1Ch evaluated by colorimeter (black) and by mass (white) with constant content of SDBS and Tex of 330 ppm. The broken line indicates the standard mixture.	137

Figure 55: Fat removal results performed via QCM as described in 5.5.2.2 at different concentrations of the pre-formulated standard mixture by BASF at 14°dH with the addition of 200 ppm cation C12EO1Ch. The measured curves are normalized to maximum removal (left), and the evaluated results of the area and end removal are summarized (right). The broken line indicates a linear decrease of the fat removal with the concentration..	139
Figure 56: Multiple contact angle measurements (grey) (left), interfacial tension against air (white) and triolein (black) (right) measured, as described in 5.5.2.7 of the standard solution at different concentration (800 ppm, 400 ppm and 200 ppm) with the addition of 200 ppm of the cationic additive C12EO1Ch, in comparison to the standard mixture without additive (Ref).	140
Figure 57: Comparison of the cmc measurement (see 5.5.2.4) of the standard mixture in millipore water (unfilled black circles), the standard mixture with the addition of 200 ppm C12EO1Ch (filled black circles), the standard mixture with the addition of 2 ppm lipase (unfilled grey squares) and the standard mixture with the addition of both, 200 ppm C12EO1Ch and 2 ppm lipase (filled grey squares) at 25 °C.	141
Figure 58: Dependence of the washing results on the pH in % measured as described in 5.5.2.3 of the standard mixture SDBS:AO7:Tex (1:1:1) 0.1 wt% + 2 ppm lipase at 25°C evaluated by color (black) and mass (white)..	143
Figure 59: Influence of the addition of 2 ppm of lipase on the standard mixture (left) and the standard mixture with 100 ppm added C12EO1Ch (right) on the washing results in %, depending on the concentration, at 25°C and pH 10 evaluated by color (blank) and by mass (shaded) as described in 5.5.2.3.	143
Figure 60: Comparison of the washing results in % of the standard mixture with the addition of 2ppm lipase (white) and 100ppm C12EO1Ch (grey) evaluated by color (blank) and by mass (shaded) at 25°C and pH 10 as described in 5.5.2.3.	145
Figure 61: Comparison of the influence of the addition of the cationic surfactant C12EO1Ch and lipase to the washing formulation ES1M (pre-formulated standard mixture by BASF) via QCM measurement as described in 5.5.2.2 in 14°dH at pH 6. The measured frequency was normalized to the value of complete removal of the Biskin layer by acetone at the end of the measurement.	146
Figure 62: Pictures of the surface of the quartz crystals from the comparison of the influence of the addition of C12EO1Ch and lipase to the washing formulation ES1M performed with a WLI (above) and a SEM (below)..	148
Figure 63: Example of a QCM measurement with the determined parameter illustrated.	153
Figure 64: In-house built washing apparatus.	154
Figure 65: Molecular structure of the azo dye Sudan black B.	154
Figure 66: The L, a and b color system, in which a* and b* correspond to the colorfulness and L* to the brightness. The picture was taken from reference ¹⁸⁴	155
Figure 67: Construction of the multiple contact angle measurement chamber	157
Figure 68: The lotus-effect on a leave after rain.	158
Figure 69: Schematical picture of the three possible ways of the formation of a droplet on a homogenous solid surface. The picture was taken from reference ¹⁷⁷	160
Figure 70: Spreading mechanisms of an aqueous surfactant solution on a hydrophobic surface according to von Bahr <i>et al.</i> (A) and according to Starov <i>et al.</i> (B). Pictures are taken from reference ¹⁸⁶	163
Figure 71: Contact angle on a polyethylene surface measured for the different ratios of the catanionic combination of the cation ACA with the anion C12EO4SO4 (above left) and C18EO4SO4 (above right) at pH 7 in millipore water and a concentration of 0.1 wt% as described in 6.5.2.1. A comparison of both anions is shown on the bottom.	166

Figure 72: Contact angle on a polyethylene measured with different ratios of the catanionic combination of the cation C12EO1Ch with the anion C12EO4SO4 (above left) and C18EO4SO4 (above right) at pH7 in millipore water and a concentration of 0.1 wt% as described in 6.5.2.1. A comparison of the anions with the data from SDS added was shown on the bottom.....	167
Figure 73: Contact angle on polyethylene of different ratios of the catanionic combination of the cation C12EO4Ch with the anion SDS (above left) and C18EO4SO4 (above right) at pH7 in millipore water and a concentration of 0.1 wt% as described in 6.5.2.1. A comparison of both anions was shown on the bottom. ..	168
Figure 74: Contact angle on polyethylene of different ratios of the catanionic combination of the cation C16EO1Ch with the anion SDS (above left) and C12EO4SO4 (above right) at pH7 in millipore water and a concentration of 0.02 wt% as described in 6.5.2.1. A comparison of both anions was shown on the bottom.	169
Figure 75: Comparison of the influence of the chain length (C12EO1Ch (black squares) and C16EO1Ch (red circles)) of the cation for the anion SDS at a catanionic concentration of 0.02 wt% (left) and the comparison of the influence of the number of EO groups (1EO (black) and 4EO (red)) for the anions SDS and C18EO4SO4 at a catanionic concentration of 0.1 wt% (right) in regard to the contact angle on polyethylene at pH 7 in millipore water measured as described in 6.5.2.1.....	171
Figure 76: Comparison of the influence of water hardness 0°dH (left) and 5°dH (middle) in regard to the contact angle after 10 secs for different ratios of the catanionic combination C18EO4SO4 - C12EO1Ch at 0.1 wt% (above), SDS - C16EO1Ch 0.02 wt% (middle) and C12EO4SO4-C16EO1Ch 0.02 wt% (below) at pH 7 measured as described in 6.5.2.1. A comparison is shown on the right.	173
Figure 77: Spreading behavior of the catanionic combination SDS-C12EO1Ch at the mass ratio 5-5 and a concentration of 0.1 wt% investigated on the leave of the benjamin fig (left above), the money tree (right above) and red cabbage (middle) in comparison to water. Below: spreading behavior of the catanionic combination SDS-C12EO1ch at the mass ratio 5-5 and a concentration of 0.002 and 0.02 wt% on the leave of the benjamin fig (left below) and on the money tree (right below).....	175
Figure 78: Observations of the spreading behavior on a polyethylene film of water and LF300 as a reference and the three catanionic samples SDS-C12EO1Ch 5-5, SDS-C16EO1Ch, and SDS-C12EO1Ch 7-3 at a concentration of 0.02 wt% recorded with a high-speed camera as described in 6.5.2.2.	176
Figure 79: Determination of the critical micelle concentration (cmc) (top left) obtained by tensiometer (see 6.5.2.5), the dynamic surface tension (ST) (top right) obtained by bubble pressure tensiometer (see 6.5.2.4) and the adsorption behavior on a hydrophobic gold-coated surface with 1-octadecane thiol (below) obtained by QCM (see 6.5.2.6), of the three investigated catanionic combinations SDS-C16EO1Ch 7-3 (black), SDS-C16EO1Ch 3-7 (dark grey) and SDS-C12EO1Ch 5-5 (light grey) at 0.1 wt% and pH 7 obtained by tensiometer.....	178
Figure 80: Schematic illustration of the influence of different physicochemical properties on the spreading behavior of the catanionic combinations.....	182
Figure 81: Construction of the high-speed camera apparatus.....	187
Figure 82: Examples of emulsions in our daily life: face cream (left), mayonnaise (middle) and milk (right).	189
Figure 83: Schematic presentation of the formation and break down of an emulsion. The picture is taken from reference ²²⁷	192
Figure 84: Schematic illustration of the total energy-distance curve of two emulsion droplets according to the DLVO theory.	195
Figure 85: Schematic illustration of the different breakdown processes of an emulsion. Figure is taken from reference ²²⁷	196

Figure 86: A typical ordering of anions and cations in the Hofmeister series. The figure is based on reference ²⁴⁷.

..... 200

Figure 87: Left: Division of alkali ions and halide ions into strongly hydrated kosmotropes (above the line) and weakly hydrated chaotropes (below the line). The medium-sized zwitterion in the left illustration represents a water molecule. Ion sizes are drawn true to scale. Right: It is shown that ions have to be similar in size to form inner sphere ion pairs. This figure is based on reference ¹⁰⁴.

..... 201

Figure 88: Overview of the ten oils used for the emulsion stability screening of the different catanionic combinations. 204

Figure 89: Pictures of the emulsion stability tests after 1 hour for the catanionic combinations with ACA as cation and the five different anions SDS, Tex, C12EO4SO4, C18EO4SO4 and C12EO6SO4 with an anion-cation molar ratio 1-1 and mass ratios 6-4, 5-5 and 4-6 at 1 wt% with ten different oils: A (octane), B (dodecane), C (hexadecane), D (rape oil), E (sunflower oil), F (biodiesel), G (Miglyol 812), H (diisostearyl malate), I (triolein) and J (pentaerythrityl tetraistearate) at room temperature evaluated as described in 7.5.2.1. 205

Figure 90: Pictures of the emulsion stability tests after 1 hour for the catanionic combinations with C12EO1Ch as cation and the five different anions SDS, Tex, C12EO4SO4, C18EO4SO4 and C12EO6SO4 at the anion-cation molar ratio 1-1 and mass ratios 6-4, 5-5 and 4-6 at 1 wt% with ten different oils: A (octane), B (dodecane), C (hexadecane), D (rape oil), E (sunflower oil), F (biodiesel), G (Miglyol 812), H (diisostearyl malate), I (triolein) and J (pentaerythrityl tetraistearate) at room temperature evaluated as described in 7.5.2.1. 206

Figure 91: Pictures of the emulsion stability tests after 1 hour for the catanionic combinations with C12EO4Ch as cation and the five different anions SDS, Tex, C12EO4SO4, C18EO4SO4 and C12EO6SO4 at the anion-cation molar ratio 1-1 and mass ratios 6-4, 5-5 and 4-6 at 1 wt% with ten different oils: A (octane), B (dodecane), C (hexadecane), D (rape oil), E (sunflower oil), F (biodiesel), G (Miglyol 812), H (diisostearyl malate), I (triolein) and J (pentaerythrityl tetraistearate) at room temperature evaluated as described in 7.5.2.1. 208

Figure 92: Summary of the macroscopic evaluation of the emulsion stability evaluated as described in 7.5.2.1 of the different catanionic combinations at the anion-cation molar ratio 1-1 and mass ratios 6-4, 5-5 and 4-6 at 1 wt% with ten different oils: A (octane), B (dodecane), C (hexadecane), D (rape oil), E (sunflower oil), F (biodiesel), G (Miglyol 812), H (diisostearyl malate), I (triolein) and J (pentaerythrityl tetraistearate) at room temperature. The evaluation parameters are the following: 0 (immediate separation), 1 (separation after 10min), 2 (separation after 1h), 3 (separation after 2h), 4 (separation overnight), 5 (separation after 24h) and 6 (stable after 24h). 209

Figure 93: Results of the spinning drop measurements of the aqueous catanionic combinations against several investigated oils: A (octane), B (dodecane), C (hexadecane), D (rape oil), E (sunflower oil), F (biodiesel), G (Miglyol 812), H (diisostearyl malate), I (triolein) and J (pentaerythrityl tetraistearate) at 25 °C as described in 7.5.2.2.

..... 211

Figure 94: Pictures of three different emulsions of catanionic systems taken with the CLSM as described in 7.5.2.5: A: SDS-C12EO1Ch, 5-5, triolein, 2 h after preparation; B: Tex-ACA, 5-5, rape oil, 2 h after preparation; C: C12EO6SO4-C12EO4Ch, 5-5, biodiesel, 2 mins after preparation. 212

Figure 95: Concentration-dependent DLS curves measured as described in 7.5.2.6 of the catanionic system Tex-ACA, mass ratio 5-5 (left); pictures of the CLSM from the catanionic system Tex-ACA, 5-5, 1 wt%, (right) performed as described in 7.5.2.5. 214

Figure 96: Influence of the addition of the salt NaCl in different concentrations on the catanionic system Tex-ACA, 5-5, 1 wt% evaluated by optical appearance (above), DLS measurement (left below) and viscosity (right below) as described in 7.5.2. 216

Figure 97: Influence of the addition of the salt Na_2SO_4 different salts in different concentrations on the catanionic system Tex-ACA, 5-5, 1 wt% evaluated by optical appearance (above), DLS measurement (left below) and viscosity (right below) as described in 7.5.2.....	217
Figure 98: Influence of the addition of the salt CaCl_2 different salts in different concentrations on the catanionic system Tex-ACA, 5-5, 1 wt% evaluated by optical appearance (above), DLS measurement (left below) and viscosity (right below) as described in 7.5.2.....	218
Figure 99: Influence of the addition of the salt NaSCN different salts in different concentrations on the catanionic system Tex-ACA, 5-5, 1 wt% evaluated by optical appearance (above), DLS measurement (left below) and viscosity (right below) as described in 7.5.2.....	219
Figure 100: Influence of the addition of ethanol (left) and butanol (right) on the catanionic system Tex-ACA, 5-5, 1 wt% evaluated by optical appearance (above), DLS measurement (middle) and viscosity measurements (below) measured after one day after preparation as described in 7.5.2.6 and 7.5.2.4.....	221
Figure 101: Influence of the pH value on the catanionic system Tex-ACA, 5-5, 1 wt% evaluated by optical appearance (A), DLS measurement (B), viscosity (C) and CLSM for the sample of pH 9 (D) as described in 7.5.2.	223
Figure 102: Measurement of turbidity with the in-house built apparatus of the catanionic system Tex-ACA, 5-5, 1 wt%, with a heating rate of 2 K/h depending on the temperature as described in 7.5.2.3.	224
Figure 103: SAXS measurement of the catanionic sample Tex-ACA at the anion-cation mass ratio 5-5 and a concentration of 1 wt% at 20 °C (black), after heating up to 40 °C (dark grey) and after re-cooling to 20 °C (light grey) measured as described in 7.5.2.7.....	225
Figure 104: Influence of temperature increase from 25 °C to 37 °C on the structure of the catanionic system Tex-ACA, 5-5, 1wt%, observed with CLSM as described in 7.5.2.5.	226
Figure 105: Switchability test due to changing the concentration of NaSCN of the emulsion combination Tec-ACA, 5-5, 1 wt% with rape oil.	227
Figure 106: Switchability tests due to the change of temperature of the emulsion combination Tec-ACA, 5-5, 1 wt% with hexadecane as oil over time. Number 1 indicates the sample where the emulsion was prepared and stored at room temperature. Number 2 indicates the sample where the emulsion was prepared at room temperature and stored at 50°C. Number 3 indicates the sample where the surfactant solution has been heated up to 50°C for 15 mins before preparation and storage at room temperature.	229
Figure 107: Switchability tests due to the change of temperature of the emulsion combination C18EO4SO4-C12EO4Ch, 5-5, 1 wt% with hexadecane as oil over time. Number 1 indicates the sample where the emulsion was prepared and stored at room temperature. Number 2 indicates the sample where the emulsion was prepared at room temperature and stored at 50°C. Number 3 indicates the sample where the surfactant solution has been heated up to 50°C for 15 mins before preparation and storage at room temperature.	230

9.2 Table of symbols

symbol	name	symbol	name
β	London dispersion constant	D	diffusion constant
γ	interfacial/surface tension	D_{eff}	effective diffusion coefficient
η	viscosity	DLS	dynamic light scattering
θ	contact angle	e	unit factor
λ	wavelength	DLVO	Derjaguin, Landau, Verwey, and Overbeek
μ	chemical potential	e	unit factor
ρ	density	E	surface elasticity
σ	surface tension	EC	effect concentration
Γ	equilibrium surface excess	EO	ethylene oxide
ϕ	volume fraction	ES1M	preformulated washing mixture from BASF
ϕ_F	surface free energy	f	fraction of material
ω	rotational velocity	g	gramm
%	percentage	G	free energy
$^{\circ}\text{C}$	degree of Celsius	G^{σ}	surface free energy
$^{\circ}\text{dH}$	degree of water hardness	G_a	attraction forces
wt%	mass percentage	$\Delta G^0_{\text{c-c}}$	standard free energy of association of methyl groups
A_H	Hamaker constant	ΔG^0_{chem}	standard free energy of covalent bonding
A	surface area	G_{el}	repulsion interaction
a	area per molecule	ΔG^0_{elec}	electrostatic interaction term
a^*, b^*, L^*	parameter of colorness	ΔG^0_{H}	standard free energy of hydrogen bonding
ABS	alkyl benzene sulfate	$\Delta G^0_{\text{H}_2\text{O}}$	standard free energy of displacement of H ₂ O molecules
ACA	Dehyquart A-CA (see page 28)	G_{mix}	mixing free energy of interaction
AO7	Lutensol AO7 (see page 122)	G_{prim}	first minimum in DLVO theory
APE	alkyl phenol ethoxylates	$\Delta G^0_{\text{s-c}}$	standard free energy of interactions between the hydrocarbon chains and hydrophobic sites
c	concentration	G_{sec}	second minimum in DLVO theory
CLSM	confocal light scanning microscope	G_{T}	total energy of interaction
cmc	critical micelle concentration	h	hour
Ch	choline	h_{sep}	separation distance
d	diameter	HLB	hydrophilic-lipophilic balance

symbol	name	symbol	name
IFT	interfacial tension	q	number of molecules per unit volume
k	experimental apparatus constant	QCM	quartz micro balance
l	length of the tail	r	separation distance
L	liter	R	universal gas constant
L	liquid	Req	equal radii
L+, L-	lamellar phase	rpm	rounds per minute
		S	substrate/solid
LAS	linear alkylbenzene sulfonate	S	entropy
LC	lethal concentration	Ssp	spreading coefficient
LES	linear alcohol ethoxylated sulfates	SAM	gold quartz crystal coated with 1-octadecanethiol
LF300	Plurafac LF 300 (see page 175)	SDBS	sodium dodecylbenzylsulfonate
m	meter	SDS	sodium dodecylsulfate
M	total molecular mass	sec	second
M+, M-	mixed micelles	SEM	scanning electron microscope
MI	molare mass of the lipophilic part of the surfactant structure	SO4	sulfate
m(ads)	adsorbed mass	ST	surface tension
m(rest)	mass rested after washing step	t	time
MES	methyl ester sulfonates	tsurf	surface age
min	minute	T	temperature
mL	milli litres	TC	total carbon content
multi- Φ	multiphase region	TKr	Krafft temperature
n	number of components	TEM	transmission electron microscope
nr	rotation	Tex	Texapon N70 (see page 122)
NA	Avogadro's number	TOTO	2,5,8,11-tetraoxatridecan-13-oate
N	Newton	v	magnification
O	oil	V	vapor
pp	packing parameter	Vt	hydrophobic tail of the surfactant vesicle
p	pressure		water
P	solid precipitate	WLI	white light interferometer
PIT	phase inversion point	X	number of C-atoms
ppm	parts per million	Y	number of EO groups

9.3 List of tables

Table 1: Results of the univariate regression analysis between the molecular properties and the determined physicochemical properties of the catanionic mixtures calculated as described in 3.5.2.6.....	62
Table 2: Results of the multivariate regression analysis between the molecular properties and the determined physicochemical properties of the catanionic mixtures calculated as described in 3.5.2.6.....	63
Table 3: Overview of the selection of catanionic components for a deeper investigation of the influences on the foaming behavior with the dynamic foam analyzer as described in 4.5.2.2.	86
Table 4: P-value results of the univariate regression analysis between the molecular physicochemical properties and the determined total foam height after 3 h (measured as described in 4.5.2.2) of the catanionic mixtures calculated as described in 4.5.2.3.....	93
Table 5: P-value results of the univariate regression analysis between the molecular physicochemical properties and the determined liquid volume (measured as described in 4.5.2.2) of the catanionic mixtures calculated as described in 4.5.2.3.	94
Table 6: P-value results of the univariate regression analysis between the molecular physicochemical properties and the determined average bubble size (measured as described in 4.5.2.2) of the catanionic mixtures calculated as described in 4.5.2.3.	95
Table 7: Evaluation of the Biskin removal experiments for the pure anionic and cationic surfactants performed with the QCM as described in 5.5.2.2.....	112
Table 8: Results of the univariate regression analysis between the molecular physicochemical properties and the determined parameter 'area' of Biskin in the QCM measurement (see 5.5.2.2) of the catanionic mixtures calculated as described in 5.5.2.8.....	116
Table 9: Results of the univariate regression analysis between the molecular physicochemical properties and the determined parameter 'end removal' of Biskin in the QCM measurement (see 5.5.2.2) of the catanionic mixtures calculated as described in 5.5.2.8.....	117
Table 10: Results of fat removal of three different fat by the standard mixture SDBS:AO7:Tex (1:1:1) with the concentration of 1000 ppm with none, with 100 ppm C12EO1Ch and with 100 ppm C12EO4Ch as additive performed with the QCM as described in 5.5.2.2 at 25 °C.	127
Table 11: Evaluation of the washing results obtained from the washing method as described in 5.5.2.3 regarding the molar amounts of anionic and cationic surfactants at the maximum of washing efficiency.	134
Table 12: Resulting parameter maximum, area and end removal in % in regard to the complete removal by acetone from the QCM measurement as described in 5.5.2.2 in 14°dH at pH 6 for the washing formulation ES1M (pre-formulated standard mixture by BASF) and the influence of the addition of the cationic surfactant C12EO1Ch and lipase.....	146
Table 13: Values of physicochemical properties of the three investigated catanionic combinations SDS-C16EO1Ch 7-3, SDS-C16EO1Ch 3-7 and SDS-C12EO1Ch 5-5 at 0.1 wt% and pH 7 obtained by tensiometer (see 6.5.2.5), bubble pressure tensiometer (see 6.5.2.4) and QCM (see 6.5.2.6).	179
Table 14: Results of the univariate regression analysis between the molecular physicochemical properties and the determined spreading performance on the polyethylene surface of the catanionic mixtures calculated as described in 6.5.2.7.	182

Table 15: Results for the P-value of the multivariate regression analysis between the molecular physicochemical properties and the determined spreading performance on the polyethylene surface of the cationic mixtures calculated as described in 6.5.2.7.....	183
--	-----

9.4 List of equations

equation 1: HLB value	6
equation 2: Definition of the packing parameter	7
equation 3: Adsorption of surfactants at a liquid interface	12
equation 4: Time dependence of the process of lowering the surface tension by Joos and Rillaerts	12
equation 5: Standard free energy of adsorption	13
equation 6: Young Laplace equation	70
equation 7: Vonnegut equation	70
equation 8: Gibbs adsorption equation	71
equation 9: Surface excess concentration	71
equation 10: Area at the surface per molecule	71
equation 11: Gibbs coefficient of surface elasticity	80
equation 12: Young's equation	106
equation 13: ΔE value	155
equation 14: Spreading coefficient	160
equation 15: Cassie contact angle	161
equation 16: Surface free energy ϕ of a drop on a solid surface	162
equation 17: Gibbs-Deuhem equation	193
equation 18: Interfacial tension γ described by Gibbs-Deuhem equation	193
equation 19: Free energy of the formation of an emulsion	193
equation 20: Attraction forces of two particles	194
equation 21: Relation of attraction forces and Hamaker constant	194
equation 22: Hamaker constant	195
equation 23: Total energy of interaction I	195
equation 24: Total energy of interaction II	195
equation 25: Calculation of the interfacial tension via spinning drop data	236
equation 26: Viscosity η by law of Stokes	237

10 References

1. D. Myers, *Surfactant science and technology*, John Wiley & Sons, 2005.
2. R. J. Farn, *Chemistry and technology of surfactants*, WILEY, 2008.
3. J. Falbe, *Surfactants in consumer products: Theory, Technology and Application*, Springer Science & Business Media, 2012.
4. S. H. Zeisel and K. A. da Costa, *Nutr. Rev.*, 2009, **67**, 615-623.
5. R. Klein, M. Kellermeier, D. Touraud, E. Müller and W. Kunz, *J. Colloid Interface Sci.*, 2013, **392**, 274-280.
6. R. Klein, D. Touraud and W. Kunz, *Green Chemistry*, 2008, **10**, 433-435.
7. O. Zech, M. Kellermeier, S. Thomaier, E. Maurer, R. Klein, C. Schreiner and W. Kunz, *Chem. - Eur. J.*, 2009, **15**, 1341-1345.
8. R. Klein, O. Zech, E. Maurer, M. Kellermeier and W. Kunz, *J. Phys. Chem. B*, 2011, **115**, 8961-8969.
9. N. Subirats, P. Castan and M. Stapels, *SÖFW-Journal*, 2009, **135**.
10. M. Bergström, *Langmuir : the ACS journal of surfaces and colloids*, 2001, **17**, 993-998.
11. D. F. Evans and H. Wennerström, in *The colloidal domain: where physics, chemistry, biology, and technology meet*, Wiley, 1999, pp. 1-44.
12. M. R. Porter, *Handbook of surfactants*, Springer, 2013.
13. L. L. Schramm, E. N. Stasiuk and D. G. Marangoni, *Annu. Rep. Prog. Chem., Sect. C: Phys. Chem.*, 2003, **99**, 3-48.
14. D. C. Cullum, in *Introduction to Surfactant Analysis*, ed. D. C. Cullum, Springer 1994, pp. 17-41.
15. J.-L. Salager, *Surfactants types and uses*, Universidad de los Andes, 2002.
16. K. Holmberg, B. Jönsson, B. Kronberg and B. Lindman, in *Surfactants and polymers in aqueous solution*, WILEY, 2003, pp. 1-37.
17. G. Wagner, *Waschmittel: Chemie, Umwelt, Nachhaltigkeit*, John Wiley & Sons, 2017.
18. B. Kronberg, K. Holmberg and B. Lindman, *Surface Chemistry of Surfactants and Polymers*, WILEY, 2014.
19. C. Yuan, Z. Xu, M. Fan, H. Liu, Y. Xie and T. Zhu, *J. Chem. Pharm. Res.*, 2014, **6**, 2233-2237.
20. W. C. Griffin, *J. Soc. Cosmet. Chem.*, 1949, **1**, 311-326.
21. T. Hargreaves, *Chemical Formulation: An Overview of Surfactant-based Preparations Used in Everyday Life*, RSC Paperbacks, 2003.
22. R. Zana, in *Dynamics of Surfactant Self-Assemblies*, ed. R. Zana, Taylor&Francis, 2005, pp. 1-36.
23. J. N. Israelachvili, D. J. Mitchell and B. W. Ninham, *J. Chem. Soc., Faraday Trans. 2*, 1976, **72**, 1525-1568.
24. J. Zhang, X. Li and X. Li, *Prog. Polym. Sci.*, 2012, **37**, 1130-1176.
25. Y. Moroi, *Micelles: Theoretical and Applied Aspects*, Springer 1992.
26. B. Kronberg, *Curr. Opin. Colloid Interface Sci.*, 2016, **22**, 14-22.
27. P. W. Atkins and J. de Paula, *Physikalische Chemie*, Wiley-VCH, 2013.
28. D. F. Evans and H. Wennerström, in *The colloidal domain: where physics, chemistry, biology, and technology meet*, Wiley, 1999, pp. 153-216.
29. M. J. Rosen and J. T. Kunjappu, in *Surfactants and interfacial phenomena*, WILEY, 2004, pp. 105-177.
30. R. G. Laughlin, in *The Aqueous Phase Behaviour of Surfactants*, Academic Press, 1994, pp. 102-154.

31. Z. G. Cui and J. P. Canselier, *Colloid Polym. Sci.*, 2001, **279**, 259-267.
32. B. Lindman, in *Handbook of Applied Surface and Colloid Chemistry (Volume 1)*, ed. K. Holmberg, Wiley, 2002, vol. 1, pp. 421-443.
33. R. Miller, E. Aksenenko and V. Fainerman, *Adv. Colloid Interface Sci.*, 2017, **247**, 115-129.
34. S. R. Milner, *Philos. Mag.*, 1907, **13**, 96-110.
35. A. Ward and L. Tordai, *J. Chem. Phys.*, 1946, **14**, 453-461.
36. P. Joos and E. Rillaerts, *J. Colloid Interface Sci.*, 1981, **79**, 96-100.
37. D. Wasan, M. Ginn and D. Shah, Marcel Dekker: New York, 1988.
38. D. Fuerstenau, *The chemistry of biosurfaces*, 1971, **1**, 143-176.
39. E. Goddard and P. Somasundaran, *Croat. Chem. Acta*, 1976, **48**, 451-461.
40. R. Zhang and P. Somasundaran, *Adv. Colloid Interface Sci.*, 2006, **123**, 213-229.
41. I. Langmuir, *JACS*, 1918, **40**, 1361-1403.
42. Z. Huang, Z. Yan and T. Gu, *Colloids Surf.*, 1989, **36**, 353-358.
43. S. Paria, C. Manohar and K. C. Khilar, *Colloids Surf. A*, 2004, **232**, 139-142.
44. T. P. Knepper and J. L. Berna, in *Comprehensive Analytical Chemistry*, Elsevier, 2003, vol. 40, pp. 1-49.
45. F. Bartnik and K. Künstler, in *Surfactants in Consumer Products*, Springer, 1987, pp. 475-503.
46. E. Smulders, W. Rähse, W. von Rybinski, J. Steber, E. Sung and F. Wiebel, in *Laundry Detergents*, Wiley-VCH 2003, pp. 203-208.
47. X. Domingo, in *Anionic Surfactants: Organic Chemistry*, ed. H. W. Stache, Marcel Dekker, 1996, vol. 56, pp. 223-312.
48. L. Huber and L. Nitschke, in *Handbook of applied surface and colloid chemistry*, ed. K. Holmberg, WILEY, 2002, vol. 1, pp. 509-536.
49. R. S. Boethling, in *Cationic Surfactants: Analytical and Biological Evaluation*, eds. J. Cross and E. J. Singer, Marcel Dekker, 1994, vol. 53, pp. 95-95.
50. C. T. Cowan and D. White, *J. Chem. Soc., Faraday Trans.*, 1958, **54**, 691-697.
51. M. J. Scott and M. N. Jones, *Biochim. Biophys. Acta*, 2000, **1508**, 235-251.
52. J. A. Perales, M. A. Manzano, D. Sales and J. M. Quiroga, *Bull. Environ. Contam. Toxicol.*, 1999, **63**, 94-100.
53. C. Van Ginkel, in *Biodegradability of surfactants*, Springer, 1995, pp. 183-203.
54. N. Schönfeldt, in *Surface Active Ethylene Oxide Adducts*, Elsevier, 2013, pp. 130-386.
55. GESTIS-Stoffdatenbank, IFA, 2018.
56. M. Á. Valenzuela, M. P. Gárate and A. F. Olea, *Colloids Surf. A*, 2007, **307**, 28-34.
57. A. Mehreteab and F. J. Loprest, *J. Colloid Interface Sci.*, 1988, **125**, 602-609.
58. C. Minero, E. Pramauro, E. Pelizzetti, V. Degiorgio and M. Corti, *J. Phys. Chem.*, 1986, **90**, 1620-1625.
59. M. Rösch, *Kolloid-Zeitschrift*, 1956, **147**, 79-81.
60. M. Hato and K. Shinoda, *J. Phys. Chem.*, 1973, **77**, 378-381.
61. A. Masuyama, T. Kawano, Y.-P. Zhu, T. Kida and Y. Nakatsuji, *Chem. Lett.*, 1993, **22**, 2053-2056.
62. X. Chen, T. J. Young, M. Sarkari, R. O. Williams III and K. P. Johnston, *Int. J. Pharm.*, 2002, **242**, 3-14.
63. Z.-G. Cui and J. P. Canselier, *Colloid Polym. Sci.*, 2000, **278**, 22-29.
64. X.-G. Li and G.-X. Zhao, *Colloids Surf.*, 1992, **64**, 185-190.
65. M. Liu, H. Fang, Z. Jin, Z. Xu, L. Zhang, L. Zhang and S. Zhao, *J. Surfactants Deterg.*, 2017, **20**, 961-967.
66. L. F. Vleugels, J. Pollet and R. Tuinier, *J. Phys. Chem. B*, 2015, **119**, 6338-6347.
67. L. Zhang, W. Kang, D. Xu, H. Feng, P. Zhang, Z. Li, Y. Lu and H. Wu, *RSC Adv.*, 2017, **7**, 13032-13040.

68. D. D. Jurašin, S. Šegota, V. Čadež, A. Selmani and M. D. Sikirć, in *Application and Characterization of Surfactants*, ed. R. Najjar, InTech, 2017, pp. 33-73.
69. S. Lu, J. Wu and P. Somasundaran, *J. Colloid Interface Sci.*, 2012, **367**, 272-279.
70. Y. Michina, D. Carrière, C. Mariet, M. Moskura, P. Berthault, L. Belloni and T. Zemb, *Langmuir : the ACS journal of surfaces and colloids*, 2009, **25**, 698-706.
71. L. Chiappisi, H. Yalcinkaya, V. K. Gopalakrishnan, M. Gradzielski and T. Zemb, *Colloid Polym. Sci.*, 2015, **293**, 3131-3143.
72. G. Kume, M. Gallotti and G. Nunes, *J. Surfactants Deterg.*, 2008, **11**, 1-11.
73. M. Dubois, J. C. Dedieu, B. Demé, T. Gulik-Krzywicki and T. Zemb, *ACS Symp. Ser.*, 1999, **736**, 86-101.
74. Y. Michina, D. Carrière, T. Charpentier, R. Brito, E. F. Marques, J.-P. Douliez and T. Zemb, *J. Phys. Chem. B*, 2010, **114**, 1932-1938.
75. R. Sharma and R. K. Mahajan, *RSC Adv.*, 2014, **4**, 748-774.
76. E. Soussan, C. Mille, M. Blanzat, P. Bordat and I. Rico-Lattes, *Langmuir : the ACS journal of surfaces and colloids*, 2008, **24**, 2326-2330.
77. I. Rico-Lattes, M. Blanzat, S. Franceschi-Messant, É. Perez and A. Lattes, *C. R. Chim.*, 2005, **8**, 807-814.
78. J. N. Israelachvili, *Intermolecular and surface forces*, Academic press, 2011.
79. E. W. Kaler, A. K. Murthy, B. E. Rodriguez and J. Zasadzinski, *Science*, 1989, **245**, 1371-1374.
80. D. Jurašin, M. Vinceković, A. Pustak, I. Šmit, M. Bujan and N. Filipović-Vinceković, *Soft matter*, 2013, **9**, 3349-3360.
81. T. Zemb, M. Dubois, B. Demé and T. Gulik-Krzywicki, *Science*, 1999, **283**, 816-819.
82. M. Dubois, B. Demé, T. Gulik-Krzywicki, J.-C. Dedieu, C. Vautrin, S. Désert, E. Perez and T. Zemb, *Nature*, 2001, **411**, 672.
83. A. Barbetta, C. La Mesa, L. Muzi, C. Pucci, G. Risuleo and F. Tardani, *Nanobiotechnology*, 2014, 152-179.
84. T. Bramer, N. Dew and K. Edsman, *J. Pharm. Pharmacol.*, 2007, **59**, 1319-1334.
85. R. Dong, R. Weng, Y. Dou, L. Zhang and J. Hao, *J. Phys. Chem. B*, 2010, **114**, 2131-2139.
86. J. Yuan, X. Bai, M. Zhao and L. Zheng, *Langmuir*, 2010, **26**, 11726-11731.
87. E. J. Danoff, X. Wang, S.-H. Tung, N. A. Sinkov, A. M. Kemme, S. R. Raghavan and D. S. English, *Langmuir : the ACS journal of surfaces and colloids*, 2007, **23**, 8965-8971.
88. H. Kahe and M. Chamsaz, *Environ. Monit. Assess.*, 2016, **188**, 601.
89. S. Javadian, A. Yousefi and J. Neshati, *Appl. Surf. Sci.*, 2013, **285**, 674-681.
90. B. Tah, P. Pal, M. Mahato and G. B. Talapatra, *J. Phys. Chem. B*, 2011, **115**, 8493-8499.
91. P. Wang, Y. Ma, Z. Liu, Y. Yan, X. Sun and J. Zhang, *RSC Adv.*, 2016, **6**, 13442-13449.
92. N. Vlachy, A. F. Arteaga, A. Klaus, D. Touraud, M. Drechsler and W. Kunz, *Colloids Surf. A*, 2009, **338**, 135-141.
93. B. Lin, A. V. McCormick, H. T. Davis and R. Strey, *J. Colloid Interface Sci.*, 2005, **291**, 543-549.
94. E. Müller, L. Zahnweh, B. Estrine, O. Zech, C. Allolio, J. Heilmann and W. Kunz, *Journal of Molecular Liquids*, 2018, **251**, 61-69.
95. M. J. Rosen and J. T. Kunjappu, *Surfactants and Interfacial Phenomena*, WILEY, 2004.
96. M. J. Rosen and J. T. Kunjappu, in *Surfactants and Interfacial Phenomena*, WILEY, 2004, pp. 353-378.
97. T. F. Tadros, *Emulsions: Formation, Stability, Industrial Applications*, de Gruyter 2016.
98. U. Zoller, *Handbook of Detergents, Part E: Applications*, CRC Press, 2009.
99. A. J. Prosser and E. I. Franses, *Colloids Surf., A*, 2001, **178**, 1-40.
100. M. J. Schick, *Nonionic Surfactants: Physical Chemistry*, CRC Press, 1987.
101. BASF, *Technical Datasheet "Lutensol"*, 2018.

102. H. Hoffmann and W. Ulbricht, in *Die Tenside*, eds. K. Kosswig and H. W. Stache, Carl Hanser Verlag, 1993.
103. K. S. Birdi, *Surface and Colloid Chemistry: Principles and Applications*, CRC Press, 2010.
104. M. E. Hayes, M. Bourrel, M. M. El-Emary, R. S. Schechter and W. H. Wade, *SPE*, 1979, **19**, 349-356.
105. K. D. Collins, *Methods*, 2004, **34**, 300-311.
106. D. Möbius, R. Miller and V. B. Fainerman, *Surfactants: Chemistry, Interfacial Properties, Applications*, Elsevier, 2001.
107. R. K. Iler, *The Chemistry of Silica: Solubility, Polymerization, Colloid and Surface Properties and Biochemistry*, WILEY, 1979.
108. E. S. Metzler, L. Kravetz, W. W. Schmidt and J. D. Skiffington, in *Proceedings of the 4th World Conference on Detergents: Strategies for the 21st Century*, ed. A. Cahn, AOCS Press, 1999, pp. 156-164.
109. J. Eastoe and J. S. Dalton, *Adv. Colloid Interface Sci.*, 2000, **85**, 103-144.
110. R. M. Weinheimer, D. F. Evans and E. L. Cussler, *J. Colloid Interface Sci.*, 1981, **80**, 357-368.
111. T. Bramer, N. Dew and K. Edsman, *J. Pharm. Pharmacol.*, 2008, **59**, 1319-1334.
112. S. R. Raghavan, G. Fritz and E. W. Kaler, *Langmuir*, 2002, **18**, 3797-3803.
113. E. F. Marques, *Langmuir : the ACS journal of surfaces and colloids*, 2000, **16**, 4798-4807.
114. M. J. Rosen, L. Fei, Y.-P. Zhu and S. W. Morrall, *J. Surfactants Deterg.*, 1999, **2**, 343-347.
115. R. L. Grant, C. Yao, D. Gabaldon and D. Acosta, *Toxicology*, 1992, **76**, 153-176.
116. S. Mishra, *Journal of oleo science*, 2007, **56**, 269-276.
117. N. Vlachy, D. Touraud, J. Heilmann and W. Kunz, *Colloids Surf. B*, 2009, **70**, 278-280.
118. E. Soussan, S. Cassel, M. Blanzat and I. Rico-Lattes, *Angewandte Chemie International Edition*, 2009, **48**, 274-288.
119. S. Consola, M. Blanzat, E. Perez, J.-C. Garrigues, P. Bordat and I. Rico-Lattes, *Chem. Eur. J.*, 2007, **13**, 3039-3047.
120. 2007.
121. D. R. Anderson, *Statistics for Business and Economics*, Thomson, 2007.
122. A. Couper, R. Newton and C. Nunn, *Colloid Polym. Sci.*, 1983, **261**, 371-372.
123. M. J. Rosen, in *Surfactants and Interfacial Phenomena*, John Wiley & Sons, Inc., 2004, pp. 34-104.
124. G. Sauerbrey, *Zeitschrift für Physik*, 1959, **155**, 206-222.
125. P. Walstra, *Principles of Foam Formation and Stability*, London, 1989.
126. R. K. Prud'homme, *Foams: Theory: Measurements: Applications*, CRC Press, 1995.
127. M. F. Ashby, T. Evans, N. A. Fleck, J. Hutchinson, H. Wadley and L. Gibson, *Metal foams: a design guide*, Elsevier, 2000.
128. T. D. Tonyan and L. J. Gibson, *J. Mater. Sci.*, 1992, **27**, 6371-6378.
129. S. L. Allen, L. H. Allen and T. H. Flaherty, in *Defoaming: Theory and Industrial Applications*, ed. P. R. Garrett, Marcel Dekker, 1993, pp. 151-177.
130. R. J. Pugh, in *Handbook of Applied Surface and Colloid Chemistry*, ed. K. Holmberg, WILEY, 2002, vol. 1, pp. 23-43.
131. D. Exerowa and P. M. Kruglyakov, *Foam and foam films: theory, experiment, application*, Elsevier, 1997.
132. S. I. Karakashev and M. V. Grozdanova, *Adv. Colloid Interface Sci.*, 2012, **176**, 1-17.
133. M. H. Pahl and D. Franke, *CIT*, 1995, **67**, 300-312.
134. Q. Sun, L. Tan and G. Wang, *Int. J. Mod. Phys. B*, 2008, **22**, 2333-2354.
135. P. Stevenson, *Foam Engineering: Fundamentals and Applications*, WILEY, 2012.
136. E. Dickinson, *Curr. Opin. Colloid Interface Sci.*, 2010, **15**, 40-49.

137. A. Parker and W. Fieber, *Soft matter*, 2013, **9**, 1203-1213.
138. D. Varade, D. Carriere, L. Arriaga, A.-L. Fameau, E. Rio, D. Langevin and W. Drenckhan, *Soft matter*, 2011, **7**, 6557-6570.
139. H.-C. Yan, Q.-X. Li, T. Geng, Y. Jiang and Y. Luo, *Tenside Surf. Det.*, 2012, **49**, 211-215.
140. J. Ferreira, A. Mikhailovskaya, A. Chennievier, F. Restagno, F. Cousin, F. Muller, J. Degrouard, A. Salonen and E. F. Marques, *Soft matter*, 2017, **13**, 7197-7206.
141. H. Fauser, M. Uhlig, R. Miller and R. v. Klitzing, *J. Phys. Chem. B*, 2015, **119**, 12877-12886.
142. S. Lam, K. P. Velikov and O. D. Velev, *Curr. Opin. Colloid Interface Sci.*, 2014, **19**, 490-500.
143. T. S. Horozov, *Curr. Opin. Colloid Interface Sci.*, 2008, **13**, 134-140.
144. J. J. Scheibel, *J. Surfactants Deterg.*, 2004, **7**, 319-328.
145. T. F. Tadros, *An Introduction to Surfactants*, De Gruyter, 2014.
146. J. Ginsberg, in *A National Historic Chemical Landmark*, American Chemical Society, 2006.
147. I. Rüdénauer and R. Griebshammer, *Produkt-Nachhaltigkeitsanalyse von Waschmaschinen und Waschprozessen* Öko-Institut e.V., Freiburg, 2004.
148. R. Stamminger and G. Goerdeler, *SÖFW-Journal*, 2007, **1**, 2-2007.
149. C. Pakula and R. Stamminger, *Energy Efficiency*, 2010, **3**, 365-382.
150. D. Aaslyng, E. Gormsen and H. Malmos, *J. Chem. Technol. Biotechnol.*, 1991, **50**, 321-330.
151. D. Bajpai, *J. Oleo Sci.*, 2007, **56**, 327-340.
152. E. Smulders, W. Rähse, W. von Rybinski, J. Steber, E. Sung and F. Wiebel, in *Laundry Detergents*, Wiley-VCH, 2003, pp. 38-98.
153. M. Zappone, A. Kaziska and G. Bogush, in *Handbook of Detergents, Part E: Applications*, ed. U. Zoller, M. Dekker, 2009, pp. 69-82.
154. T. Becker, G. Park and A. L. Gaertner, in *Enzymes in Detergency*, eds. J. H. van Ee, O. Misset and E. J. Baas, Marcel Dekker, 1997, vol. 69, pp. 300-323.
155. M. R. Egmond, in *Enzymes in Detergency*, eds. J. H. Van Ee, O. Misset and E. Baas, Marcel Dekker, 1997, vol. surfactant science series, pp. 61-74.
156. A. M. Wolff and M. S. Showell, in *Enzymes in Detergency*, eds. J. H. Van Ee, O. Misset and E. J. Baas, Marcel Dekker, 1997, vol. 69, pp. 93-107.
157. E. Kissa, *Text. Res. J.*, 1981, **51**, 508-513.
158. Z. S. Derewenda, in *Advances in Protein Chemistry*, eds. C. B. Anfinsen, J. T. Edsall, F. M. Richards and D. S. Eisenberg, Academic Press, 1994, vol. 45, pp. 1-52.
159. M. Zappone, A. Kaziska and G. Bogush, in *Handbook of Detergents, Part E: Applications*, ed. U. Zoller, CRC Press, 2008, pp. 70-81.
160. E. Smulders, W. Rähse, W. von Rybinski, J. Steber, E. Sung and F. Wiebel, in *Laundry Detergents*, Wiley-VCH 2002, pp. 7-38.
161. T. Young, *Philos. Trans. Royal Soc.*, 1805, **95**, 65-87.
162. W. G. Cutler and E. Kissa, *Detergency: Theory and Technology*, Marcel Dekker, 1987.
163. T. F. Tadros, *Applied surfactants: principles and applications*, WILEY, 2006.
164. G. Broze, in *Detergents and Cleaners*, ed. K. R. Lange, Hanser Publishers, 1994, pp. 29-41.
165. E. Verwey, *J. Phys. Chem.*, 1947, **51**, 631-636.
166. B. Deraguin and L. Landau, *Acta Physicochim: USSR*, 1941, **14**, 633-662.
167. J. B. St. Laurent, F. de Buzzaccarini, K. De Clerck, H. Demeyere, R. Labeque, R. Lodewick and L. van Langenhove, in *Handbook for Cleaning/Decontamination of Surfaces*, ed. P. Somasundaran, Elsevier 2007, pp. 57-102.
168. M. F. Cox and K. L. Matheson, *J. Am. Oil Chem.' Soc.*, 1985, **62**, 1396-1399.
169. Y. Yu, J. Zhao and A. E. Bayly, *Chin. J. Chem. Eng.*, 2008, **16**, 517-527.
170. B. Borgström, *Biochim. Biophys. Acta, Lipids Lipid Metab.*, 1977, **488**, 381-391.
171. S. Bornemann, D. H. Crout, H. Dalton and D. W. Hutchinson, *Biocatalysis*, 1994, **11**, 191-221.

172. M. D. O'Donnell and K. McGeeney, *Enzyme*, 1974, **18**, 356-367.
173. S. S. Magalhaes, L. Alves, M. Sebastiao, B. Medronho, Z. L. Almeida, T. Q. Faria, R. M. Brito, M. J. Moreno and F. E. Antunes, *Biotechnol. Progr.*, 2016, **32**, 1276-1282.
174. S. Mahiuddin, A. Renoncourt, P. Bauduin, D. Touraud and W. Kunz, *Langmuir : the ACS journal of surfaces and colloids*, 2005, **21**, 5259-5262.
175. G. Kuhnt, *Environ. Toxicol. Chem.*, 1993, **12**, 1813-1820.
176. M. Schwuger, *Ber. Bunsenges. Phys. Chem.*, 1979, **83**, 1193-1205.
177. E. V. Gribanova, A. E. Kuchek and M. I. Larionov, *Russ. Chem. Bull.*, 2016, **65**, 1-13.
178. Y. Yuan and T. R. Lee, in *Surface science techniques*, Springer, 2013, pp. 3-34.
179. N. B. o. C. Engineers, *Soaps, Detergents and Disinfectants Technology Handbook*, Ajay Kr. Gupta, 2007.
180. T. Christ, W. M. Morgenthaler and F. Pacholec, in *Detergents and Cleaners*, ed. K. R. Lange, Hansers Publishers, 1994, p. 133.
181. P. K. Robinson, *Essays Bionchem.*, 2015, **59**, 1-41.
182. S. Duinhoven, Wageningen University, 1992.
183. J. H. Van Ee and O. Misset, *Enzymes in detergency*, CRC Press, 1997.
184. T. Fujii, T. Tatara and M. Minagawa, *J. Am. Oil Chem. Soc.*, 1986, **63**, 796-799.
185. N. Pauler, *Optische Eigenschaften von Papier*, AB Lorentzen & Wettre: Schweden, 2012.
186. D. Palacios, M. D. Busto and N. Ortega, *LWT - Food Sci. Technol.*, 2014, **55**, 536-542.
187. K. Lee, N. Ivanova, V. Starov, N. Hilal and V. Dutschk, *Adv. Colloid Interface Sci.*, 2008, **144**, 54-65.
188. H. J. Lee and S. Michielsen, *J. Text I.*, 2006, **97**, 455-462.
189. H.-J. Butt, K. Graf and M. Kappl, *Physics and Chemistry of Interfaces*, WILEY-VCH, 2006.
190. D. Bonn, J. Eggers, J. Indekeu, J. Meunier and E. Rolley, *Rev. Mod. Phys.*, 2009, **81**, 739.
191. S. Rafaï, D. Sarker, V. Bergeron, J. Meunier and D. Bonn, *Langmuir*, 2002, **18**, 10486-10488.
192. X. Zhao, M. J. Blunt and J. Yao, *J. Pet. Sci. Eng.*, 2010, **71**, 169-178.
193. M. Sakai, T. Yanagisawa, A. Nakajima, Y. Kameshima and K. Okada, *Langmuir : the ACS journal of surfaces and colloids*, 2009, **25**, 13-16.
194. J. Perelaer, C. E. Hendriks, A. W. de Laat and U. S. Schubert, *Nanotechnology*, 2009, **20**, 165303.
195. J. Radulovic, K. Sefiane and M. E. R. Shanahan, *J. Bionic. Eng.*, 2009, **6**, 341-349.
196. N. Ivanova and V. M. Starov, in *Surfactant Science and Technology: Retrospects and Prospects*, ed. L. Romsted, CRC Press, 2013, pp. 171-193.
197. P. G. de Gennes, *Rev. Mod. Phys.*, 1985, **57**, 827-863.
198. G. Jain, R. K. Khar and F. J. Ahmend, *Theory and Practice of Physical Pharmacy*, Elsevier Health Sciences, 2013.
199. R. N. Wenzel, *The Journal of Physical Chemistry*, 1949, **53**, 1466-1467.
200. A. Cassie, *Discuss. Faraday Soc.*, 1948, **3**, 11-16.
201. J. Radulovic, K. Sefiane, V. M. Starov, N. Ivanova and M. E. R. Shanahan, in *Drops and Bubbles in Contact with Solid Surfaces*, eds. M. Ferrari, L. Liggieri and R. Miller, CRC Press, 2013, pp. 37-71.
202. M. von Bahr, F. Tiberg and V. Yaminsky, *Colloids Surf. A*, 2001, **193**, 85-96.
203. V. Dutschk, K. G. Sabbatovskiy, M. Stolz, K. Grundke and V. M. Rudoy, *J. Colloid Interface Sci.*, 2003, **267**, 456-462.
204. V. M. Starov, S. R. Kosvintsev and M. G. Velarde, *J. Colloid Interface Sci.*, 2000, **227**, 185-190.
205. H. A. Ritacco, F. Ortega, R. G. Rubio, N. Ivanova and V. M. Starov, *Colloids Surf. A*, 2010, **365**, 199-203.

206. Y. Wu and M. J. Rosen, *Langmuir : the ACS journal of surfaces and colloids*, 2005, **21**, 2342-2348.
207. N. Kovalchuk, A. Barton, A. Trybala and V. Starov, *J. Colloids Interface Sci. Comm.*, 2014, **1**, 1-5.
208. N. Kovalchuk, A. Barton, A. Trybala and V. Starov, *J. Colloid Interface Sci.*, 2015, **459**, 250-256.
209. D. A. L. Leelamanie and J. Karube, *Soil Sci. Plant Nutr.*, 2013, **59**, 501-508.
210. N. Sghaier, M. Prat and S. Ben Nasrallah, *Chem. Eng. Sci.*, 2006, **122**, 47-53.
211. BASF, *Technical Information - Plurafac LF types*, 2014.
212. K. Holmberg and Editor, *Handbook of Applied Surface and Colloid Chemistry, Volume 1*, WILEY, 2002.
213. A. S. Adheeb Usaid and J. Premkumar, *Int. J. Eng. Res. Appl.*, 2014, **4**, 241-248.
214. F. Leal-Calderon, V. Schmitt and J. Bibette, *Emulsion science: basic principles*, Springer 2007.
215. J. Boyd, C. Parkinson and P. Sherman, *J. Colloid Interface Sci.*, 1972, **41**, 359-370.
216. F. O. Opawale and D. J. Burgess, *J. Colloid Interface Sci.*, 1998, **197**, 142-150.
217. G. Chen and D. Tao, *Fuel Process. Technol.*, 2005, **86**, 499-508.
218. S. Melle, M. Lask and G. G. Fuller, *Langmuir : the ACS journal of surfaces and colloids*, 2005, **21**, 2158-2162.
219. 2009.
220. J. Wadhwa, A. Nair and R. Kumria, *Acta Pol Pharm*, 2012, **69**, 179-191.
221. A.-T. Kuo and C.-H. Chang, *J. Oleo Sci.*, 2016.
222. C. Vautrin, T. Zemb, M. Schneider and M. Tanaka, *J. Phys. Chem. B*, 2004, **108**, 7986-7991.
223. C. Vautrin, M. Dubois, T. Zemb, S. Schmölzer, H. Hoffmann and M. Gradzielski, *Colloids Surf. A*, 2003, **217**, 165-170.
224. W. Kunz, E. Maurer, R. Klein, D. Touraud, D. Rengstl, A. Harrar, S. Dengler and O. Zech, *J. Disper. Sci. Technol.*, 2011, **32**, 1694-1699.
225. B. P. Binks, in *Modern aspects of emulsion science*, ed. B. P. Binks, Royal Society of Chemistry, 2007, pp. 1-48.
226. J. Sjöblom, *Emulsions and Emulsion Stability*, CRC Press, 2005.
227. T. F. Tadros, in *An Introduction to Surfactants*, De Gruyter, 2004, pp. 73-103.
228. T. F. Tadros, *Emulsion formation and stability*, John Wiley & Sons, 2013.
229. S. Madhav and D. Gupta, *Int. J. Pharm. Sci. Res.*, 2011, **2**, 1888.
230. M. Fanun, *Microemulsions: Properties and Applications*, CRC Press, 2009.
231. H. Hamaker, *physica*, 1937, **4**, 1058-1072.
232. D. N. Petsev, in *Emulsions: Structure, Stability and Interactions*, ed. D. N. Petsev, Elsevier, 2004, pp. 313-351.
233. G. M. Kontogeorgis and S. Kiil, in *Introduction to Applied Colloid and Surface Chemistry*, eds. G. M. Kontogeorgis and S. Kiil, Wiley, 2016, pp. 269-283.
234. V. Schmitt, S. Arditty and F. Leal-Calderon, in *Emulsions: Structure, Stability and Interactions*, ed. D. N. Petsev, Elsevier, 2004, pp. 607-641.
235. S. U. Pickering, *J. Chem. Soc.*, 1907, **91**, 2001-2021.
236. W. D. Bancroft, *J. Phys. Chem.*, 1913, **17**, 501-519.
237. B. Binks and S. Lumsdon, *Langmuir : the ACS journal of surfaces and colloids*, 2001, **17**, 4540-4547.
238. N. Ashby and B. Binks, *Phys. Chem. Chem. Phys.*, 2000, **2**, 5640-5646.
239. Y. Chevalier and M.-A. Bolzinger, *Colloids Surf. A*, 2013, **439**, 23-34.
240. L. M. Surhone, M. T. Timplendon and S. F. Merseken, *Pickering Emulsion*, VDM Publishing, 2013.
241. G. May-Alert, Philipps Universität Marburg, 1985.

- 242. N. Schelero, H. Lichtenfeld, H. Zastrow, H. Moehwald, M. Dubois and T. Zemb, *Colloids Surf., A*, 2009, **337**, 146-153.
- 243. N. Schelero, A. Stocco, H. Moehwald and T. Zemb, *Soft matter*, 2011, **7**, 10694-10700.
- 244. K. Margulis-Goshen, B. F. B. Silva, E. F. Marques and S. Magdassi, *Soft matter*, 2011, **7**, 9359-9365.
- 245. N. Zhang, Y. Fu, G. Chen, D. Liang, A. Abdunaibe, H. Li and J. Hao, *Colloids Surf., A*, 2016, **495**, 159-168.
- 246. F. Hofmeister, *Arch. Exp. Path. Pharm.*, 1888, **25**, 1-30.
- 247. W. Kunz, *Specific ion effects*, World Scientific, 2010.
- 248. W. Kunz, *Curr. Opin. Colloid Interface Sci.*, 2010, **15**, 34-39.
- 249. P. Jungwirth and D. J. Tobias, *Chem. Rev.*, 2006, **106**, 1259-1281.
- 250. C. R. Harrison, J. A. Sader and C. A. Lucy, *J. Chrom. A*, 2006, **1113**, 123-129.
- 251. N. Vlachy, B. Jagoda-Cwiklik, R. Vácha, D. Touraud, P. Jungwirth and W. Kunz, *Adv. Colloid Interface Sci.*, 2009, **146**, 42-47.
- 252. S. Kronawitter, Universität Regensburg, 2018.
- 253. R. D. O'Brien, *Fats and Oils: Formulating and Processing for Applications*, CRC Press, 2009.
- 254. A. Sarin, *Biodiesel: Production and Properties*, RSC Publishing, 2012.
- 255. D. J. Burgess and J. K. Yoon, *Colloids Surf. B*, 1995, **4**, 297-308.
- 256. J. Jiao and D. J. Burgess, in *Multiple Emulsion: Technology and Applications*, ed. A. Aserin, John Wiley & Sons, 2008, pp. 1-29.
- 257. H.-J. Butt, K. Graf and M. Kappl, *Physics and Chemistry of Interfaces*, WILEY-VCH, 2003.
- 258. C. Walser, Universität Regensburg, 2018.
- 259. L. Cheng, L. Liu and D. Mewes, in *Advances in Multiphase Flow and Heat Transfer*, eds. L. Cheng and D. Mewes, Bentham Books, 2012, vol. 4, pp. 149-175.
- 260. G. M. Førland, J. Samseth, M. I. Gjerde, H. Høiland, A. Ø. Jensen and K. Mortensen, *J. Colloid Interface Sci.*, 1998, **203**, 328-334.
- 261. K. Rauscher, J. Voigt, I. Wilke and K.-T. Wilke, *Chemische Tabellen und Rechentafeln für die analytische Praxis.*, Deutscher Verlag für Grundstoffindustrie, 1982.
- 262. L. L. Schramm, *Emulsions, Foams, Suspensions, and Aerosols: Microscience and Applications*, Wiley-VCH, 2014.
- 263. K. L. Stellner, J. C. Amante, J. F. Scamehorn and J. H. Harwell, *J. Colloid Interface Sci.*, 1988, **123**, 186-200.
- 264. X. Pei, Z. Xu, B. Song, Z. Cui and J. Zhao, *Colloids Surf., A*, 2014, **443**, 508-514.
- 265. A.-L. Fameau and T. Zemb, *Adv. Colloid Interface Sci.*, 2014, **207**, 43-64.
- 266. A. Zgoła-Grześkowiak, T. Grześkowiak, J. Zembruska and Z. Łukaszewski, *Chemosphere*, 2006, **64**, 803-809.

11 Eidesstattliche Erklärung

Ich erkläre hiermit an Eides statt, dass ich die vorliegende Arbeit ohne unzulässige Hilfe Dritter und ohne Benutzung anderer als der angegebenen Hilfsmittel angefertigt habe; die aus anderen Quellen direkt oder indirekt übernommenen Daten und Konzepte sind unter Angabe des Literaturzitats gekennzeichnet.

Weitere Personen waren an der inhaltlich-materiellen Herstellung der vorliegenden Arbeit nicht beteiligt. Insbesondere habe ich hierfür nicht die entgeltliche Hilfe eines Promotionsberaters oder anderer Personen in Anspruch genommen. Niemand hat von mir weder unmittelbar noch mittelbar geldwerte Leistungen für Arbeiten erhalten, die im Zusammenhang mit dem Inhalt der vorgelegten Dissertation stehen.

Die Arbeit wurde bisher weder im In- noch im Ausland in gleicher oder ähnlicher Form einer anderen Prüfungsbehörde vorgelegt.

Regensburg, den

(Lydia Zahnweh)